

*Nasa CR 65578*

FINAL REPORT TO  
NATIONAL AERONAUTICS AND SPACE ADMINISTRATION

Research Contract NAS 9-1970

Computer Analysis of EEG Data for a  
Normative Library

September 23, 1963 to January 31, 1966

GPO PRICE \$ \_\_\_\_\_

CFSTI PRICE(S) \$ \_\_\_\_\_

Hard copy (HC) 3 00

Microfiche (MF) .65

( Dr. J. D. French

Dr. W. R. Adey

Dr. D. O. Walter

# 653 July 65

Brain Research Institute

University of California, Los Angeles

April 15, 1966

FACILITY FORM 602

**N67 18723**

(ACCESSION NUMBER)

191

(PAGES)

CR-65578

(NASA CR OR TMX OR AD NUMBER)

(THRU)

(CODE)

(CATEGORY)

1

04

## TABLE OF CONTENTS

### VOLUME I

d I.	INTRODUCTION Concerning Analytic Methods . . . . .	1
II.	METHODS . . . . .	14
	Scenario. . . . .	15
	Sleep Definitions . . . . .	20
	Selection of Segments . . . . .	23
	Spectral Methods. . . . .	24
	Summarizing Techniques. . . . .	31
	Programs. . . . .	35
	Sample Output . . . . .	48
III.	RESULTS	
	Waking EEGs . . . . .	62
	Sleep Heads . . . . .	77
	REFERENCES . . . . .	85
	APPENDIX I . . . . .	86
	APPENDIX II (Preliminary Report on Discriminant Analysis). . . . .	91
	APPENDIX III (Figures) . . . . .	108

### VOLUME II (In Preparation)

- I. INTRODUCTION concerning relation of this study to previous attempts at normative series.
- II. METHODS of comparing individual patterns with means of the entire group and of selected subgroups.
- III. RESULTS: Selected subgroups.
- IV. RESULTS: Comparison of selected individuals with means.
- V. RESULTS: Additional applications of discriminant analysis.
- VI. DISCUSSION of implications of this study for NASA.

## ACKNOWLEDGEMENTS

Financial support for this study came from various federal agencies. Some of the calculations were done on a digital computer (Scientific Data Systems, Model 930) by the Data Processing Laboratory of the Brain Research Institute, partially supported by USPHS Grant NB02501 through the NINDB, by AFOSR Contract AF 49(638)-1387, and ONR Contract 233(91). The spectral and the discriminant computations were done on an IBM 7040-7094, by the Health Sciences Computing Facility under Dr. W. Dixon, sponsored by NIH Grant FR-3, whose long-continued cooperation is greatly acknowledged. The normative library analysis was supported in part by NASA Contract 9-1970, and we are also happy to acknowledge assistance from NASA Grant NsG 237-62. The technical excellence of the many recordings was due to Drs. P. Kellaway and R. Mauksby, of the Methodist Hospital, and Dr. M. Grahame of Rice University, Houston, Texas. The stimulus-control devices were designed and constructed in our laboratory by R.T. Kado and others. It is a pleasure to acknowledge the enthusiastic programming assistance of Mr. A. Parmelee. Dr. J. M. Rhodes has been a valued member of the scientific analysis group at several stages of this work, and Mr. D. Brown created many of the concepts applied in these programs.

## I. INTRODUCTION

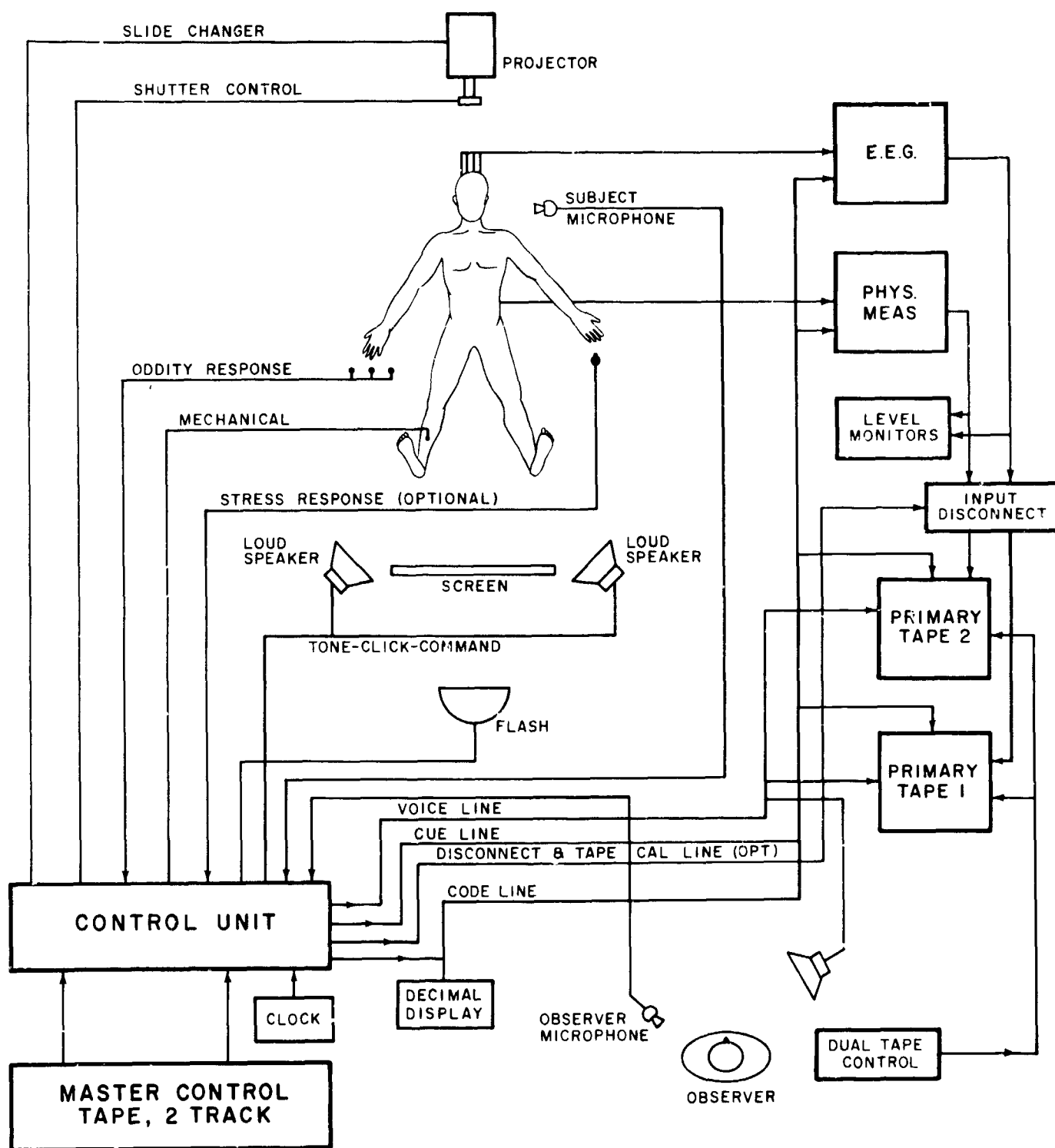
The scientific setting of the research effort reported here cannot be better introduced than by selected direct quotations from the chapter, Computer Analysis in Neurophysiology, written for general dissemination in the book, Computers in Biomedical Research (Adey, 1965) by the principal investigator of this contract:

It is the hallmark of the long history of man's attainment of a unique place among the primates that he finds himself fascinated and challenged by his own mental processes. He alone in the gamut of living things displays abilities to test and evaluate his own nature, and to seek the substrates and correlates of psychological events in physiological processes. He has long been aware of essential functions of his nervous system in the transmission, transaction, and storage of information. In the last century, structural and functional organization of the central nervous system has been substantially unraveled in the transmission of information. Only in the last decade, however, has progress been made in establishment of correlates between behavioral and neurophysiological processes. In our first glimpses of these exceedingly complex physiological events, it is apparent that their full comprehension requires the detection of patterns in a vast uncharted sea of seemingly random processes. Our frame of reference in brain tissue must necessarily consider redundancy in transmission and transaction of information, and stochastic modes of operation in the recall of previous experience.

The philosophies in application of computers to neurophysiology have been guided in the first instance by needs in data analysis, including detection of patterns of electrical activity. Arising from this new knowledge of intrinsic organization from the single cell to the integrated activity of major brain systems has been the development of a series of realistic and increasingly sophisticated models of brain functions, which are themselves susceptible of evaluation by data analysis in actual brain systems. There remains a less tangible area of endeavor, where achievements remain potential rather than actual, in which knowledge of transactional and storage processes in nervous structures may provide the basis for new computational devices. It would seem that knowledge of these properties in nervous tissue and developments in artificial

self-organizing systems may proceed in parallel rather than in lineal descent, with each providing appropriate stimuli to the other, but without critical interaction in the immediate future. At all events, it appears that the need to consider central nervous organization on a redundant and probabilistic basis, particularly at the level of cerebral associative mechanisms, requires models vastly removed from simple pulse-coded nerve nets, and implicates systems of parallel processing for information reaching the citadel of the single nerve cell in a variety of modes. It is to this exquisite uniqueness in organization of cerebral systems as revealed by computational analysis that this discussion will be primarily directed.

Neurophysiological research poses special problems in experimental design and data acquisition for subsequent computational analysis. In brain tissue, there are two widely divergent types of electrical activity recorded by appropriate means from any domain of cortical or subcortical gray matter. There are the fast action potentials of single nerve cells, recorded with micro-electrodes adjacent to or actually within the cell, with a typical duration of about 1 millisecond and repetition rates up to several hundred per second. In the same domain of tissue, we may record slower wave processes with a spectrum from 1 to 100 cycles per second or more. These waves are not the "envelope" of pulse-coded firing of nerve cells, but may have their origin partly in postsynaptic or dendritic potentials. We thus have the notion of at least a dual system in the processing of information in brain tissue. Moreover, it is necessary in virtually all experiments to record simultaneously from a series of interrelated points comprising a particular cerebral system. These simultaneous records may be of a series of electroencephalographic wave processes, or a combination of single action potentials and waves in different channels. In either case, detection of informational patterns requires due attention to acquisition of analog records free from frequency or phase distortions, or accurate assessment of the nature of such artifacts.



### PSYCHO-PHYSIOLOGICAL TESTING AND DATA ACQUISITION SYSTEM BLOCK DIAGRAM

Fig. 1. Scheme for presentation of auditory and visual stimuli and learning situations from a master control magnetic tape to a subject for computer analysis of EEG records. The system utilizes a twin-track recorder for a voice protocol and command signals. The latter are carried on IRIG subcarrier oscillators. The data acquisition tapes include the command signals and the EEG records.

## Neurophysiological Data Acquisition for Computer Analysis

PSYCHOPHYSIOLOGICAL PROGRAMMING APPARATUS FOR USE WITH COMPUTATIONAL TECHNIQUES. The rapid growth of behavioral neurophysiology in the past decade has led to evaluation of neurophysiological correlates of classical training procedures, including both classical and operant paradigms. It has become obvious that in the detection of neurophysiological correlates it is of critical importance to accurately signal subtle aspects of task performance and subject orientation, as well as the traditional signals indicating initiation of the test situation and moment of task completion. Only in this way can we hope to detect aspects of pattern in subtly and swiftly changing EEG activity. It is essential that tasks be presented with accurate and repeatable timing from one subject to another, and to the same subject from one day to another.

We have developed a system of human psychophysiological testing in collection of baseline EEG records from 200 subjects in a research program for the NASA Manned Spacecraft Center at Houston. Developed by Raymond Kado, the testing procedure centers about an accurately recorded 0.25-inch master program tape (Fig. 1). Using a twin-track recorder, command signals for the presentation of visual, auditory, and tactile stimuli, and for the test tasks to be learned by the subject during EEG recording, are multiplexed on subcarriers which operate on IRIG channels 1 through 9. One subcarrier carries a BCD three-digit "situation" code number. Each of the other subcarriers can initiate an operation when present; no situations may be presented unless both the situation subcarrier and an epoch marker subcarrier are present. Moreover, the situation subcarriers must be continuously present for 5 milliseconds before the situation gate is generated. This degree of redundancy is adequate to prevent presentation of a situation on noise pulses originating within the system.

At the onset of recording, the subject's number is encoded on the code-cue channel of a fourteen-channel 1-inch data tape, and the subject is verbally identified on the observer comment channel.

The multiplexed control signals and the voice protocol thus become part of the data acquisition tape, and it is possible to secure a rigorous duplication of tests from one subject to another. On initiation of the recording session, output of the physiological preamplifiers may be disconnected from the tape recorders during the blocking period which follows input switching from "calibrate" to "use" modes, and a square wave at 1 per second, 2 V p-p, is applied directly to the tape inputs, providing an independent calibration for the tape system. Calibration procedures are repeated at the end of the session. The last calibration is followed by an "end code" to facilitate tape digitization.

#### Analysis of Analog Wave Processes in Brain Tissue

The presence of wave processes in cortical and subcortical structures has challenged and baffled the physiologist ever since the observation by Caton (1875) that a galvanometer connected to the scalp undergoes ceaseless perturbations in its baseline. However, early optimism that easy and simple relationships might be found between informational processes and the EEG was not sustained. In the past 20 years attempts to detect patterns in these wave processes have been increasingly successful through techniques of automatic analysis.

In clinical use, early methods involved frequency analysis with analog techniques. A measure of spectral density distributions in epochs of EEG records 5 to 10 seconds in length can be obtained by multiple filters, each having a bandwidth of 1 to 2 cycles per second, and covering a band from 1 to 50 cycles per second. Such devices as resonant reeds and resistance-capacitive filters have been successfully used (Grey Walter, 1950), and typically provide continuous or periodic analyses of one or two channels.

This trend toward the use of analog techniques reached its peak almost a decade ago with the development of drum storage and tape loop devices capable of averaging evoked responses and performing correlation analyses (Brazier and Casby, 1952; Brazier and Barlow, 1956; Dawson, 1951). Toposcopic displays, in which the EEG signals intensity-modulated the beams of an array of cathode ray oscilloscopes as they synchronously traced polar plots (Grey Walter, 1943 a, b; Grey Walter and Shipton, 1951; Kozhevnikov,



1958; Livanov, 1960; Petsche and Stumpf, 1960), gave an early glimpse of possible ways in which phase patterns in an array of recording leads might be detected and displayed. Detection of patterned activity in the cortical mantle as a whole, or in the activity of corticosubcortical systems, has remained the goal of these analyses. However, the demand for ever-increasing complexity of analysis, often involving a series of separate analyses performed in a predetermined sequence, has led to the preponderance of special and general purpose digital computers in neurophysiological analysis.

It would appear that the logical development of digital computer utilization in this field will involve successive feasibility studies on the general purpose computer, leading in time to engineering of smaller, highly efficient special-purpose instruments to perform the same functions. Philosophically, it may be suggested that too early commitment to a particular technique of analysis through the availability of a particular "black box" computer, without the critical flexibility and opportunity to retract and regroup when trial of a particular technique indicates that its modification or even rejection may be desirable, would predicate the application of computers to categories of experiments solely on the basis of availability of a particular special-purpose computer. As the following account may make clear, the evaluation of a series of biological concepts may very well require the development of mathematical techniques peculiarly suited to the particular experiments in hand. It is here that the flexibility of the general-purpose digital computer is so clearly manifested.

The following account of the analysis of patterns of EEG activity suggests a sequence in which attempts to understand the role of cerebral wave phenomena has gone hand in hand with the development of new analysis techniques. These methods are suited to the examination of either short or long epochs of EEG records. They thus permit evaluation of brief states of focused attention, orienting behavior, and decision making on the one hand, and on the other, evaluation of long-term changes associated with fatigue, drowsiness, sleep states, alerting, and emotional perturbation.

## Computer Analysis of Short Epochs of EEG Record

SPECTRAL ANALYSIS OF THE EEG. From the earliest applications of techniques of frequency analysis to EEG records (Grass and Gibbs, 1938; Grey Walter, 1943 a,b) it was apparent that the EEG represented an essentially continuous spectrum of frequencies from under 1 cycle per second to well over 50 cycles per second. Functions relating intensity to frequency in any one lead are classified as autospectra, whereas cross-spectra describe shared intensities across a band of frequencies (Walter, 1963).

Both analog and digital spectral analyses have been applied to EEG records. Earlier analog devices converted functions of time into functions of frequency by sets of filters whose summed passbands covered the desired spectrum. Each filter accommodated a narrow band of frequencies, with minimal response at adjacent frequencies. Problems of designing physical filters with appropriately narrow skirt characteristics have led to the development of digital filters, in which the digital computer provides weighting functions by which the time function is multiplied. The sum of these products is taken as the output of the digital filter. The weighting function can be considered as having a narrow bandpass characteristic, as in an analog filter, or the application of a set of digital filters to a function of time can be viewed as a discrete version of a Fourier transform.

Spectral functions can be estimated in the digital computer from correlograms, rather than raw data, and this route may be economical for analysis of one or a few simultaneous traces. It is mathematically equivalent and more economical to apply digital filters directly to the digital data of each channel, as explained below in another connection. In this method, mean square filter outputs become the spectral intensities in each band. Digital filters of high quality have been developed for this application.

It is an essential step to emphasize the regular activity relative to the irregular, as occurs in the correlogram, or in properly designed filters, in order to ensure that the variance of the spectrogram decreases with increasing record length. Blackman and Tukey (1959) point out that omission of such a step

prevents the periodogram from being a statistically consistent estimator of the population spectrum, and may lead to interpretation of peaks due to sampling variability as relating to phenomena in the data.

a. Cross-Spectrograms. This technique was first applied to EEG data by Adey and Walter (Adey and Walter, 1963; Walter and Adey, 1963; Walter, 1963). It relates two EEG traces, and not only displays the intensity of the relationship as a function of frequency but provides much additional information about common wave processes and phase relationships at each frequency. These phase relations represent significant spatiotemporal relations of the activity in these brain structures. This technique provides objective measures of wave-for-wave relationship between different EEG traces, as a basic advantage of spectral analysis over conventional frequency analysis. Cross-spectrograms will display the relative amplitude of activity shared by the two traces at each frequency of the spectrum, and the phase relations of the shared activity at each frequency. It is also possible to establish a coherence function and a transfer function, and to evaluate their statistical variability.

b. Coherence and Transfer Ratio. The coherence function is also a function of frequency, and may be between 0 and 1. Values near 1 indicate that, at the frequency where they occur, nearly all the activity in one record could be explained as a linear transformation of activity in the other record. Coherence values near 0 indicate almost no linear relation between the records at that frequency. The coherence function thus resembles the coefficient of correlation between the records. As Walter (1963) pointed out in an earlier communication, the formula for the magnitude of the coherence may be expressed.

$$\text{coh}(f) = \text{MAGS}(f) / \text{ASX}(f)\text{ASY}(f)$$

where  $\text{MAGS}(f)$  is the mean cross-spectral magnitude at frequency  $f$  and  $\text{ASX}(f)$  is the autospectrum of  $X$  and  $\text{ASY}(f)$  the autospectrum of  $Y$ , at the respective frequencies. However, the term coherence is now commonly applied to the square of the function described in this equation.

In each frequency band, the phase angle of the coherence function is identical with that of the cross-spectrogram. A high coherence magnitude at a phase angle of 0° is analogous to high positive correlation in ordinary statistics, whereas the same at a phase angle of 180° is analogous to high negative correlation.

The transfer ratio is closely related to the coherence function. Whereas coherence resembles the ordinary correlation coefficient, the transfer ratio is analogous to the regression coefficient of one variable on another. Its formula is

$$tr(f) = MAGS(f)/ASX(f).$$

This transfer ratio is actually the magnitude of the transfer function, widely used in electrical engineering, and its phase angle is that of the cross-spectrogram. Descriptively, the transfer ratio indicates the ease of transmission of each frequency from one recording site in the brain to another. With bipolar electrodes, the amplitude of recorded wave trains is dependent on direction of approach; thus changes in transfer ratio are more likely to have a simple physiological interpretation than are particular values of the ratio, and are mainly attributable to changes in electrical characteristics of tissue lying between the sites of the electrode pairs.

As the requisite techniques become available, it would seem desirable to apply the techniques of multiple regression coefficients to spectral analysis, since bivariate regression may not be the most appropriate technique to apply to several simultaneous EEG records (Walter and Adey, 1963).

Walter (1963) has described a useful extension of these cross-spectral measures of transfer ratios and phase angles in EEG traces. This involves a treatment of their statistical variability through the application of Goodman's techniques (1957) for deriving the joint distribution of autospectra, the transfer ratio, and the phase angle. His equations allow establishment of joint confidence bounds on the transfer ratio and phase angle for each frequency. The method uses a polar display; in the first applications, upper and lower bounds on angle established a sector, while bounds on transfer ratio defined an annulus. The zone so delimited on the polar plot is the region of the true transfer function, with the specified confidence probability. Walter has designated these

regions as "fans" and examples will be described below. The formulas for the actual bounds are

$$\sin \theta(f) = \sqrt{\frac{1 - \text{coh}^2(f)}{\text{coh}^2(f)}} \sqrt{[(1 - P)^x - 1]}$$

$$x = -m/(N-m)$$

$$L(\text{tr}) = \frac{\text{tr}(f)}{1 + \sin \theta(f)}; \quad U(\text{tr}) = \frac{\text{tr}(f)}{1 - \sin \theta(f)}$$

$$L(\phi) = \phi(f) - \theta(f); \quad U(\phi) = \phi(f) + \theta(f)$$

where P is the specified confidence coefficient, N is the number of sampling times, and m is the number of filters. There is a critical value of coherence where  $\sin \theta = 1$ , below which the bounds are too wide to be meaningful. For proper statistical inference, the unknown population value of coherence should be substituted in these formulas rather than the sample estimate. Recently, Goodman, in unpublished work, has made possible the calculation of circles of uncertainty for transfer ratio and phase, based solely on the sample value of coherence.

c. Examples of Cross-Spectral Analyses, with Calculation of Coherence, Transfer Ratios, and Variability Bounds. The superior ability of spectral analysis by comparison with correlation techniques to reveal differences between brief epochs of record, such as those accompanying a cat's performance of a discriminative task in a T maze, is exemplified in Figure 2. The use of correlation techniques to detect different phase patterns between correct and incorrect responses has been described above. By spectral analysis, interrelations between two parts of the hippocampal system in an animal making occasional errors are shown to be modified clearly in ways not revealed by cross-correlation (Adey et al., 1961).

In the correct response, the relative amplitudes of activity between the dorsal hippocampal and entorhinal traces showed a clear single maximum at about 6 cycles per second. In the incorrect response, there was a secondary peak at 2 cycles per second and the peak at 6 or 7 cycles per second was much smaller. Comparison of average phase angles between traces at each frequency showed a striking difference between correct and incorrect responses. In the correct response, the average phase angle between the two

CAT LC 55, 8<sup>th</sup> DAY OF TRAINING,  
2<sup>nd</sup> APPROACH: CORRECT

CAT L: 5E, 8<sup>th</sup> DAY OF TRAINING,  
3<sup>rd</sup> APPROACH: INCORRECT

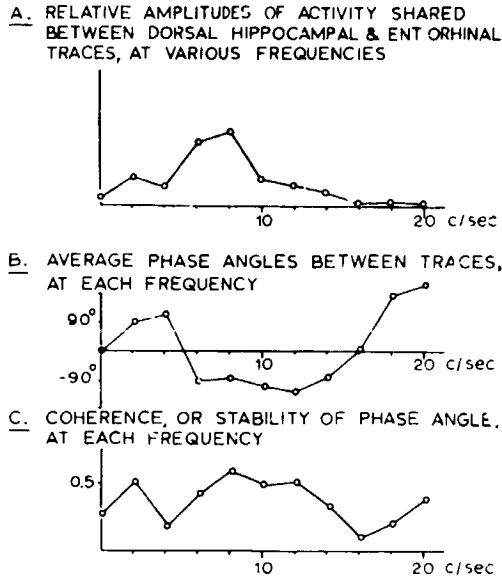
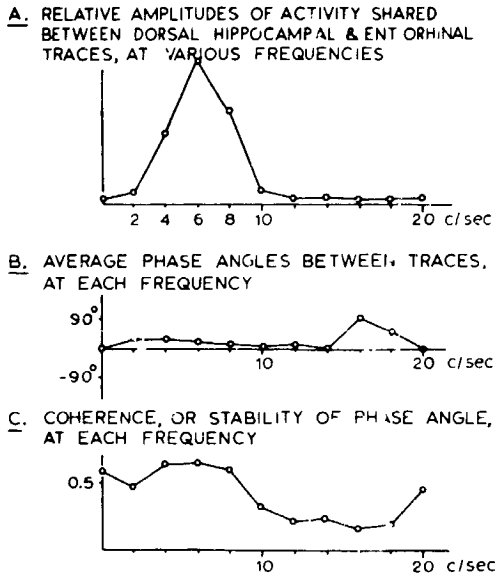


Fig. 2. Cross-spectral analyses of shared and unshared (A), average phase angles (B), coherence (C) in successive approaches. All three parameters are significantly different between correct and incorrect responses, with a sharp reversal of average phase angle at 6 cycles per second in the incorrect response. From Adey et al (1961).

### STOCHASTIC MODELS OF EEG

PROBABILITY BOUNDS ON COMPLEX TRANSFER FUNCTIONS,  
DORSAL HIPPOCAMPUS TO ENTORHINAL CORTEX

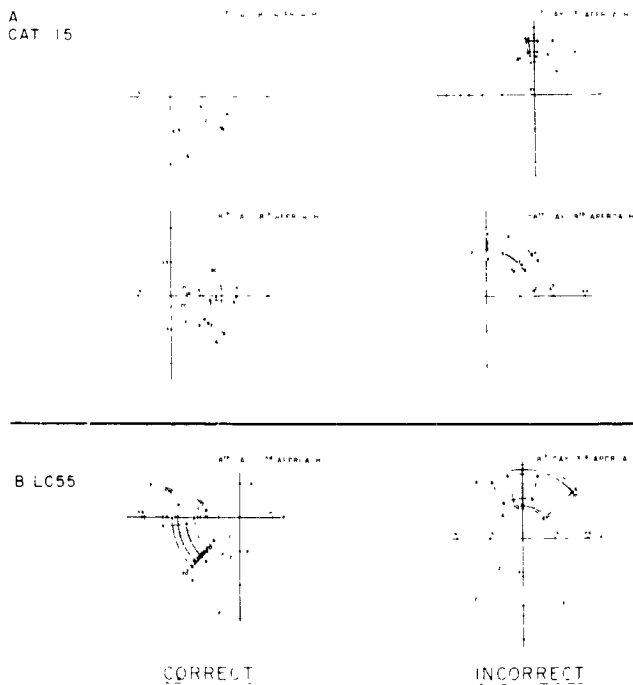


Fig. 3. Stochastic models of EEG. Examples of polar coordinate plots of probability bounds on complex amplitude transfer functions, dorsal hippocampus to entorhinal cortex. Phase angles are depicted on angular coordinates, and transfer functions are shown on radii. Shaded fans enclose 6 cycles per second portions of spectrum, and are maximum energy zones. Note consistency between correct responses and differences from incorrect responses in one animal (above), and similar wide differences between correct and incorrect responses in another animal (below line). From Adey and Walter (1963).

traces was fairly uniform at  $+20$  to  $30^\circ$  in the spectrum between 2 and 10 cycles per second, with an increase to  $90^\circ$  at 16 to 18 cycles per second. In the incorrect response, a sharp reversal in average phase angle appeared at about 5 cycles per second, and persisted throughout the spectrum between 5 and 14 cycles per second at about  $-90^\circ$ . Coherence was high (in excess of 0.5) from 2 to 9 cycles per second in the correct response, with a sharp dip at 4 cycles per second.

These findings strongly support the reversal in phase patterns between correct and incorrect responses noted above in cross-correlation analysis in another animal. Continuing interest centers around the extent to which such findings may reflect a general difference in phase patterns between correct and incorrect decisions in fully trained animals. A further series of analyses (Adey and Walter, 1963) indicates that such changes do not always occur, and that incorrect responses may be isophasic with the correct ones, but this ambiguity may relate to the complexity of the behavioral response pattern in this discriminative task and levels of attention necessary for its successful performance.

Extension of these cross-spectral analyses to treat aspects of statistical variability with a display of relative phase angles and transfer ratios on a polar plot is shown in Figure 3 . The same 6 cycles per second band which shows the maximum energy peak in the two records separately is also that in which the transfer vector relating the hippocampal with the entorhinal waves is most narrowly limited, as indicated by the shaded areas. The boundaries of this and other zones shown are established at the 50% level of probability that the mean transfer vector lies within the zone delineated. There is good general agreement between the calculations relating to correct responses on two different days, in the phase relations at and near this best-related frequency. By contrast, the findings in incorrect responses from each of the same 2 days show a totally different location for the 6 cycles per second zone, although there was again good agreement between these incorrect responses in the location of those zones. The incorrect responses also showed a much wider scatter in the

distribution of other spectral zones than was seen in the correct responses. A further example from a different animal showed a major change in phase relations between entorhinal cortical and hippocampal records in correct and incorrect responses.

These spectral techniques have also been used to study the changes in hippocampal rhythms after lesions in the remote sub-cortical zone of the subthalamus, during discriminative performances (Walter and Adey, 1963). These studies indicated nonlinear interrelations between hippocampus and adjacent entorhinal cortex, in addition to the linear one. Nonlinear relations were also detected between the hippocampus and the midbrain reticular formation. Characteristically, it appears that irregular activity in the frequency of the slow wave trains is unshared between the rhinencephalic leads, whereas regular activity is shared.

#### References

- Adey, W. R., and D. O. Walter, (1963), Exptl. Neurol. 7, 186.
- Adey, W. R., D. O. Walter, and C. E. Hendrix. (1961) Exptl. Neurol. 3, 501.
- Blackman, R. B., and J. W. Tukey. (1959). "The Measurement of Power Spectra". Dover, New York.
- Brazier, M. A. B., and J. S. Barlow. (1956). Electroencephalog. Clin. Neurophysiol. 8, 325.
- Brazier, M. A. B., and J. U. Casby. (1952) Electroencephalog. Clin. Neurophysiol. 4, 201.
- Caton, R. (1875). Brit. Med. J. 2, 278.
- Dawson, G. D. (1951). J. Physiol. (London) 115, 2 P.
- Goodman, N. R. (1957). "On the Joint Estimation of the Spectra, Cospectrum and Quadrature Spectrum of a Two-dimensional Stationary Gaussian Process." Ph.D. Dissertation, Princeton University, Princeton, New Jersey.
- Grass, A. M., and F. A. Gibbs. (1938) J. Neurophysiol. 1, 521.
- Grey Walter, W. (1943a). Electron. Eng. 16, 8.
- Grey Walter, W. (1943b). Electron. Eng. 16, 236.
- Grey Walter, W. (1950). In "Electroencephalography" (D. Hill and G. Parr, eds.). Macdonald, London.
- Grey Walter, W., and H. W. Shipton (1951). Electroencephalog. Clin. Neurophysiol. 3, 281.
- Kozhevnikov, V. A. (1958). Fiziol. Zh. SSSR 43, 983.



Livanov, M. N. (1960). "Electroencephalography." State Publishing House, Moscow.

Petsche, H., and C. Stumpf. (1960). Electroencephalog. Clin. Neurophysiol. 12, 589.

Walter, D. O. (1963). Exptl. Neurol. 8, 155.

Walter, D. O., and W. R. Adey. (1963). Exptl. Neurol. 7, 481.

## II. METHODS

### General Comment on Methods of Data Analysis

In any application of statistics, there are several possible attitudes toward the variability of experimental results. One can assume that there is a True Value, but fluctuating errors of measurement are frustrating our striving to know that Value. Or one can view the fluctuations as due to interfering processes within the subject, whose irrelevant contributions we are trying to minimize. Or (and this is the attitude taken in this report) one can assume that 'values' are always fluctuating, as well as being obscured by irrelevant activity; then it is significant not only to attempt to minimize irrelevant fluctuations, but also to delimit and describe those parts of the observed variability which do not seem to be due to instrumental or interfering processes.

While this approach assumes, in modern jargon, that the individual is a 'stochastic process', it unfortunately is also one which maximizes the methodological effort, for we need to study not only means but higher moments of the distributions of this stochastic process. The number of samples required to do so is often greater than that required for estimation of means; and the detection and validation of differences between subjects or between situations, etc., requires considerably more statistical technique and calculation. As a further disadvantage of the stochastic process assumption, different questions about the data require different transformations of the data, so there is not even a single preferred method of summarization of data, no 'all-purpose summary'. Thus we have had to develop a number of different transformations of the data, depending on the question being asked. Nevertheless, we feel that this assumption is so much better at representing physiological processes, that the added effort is justified by better and more suggestive results.

Preparation of Subjects, Subjects' Experiences, and Data Collection.

All of these procedures were developed under other contracts, to whose reports the reader is referred. Preparation of subjects and the collection of data, as well as the copying of the data tapes, was covered by a contract with Dr. P. Kellaway. The experiences which the subject underwent were controlled by a device developed at the Space Biology Laboratory by Mr. Raymond T. Kado and others, under NASA Contract 9-1200. The 'scenario' for the actual stimulus series was written by Dr. J. M. Rhodes, and approved by the Normative Library Planning Committee. It is reproduced as the next section of this report.

## Revision of N.A.S.A. Scenario

Code 000

Pre-examination Instructions

This part of the examination is to record a variety of measures during different tasks or types of activity. You will see flashes, hear clicks, and receive mild taps. You will be told to open or close your eyes at various times. If you are told to open your eyes or close them, stay in that position until a new instruction; for example, if told to close your eyes do not open them until told to do so. You will also be asked to make verbal responses and to push various buttons. These buttons are attached to the chair on the right-hand side. There are three buttons, test them by pushing first the left, then the middle, and lastly the right. Most of these instructions will be repeated during the examination proper.

Now we want to adjust our calibration for eye movements. Place your head in a comfortable position and focus your eyes on the center of the screen. You will see a light come on to the left; without moving your head, focus your eyes on the light. Other lights will come on one by one, each time, without moving your head, focus your eyes on the new light. Remember, do not move your head. Ready - (wait for stabilization).

<u>Code</u>	<u>Situation</u>
001	Identification (10 sec.)
002	Calibration: positive, negative and sine wave (30 sec.)
003	Linkage (10 sec.)
004	"Close your eyes." (3 sec.)
005	Rest (15 sec.)
006	"open your eyes." (6 sec.)
007	"Close your eyes." (5 sec.)
008	Rest (10 sec.)
009	"Keep your eyes closed for the present. Now the examination proper will begin. As you have been told, you will see flashes, hear clicks, receive slight taps, and have various tasks to perform. All parts of the examination including these instructions have been pre-recorded so no questions can be answered. If at some time during the examination you feel the instructions are not clear or are coming too fast, do the best you can on the following tasks. This part of the examination will take approximately 40 minutes. Please do not ask to stop during this time." (30 sec.)
010	Rest (10 sec.) (Tell subject to close his eyes, if necessary).
011	Presentation of 100 flashes at 1/c.p.s. (100 sec.)
012	Rest (15 sec.)
013	"clench your right hand in a fist and hold it clenched." (5 sec.)
014	"Release." (5 sec.)
015	Rest (10 sec.)
016	Presentation of 100 Mechanical Stimulations at 1 c.p.s. (100 sec.)

<u>Code</u>	<u>Situation</u>
017	Rest (15 sec.)
018	Presentation of 100 clicks at 1/cps. (100 sec.)
019	Rest (15 sec.)
020	Presentation of 200 flashes at 12 c.p.s. (17 sec.)
021	Rest (18 sec.)
022	Presentation of 200 clicks at 12 c.p.s. (17 sec.)
023	Rest (18 sec.)
024	Presentation of 200 taps at 12 c.p.s. (17 sec.)
025	Rest (18 sec.)
026	"Open your eyes." (5 sec.)
027	Rest (7 sec.)
028	Presentation of 200 clicks at 12 c.p.s. (17 sec.)
029	Rest (18 sec.)
030	Presentation of 200 taps at 12 c.p.s. 17 (sec.)
031	Rest (18 sec.)
032	Presentation of 200 flashes at 12 c.p.s. (17 sec.)
033	Rest (18 sec.)
034	Presentation of 100 clicks at 1/sec. (100 sec.)
035	Rest (15 sec.)
036	Presentation of 100 flashes at 1 c.p.s. (100 sec.)
037	Rest (15 sec.)
038	Presentation of 100 taps at 1 c.p.s. (100 sec.)
039	Rest (5 sec.)
040	"During the rest of the examination at different times you will see three symbols light up, two of which will be the same. You are to push one of the three buttons on

<u>Code</u>	<u>Situation</u>
040 (cont.)	the right-hand side corresponding to the odd symbol on the panel; for example, if the middle symbol is the odd one, push the middle button. When you have pushed the proper button the screen will go dark until the next presentation. The presentations may come at any time from now on." (40 sec.)
041	Presentation of single flash (5 sec.)
042	Rest (5 sec.)
043	Presentation of oddity problem Slide and shutter time (5 sec.)
044	"You will now be asked to do some mental calculations. When you have the answer, speak out clearly. If you have not finished one problem before the next is asked, start to work on the new one. Now close your eyes." (20 sec.)
045	Rest (5 sec.)
046	Presentation of loud white noise (5 sec.) (Noise duration - 5 sec.)
047	Rest (10 sec.)
048	"What is $21 \times 45$ ?" Answer: 945 (50 sec.)
049	"What is $45 \times 21$ ?" Answer: 945 (15 sec.)
050	"What is $12 \times 45$ ?" Answer: 540 (30 sec.)
051	"Open your eyes." (5 sec.)
052	Presentation of oddity problem Slide and shutter time (5 sec.)
053	"You will now hear groups of three tones like this (three tones). When you hear the third tone you are to push the button under your first finger on the right side of your chair. Remember to wait for the third tone of each group before pushing the button. Now close your eyes." (40 sec.)

<u>Code</u>	<u>Situation</u>
054	Presentation of single tap (5 sec.)
055	Rest (5 sec.)
056	(Presentation of the tones, three tones with an interval of 1 second, 3 seconds between series of tones, on the 40th presentation the third tone has an interval of 2 seconds, on 80th presentation the third tone has an interval of 3 seconds.) (485 sec.)
057	Rest (12 sec.) "Open your eyes." (after 5 sec.)
058	Oddity presentation Slide and shutter time (5 sec.)
059	"You will now be shown on the screen before you a series of slides. Each slide will have six circles numbered 1 to 6; one of the six will always be larger or smaller than the other five. You are to say loudly which is the odd circle. If you cannot do this before the circles are taken off the screen, or if you make a mistake you will hear this (loud tone manually operated)." (35 sec.)
060-079	Presentation of Slide Series 1, 2 and 3 Slide-exposure period: 3 sec.
080-099	Slide-exposure period: 2 sec.
100-119	Slide-exposure period: 1 sec. Slide-shutter interval constant = 5 sec. (420 sec.)
120	Rest (33 sec.)
121	Linkage (10 sec.)
122	Calibration: positive, negative and sine wave (30 sec.)

Total time: 44 minutes 15 seconds.

## Sleep Segment of Data Tapes

[The following is quoted from Dr. Kellaway's report.]

## Procedure:

After completion of the programmed waking scenario, subject's electrodes are unplugged from the terminal board. The two EMG electrodes on the right arm and the GSR electrode on the left digit #3 are removed. The remaining electrodes are left in place, their wires being taped to the subject's shoulders in a coil. The subject is then conducted to a private waiting room where he eats lunch, relaxes and reads magazines for about one hour until ready to begin the sleep record.

The sleep portion of the test is conducted in the same recording room used for the waking program. A folding bed is made ready, and the terminal box on the back of the recording chair is turned to face the head of the bed. The room is made completely dark and relatively sound-proof.

The same montage is used during sleep as was used during the waking record, with one exception -- the EMG electrodes are placed over the platysma muscle under the chin. The GSR electrode is reapplied to its former position.

Unused magnetic tapes are placed on the machines and the system is re-calibrated before data is recorded. The gain in the EMG channel is generally 4 to 8 times higher during the sleep record than it was during the waking portion.

The subject is instructed only to close his eyes and relax. He may lie in any position, but he is asked not to turn over during the recording.

The data tapes are started and codes are simultaneously recorded on both tapes every 6 seconds during sleep. The subject is allowed to go to sleep and remains undisturbed until he reaches the level of sleep characterized by fairly continuous high voltage very slow activity in the EEG. This level may be reached within one-half hour or it may take longer. (If the subject fails to sleep deeply in the afternoon, the electrodes are removed and the subject brought back in the evening for another attempt to obtain a sleep record.)

After a sufficient amount of "high voltage slow sleep" has been obtained, relatively weak auditory stimuli, such as clicks, are given to the sleeping subject in order to elicit a well defined "K-complex". Strong auditory stimuli are then administered in order to obtain actual arousal. After a brief post-arousal recording, the system is re-calibrated and the subject is released.

Dubbing portions of sleep on to the final data tape:

The paper write-out of the magnetic tape recording taken during sleep is visually scanned by an electroencephalographer who chooses various segments of the record to be dubbed on to the final data tape.

The table below includes a brief description of the criteria used for choosing the different portions of sleep. Note that level or stage of sleep is based purely upon EEG pattern. Situation codes, identifying the various stages, are recorded on the final data tape during the process of dubbing and are not quite synchronous on tapes A and B. Synchronization between the data on tapes A and B can only be obtained by reference to the time codes which were recorded on both A and B tapes simultaneously every six seconds while the original sleep record was being made.

<u>Situation Code</u>	<u>Description</u>	<u>Approx. Length</u>
123	Start calibration	Variable 20-60 sec.
124	<u>Sleep 0.</u> subject resting with eyes closed but awake as judged by presence of alpha rhythm.	30 sec.
125	<u>Sleep I.</u> "drifting" or drowsy stage when alpha rhythm greatly diminishes or disappears and record is generally low in voltage. Some subjects may have anterior dominant theta activity.	30 sec.
126	<u>Sleep II.</u> light sleep when vertex transient wave forms or "parietal humps" first appear.	30 sec.
127	<u>Sleep III.</u> medium sleep when 14 per sec. sleep spindles as well as vertex transients are prominent.	30 sec.
128	<u>Sleep IV.</u> deep sleep when high voltage slow waves are present in all leads.*	30 sec.

\*In the few individuals who show a "paradoxical" phase of sleep with rapid eye movements and low voltage EEG pattern, this segment will be included in situation 128 instead of high voltage slow sleep.



<u>Situation Code</u>	<u>Description</u>	<u>Approx. Length</u>
129	<u>Sub-arousal.</u> well defined "K-complex" in response to auditory stimulus. Timing of the stimulus is indicated by short pulse in code channel.	30 sec.
130	<u>Arousal.</u> actual arousal from sleep in response to an auditory stimulus. Several stimuli are delivered after arousal in order to prevent subject from going back to sleep	Variable 60-180 sec.
131	End Calibration	Variable 20-60 sec.

## SELECTION OF SEGMENTS TO BE ANALYZED

It was desired to study a considerable range of the many situations experienced by the subjects, yet the large amounts of computer time required, both in spectral analysis and in its summarization, dictated selection of a restricted set. Nevertheless, selections included several periods of eyes-closed rest (between stimulation periods), several periods of eyes-open rest, the entirety of the periods of the three kinds of stimulation (flashes, clicks and taps) at 1/sec., both eyes-open and -closed, selected epochs from the vigilance task (Code 56), all of the visual discriminations for 3-sec exposure, all for the 1-sec exposure, and all the sleep segments chosen by the recording team. The definition of these segments is given in Appendix 1. It happens that the segments as described (with the exception that the 3-sec discrimination segments are separated into first 10 and second 10) each add up to close to 100 sec in each situation. This is convenient, since it approximately equalizes the variability of spectra and coherences when they are averaged over these periods. Thus, after the analysis by separate epochs was done for each subject, an 'average case' for each of the analysed situations was calculated; these form a considerable part of the basis for further study and comparison between subjects' responses. Since there seldom appeared to be a trend of change during a situation, little information of physiological interest seems to be lost by this averaging.

The exact list of periods defined is given in APPENDIX 1. It would be pleasant to extend the analysis of the same subjects to further conditions, to compare their responses to 12/sec vs 1/sec stimulation, their reactions during mental arithmetic, fist-clenching, etc., but as noted above, computer time limited the selections which have been spectrally analysed for this study.

During computation, the digital data tape was positioned to the requested segment by definition, first, of the preceding code number, then, if applicable, by the stimulus pulse number thereafter, and/or a starting time relative to the previous definitions.

Since this starting time offset could be negative, it was possible to position before a given stimulus pulse, although this ability was not exploited in this series. Ending times for an analysis epoch could be defined in a similar way, either by elapsed time only, or with reference to a stimulus pulse. The ability to position either beginning or ending of the epoch with respect to response pulses was also included in the capabilities of the program, but has not been employed in this series.

Some difficulty was encountered in positioning in the specified way for occasional codes, due to a variety of tape errors, mainly on digital tapes, but occasionally affecting the analog tape. Usually, one attempt was made to recover isolated cases missing from otherwise acceptable subjects; if the attempt failed again in the same way, the case was left out of the summarization. If such a problem affected more than five cases out of 50 or more than three adjacent cases, the whole subject was redigitized; if the trouble persisted, the subject was dropped.

#### SPECTRAL METHODS

##### Sampling Rate, Low-pass Filtering, and Aliasing.

Records reported in this study were all sampled at 200 samples per second, with 50 microsecond delay between channels. Digital low-pass (zero phase-shift) filtering was applied as part of the NEEG processing of every segment analyzed. The output rate of this low-pass filtering was 100 samples per second, giving a folding frequency after filtering of 50 c/sec. The shape of the low-pass filter was designed to be flat from 0 to 25 c/sec, after which it entered a linearly decrementing region from 25 to 37.5 c/sec, beyond which it was nominally zero. An actual test of this filter was made, with the results shown in Fig. FM-1 (p. 30, see section on Digital Filtering).

Because of the filtering before secondary sample-rate reduction, the reduction should not introduce any aliasing, since only activity between 75 and 100 c/sec would be folded onto the range analysed, and it is severely attenuated by the filtering. However, there is another possibility for aliasing, namely of those frequencies which are folded into the analysis band of 0-25 c/sec by the original sampling during digital-analog conversion. Such frequency ranges of the analog playback are 175-225, 375-425,

575-625, etc. c/sec. Ordinarily one would not anticipate a significant amount of narrow-band activity in those ranges; but unfortunately the sensitivity of spectral analysis is so great that the third harmonic of the power-line frequency at 180 c/sec is quite visible, and folds onto the activity at 20 c/sec in the original recording. The amounts of such activity are not great, but unfortunately they are coherent between channels; an analogous situation for a different instrumental artifact is described in Walter, et al. (1966). The interchannel delay which is negligible for frequencies in the EEG range, amounts to  $3.24^\circ$  per channel at 180 c/sec, which is still negligible for adjacent channels in comparison with the usual statistical error in estimating phase angles, but contributes signals more than  $20^\circ$  out of phase between channels 2 and 9, for example, which are recorded (on the A tape) from geometrically adjacent regions of the scalp. This effect misled us until we recognized its origin in aliasing. It is uncertain whether the 180-c activity was present in the original recording, during the dubbing (when it would have had to be 720 c/sec because of the tape speed multiplication), during reproduction for digitization, or some combination of these. Since the amount of this activity is about 1 microvolt r.m.s., something of the kind could not really have been avoided by more sanitary engineering; it is merely another of those difficulties brought on by the new order of sensitivity of these methods. Thus, any activity nominally at exactly 20 c/sec in these records must be interpreted with that difficulty in mind; in addition, we must discount a spuriously high impression of coherence in this band.

#### Muscle Filtering

The muscles of the cranium produce a signal which mixes with the signals from the brain, when both are active. It is common in electroencephalographic practice to employ 'muscle filters' when such activity cannot be avoided by exhorting the subject. In this library, there was no opportunity for us to communicate with the subjects, and so those sections of record which appeared to contain significant muscular activity were also filtered before digitization, so that the sampling rate would not have to be inordinately increased. The filters' characteristics,

shown in Fig. AF (p. 30), were compensated digitally, after frequency analysis. Being realizable, these networks of course introduced phase shifts which differed at different frequencies. However, the difference in phase shift between two such filters at the same frequency will be much less than the statistical sampling errors inherent in measuring phase angle differences between brain waves, so that no compensation for phase changes was used.

### Digital Filtering

Frequency analyses were accomplished for this study by digital filtering of the data. By this technique the digital computer produces results directly analogous to those produced by analog frequency-selective filters, but of a design quality often unattainable by analog equipment. The method operates by the technique of convolution of a set of numbers representing the filtering action desired, with the set of numbers which constitute the data for a given channel for the chosen period of time. Convolution means essentially multiplying and adding the products together. The sense in which a set of numbers (called 'filter weights') represents the filtering action desired is that the filter weights are the samples (at a sampling rate equal to that applied to the data) of the response which the desired analog filter would have had to a unit impulse input. Textbooks show that convoluting such a set of numbers with a section of data is equivalent to filtering it; that is, the result of this multiplying and adding is a number which is equal to what the desired analog filter would have produced, if the same data (in analog form, of course) had been applied as input to the filter.

A major advantage of the digital filter as against a real analog filter is that it is a practical impossibility to produce an analog filter which does not introduce phase delays, and phase delays which differ in different parts of the filter's pass band. It is easy to make a non-phase-shifting digital filter, and this is important for our work where differences of phase angles between channels are an important aspect of the data. Phase shifts are more critical in the narrow-band filters used for cross-spectral analysis, than in the broad-band muscle filters mentioned above.

The operation of convolution just described is required for each filter output value, for each frequency, for each channel; since each convolution involves many multiplications, this operation occupies the major time of the computer performing a frequency analysis by NEEG. Many filter output points for each frequency are necessary in order to accumulate a useful estimate of the spectral intensities during an analysis epoch. It is wasteful of computer time to convolute, beginning again at every sampling time, for the filter outputs so generated would be highly interdependent statistically. It is also wasteful of data to begin a convolution too seldom. In NEEG, a compromise rate of application was chosen, which sacrifices 50% in statistical efficiency, but requires less than 25% the computer time of the rate which would be 98% statistically significant.

The rate of application chosen requires several convolutions to be applied to each data reading; the exact number varies with the sampling rate and maximum analysis frequency, and is automatically chosen by the program. One of the innovations that allows NEEG to save much space in comparison with many spectral analysis programs, is the method called 'sideways filtering', originated by Dan Brown under this contract. In this method of applying digital filters to data, all the convolutions which are to be applied to a given sample of data are applied to it the first time it enters the machine's memory; thus only one sample of data from a given channel need be stored at a time. In practice, for economy of tape usage, a block of 12-20 values for each channel under analysis is in memory at a time, but only one of these for each channel is being processed by NEEG.

Since convolution consists of multiplying and adding (or accumulating), several simultaneous convolutions require that several accumulators be storing partial convolution results. These are referred to as 'rotating accumulators', since as soon as a convolution is complete, its accumulator is cleared and assigned to begin accumulating the filter output for a considerably later time. In order to make our digital filters have no phase shift, it is necessary to carry the convolution 'into the future';

that is, the filter weights and data whose products contribute to the filter output associated with a given time must include data which occurred later than that given time. It is this requirement that makes impractical analog filters having no phase shift; but it also makes diagrams like Fig. FM-2 contain points on both sides of the starting time for the first accumulator (p.38)..

An additional feature which conserves computer time in NEEG is the use of two filtering passes. The data is first treated by a low-pass filter, which removes frequencies above the maximum frequency it was desired to include in the spectral analysis. Thus, for many of the NEEG calculations, the data was originally sampled 200 times per second, but the maximum frequency included in the spectral analysis was 25 c/sec.

Thus, if in the original reproduction for digitization, an ideal low-pass filter had been used that allowed all frequencies below but not above 25 c/sec to reach the digitizer, a sampling rate of only 50 c/sec would have sufficed, thus saving many multiplications in the later convolutions. Alternatively, if an ideal digital low-pass filter could have been applied to the data after digitization, the effective sampling could thereafter have been reduced to 50/sec. Since ideal filters are not available in applied mathematics, a compromise digital low-pass filter was applied. This filter introduced zero phase shift at any frequency; it had essentially no attenuation (unity gain) between 0 and 25 c/sec, at which point its gain falls linearly to zero (attenuation rises to infinity) over the range 25-37.5 c/sec. Above 37.5 c/sec, its maximum gain is 0.01 in amplitude, which means 0.0001 in power; the asymptotic loss rate is 18 db/octave. The output of such a filter could be adequately represented without aliasing by data sampled at 75 c/sec, but to avoid timeconsuming interpolations, the next larger factor of the original sampling rate is used: thus in this case the low-pass filter has an output at 100/sec. Since there are 25 band-pass filters in our typical analysis, the reduction of a factor of 2 in the number of multiplications for each one accomplished by this low-pass filtering is a worthwhile saving.

In our typical analysis, the band-pass filters are centered at intervals of 1 c/sec from 0 to 25 c/sec. There is considerable discussion as to the precise optimum filter shape and disposition

that are best for spectral analysis, but all agree that some overlap in frequency response (between adjacent filters) is desirable. The band-pass filters in NEEG were designed to give close to constant total power for extremely narrow-band inputs anywhere within their combined range. Filter responses reach zero for bands more than 1 c/sec from their center frequency. A plot of the responses to synthetic pure sine-wave inputs is shown in Fig. FM-1. . (p. 30).

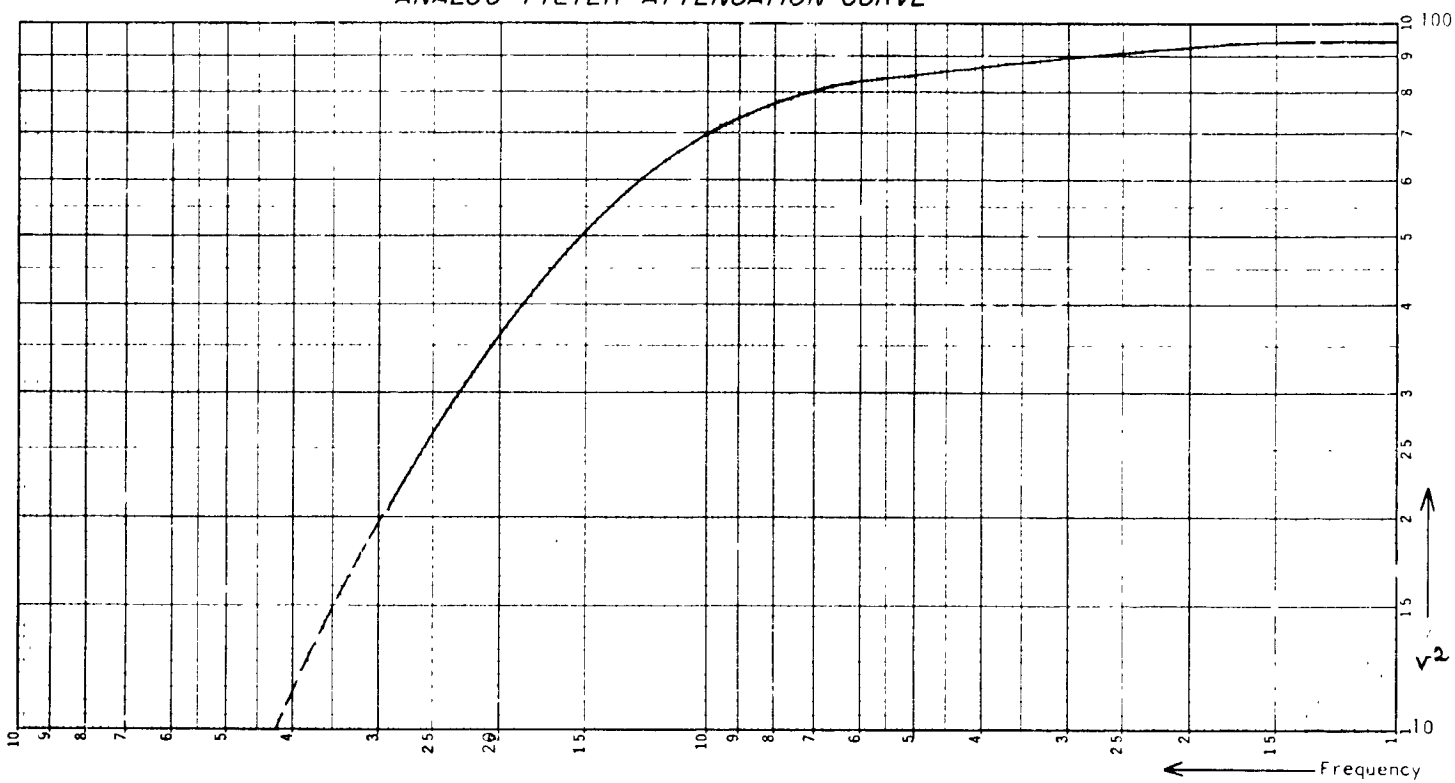
#### Band-pass Filtering

Band-pass filtering in NEEG is very similar to low-pass filtering, although of course the filter weights are arranged for narrower response, and centered at many different non-zero frequencies. The major difference is that, in order to preserve the same statistical efficiency, at the same ratio of input to output rates, it is necessary to define and apply two convolutions simultaneously. One of these is of zero phase shift, like the low-pass weights, and the other is of precisely  $90^\circ$  phase shift. It is the squares of both of these filters' outputs that are cumulated to make spectra; the products of these outputs (from different channels) are cumulated to make cross-spectra, from which coherences and phase angles are calculated.

Because of the filters' extension both before and after the nominal ends of the interval to be analysed, the data tape must also be positioned beyond, by an amount calculated by the program. This time-extension is essential in any frequency-domain analysis. Unfortunately there was an error in this feature of NEEG which resulted in many of the intervals' being too short, causing the spectra from these intervals to be too small in all frequencies. The effect is within the sampling variability of our spectral estimates, and was uniform for all subjects, so we felt that recomputation was not justified. The error has now been corrected, which may result in some slight biases in comparisons with future work.



ANALOG FILTER ATTENUATION CURVE



Log Power Ratio

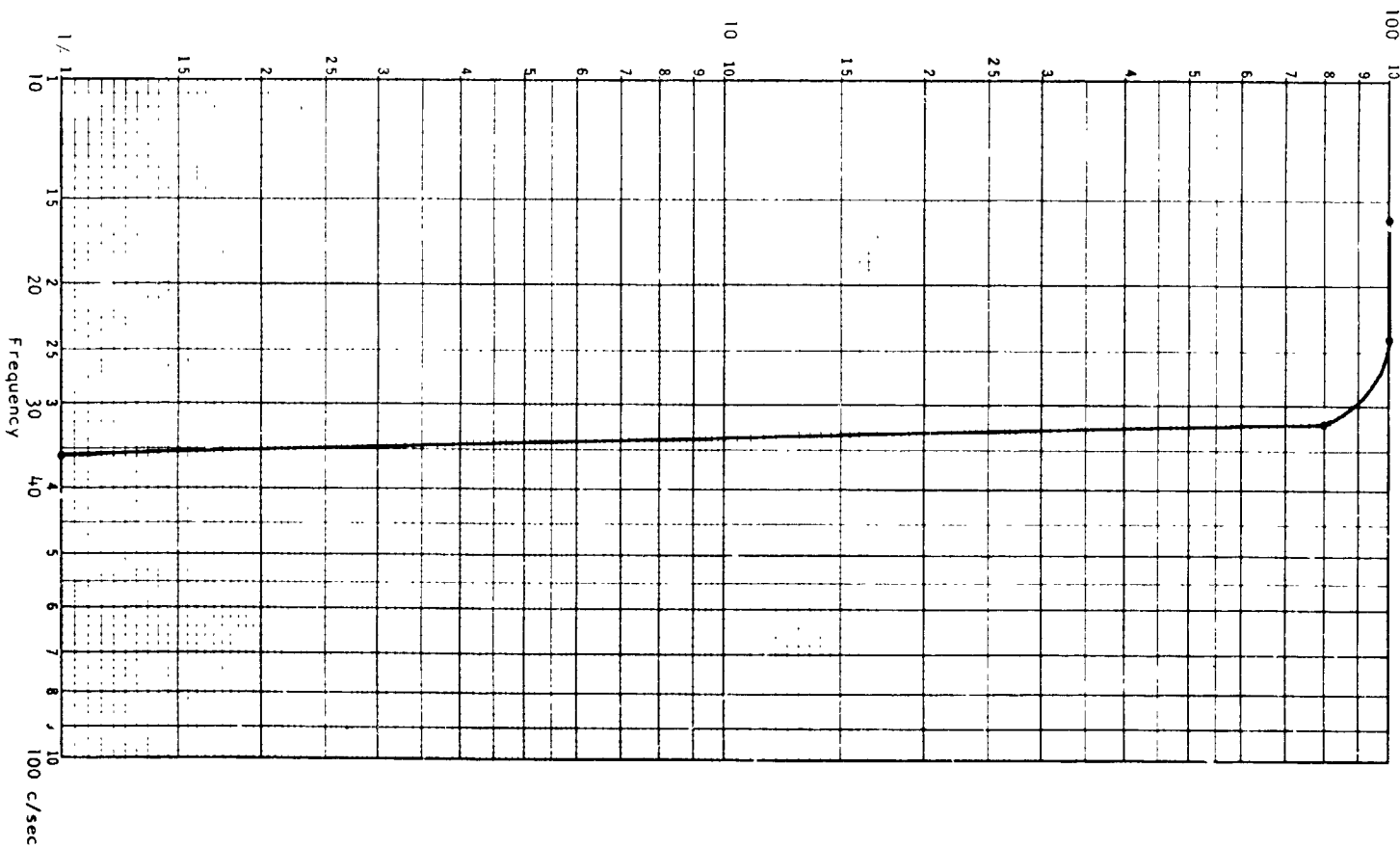


Fig. FM-1

## SUMMARIZING TECHNIQUES

Formulas Used in Averaging

In summarizing such an extensive library of numerical data, we have used averaged parameters -- in some cases averaged over time, in others across subjects, and occasionally over frequencies. Average intensities have a clear interpretation, although for reasons given below we have used geometric rather than arithmetic means in averaging intensities. The averages of cross-spectral parameters have to be more carefully developed.

## 1. Averaging autospectra

In many segments analyzed, some or all of a subject's leads contained muscle artifact. While muscle filters were used, this activity still greatly increased calculated spectral intensities in almost all frequency bands. Rather than attempt to identify such leads and segments, and exclude them from "averaging in" with other segments, we usually chose to use an averaging formula which de-emphasizes their contribution. Since muscle-affected spectra were increased approximately equally in each frequency band, the characteristic shape of the spectra will be preserved.

The formula used for each frequency is that for geometric mean of values in each 'case':

$$\begin{aligned} x &= \left( \prod_{i=1}^N X_i \right)^{1/N} \\ &= \exp \left( \frac{1}{N} \sum_{i=1}^N \log X_i \right). \end{aligned}$$

It is easy to see by experiment or theory that the geometric mean is less perturbed by one or two "outlying" cases, than is the arithmetic mean.

## 2. Averaging Coherence and Phase

If two channels have a high coherence in each of several epochs and a low coherence in others, the average coherence is of course medium. But if the calculated phase angle is close to 180° when the coherence is high, but varies between 0° and 360° when coherence is low, we will get a more proper idea of the average phase angle if we weight more heavily those epochs where

(see Appendix III for all figures) the coherence was high (hence the angle was well determined). Another annoyance in averaging angles is clear from the question, "What is the average of  $1^\circ$  and  $359^\circ$ ?" Obviously, the answer is  $0^\circ$ , but there is some difficulty in defining a generally applicable formula.

To avoid both these troubles, averaging of both coherence and phase angle was done indirectly, by going back to the original cross-spectra and averaging them. The average coherence and phase were then derived from the averaged cross-spectra.

Since muscle artifact is essentially incoherent between channels, resulting in small cross-spectra in such epochs, the geometric mean was not used for cross-spectra. Calculating average coherence as the quotient of an arithmetic mean for cross-spectra and a geometric one for autospectra results in a biased estimator. The amount of the bias was estimated by a Monte Carlo simulation, which showed that bias to be entirely negligible for our ranges of parameters.

#### PRESENTATION OF RESULTS

In addition to choosing methods of averaging which are adapted to the special properties of EEG data, we had to develop methods of presenting the results in reasonably comprehensible form. One of the difficulties in this connection was posed by wide range of the data, as between frequencies within the same channel, as well as between the intensities in the same frequency under different conditions.

For illustration of the difficulties of presentation posed by the wide range of our data, and the method developed for solving them, consider the following synthetic spectral output:

<u>Frequency</u>	<u>Case 1</u>	<u>Case 2</u>	<u>Case 3</u>	<u>Case 4</u>	<u>Case 5</u>	<u>Case 6</u>
1	1000	900	1000	900	1000	900
2	100	200	100	200	100	200
3	10	20	10	20	10	20
4	2	2	2	1	1	1
5	100	0	0	0	0	0

Such extreme range does not ordinarily occur within such a narrow frequency range, but does frequently occur in a single channel within the range of the 1-25  $\mu$  which is used in this study.

The data for each of the five "frequencies" is plotted in one set of bars in Fig. VM-Data, so that the six sets of bars represent all the data from the six "situations"; "frequency" 1 at the left of each set, then frequency 2, etc. When plotted on a linear scale, as in Fig. VM-Data, the picture is not very expressive of the variations in the weaker "frequencies". Some improvement is shown in the following Figures, Fig. VO-Mean and Fig. VO-Standard Deviations, where a logarithmic scale is used. The numbered bars to the left of the Mean plot show the original data values that would have resulted in a bar of the height they label, which are rounded off from constant logarithmic steps. Since we consider relative variation significant, it is natural to consider the coefficient of variation of these same data, which is shown in Fig. VM-Coefficient of Variation: the much greater relative variability of the "5¢" activity is immediately apparent, as is the equality of relative variability in "frequencies" 2-4, and the relatively quite small variability in the "1¢" activity. A transformation more expressive of variation from "code" to "code" is shown in Fig. VO-Variations. Each of the bars in these "spectra" is found by taking the mean (plotted in Fig. VM-Mean) from each value, and dividing that difference by the standard deviation. Thus,

$$V(f,s) = (X(f,s) - \bar{X}(f,.)) / \sigma(f,.)$$

where  $V(f,s)$  is the variation at any particular frequency for a particular situation,  $X(f,s)$  is the original data for the same frequency and situation,  $\bar{X}(f,.)$  is the average data for that frequency, but averaged over all situations, and  $\sigma(f,.)$  is the standard deviation for the data at that frequency, over all situations.

Attending to "frequency" 1, over all 6 situations, we see that

$$\begin{aligned} \bar{X}(1,.) &= \frac{1}{6} (1000 + 900 + 1000 + 900 + 1000 + 900) = 950 \\ \sigma(1,.) &= \sqrt{\frac{(50)^2 + (-50)^2 + (50)^2 + (-50)^2 + (50)^2 + (-50)^2}{6}} = 50 \\ V(1,1) &= (1000 - 950)/50 = 1 \\ V(1,2) &= (900 - 950)/50 = -1, \text{ etc.} \end{aligned}$$

Thus, in the first situation, its strength was  $1\sigma$  above the mean for frequency 1, while in situation 2 the value was  $-1\sigma$  from that mean; and of course this oscillation continues throughout. The relative variations in frequencies 2 and 3 are similarly calculated, since

$$\bar{X} (2, \cdot) = \frac{1}{6} (100 + 200 + 100 + 200 + 100 + 200) = 150$$

$$\sigma (2, \cdot) = \sqrt{\frac{(-50)^2 + (50)^2 + (-50)^2 + (50)^2 + (-50)^2 + (50)^2}{6}} = 50$$

$$v (2, 1) = (100 - 150)/50 = -1$$

$$v (2, 2) = (200 - 150)/50 = 1, \text{ etc.}$$

$$\bar{X} (3, \cdot) = \frac{1}{6} (10 + 20 + 10 + 20 + 10 + 20) = 15$$

$$\sigma (3, \cdot) = \sqrt{\frac{(-5)^2 + (5)^2 + (-5)^2 + (5)^2 + (-5)^2 + (5)^2}{6}} = 5$$

$$v (3, 1) = (10 - 15)/5 = -1$$

$$v (3, 2) = (20 - 15)/5 = 1, \text{ etc.}$$

Thus, the relative variations in "frequencies" 2 and 3 are equal to each other, and equal in magnitude but opposite in sign to those of frequency 1. Frequency 4 had variations of equal size, but differently distributed among the situations. Finally, frequency 5 was positive by almost  $2\sigma$  in situation 1, and uniformly negative (in variation) in all succeeding situations. Thus, we see that the relative variation of widely different sizes of data is brought to a standardized plot for ease of visual comparison.

## PROGRAMS

## General Outline of NEEG Operations

1. Read NEEG parameters (see Note 1)
2. Generate low pass and band-pass filter weights (see Note 2)
3. Position the input tape(s). Positioning is done in the following order:
  - a. Find experiment code (EXPNO, on code channel (EXPCODE); tape positioned one scan after last pulse in code.
  - b. Find starting pulse (PSTART) on pulse channel (STIMUL; EXPCODE used if not on tape). Tape positioned one scan after pulse STIMUL.
  - c. Find response of length BRESP. Tape positioned one scan after response.
  - d. Move tape START seconds (may be negative)

If any of the above parameters are not defined, the corresponding section of positioning is ignored.

Once the tape is positioned, NEEG reads one scan (one data value per channel) at a time, until the stop condition occurs, the stop condition is defined as follows:

- a. Find ending stimulus pulse (PEND)
- b. Then find response of length (ERESP)
- c. Then go TEND seconds (may not be negative).

If any of the above parameters are not defined, the corresponding section is ignored.

4. Number of channels analyzed (see Note 2)
  - X = One scan from input tape  $\underline{X}(1)$ ,  $1 = 1, N$ ; X is put through the low-pass filter routine which may or may not return Y.
  - Y = One scan of low-pass outputs  $\underline{Y}(1)$ ,  $1 = 1, N$ ; if Y is not returned, get another X. If Y is returned, go to section 5.
5.  $NF = (FMAX - FMIN)/DELF$ 
  - = Number of filters (maximum number is 35)
  - Y is put through the band-pass filter routine NF times (once for each filter frequency). The band-pass filter routine may or may not return Z.
  - Z = One scan of band-pass filter
    - outputs  $Z(1)$ ,  $1 = 1, N$  - in phase filter
    - $Z(1)$ ,  $1 = N + 1, 2N$  - quadrature filter

If no Z is delivered, get another X and return to section 4.

If Z is delivered, we get two values  $Z(1)$ ,  $Z(1+N)$  for every channel for every frequency band (except the zero frequency band for which there is no quadrature filter).

$FN$  = Number of Z's per frequency per channel.

6. From Z the following preliminary results are formed:
  - a. Zero frequency auto spectra

$$AS_0(J) = \sum_{1}^{EN} Z_0(J)^2 \quad J = 1, N$$

- b. Auto spectra for remaining bands

$$AS_1(J) = \sum_{1}^{EN} (Z_1(J)^2 + Z_1(J+N)^2) = \text{Sum of squares of inphase and quadrature filter outputs for } i\text{th band.}$$

- c. Cross spectra for remaining bands  
cross of channel a with channel b

$$CS_{i1} (a/b) = \sum_1^{EN} (Z_i(a) * Z_i(b) + Z_1(a+N) * Z_1(b+N))$$

$$CS_{i2} (a/b) = \sum_1^{EN} (Z_i(a) * Z_i(b+N) - Z_1(a+N) * Z_1(b))$$

- a. a + N refers to inphase and quadrature for channel a.  
b. b + N refers to inphase and quadrature for channel b.

7. Formulas for variables appearing in the NEEG printout (see Sample Output page 54).

FN = Number of band-pass filter outputs per frequency band  
(same for all bands) (number of Z's).

FNL = Number of low-pass filter outputs (number of Y's).

Number of degrees of freedom = 2 \* FN

NF = Number of frequency bands

$$YAV = \frac{1}{FN} \sum_1^{FN} Z_0 = \text{Average zero frequency output (this is named AVG on the printout)}$$

Quantities actually printed out:

Auto spectra

- a. Zero frequency

$$SPCT_0 (J) = \left[ \frac{AS_0 (J)}{FN} - YAV (J)^2 \right] * \frac{2.0}{DEL F} \quad (J=1, N)$$

- b. Remaining frequencies

$$SPCT_i (J) = \frac{AS_i (J)}{DEL F * 2.0 * FN}$$

- c. Other parameters

$$AVG.(J) = \frac{1}{FN} \sum_1^{EN} Z_0(J) \quad (J=1, N)$$

$$VAR(J) = \frac{1}{FNL} \sum_1^{EN} (Y(J)^2 - (YAV(J))^2)$$

$$SUMSP(J) = \sum SPCT_i (J) * DEL F \quad (i = 1, NF)$$

$$B.W.(J) = \frac{SUMSP(J)}{\max (SPCT_i (J))}$$

$$\frac{TAU(J)}{T} = \frac{SUMSP(J)}{XMAXSQ(J)}$$

$$XMAXSQ(J) = \max (Y(J)^2) = \text{Largest low-pass output for channel J, squared}$$

$$FBAR(J) = \frac{\sum_i SPCT_i(J) * DELF * F}{\sum_i SPCT(J) * DELF}$$

that is, (F = FMIN, FMIN + DELF, . . . . ., FMAX)  
F = FMIN, FMAX, DELF

Cross spectra

a/b  $\implies$  channel a crossed with channel b.

$$AMP_i(a/b) = \sqrt{CS_{i1}(a/b)^2 + CS_{i2}(a/b)^2}$$

$$PHASE_i(a/b) = \frac{180}{\pi} \text{Arctan} \left( \frac{CS_{i2}(a/b)}{CS_{i1}(a/b)} \right) \quad \begin{array}{l} i = \text{Frequency band} \\ i \neq 0 \end{array}$$

-90  $\leq$  PHASE<sub>i</sub> < 270

$$COH_i(a/b) = \frac{AMP_i(a/b)^2}{SPCT_i(a) * SPCT_i(b)}$$

$$CBAR(a/b) = \frac{1}{NF-1} \sum_i COH_i(a/b) * DELF$$

$$FHAT(a/b) = \frac{\sum_i COH_i(a/b) * DELF * F}{\sum_i COH(a/b) * DELF}$$

(for F = FMIN, FMIN + DELF, . . . . ., FMAX)  
F  $\neq$  0

interpowers (RIP and RIQ)

$$RIP(a/b) = \frac{\sum_i SPCT_i(b) * COH_i(a/b)}{\frac{SUMSP(b) - SPCT_0(b)}{DELF}}$$

$$RIQ(a/b) = \frac{\sum_i SPCT_i(a) * COH_i(a/b)}{\frac{SUMSP(a) - SPCT_0(a)}{DELF}}$$



NOTE 1: NEEG Parameters

BCODE - Height of the base level of codes on the code channel.  
 BPULSE - Height of the base level of pulses on the pulse channel.  
 BRESP - Length in milliseconds of the beginning response.  
 CHAN - Names of those channels for which autospectra is desired.  
 CHAN1 - Names of the channels on first input tape.  
 CHAN2 - Names of the channels on second input tape.  
 DATE - Identifying date in 30 alpha-numeric characters.  
 DELF - Resolution in cyc/sec desired in analysis.  
 ERESP - Length in milliseconds of the ending response.  
 EXPNO - Three digit experiment code No. on code channel.  
 FMAX - Maximum frequency desired in analysis.  
 FMIN - Minimum frequency desired in analysis.  
 FS - Digitized sampling rate in scans/second.  
 H1 - Experiment identification for entire run in 72 alpha-numeric characters.  
 H2 - Experiment identification for single case in 72 alpha-numeric characters.  
 HCODE - Height above the base level (BCODE) of experiment code on code channel.  
 HPULSE - Height above the base level (BPULSE) of pulses on pulse channel.  
 IDER - =1 means autospectra of the first derivative is desired also.  
 K - ignore - has no function.  
 LBTAPE - Fortran Logical Unit No. for binary output tape.  
 LIST - Names in pairs of those channels named in CHAN for which cross spectra are desired.  
 LISTXY - Ignore - has no function.  
 LONG - Length in scans of each pulse in experiment code on code channel.  
 LPTAPE - Fortran Logical Unit No. for filter output tape.  
 LTAPE1 - Fortran Logical Unit No. for first input tape.  
 LTAPE2 - Fortran Logical Unit No. for second input tape.  
 N - Number of channels in CHAN.  
 NBFIL - Number of end of file marks after which to position the binary output tape.  
 NCHAN - Number of channels in CHAN1.

NDEN1 - Density (566 or 800) of first input tape.  
 NO GO - = 0 means position the input tape but do no analysis.  
       = 1 mean: position and analyze.  
 NPFILE - Number of end of file marks after which to position the  
           filter output tape.  
 NTAPES - Number of input tapes.  
 NX - Number of pairs in LIST.  
 OUT - = 1 binary output desired.  
       = 2 list is desired - ignore - has no function.  
       = 4 filter output desired - ignore - not in production  
           status.  
       = 8 filter printout desired - gives reams of output.  
 PEND - Pulse No. to end analysis.  
 PSTART - Pulse No. to start analysis.  
 RECRD - Experiment record No.  
 SCALE - Scale factor for each channel in CHAN.  
 SUBNO - Experiment subject No.  
 TEND - Ending time in seconds for analysis.  
 TSTART - Starting time in seconds for analysis.

Limitations and Comments - All parameters are set to zero if not  
 read in except LONG, NDEN1, and NTAPES.

CHAN2 - Not operational in NEEG03.  
 FMAX -  $(FMAX-FMIN)/DELTA \geq 35$ .  
 FMIN - Not operational in NEEG03 - set to zero.  
 LONG - Set to 30 if not read in.  
 LPTAPE - Not for production in NEEG03.  
 LTAPE2 - Not operational in NEEG03.  
 NBFILE - ignore if stacking binary output. There must be at  
           least one job already on the output tape. A new output  
           tape is started by reading in (NBFILE) = 0B or by putting  
           three END OF FILE marks at the beginning of the tape.  
 NDEN1 - Set to 556 if not read in.  
 NDEN2 - Not operational in NEEG03.  
 NOGO - (NOGO) = 0B read in for the first case will nullify all  
           binary output requests. Hence a NOGO on the first case  
           should be done with (TEND) = 0 unless the entire job is  
           to be NOGO.  
 NPFILE - Not for production in NEEG03.  
 NTAPES - Non functional in NEEG03 - set to 1.  
 TSTART -  $TSTART * FS \leq 2^{17} - 1$  (=131071).

NOTE 2: Low-Pass Filtering in NEEG

- $FS$  = Sampling rate in samples per second.  
 $F_{MAX}$  = Maximum frequency analyzed.  
 $\Delta F$  =  $F_{MAX}/2$   
 $I_{SP}$  =  $2.4 * FS / F_{MAX}$   
 $I_S$  =  $2 * SP + 1$  = Number of filter weights to be used.  
 $AC_i$  =  $i$ th accumulator -  $i = 1, 20$   
 $START$  = Location of first data point requested.  
 $I_V$  =  $2 * FS / (5.0 * F_{MAX})$  = Decimation factor.  
 $FSZ$  =  $\frac{FS}{I_V}$  = Reduced sampling rate.

Idealized Filter

The filter (Fig. FM-1, p. 30) is constructed with a roll-off frequency of  $F_{MAX}$  and a cut-off frequency of  $F_{MAX} + \Delta F = F_2$ .  $M = (F_{MAX} + F_2)/2$ .

2M cyc/sec is the minimum sampling rate that will avoid aliasing error due to folding. The output rate of the filter is reduced to  $FSZ$  which is the smallest factor of  $FS$  greater than  $2M$ . If  $FS$  and  $F_{MAX}$  are such that no reduction of the filter output rate is possible, i.e., if  $2 * FS / (5 * F_{MAX}) < 2$  then no low-pass filtering is done.

Examples:

	<u><math>F_{MAX}</math></u>	<u><math>F_{MAX} + \Delta F</math></u>	<u><math>M</math></u>	<u><math>2M</math></u>	<u><math>FSZ</math></u>	<u><math>FS</math></u>	<u><math>I_V</math></u>
1.	40	60	50	100	100	200	2
2.	50	75	62	124	200	200	1
3.	25	37	31	62	67	200	3

The low-pass filtering is done with rotating accumulators. We will illustrate the process by going through an example step by step. To illustrate the process of output rate reduction, we wish to use a case where  $IV = 2$ .

For simplicity we will say that  $ISP = 3$  even though this is impossible if  $IV = 2$ .

$ISP = 3$  = Number of rotating accumulators  
 $IS = 7$  = Number of elements in the weights vector.  
 $IV = 2$  = Decimation factor.

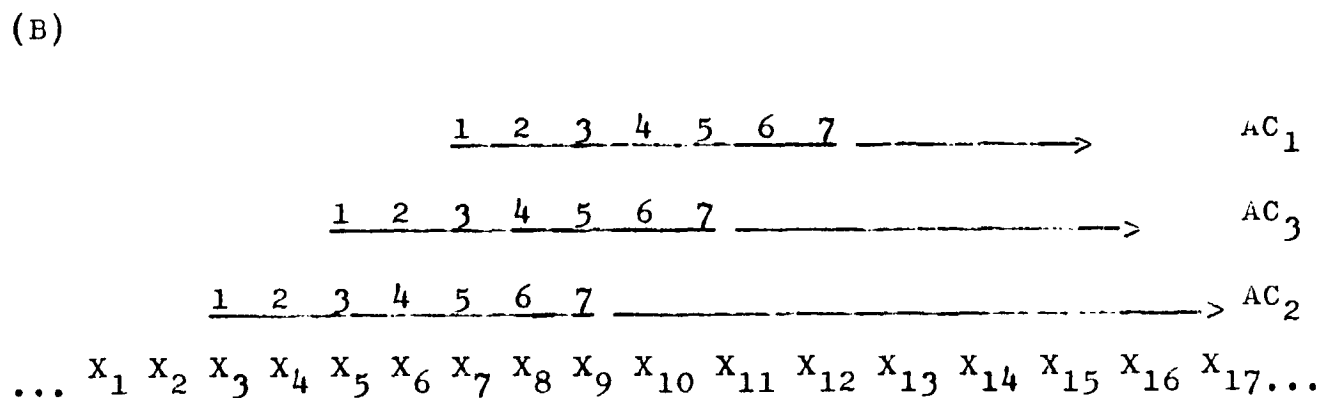
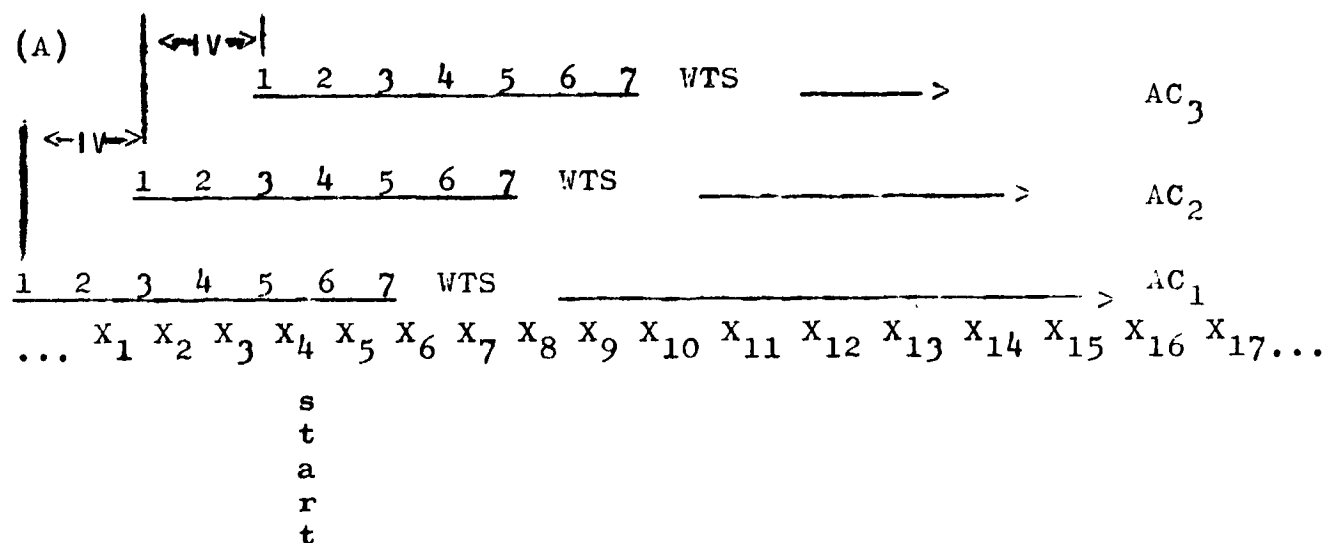


Fig. FM-2

The process is identical for all channels of data; so we will discuss the process for a single channel only. We select a data point somewhere in our data (see SELECTION OF SECTIONS TO BE ANALYSED) and request that this point (here labeled START) be the starting point for the analysis. In the illustration this point is referred to as  $X_4$  where  $4 = \text{ISP} + 1$ . To force the first filter output to correspond with  $X_4$ , the program backs up ISP (=3) data points and that point (labeled  $X_1$ ) is the first data point read. As the data is read, one point at a time starting with  $X_1$ , the following process goes on.  $AC_1$ ,  $AC_2$ ,  $AC_3$ , are initially set to zero. See below; note that "=" is used in the FORTRAN sense of "is replaced by".

<u>Data Point Read</u>	<u>Accumulation (FORTRAN)</u>	<u>Usual Notation</u>
$X_1$	$AC_1 = AC_1 + X_1 * WTS_1$	$AC_1(1) = AC_1(0) + X_1 WTS_1$ $AC_2(1) = AC_2(0)$ $AC_3(1) = AC_3(0)$
$X_2$	$AC_1 = AC_1 + X_2 * WTS_2$	$AC_1(2) = AC_1(1) + X_2 WTS_2$ $AC_2(2) = AC_2(1)$ $AC_3(2) = AC_3(1)$
$X_3$	$AC_1 = AC_1 + X_3 * WTS_3$ $AC_2 = AC_2 + X_3 * WTS_1$	$AC_1(3) = AC_1(2) + X_3 WTS_3$ $AC_2(3) = AC_2(2) + X_3 WTS_1$ $AC_3(3) = AC_3(2), \text{ etc.}$
$X_4$	$AC_1 = AC_1 + X_4 * WTS_4$ $AC_2 = AC_2 + X_4 * WTS_2$	
$X_5$	$AC_1 = AC_1 + X_5 * WTS_5$ $AC_2 = AC_2 + X_5 * WTS_3$ $AC_3 = AC_3 + X_5 * WTS_1$	
$X_6$	$AC_1 = AC_1 + X_6 * WTS_6$ $AC_2 = AC_2 + X_6 * WTS_4$ $AC_3 = AC_3 + X_6 * WTS_2$	
$X_7$	$AC_1 = AC_1 + X_7 * WTS_7$ $AC_2 = AC_2 + X_7 * WTS_5$ $AC_3 = AC_3 + X_7 * WTS_3$	Full; read out, set to zero, restart then set $AC_1 = X_7 * WTS_1$
$X_8$	$AC_1 = AC_1 + X_8 * WTS_2$ $AC_2 = AC_2 + X_8 * WTS_6$ $AC_3 = AC_3 + X_8 * WTS_4$ etc.	

After point 7 is read,  $AC_1$  is full and the contents of  $AC_1$  are recorded by NEEG as the first low-pass filter output. This number is the filter output "for" the data point lined up with the center weight ( $WTS_4$ ) for  $AC_1$ , i.e.,  $X_4$ , the starting position.

$AC_1$  is set to zero, shifted over as in part B of Fig. FM-2; then  $AC_1 = X_7 * WTS_1$ . Two scans later  $AC_2$  is full and a filter output value "for"  $X_6$  is delivered, and  $AC_2$  is shifted over. Two scans later we get an output from  $AC_3$ . We continue to get an output every 2 (= IV) data points until the output for the last data point requested is delivered. Hence 3 (= ISP) points past the ending point will be read. The low-pass filter weights are an even function around the center weight, with a shape something like a damped co-sine wave.

Hence only half the filter weights are stored. In the above illustration for example,  $WTS_1 = WTS_7$ ,  $WTS_2 = WTS_6$ , and  $WTS_3 = WTS_5$ , so that only  $WTS_1$  through  $WTS_4$  need be stored in computer memory; proper address calculation causes the correct convolution to be performed.

## BPWTS

## A. IDENTIFICATION

Program Code Name: BPWTS  
 Classification: 2.2 S 040  
 Programmer: Dan Brown BRI/DPL UCLA Health Sciences Center  
 Machine: 7094  
 Language: FAP  
 Date: January 22, 1964

## B. PURPOSE

Generates sets of in-phase and quadrature band pass filter weights for BPF for frequencies FNDELFF, 2.\*FNDELFF, FNMAX. A single set of LP filter weights is obtained from OWTs for frequency 0.

## C. METHOD

The number of weights, NWTS, required for resolution FNDELFF is computed as  $3.2/\text{FNDELFF} + 1$ . OWTs ( $1.6/\text{FNDELFF}$ ,  $\text{FC}=\text{FNDELFF}/4$ ,  $\text{FR}=3*\text{FNDELFF}/4$ , WTS) is called to supply the low-pass weights  $L_i$ ,  $i=1, 2, \dots, 1.6/\text{FNDELFF}+1$ . The in-phase Jth band weights,  $F_{1Ji}$ , are computed as  $F_{1Ji}=2*L_i*\cos(2\pi*\text{FNDELFF}*J)$  and the quadrature Jth band weights,  $F_{QJi}$ , are computed as  $F_{QJi}=2*L_i*\sin(2\pi*\text{FNDELFF}*J)$  where  $J=1, 2, \dots, 2*2*\text{FNMAX}/\text{FNDELFF}$ .

## D. EXTERNAL REFERENCES

## 1. Entry Point Names:

BPWTS

## 2. Called Subroutines:

OWTS

## E. USAGE

## 1. Calling Sequence:

CALL BPWTS (WTS, FNDELFF, NWTS, FNMAX)

## 2. Parameters, Arguments:

WTS = a vector for the weight storage. It should be dimensioned as  $\lfloor \sqrt{2}(\text{FNMAX}/\text{FNDELFF})+1 \rfloor * \lfloor 1.6/\text{FNDELFF}+1 \rfloor$  in the calling program.

FNDELFF = desired resolution, cycles per scan.

NWTS = Number of weights required per band. Value returned includes both sides and center of weight vector.

FNMAX = desired maximum frequency, cycles per scan.

### 3. Input/Output Data:

FNDELFF and FNMAX must be supplied by the user.

PPWTS returns WTS and NWTS.

### F. STORAGE REQUIREMENTS

#### 1. Space Required:

142 octal cells

### G. RESTRICTIONS & CODING INFORMATION

#### 1. Data Format:

For each band, only one side (plus the center) of the weight vector is computed.

WTS(1)-WTS(M) = low-pass filter weights (from OWTS),  
of width  $\approx$  FNDELFF/2

WTS(M+1)-WTS(2M) = in-phase band-pass weights for  
first band centered at FNDELFF.

WTS(2M+1)-WTS(3M) = quadrature band-pass weights for  
first band centered at FNDELFF.

WTS(3M+1)-WTS(4M) = in-phase band-pass weights for second  
band centered at 2\*FNDELFF.

... ..

WTS(2N\*M+1)-WTS((2N+1)\*M) = quadrature band pass weights  
for the Nth band centered at N\*FNDELFF,

where:

$M=1.6/\text{FNDELFF}+1$  and the number of bands  
N (not counting Frequency 0) is given  
by  $2*\text{FNMAX}/\text{FNDELFF}$ .

#### 2. Cautions to Users:

$\text{FNMAX}/\text{FNDELFF} \ll 1$  causes an exit with only the low-pass filter  
weights obtained from OWTS. Minimum frequency is assumed  
to be zero.



BRF Revision No. 3

## A. IDENTIFICATION

Program Code Name: BPF Revision No. 3  
 Classification: 2.1 S 012  
 Programmer: Dan Brown/Joyce Cootz BRI/DPL UCLA Health  
 Sciences Center  
 Machine: 7090/94  
 Language: IBCMAP  
 Date: September 30, 1964

## B. PURPOSE

To filter data sampled at equal time intervals given symmetric or antisymmetric weights.

## C. METHOD

Given the  $N$  data series  $\{Y_i(t_j)\}$ ;  $i=1, N$ , a frame at a time, filter products are updated in a set of rotating accumulators,  $\{A_{i,k}\}$ :

$$A_{i,k+s} \leftarrow \sum (W_{p+vs-N_w/2}) Y_i(t_j) + A_{i,k+s}$$

where:

$v$  = ratio of input to output sampling rate  
 $p$  = number of input points since the last output  
 $s = 0, 1, 2, \text{ etc.}, \text{ until } p+vs \leq N$

where:

$N_w$  = the number of filter weights (two-sided)

$k+s$  is computed modulo  $N_w/v+1$ . When  $p+vs = N_w$ , a filter output frame  $\{Z_i\}$  is stored:

$$Z_i(t_{j-N_w/2}) \leftarrow A_{i,p+vs}$$

$$A_{i,p+vs} \leftarrow 0$$

when  $p = v$ ,  $p$  is set to zero, and the accumulators are "backed up" by setting  $k \leftarrow k-1$ .

Only the future weights,  $W_0, W_1, \dots, W_{N_w/2}$ , are given in the routine.

The past weights are assumed:

$$\text{If } W_0 \neq 0; W_{-n} = W_n$$

$$\text{If } W_0 = 0; W_{-n} = -W_n$$

## E. USAGE

## 1. Entry Point Names:

Two entrances are provided:

## a. CALL SMFIL (NW, IV, IAC, NP)

where:  $NW = N_w =$  number of weights

$IV = v =$  input/output ratio

$IAC = 0 =$  initial accumulator index (set internally)

$NP = P =$  inputs since output (set internally)

This entrance sets up the routine for proper indexing and initializes IAC and NP.

## b. CALL MFIL (Y,Z,N,WTS,ACC,NP,IAC,IO,ISET)

where:  $Y = Y_i =$  input vector

$Z = Z_i =$  output vector

$N =$  number of channels in Y and Z

$WTS = W_0 =$  weight vector

$ACC = A_{0,0} =$  rotating accumulators (block of at least  $N*(N_w/v+1)$  cells)

$NP = P =$  (updated internally)

$IAC = Nk =$  index of accumulators (updated internally)

$IO = I =$  output point stored in Z

0 = no output

$ISET \neq 0 =$  skip setup part of entrance (address of all parameters unchanged)

If one weight vector is used, maximum speed is attained by use of the MFIL entrance with  $ISET \neq 0$  after the first entrance.

## F. STORAGE REQUIREMENTS

## 1. Space Required:

247 octal cells

## G. RESTRICTIONS &amp; CODING INFORMATION

1. The accumulator block should be set to zero before each case.
2. The routine assumes a 7094 (or 7090 with seven index registers) not in the multiple tag mode.
3. This routine does not work for  $IV < NW$ .

## H. TIMING

Average execution time per entry ( $ISET \neq 0$ ) in microseconds (7094):

$$T = 38 + \frac{13N+22}{v} + \frac{N_w}{v} \quad (19 + 36N)$$

Sample Processing of Normative Data (taken from Monthly Progress Report for January 8, 1964)

An example of specification of an actual analysis, together with a selection of the resulting output is included in this section.

It relates to the digital tape representing the B tape (additional EEG leads, and somatic channels) for Subject 207, and beginning with situation 54 (Explanation of the Three-tone task). This digital tape is one of eight for this subject, and is in use for program checkout; the tape used was one copied from the reel onto which the original digitization was made, onto a reel belonging to the Health Sciences Computing Facility, both in order to physically conserve our tape, and in order to make access more convenient for the HSC personnel.

We analysed several successive sections of situation 56 (three-one series); for illustration, we consider the first such analysis, which began with the subject's first button-pushing response, included the second, and stopped somewhat short of his third response. Later analyses continued from this point.

The load sheets specifying this entire analysis are pp. 51-53. Page 1 of these load sheets describes the tape and the computer set-up; page 2 describes the channels to be analysed, and page 3 defines the epoch for this case. Ordinarily, many analyses will be made with pages 1 & 2 constant, and the few parameters specifying the new epoch will be put on continuation pages like page 3. Some of the output resulting from this particular specification is also attached on pp. 54-57. The first output page has the tape and run description. The first line consists of a constant heading, and the page number. The second line is the descriptive title given for this tape on page 1 of the load sheets; the third is the descriptive title of the first case, given on page 3 of the load sheets. The run description reprints the information that one data tape is in use, mounted on the computer's tape unit 14; that the output results are saved for further processing on the tape on unit 15. The descriptions of the heights of code and stimulus pulses, taken from the first load sheet, by which the program will be positioning the data tape, are listed (these numbers were derived immediately after the digitization process,

as part of the validation of the digital tape, by plotting out, via the CDC 160A, sections of the code channel containing each kind of pulse).

The channel names given in this example are of no interest to the user, but merely numbers given for computer identification purposes, for this checkout run. For computations of greater physiological interest, more meaningful names would of course have been given on page 2 of the load sheets, and used for computer reference. For ease of understanding for the present, we note that C1 = C3-P3, C2 = C4-P4, C3 = P3-01, C4 = P4-02, C5 is a synthetic channel explained later, C6 = 01-02, C7 is another synthetic channel, and the rest of the channels are not used in this example, except channel 13, which is the code and stimulus pulse channel, and necessarily has the name EXCODE, in order for the program to treat it as the code channel. The last note on page 1 of the output informs us that the program has determined that the data tape has been recorded in low density (200 characters per inch), as are all tapes from the CDC 160A (until the installation this month of units which will record at 556 ch/in); when tapes are copied onto HSC reels, however, it is usually preferable to use high density (800 ch/in). In order to assure that jobs would not be delayed by an error in manual specification of tape density, a computer subroutine to determine the actual density, and properly set the reading unit, has been included; this is its note on the present data tape.

Page 2 of the output begins describing the case, with the channels to be analysed (taken from page 2 of the load sheets), and the frequency range and resolution requested. Then a note from the program informs us that a filter was constructed which will pass frequencies up to 25 cyc/sec unchanged, and gradually drops off to complete attenuation over the next 12.5 cyc/sec; on this basis, a reduced sampling rate is derived, in the present situation 76.92 samples/sec. This means that only one third as many samples will be analysed further, than if this low-pass filtering had not been done; but since the sample-rate reduction follows filtering, no aliasing is incurred.

Then the output mentions that the computer is searching for code 56, that the analysis will start after stimulus pulse 3, and continue to 5 seconds following stimulus pulse 6. Unfortunately the printout has not been updated so as to mention that it is actually searching for the response pulses following the named stimulus pulses, in accord with page 3 of the load sheets.

Now begins a series of printouts concerning the positioning of the tape, and the interpretation the program is making of the various pulses it is encountering on the code channel. These printouts will be suppressed in a production version, but give a sketch of the progress of positioning and computation. When five seconds' data following the second response pulse have been entered into the filters, computation stops, and the printout of the requested autospectra begins. Note that the time since beginning the case description is about 1.5 minutes of 7094 time, to initially position the data tape, make these 7 spectra and 21 cross-spectra, phase angles and coherences, for 25 different frequencies. About 1.25 minutes is required for the calculations.

The autospectral printout begins by telling of the number of degrees of freedom of each spectral estimate; this can be used to enter tables of chisquare, to approximate the variability of any particular value. Each column is headed by the name of the channel to which it applies, and the spectral intensity at each frequency for each of them is printed. Note that the frequencies given are integers, since we chose DELF to be 1 on page 3 of the load sheets. Any other frequency increment is equally possible, subject to the limitation to about 30 frequencies total. Thus if an analysis up to 60 cyc/sec were desired, the present program is limited to a minimum frequency increment of 2 cyc/sec.

Note that channels 1, 2, 3 and 4 have all a high intensity at zero cyc/sec (this really means, less than 0.5 cyc/sec), and all four have quite a narrow peak at 11 cyc/sec. These four leads are A-P (antero-posteriorly) oriented, in contrast to channel 6, which is laterally oriented between symmetric occipital placements. The peak in the bi-occipital spectrum is not at 11 cyc/sec at all, but almost exactly at 10. This is in spite of the fact that channel 6 shares an electrode with both C3 and C4!

LOAD SHEET  
NASA EEG SPECTRAL ANALYSIS PROGRAM, NEEG

INPUT TAPE PARAMETERS

To Keypuncher:

Keypunch into col. 1-72. Do not leave blank columns unless specified by (n)

To Preparer:

Cross out whole entry for parameters not needed

(H1)H12= HSC0TAPE03,0  
SUBJ0207B0C0PJED

Do not keypunch

Tape Description (72 characters maximum)

(SUDN0)= 207 B (~~REGRD~~) ~~\_\_\_\_\_~~ B

Subject Number(integer). Recording date: 6-digit number, 2 for month, 2 for day, 2 for year.

(NTAPES)= 1 B (NCHAN)= 13 B

Number of simultaneous input tapes(1 or 2)  
Number of Channels on Tape (must be the same if two tapes)

(FS)= 230.77

Input Sampling Rate Per Channel, in samples per second of the original Subject's time.

(left justify) (rel)  
(CHAN1) H1= C1 ♀ H1= C2 ♀  
H1= C3 ♀ H1= C4 ♀  
H1= C5 ♀ H1= C6 ♀  
H1= C7 ♀ H1= C8 ♀  
H1= C9 ♀ H1= C10 ♀  
H1= C11 ♀ H1= C12 ♀  
H1= EXC0DE ♀ H1= \_\_\_\_\_ ♀

Sequential List of Mnemonic Names of Channels on Tape 1 (first two in first line, etc.) Describe each by 6 or less characters.

The Experiment Code Channel must be named 'EXC0DE', if present. The Stimulus Pulse Channel must be named 'STIMUL', if it is separate.

~~(CHAN2) H1= \_\_\_\_\_ ♀ H1= \_\_\_\_\_ ♀  
H1= \_\_\_\_\_ ♀ H1= \_\_\_\_\_ ♀  
H1= \_\_\_\_\_ ♀ H1= \_\_\_\_\_ ♀  
H1= \_\_\_\_\_ ♀ H1= \_\_\_\_\_ ♀  
H1= \_\_\_\_\_ ♀ H1= \_\_\_\_\_ ♀  
H1= \_\_\_\_\_ ♀ H1= \_\_\_\_\_ ♀  
H1= \_\_\_\_\_ ♀ H1= \_\_\_\_\_ ♀~~

Names for second input tape, including EXC0DE and STIMUL, which must be on the same channels as on Tape 1.

(ZCODE)= -25 B (LTR)= 62 B

Pulse Descriptions

Position of baseline for and height of experiment code pulses(In digitizer counts)  
Same for stimulus pulses

(ZPUL)= 60 B (LPULSE)= 50 B

Date of 1st submission, alphanumerically expressed

(DATE) H5= 290DEC,01963 ♀

Logical Unit Number of first tape (ordinarily 15), and of the second tape (ordinarily 14, if used)

(LTAPE1)= 14 B (~~LTAPE2~~) ~~\_\_\_\_\_~~ B

(rel)



CASE PARAMETERS

keypunch into col. 1-72

ignore blanks unless specified by (n)

cross out parameters not needed

do not keypunch

(H2)H12 = SUBJECT 207B

Case Description  
(72 Characters, Max.)

(EXPNO) = 56 B (rel)

3 digit experiment or situation  
code number

(PSTART) = 3 B

Analysis Interval

Stimulus Pulse No. to start

(BRESP) = 20 B

After finding PSTART, go to  
first succeeding response of  
length BRESP (20,40, or 80)  
milliseconds. Ignored if zero.

(TSTART) = 0

After above positioning, Go  
TSTART seconds. (May be negative)

(PEND) = 6 B

Stimulus Pulse No. to end

(ERESP) = 20 B

After Finding PEND,  
Go to first succeeding response  
of length ERESP (20,40, or 80)  
milliseconds. \*

(TEND) = 5 (rel)

After above positioning,  
Go TEND Seconds (may not be neg.)

Frg. Analysis Parameters

(FMAX) = 25

Max. Freq. to be analyzed (c.p.s.)

(DELF) = 1

Freq. Resolution (c.p.s.)

(OUT) = 1 B

Outputs

Output option; 1 = binary tape,  
2 = listing, 4 = plot tape,  
8 = filtered data. Any sum  
allowed.

(LBTAPE) = 15 B

Logical tape for binary output

~~(LPTAPE) =            B~~

Logical tape for plot output

\$ \* END OF CASE (rel)

~~\$ \* END OF JOB (rel)~~

\*If BRESP = 140, response  
pulse of any length is used  
for start positioning.  
Similarly for ERESP = 140.



SAMPLE OUTPUT

NASA EEG SPECIAL ANALYSIS PROGRAM

PAGE 1

54

HSC TAPE 3, SUBJ 2076 COPIED

SUBJECT 2078

0 HCURS 3 MINUTES 24.9343 SECONDS. 29 DEC, 1963

RUN DESCRIPTION

1 INPUT TAPE(S) CN LOGICAL UNITS 14, 0

OUTPUT RESULTS

SAVED IN BINARY CN LOGICAL TAPE 15

BCC EXPERIMENT CCDE CN CHANNEL 13

WITH HEIGHT = 52 COUNTS AND

MAXIMUM LENGTH = 30 SAMPLES

STIMULUS PULSES CN CHANNEL 13

WITH HEIGHT = 50 COUNTS

SAMPLING RATE = 230.77 SAMPLES PER SECOND PER CHANNEL

INPUT TAPE LIST

TAPE1	TAPE2
1	C1 000000
2	C2 000000
3	C3 000000
4	C4 000000
5	C5 000000
6	C6 000000
7	C7 000000
8	C8 000000
9	C9 000000
10	C10 000000
11	C11 000000
12	C12 000000
13	EXCODE 000000

LOGICAL TAPE UNIT 14 HAS BEEN SET TO LOW DENSITY

NASA EEG SPECTRAL ANALYSIS PROGRAM

F-SC TAPE 3, SUBJ 207B COPIED

SUBJECT 207B

0 HOURS 3 MINUTES 25.4833 SECONDS, 29 DEC, 1963

CASE 1 DESCRIPTION

THE FOLLOWING CHANNELS ANALYZED

FROM 0 TC 25.00 C.P.S.

AT A RESOLUTION OF 1.00 C.P.S.

1 C1

2 C2

3 C3

4 C4

5 C5

6 C6

7 C7

INPUT DATA WERE PREFILTERED WITH

A LOW PASS FILTER (FC = 25.00, FR = 12.50 C.P.S.

AND THE SAMPLING RATE REDUCED TO 76.92 C.P.S.

TAPE(S) SEARCHED FOR SITUATION CODE 56

THIS CASE STARTS 0. SECONDS AFTER STIMULUS PULSE 3

ENDS 5.00 SECONDS AFTER STIMULUS PULSE 6

TAPE 14 IS 0. SEC. FROM CODE

LEGAL CODE FOUND. VALUE = 54 CNT= 335

ILLEGAL CODE, 0 227 0

LEGAL CODE FOUND. VALUE = 55 CNT= 1642

LEGAL CODE FOUND. VALUE = 56 CNT= 1570

ENTRY ACCUMULATOR

NO

XR1

XR2

XR3

XR4

XR5

XR6

XR7

NASA EEG SPEC' L ANALYSIS PROGRAM  
 HSC TAPE 3, SUBJ 2078 COPIED

SUBJECT 2078

0 HOURS 5 MINUTES 0.5167 SECONDS, 29 DEC, 1963  
 TCTAL TIME = 11.68 SECONDS

AUTC - SPECTRA WITH 12 DEGREES OF FREEDOM

FREQ	C1	C2	C3	C4	C5	C6	C7
0.	11.272	10.077	13.800	21.903	21.570	21.518	9.051
1.000	7.329	4.065	5.875	3.060	10.065	4.503	6.215
2.000	5.048	3.488	4.323	0.905	1.396	4.728	0.810
3.000	0.956	0.579	3.766	2.480	1.114	2.488	0.905
4.000	0.451	0.462	1.291	0.937	1.367	0.947	1.240
5.000	0.730	1.118	1.362	1.022	2.726	2.430	1.440
6.000	0.681	0.250	0.830	0.301	2.366	2.970	1.787
7.000	0.786	0.242	1.104	0.740	1.852	2.479	1.149
8.000	1.324	0.854	2.664	1.365	1.633	3.471	1.083
9.000	2.123	0.930	2.448	0.918	7.470	10.911	2.669
10.000	9.000	5.632	15.071	5.235	17.194	23.919	9.009
11.000	14.282	14.080	37.116	31.531	15.118	12.760	9.379
12.000	1.680	1.255	2.281	3.171	1.585	2.725	1.834
13.000	0.368	0.300	0.623	0.900	1.196	2.103	1.874
14.000	0.382	0.214	0.571	0.327	2.161	2.294	1.372
15.000	0.693	0.209	0.938	0.183	0.647	1.480	1.259
16.000	0.258	0.171	0.573	0.322	1.405	0.761	1.394
17.000	0.778	0.423	0.974	0.254	2.920	1.618	3.822
18.000	0.536	0.364	0.673	0.243	1.828	1.073	2.361
19.000	0.722	0.363	0.410	0.205	0.954	1.588	1.172
20.000	0.632	0.428	0.395	0.564	0.922	1.135	1.366
21.000	0.914	0.164	1.166	1.188	1.882	0.626	3.136
22.000	0.843	0.469	0.988	0.922	2.685	2.607	2.269
23.000	1.064	0.033	0.534	0.376	1.249	1.310	2.816
24.000	0.476	0.053	0.352	0.269	0.386	0.291	0.772
25.000	0.113	0.075	0.213	0.192	0.348	0.246	0.356
AVG.	3.54	-0.61	16.41	2.63	13.94	0.15	18.09
VAR.	55.52	43.39	119.71	64.93	115.83	130.32	87.70
SUMSP	63.54	46.36	100.34	79.51	104.04	112.98	70.54
B.W.	4.42	3.29	2.70	2.52	4.82	4.72	7.52
TAU/T	0.081	0.107	0.042	0.090	0.042	0.073	0.031
XMAXSQ	784.77	435.25	2416.10	882.69	2451.26	1547.73	2244.79

F-SC TAPE 3, SUBJ 2078 COPIED

SUBJECT 2078

0 HOURS 5 MINUTES 1.1833 SECONDS, 29 DEC, 1963

CROSS - SPECTRA WITH 12 DEGREES OF FREEDOM

FREQ	AMP	PHASE	CCH	AMP	PHASE	COH	AMP	PHASE	COH	AMP	PHASE	COH	AMP	PHASE	COH
1.00	2.561	0.6	0.220	3.526	27.9	0.289	2.069	-20.2	0.191	4.396	115.4	0.262	3.455	152.4	0.362
2.00	4.095	0.4	0.952	3.876	-8.3	0.688	1.413	-3.7	0.437	0.953	145.4	0.129	3.365	162.6	0.474
3.00	0.561	-14.3	0.568	1.661	-17.1	0.766	1.302	18.5	0.715	0.662	225.1	0.411	0.926	152.2	0.361
4.00	0.364	-49.3	0.637	0.506	-34.1	0.440	0.350	-9.7	0.290	0.501	-83.6	0.407	0.273	266.1	0.175
5.00	0.553	-29.1	0.375	0.564	-10.1	0.320	0.583	-17.3	0.456	0.239	266.9	0.029	0.313	268.0	0.055
6.00	0.215	32.2	0.270	0.559	7.7	0.554	0.209	23.0	0.213	0.434	104.0	0.117	0.633	137.5	0.193
7.00	0.234	4.7	0.289	0.806	-32.8	0.748	0.585	-18.4	0.589	0.663	172.8	0.302	0.849	156.8	0.370
8.00	0.766	3.3	0.519	1.524	-15.7	0.659	0.718	13.8	0.285	0.783	141.0	0.284	1.749	142.0	0.666
9.00	0.514	19.3	0.134	1.829	18.2	0.644	0.463	32.8	0.110	2.417	164.2	0.368	3.688	174.8	0.587
10.00	5.590	-7.5	0.616	10.314	21.4	0.784	5.276	56.1	0.590	1.034	133.9	0.007	7.498	169.6	0.261
11.00	12.834	-7.7	0.813	21.758	36.6	0.887	19.616	51.3	0.849	4.248	7.8	0.083	3.104	109.0	0.053
12.00	1.136	-4.5	0.612	1.555	28.7	0.631	1.729	38.8	0.561	0.892	118.6	0.299	1.205	111.6	0.317
13.00	0.030	-34.9	0.008	0.331	64.6	0.477	0.347	101.1	0.364	0.064	46.0	0.009	0.186	151.9	0.045
14.00	0.188	-77.9	0.430	0.159	46.8	0.116	0.207	262.7	0.343	0.507	173.2	0.311	0.690	202.3	0.543
15.00	0.102	-1.6	0.071	0.639	-19.6	0.627	0.192	16.4	0.289	0.439	261.2	0.430	0.513	198.9	0.256
16.00	0.021	-79.2	0.010	0.131	90.4	0.116	0.166	135.2	0.331	0.081	-14.1	0.018	0.051	222.3	0.013
17.00	0.334	-0.8	0.339	0.693	31.0	0.633	0.042	-36.0	0.009	0.764	62.2	0.257	0.357	124.7	0.101
18.00	0.238	-2.0	0.290	0.384	18.7	0.409	0.066	1.4	0.033	0.391	85.4	0.156	0.378	134.9	0.248
19.00	0.168	31.4	0.108	0.296	9.4	0.296	0.145	-88.9	0.142	0.340	190.6	0.168	0.674	202.3	0.396
20.00	0.139	230.9	0.072	0.368	8.5	0.544	0.193	-82.8	0.104	0.120	188.4	0.025	0.529	209.8	0.390
21.00	0.296	-31.3	0.583	0.716	14.9	0.626	0.516	25.7	0.245	0.553	-4.8	0.178	0.229	-8.1	0.092
22.00	0.304	-6.2	0.233	0.861	41.4	0.892	0.527	79.0	0.358	0.305	83.7	0.041	0.572	153.8	0.149
23.00	0.208	14.6	0.436	0.691	3.3	0.838	0.396	-9.6	0.391	0.656	20.2	0.324	0.339	21.0	0.082
24.00	0.121	43.2	0.583	0.202	53.4	0.243	0.065	56.2	0.033	0.084	-36.0	0.038	0.207	247.8	0.309
25.00	0.072	-37.7	0.582	0.120	13.0	0.600	0.072	-22.8	0.239	0.064	-36.0	0.103	0.092	-89.5	0.307

The additional lines below the spectral intensities are other parameters describing the same data. Those most interesting for physiological interpretation are B.W. (equivalent noise bandwidth) and  $\text{TAU}/T$  (characteristic duration). These parameters have been applied to EEG classification and analysis by D. Brown; (see Rhodes et al, 1965); their interpretation is described in a paper now in preparation. Briefly, the band-width is an index of regularity of the wave process, while the characteristic duration is related to "ringing" (in the sense of a filter's ringing) shown in that channel.

The next page of printout, and the last one included in this illustration, has the first 5 of the 21 cross-spectra and related functions. The names of the two channels being related head the columns, and we note for instance that the 11-cyc peaks in channels 1, 2, 3 and 4 are remarkably coherent, in that 88%, for instance, of the 11-cyc activity in C5 could be explained as a linear transformation of that in C1. This is a very high coherence, especially in view of the fact that sampling errors in estimated coherence are less for higher values, so that lower values are in general less accurately known than these high ones. But note that the coherence between C1 and C6 is extremely low, essentially zero. The same is shown, on pages not reproduced, for the relation with C2, 3 and 4, again in spite of the fact that C6 shares electrodes with C3 and C4. Interpreting these findings according to the classical models for generation of the EEG, this seems to be a strong indication of an 11-cyc generator, located in the midline, oriented A-P.

### MERGE

#### Retrieval of NEEG Output Data

Since many different methods of further processing may be applied to the auto- and cross-spectra calculated by NEEG, it is necessary that there be a method of selecting desired items from the mass of data written on magnetic tape by the program. MERGE serves this purpose.

NEEG writes the data which it calculates for each case in five separate blocks on tape, in addition to printing it. The first of these blocks, referred to as type one data, consists of

channel names used and a brief description of the case. Type two data is auto spectra. Type three data consists of certain summary data calculated from the auto spectra and from the input data itself. These data (AVG, VAR, SUMSP, BW, TAU/T, XMAXSQ, FBAR) appear below the auto spectra in the printout. Type four data is cross spectra (AMP, PHASE, COH). The last of these data blocks, called type eight data, consists of summary data calculated from the cross spectra (INTERPOWERS, FHAT, CBAR, FBAR). These data appear below the associated cross spectra in the print-out. If no cross spectral calculations are done in a given NEEG case, type four and type eight data are not written on tape for that case.

Each block of data is prefaced by a string of 21 numbers describing it and the case from which it was derived (see Note 1). This string is referred to as the ID vector of the data which it prefaces.

The program MERGE is designed to read selected data from one or more NEEG output tapes and to put them on a new tape for further use; its output tape is similar to its input, so that MERGE output may later become MERGE input, when desirable. It selects and orders data according to the values in one or more positions of the ID vectors of the data. Data requests to MERGE are organized into 'items', and output is sequential by item: all data specified by the first item is put out before any from the second, etc.

Parameters to the program specify input and output tapes, in which file or files of each input tape the desired data is located, and, for each of up to 100 items, the criteria (in terms of specified values of specified ID vectors positions) according to which a given block of data is to be included in or excluded from a given item.

Having read its parameters, MERGE proceeds in two phases, first selecting, then sorting the requested data.

In the selecting process, the specified files of the input tapes are read, and each block of data whose ID vector satisfies the requirements of any item is written, along with its ID vector, on a temporary storage tape. When all the desired data have been selected (or found to be not available in the specified tape files) the sorting phase begins.

In the sorting phase, the data requested in each item in order is selected from the temporary storage tape and written, with its ID vector, on the output tape. If ordering of the data within this item has been requested, it is done at this time.

A variation of MERGE operates as described above except that, rather than writing on tape each case requested for a given item, an "average case" (of auto- and cross-spectra only) is made of them; it is both printed and written on tape when all its components have been "averaged in" (see Note 2 for formulas used).

Built into both versions of the program is a facility for compensating spectral intensities for attenuation introduced by analog filters, if these were used in the digitization process of the raw data. Application or non-application of this compensation is under control of a parameter in each item.

#### NOTE 1: The ID Vector

Except where noted, these numbers are parameters to NEEG. See Note 1 of the NEEG write-up for an explanation of their significance.

<u>Position</u>	<u>Contents</u>
1	Data type (see text of this memo)
2	Page number of cross spectra (in general, there is a great deal more cross spectra data than any other type so it is broken down into smaller blocks, one for each printed page of it).
3	SUBNO
4	NREC
5	number of degrees of freedom for this case
6	case number
7	FS
8	NCHAN
9	NCROSS
10	EXPNO
11	PSTART
12	BRESP
13	TSTART
14	PEND
15	ERESP
16	TEND

Note 1 (continued)Position

17	FMAX
18	DELF
19	OUT
20	Used for cross data only, this contains the number of crosses in the following data block.
21	This contains the number of frequencies covered in the associated spectral data.

NOTE 2: Formulas Used in Average Merge

$$\bar{S} = (S_1 \cdot S_2 \cdot \dots \cdot S_n)^{1/n},$$

where  $\bar{S}$  is the average auto spectral intensity for a given channel and frequency and each  $S_i$  is the corresponding auto spectral intensity for the  $i$ th case in the item.

$$\bar{X} = \frac{1}{n} \sum_{i=1}^n X_i,$$

where  $X$  is cross spectral intensity

$$\bar{\theta} = \tan^{-1} \left[ \frac{\sum_{i=1}^n X_i \sin \theta_i}{\sum_{i=1}^n X_i \cos \theta_i} \right], \quad \text{where } \theta \text{ is phase angle}$$

$$\bar{C} = \frac{\left( \sum_{i=1}^n X_i \sin \theta_i \right)^2 + \left( \sum_{i=1}^n X_i \cos \theta_i \right)^2}{\left( \sum_{i=1}^n S_{ai} \right) \left( \sum_{i=1}^n S_{bi} \right)},$$

where  $\bar{C}$  is 'average' coherence,  $S_a$  is auto spectra from one channel making up the cross and  $S_b$  is auto spectra from the other.



### III. RESULTS: MAKING EEG'S

#### Contours of Intensity and Coherence

The time history of activity in a given channel, as an average over the fifty subjects, can be read for each group of situations from contour maps of intensity like Fig. LFP-LF (see Appendix III). Here, not only are all fifty subjects' spectra averaged together, but the spectra for similar situations (all eyes-closed rest periods, all eyes-open rest, etc.) are averaged together, so as to give only twelve archetypal situations. They are called "25" (which is the heading under which the cross-subject averages for all eyes-closed rest situations are plotted), "53" (all eyes-open rest), "11" (all eyes-closed flashes) and so on for the periods of simple stimulation; then, "69" (the first ten periods of visual discrimination with a 3-sec exposure), "79" (the second ten periods of 3-sec discrimination), "119" (all 1-sec exposures), and "56" (the eyes-closed vigilance task). Situations "69" and "79" were separated since in this grouping, the twelve summarized situations came fairly close to having the same total number of seconds (approximately 100), thus the same variability due to sampling error.

Beginning with Fig. LTP-L0 as an illustration, we note that on the average it peaks in the 10  $\phi$  band as well as in the lowest frequencies, and that it has a stable valley at 6  $\phi$ , as well as a less stable one in higher frequencies. Remembering that we must discount most of the 20  $\phi$  activity as due to aliased (3rd harmonic) hum, there is still a relative low at 17  $\phi$  in "38" (eyes-open taps), then a sizeable (relatively) rise in "69" through "119", with a drop (but not to earlier levels) in the 17  $\phi$  band in "56". The variations for LTP-L0 show that 1-3  $\phi$  are particularly low in "25" and "16" (both these times, 14-16  $\phi$  are also low), particularly high in "69"-79"; 4-7  $\phi$  are low in "53" and 6-7  $\phi$  have an isolated (relative) high in "38". 7-10  $\phi$  has a low in "69-119", and a high in "56".

Consider now the symmetric placement, RO-RTP. Its average is very similar in its major features to those of LTP-LO, except for being of slightly lower level generally. The variations of RO-RTP are even more similar to those of its symmetric partner, partly because the difference in level is thereby compensated for. The concordant variations emphasize some previously dubious features: a high at 4-6  $\phi$  in "11", another around 6  $\phi$  in "38". The great similarity between the averages in these two symmetric placements is encouraging; let us see how much activity is coherent between them, so that some of the concordances could be attributed to the same generator. Examining the Figure LTP-LO/RO-RTP, we must note that the contours have been drawn for levels of coherence (0.16 and 0.27) which would be independently significant (approximately at the "5%" and "1%" levels) even for a single subject, in view of the averaging over cases which we have done; and so are much more than that for this average of 50 subjects. Thus the contours have been drawn so that strong coherences are emphasized; but coherences of values less than 0.16 (in this cross-subject average plot) may still be dependably different from 0.

Thus there is a band from 9-11  $\phi$  where coherences between these channels are above 0.27 in all situations except "69-119", where they are between 0.16 and 0.27. At 1-5  $\phi$  in "11", the coherence is also above 0.16, which persists at 2  $\phi$  through "16-18", and comes again at 1-3  $\phi$  in "36" and 5-7  $\phi$  in "38". These are the only time-frequency loci where the coherences between these two space loci rise above 0.16, but other features are shown in the variations part of Fig. LTP-LO/RO-RTP. For instance, all frequencies except 8-10  $\phi$  and 20  $\phi$  have a notably high coherence in "11", which is carried over at high frequencies into "16-18". Also, the coherence at 6  $\phi$  in "38" is particularly high among 6  $\phi$  coherences, so the peak at this frequency-time locus in the two contributing autospectra is no doubt due to the same generator. Coherences are particularly low at middle frequencies in "69-119"; also at 2-7  $\phi$  in both "119" and "56", two situations otherwise so dissimilar.

Let us compare these channels' reactions with those of two anatomically adjacent channels, which were recorded on the other ("B") data tape, LP-LO and RP-RO. LP-LO has an average spectrum very much like that of LTP-LO, except for being at a higher level throughout; but the peak activity is still at 10  $\phi$ , with a valley at 6  $\phi$ ; the drop-off in intensity toward higher frequencies does not go below 100  $\mu\text{V}^2$  (c/sec), but the proportion of activity in this band is essentially the same as in LTP-LO. The ridge at 6  $\phi$  in "36" is distinct from the (variationally noted) peaks at 6  $\phi$  in LTP-LO and RO-RTP, which are in "38". Therefore, we have two different eyes-open stimulation situations in which there is a rise in the 6  $\phi$  activity in P-O channel activity: one in the lateral pair during "38" (eyes-open taps), the other in the medial pair during "36" (eyes-open flashes). We saw that the peak in the lateral pair was coherent; but reference to Fig. LP-LO/RP-RO indicates that the medial peaks are coherent more than 0.26 for all frequencies below 10  $\phi$ , except for a few situations. In fact, although there is not a peak of intensity at 6  $\phi$  in "38" for LP-LO or for RP-RO, there is a peak of coherence between them then.

Reserving the coherence LP-LO/RP-RO for later study, note that except for the difference at 6  $\phi$  just discussed, the variations of LP-LO and RP-RO are quite similar to those of their lateral neighbors, below 12  $\phi$ . In fact, the similarity does not end there, for the medial ones have all the highs and lows of variation that the lateral channels have, but the medial ones have additional highs (particularly) and lows (a few). One of the additional highs shown by both medial channels is the upward extension of one previously noted in "11", which in these medial channels extends not only over 11-13  $\phi$ , but also 16-21  $\phi$  in both (beginning a little lower in RP-RO). Since the whole frequency range from 11-19 and 21-25  $\phi$  was unusually coherent between the lateral channels in "11", the higher extension of high intensity in the medial channels may not indicate a new generator, but merely the fuller expression of one noted before.

In view of the complexity of interpretation of relationships among many neighboring channels, it is better for many purposes to use a different presentation of the variation data, such as

is included in the next section. It is still of value to examine other channels' history, as presented in these diagrams. For example, LO-RO shows an average spectrum quite similar to that of LP-LO, not only in the peak at 10  $\phi$  but also in the valley at 6 $\phi$ ; but, LO-RO is higher in intensity than LP-LO, so that again, its variations are more helpful in comparing the two leads' responses. Like LP-LO, LO-RO shows a relative high at 11-19 and 21-24  $\phi$  in "11"; but, as we have noted in the paper first reporting results from this study (see Walter, et al. 1966) coherences LP-LO/LO-RO are very low, there is no coherence as high as 0.16 in the figure giving average coherences between the two leads; indeed the average coherence across all subjects and all situations is less than 0.05 at all frequencies. Thus, in "11", also, we seem to have another example of LO-RO's becoming active at the same time, and in the same frequency bands in which LP-LO and RP-RO do (and in which those two are coherent), without LO-RO's becoming coherent with them. Another feature which LO-RO's variations share with the other leads mentioned is a valley at middle frequencies in "69-119", although it is considerably wider in band in LO-RO than elsewhere, extending from 4  $\phi$  to as high as 12  $\phi$ . In "56", LO-RO is more than one standard deviation above its own mean in all frequencies (except 0-1  $\phi$ )! In none of these variations, of course, is there any sizeable coherence with LP-LO. Another feature that LO-RO shows, which is not notable in other leads, is a high at 4-6  $\phi$  in "18" (eyes-closed clicks).

A particularly instructive example is provided by LC-CZ and CZ-RC. They are adjacent and share an electrode and should be over homologous areas of sensori-motor cortex. Their intensity maps (see Figs. LC-CZ and CZ-RC) both show a large amount of low-frequency activity, with a secondary peak at 10  $\phi$ , and a not very sharp valley, bottoming as much at 7  $\phi$  as at 6  $\phi$ . Their 10  $\phi$  peaks are much weaker than those of the typical "alpha" producers like LP-LO; both central channels have noticeable 20  $\phi$  peaks, possibly due mostly to aliasing. There is again a difference of level, which the variations compensate for: their variation maps are quite similar, with parallel highs in "18" at 6  $\phi$  (with LC-CZ showing a non-paralleled growth to cover 6-8  $\phi$  in "34" -- eyes-open clicks versus "18's" eyes-closed clicks -- while CZ-RC shows

no high in this range in "34"); in "38" at 6-8  $\phi$ ; in "69" at 1-4  $\phi$  becoming 1-5  $\phi$  in "79"; at 11-12  $\phi$  in "34-35", becoming 13-17  $\phi$  in "38", dropping out in "69", returning in "79", along with 19 and 24-25  $\phi$ ; finally, parallel highs at 9-10  $\phi$  in "56". The lows in the two channels show a parallelism just as strong. Thus a remarkable parallelism is clear between these neighboring structures.

The coherence map (Fig. LC-CZ/CZ-RC), by contrast, is extremely sparse, and has no values as high as 0.16 before "38", and none ever below 13  $\phi$ . This means that virtually all the activity in these two channels, with their impressively parallel variations of strength, is incoherently caused, that is, cannot be due to linear propagation of waves arising from the same generator. By contrast, and to scotch the impression that this might arise from instrumental or computational error or peculiarity, the channels LT-LC and RC-RT, channels further apart than the pair just mentioned, but sharing an electrode with each of them, have coherences above 0.26 at 1-10  $\phi$ , much of the time when the subjects' eyes are closed (although, incidentally, neither of these channels has a high in that band during such times).

Such contrasts, between pairs of leads showing similar reactions, coherently caused, and similar reactions incoherently connected, are one of the major contributions of cross-spectral calculations to EEG analysis.

#### The Variations: Basic Heads

While it might be thought that displays of averages would be the most graphic way to present our multidimensional results, it seems in fact that the average spectra differ remarkably little between leads (see Fig. WV-Average). Furthermore, the difference between the intensity in lower versus higher frequency bands is much greater than the difference between leads at the same frequency.

Therefore, a display which equalizes means will help us to grasp the picture over the whole head and over the whole frequency range. In addition, however, when the mean is small, the range of possible variability is correspondingly small, since spectral intensities are inherently non-negative (see Fig. WV-Standard Deviation). A presentation which compensates for this aspect of the data, as well as the different strengths, is one which we call variations of spectra, explained in an earlier section. An additional transformation of the average data, which is of some interest in comparing frequencies and locations, is the coefficient of variation (Fig. WV-Coefficient). This is derived, for each frequency and location, by dividing the mean into the standard deviation. While there are many different standard deviations which might be used, we used the deviations of each frequency as between situations: that is, for the average subject, how much did 1- $\phi$  activity change between eyes-open rest, eyes-closed rest, flashes, clicks, etc?

When this deviation is divided by the corresponding mean (that is, by the average over all situations), we see in the Figure (WV-Coefficient) that the relative variability of the lower frequencies is distinctly above that for others from 5-25  $\phi$ . Thus, in addition to being much stronger (Fig. WV-Average), these frequencies are more variable, even when the variability is rescaled by being divided by their larger averages. It seems that these very low frequencies have been unduly ignored in conventional electroencephalography; later, we will see that the same conclusion arises from some exploratory work in discriminant analysis.

#### Topographic Plots of Variations of 50 Subjects' EEG Intensities

A form of summary which allows comparison between the changes in each frequency band is called "Variations of Spectra". This presentation is based on the set of spectra for the whole range of situations, keeping the channels separate. Thus, there is a value of "variation" for each channel, frequency, and situation. A value of variation is derived by first taking the average over situations (for each channel and frequency), as well as the corresponding standard deviation. Then each spectral value which

contributed to an average is reduced by that average, and the result divided by that standard deviation (this is the transformation to 'standard scores'). Thus each value of variation represents the amount by which intensity in that frequency and channel differs in this situation from the mean across situations, in units of its own standard deviation. It is a mathematical consequence of the definition of variations that the mean of the squares of the variations in any one frequency in any one channel (i.e. of the variations appearing in the corresponding location in each "head") is 1.00. That is, the variability of each frequency in each location has been standardized (see SUMMARIZING TECHNIQUES).

While it would be theoretically possible for adjacent frequencies to behave quite independently, this seldom happens. This is partly due to the fact that different subjects' spectral maxima occur as different frequencies, so that the average graph is "smeared" somewhat more than a single subject's graph would be. However, we will see later in this section of the report that for most subjects, it is still unusual for a single frequency to behave quite independently of its neighbors.

Turning to Fig. WV-CODE 25, we see that in situation 25 all but five leads (frontals F'1-F3, F'2-F4, F3-T3, F4-T4, and the caudalmost O1-O2) have a very similar variation pattern, with all frequencies except 8, 9, 10  $\phi$  (and sometimes 7  $\phi$ ) having negative variations, generally of about 1  $\sigma$ ; and that the variations for 8, 9, 10  $\phi$  are positive by about 0.5  $\sigma$ . This general picture is slightly varied in the P-0 leads, which have a positive variation (or much less negative) at 19  $\phi$ , which seems very likely to be the first overtone of the 9  $\phi$  peak; this is shared to some extent by C-P leads, which, however, are lower in other bands above 12  $\phi$ , reaching about -1.5  $\sigma$  from 12-25  $\phi$  (except 19  $\phi$ ) in C3-P3 and C4-P4. In this situation, the frontal leads are uniformly depressed by about 1  $\sigma$  at all frequencies; O1-O2 has an idiosyncratic pattern.

In the situation plotted next (Fig. WV-CODE 53, eyes-open rest), the picture is radically different with all intensities lower than their means, in accord with the classical description of low-voltage waves with eyes open. In the alpha band posteriorly, the depression is slight, whereas

in the transversal leads it is large. It is odd that C3-P3 & R are, except for the alpha bands, more active than in eyes-closed rest (#25).

Figure WV-CODE 56, eyes-closed button-pressing to tones, shows a great exaggeration and spatial spread of the alpha bands centered at 9  $\mu$ , wider the further posterior, together with exaggeration of the possible harmonic peaking at 19  $\mu$ . O1-O2 is quite different from other leads in this code, being very positive in variation at all frequencies.

The next three situations are all eyes-closed stimulation: flashes (Fig. WV\_CODE 11), taps (Fig. WV\_CODE 16) and clicks (Fig. WV\_CODE 18); they are paralleled by the following three situations of eyes-open stimulation, but in a different order: clicks (Fig. WV\_CODE 34), flashes (Fig. WV\_CODE 36), and taps (Fig. WV\_CODE 38). Thus #11 is paired with #36; #16 with #38; and #18 with #34.

All three eyes-closed stimulation situations show a degree of similarity with eyes-closed rest, #25. The eyes-closed flashes of #11 produce a considerable difference from #25, most obviously in all occipital channels, which are above average in all except the very highest and lowest frequencies; they are especially high at 10, 11 and 12  $\mu$  which is higher in frequency than their resting peaks, which were at 9. A curious finding is the great similarity of variations for T5-T7 and T6-T8, together with their relative peak at 11  $\mu$  and absolute average value at 12  $\mu$ , in contrast to more medial or posterior leads which have their greatest relative positivity at 12  $\mu$ .

Under eyes-closed taps (#16), the posterior leads return to being extremely similar to their rest patterns. The major differentiation introduced by the taps is quite narrow band increase in all transversal leads, which reaches about +10 at 9 or 10  $\mu$ ; the vertex is also less negative than in rest, at all frequencies from 9  $\mu$  up.



Eyes-closed clicks (#18) leads to a different pattern with the 10-11  $\phi$  range reduced in all leads except CZ-FZ, and the range 5-9  $\phi$  raised in most central and posterior leads, 6 or 7  $\phi$  having a relative peak in several leads.

The three succeeding situations of eyes-open stimulation are very similar in their pattern, and different from the fluctuating eyes-open rest pattern. In these three situations, most leads are quite close to their means in all frequencies, which is not a meaningless neutral finding, but rather a definitely unlikely event, requiring as much explanation as do the variations from the means observed in other situations.

To discuss the eyes-open stimulations in the same modality order as the eyes-closed ones, we consider #36, the eyes-open flashes. In contrast to the other eyes-open stimulations, #36 shows very high vertex from 12  $\phi$  up, and relative peaks around 5-7 and 12-13  $\phi$  in C3-CZ and CZ-C4, as well as peaks in C3-P3-01 and C4-P4-02 in all frequencies except 8-11 and 18-20  $\phi$ . In one of the few instances of trustworthy asymmetry seen in these maps, C3-P3-01 are further above their means in most frequencies than are their right-side counterparts.

Situation #38 (eyes-open taps) is like #36 (flashes) in having high positive vertex variations at 14  $\phi$  and above, but differs from it by having considerable negative variations at 8, 10, 11 and 13  $\phi$ . C3-CZ and CZ-C4 are positive, especially 5-9 and 13-17  $\phi$  (here the right side is perhaps significantly more peaked than the left). C3-P3-01 and C4-P4-02 are lower than in situation #36, and have negative variations in mid-frequencies, particularly at 11-12  $\phi$ . O1-02 has a pattern contrasting with what it shows in #36. #34, eyes-open clicks, has most leads very close to their means in all frequencies; the major exceptions are C3-CZ-C4, and to a smaller extent T5-C3, C4-T6, and O1-02. C3-CZ has positive variations at 3-25  $\phi$ , as does CZ-C4 to a lesser extent. T5-C3 and C4-T6 have small peaks around 8  $\phi$  and O1-02 is generally below means, except 7-12  $\phi$ .

Codes #69, #79 and #119 (see Figs. WV-CODE 69, WV-CODE 79, and WV-CODE 119 respectively) are again a similar group, and are best characterized as showing the exact opposite to situation #25. Code #79 is the most extreme of the three, with both frontal leads having almost uniformly  $+3\sigma$  variations at all frequencies. Some of this is no doubt due to muscle artifact, but certainly muscle artifact cannot have produced the great gouges centered at 9  $\phi$  in all the other leads. In conformity with the statement that this represents the direct opposite to the eyes-closed rest situations, there is another valley at 19 and 20  $\phi$  in those leads which had a peak there in situation #25. The variations for code #69 are very similar indeed to those of #79, with almost uniform subtraction of  $1\sigma$  from all values. Code #119 is very much like #69 in all the leads around the edges of the montage, but somewhat different in C3-CZ-C4, FZ-CZ, C3-P3-01 and C4-P4-02. These differences consist of a wider-band negativity 5-13  $\phi$  and a lesser one (but still greater than in #69) in 16-20  $\phi$ .

#### Coherence Heads

With such remarkable similarity shown between symmetric placements, when each frequency is shown against its own mean strength and in terms of its own variability of strength, and with such other clear progressions of pattern as have been described above, it is natural to wonder whether those equally improbable peaks (and perhaps valleys) can be understood by the distribution of the same wave processes to the various sites showing unexpected parallelisms. In other words, are the similar peaks of variation shown by left and right temporo-parietal in situation #25 due to a shared cause, linearly propagating between the hemispheres? Coherences provide the answer, and so we have prepared a parallel series of head diagrams expressing the average coherences in each situation.

Unfortunately, there are some difficulties in doing this. For one thing, there are many more possible pairings than there are single leads, and so there are many more coherences that may be displayed. We have selected for display only those pairings that were expected to have more than a redundant interest: symmetric pairs and adjacent pairs, either longitudinally or laterally.

These three sets are displayed separately, in order to fit them into a reasonable size. The other difficulty is that there are two equally defensible ways of averaging coherences together to give an over-all impression. One averaging method (Method "A") ignores the phase angles, as they may differ from subject to subject or from situation to situation, and merely asks, "How great were the coherences between these two leads?" The other averaging method (Method "B") incorporates the differences of phase angles, and in effect asks, "How coherent are these two leads, if we assume them to arise from the same process in all cases?"

The "B" form is the more appropriate when we are interested in analyzing the symmetries of the averaged variations, for instance; "A" is more appropriate when we wish to compare the coherences shown by a single individual with those shown by a group. Thus both kinds of average coherence diagrams have been produced; method "B" is appropriate to this volume, concerning summaries; method "A" to the second volume, relating single subjects to groups.

A further step of averaging can be taken, of course, on either of the above -- namely, averaging across situations to get the mean coherence (either "A" or "B" sense) independent of situation. They will be described first.

Two notational conventions will shorten the references to leads and pairs of leads in what follows. The coherence between a channel and its (right-sided) symmetric channel will be denoted by '/R'; for example, F'1-F7/F'2-F8 will be abbreviated F'1-F7/R. Somewhat analogously, if a description applies to a certain one-sided pairing of channels, and to the symmetric (one-sided) pairing on the right, we will abbreviate this '& R'; for example, T3-T5/T3-C3 and T4-T6/T4-C4 will be abbreviated T3-T5/T3-C3 & R.

#### Cross-Situation Average Coherences (Method "B")

We begin by considering Fig. WC-1-Average, which shows several L/R average coherences.

Between left and right frontal leads (i.e. F'1-F7/R), coherence is about 0.2 from 2-10  $\phi$ , sharply lower elsewhere; F7-T3/R is equally coherent @ 2-4  $\phi$ , and again, though less, 8-10  $\phi$ . The

peak @ 8-10  $\phi$  becomes successively more marked, and the 2  $\phi$  one less so, as we move to T3-T5/R and T5-01/R where the 10  $\phi$  peak reaches an average coherence of 0.6. The nearer pairs C3-P3/R and P3-01/R are more coherent throughout than those mentioned above, especially @ 2-10  $\phi$  (with a small peak at 20  $\phi$ ).

The second average-coherence head (Fig. WC-2-Average) is concerned mostly with the relations between temporal and parietal leads. There is another broad symmetry shown in the coherence functions relating symmetric pairs of pairings. For instance, the coherence graph relating T3-C3 with C3-CZ is very like that relating CZ-C4 with C4-T4, being about 0.2 @ 1-4  $\phi$ , gradually less 5-10  $\phi$ , and finally essentially zero, 10-25  $\phi$ . Similarly, T3-T5/T3-C3 is very parallel to T6-T4/C4-T4, though the left-hand pair does seem uniformly slightly higher in coherence.

Easier of interpretation, though somewhat surprising, are the uniformly low coherences plotted as relating C3-CZ and CZ-C4, only a small peak at 20  $\phi$  rising slightly above the general incoherence. The fact that coherences at 1-10  $\phi$  are considerably higher between the distant pair T3-C3/R than between the closer pair remarked above requires explanation: are the hands better coordinated (neurally) than the feet?

The third head (Fig. WC-3-Average) attends principally to longitudinal pairings, and shows clear evidence of what one is tempted to call a "posterior longitudinal system" of relatively highly coherent (that is, presumably well distributed) wave activity in these pairs from 1-5  $\phi$  (with some local differences, to be sure) at 9 and 10  $\phi$ , and at 20  $\phi$ . In counterpoint to this there is the marked anti-coherence of F7-T3/T3-T5 and R in the band 3-7 C; perhaps this can be attributed to these pairs' spanning the lateral fissure separating the temporal pole (with its hippocampus) from the frontal lobe.

Also notable are the low coherence levels of P3-01/01-02 and P4-02/01-02; but in one of those fascinating asymmetries contrasting with a generally highly symmetric picture, the P4-02/01-02 is significantly higher than the P3-01/01-02 at all frequencies (though rather low in themselves).

Coherences in Differing Situations as Discriminanda

The general impression is of a great degree of stability between situations, with relatively few instances of great variation from the means previously described. From the point of view of cerebral organization, then, stability is more noticeable than variation. From the related point of view of discriminant analysis, however, it should be pointed out that what is plotted here is not variations of coherence, in the sense that variations of intensity were plotted. A numerically small change in intensity, if superimposed on a small cross-situation variability in that band, was plotted as a large variation, and could well be exploited for discrimination between situations; but a corresponding small change of coherence will be here plotted as small, and not magnified by variation plotting. Although this could be done (indeed variations of coherence were plotted as contour maps), we have spared the reader the particular transformation of that data into variation heads. One reason is the differing statistics of intensity and coherence samplings, which make a small calculated coherence less trustworthy than a larger one. Thus discriminant analysis may fasten on differences of coherences too small to be visually notable in these heads. In any case, those that we can perceive in these pictures are presumably available for discrimination, unless within-situation variability (not plotted here) is too great.

Code #25 differs from the mean in the left-right coherences (Fig. WC-1-CODE 25), by being higher @ 5-10  $\epsilon$  in F'1-F7/R and lower @ 2-5  $\epsilon$  in F7-T3/R; in the second set (Fig. WC-2-CODE 25), it is perhaps a little more coherent in T3-C3/R @ 5-10  $\epsilon$ , but otherwise the coherences in eyes-closed rest periods are quite similar to the average ones of this set; in the third set (Fig. WC-3-CODE 25), lower values @ 11-25  $\epsilon$  in F'1-F7/F7-T3 and R are notable.

Code #53 has above-average coherences outside the alpha bands in several pairings, particularly in Fig. WC-2-CODE 53. Unfortunately, the machine here encountered a tape-reading error which gave foolishly high stated values @ 18  $\epsilon$  in T3-C3/R and @ 1  $\epsilon$  in C3-C2/R (as well as @ 25  $\epsilon$  in Fig. WC-2-CODE 69). We will re-do some of the machine processing, in order to check the very interesting idea that coherences are high whereas intensities are low.

Code # 11 differs from the average as to coherences (see Fig. WC-1-CODE 11) by slightly higher values @ 1-5  $\phi$  in T5-01/R, @ 1-10  $\phi$  in T3-C3/R (Fig. WC-2-CODE 11), generally slightly higher values @ 12-25  $\phi$  in T3-T5/T3-C3 and R (in spite of R's considerably lower general coherences). # 11 is like #25 in being above average @ 8-12  $\phi$  in T3-T5/T5-01 & R (Fig. WC-3-CODE 11), and in being lower than average coherence @ 12-25  $\phi$  in F'1-F7/F7-T3 & R, but unlike it in lacking relatively high coherences @ 1-2  $\phi$  in C3-P3/CZ-FZ & R.

Code #16 (eyes-closed taps) differs in coherence from the mean almost identically with #11; the only difference in their coherences (see Fig. WC-3-CODE 16) seems to be @ 16-18  $\phi$  in F7-T3/T3-T5. Whether so small a band of frequencies can be expected to yield a reliable discrimination seems doubtful, although this might be thought to be part of the somatic evoked potential (even though the ankle, where the stimulus was applied, should be represented rather beneath C3-CZ). (The symmetric intensity variation peaks @ 9-11  $\phi$  in T3-T5 and T4-T6, which would serve to distinguish #11 from #16, are not mirrored in any contrast of L/R coherences between the two situations.)

Code # 18 (Fig. WC-1-CODE 18), on the other hand, can be seen immediately to differ from the average and from #11, at least posteriorly, coherences being distinctly lower (outside the range 8-12  $\phi$  in C3-P3/R, T5-01/R, and P3-01/R. In the second head (Fig. WC-2-CODE 18), the posterior leads are again slightly less coherent, especially @ 1-5  $\phi$ , and a similar variability affects the central/posterior pairings in the third head (Fig. WC-3-CODE 18). It is worth stating that at an earlier stage in the development of the data, when only 15 subjects were available for averaging, code #18 was very remarkable for having absolutely the lowest coherences (outside the band 8-12  $\phi$ ) of any situation, in quite a few different pairings. Apparently so unambiguous a result was a statistical fluctuation not true of all 50 subjects, but the trace of it still remains; many coherences are indisputably smaller than their means, during this situation of eyes-closed clicks.

Turning to the eyes-open stimulations, the eyes-open flashes (#36) are clearly different in coherence from the average, by having higher coherences @ 1-3  $\phi$  in symmetric pairings (Fig. WC-1-CODE 36); this may perhaps be due to the evoked response and its harmonics, although one does not ordinarily think of large temporal evoked responses. An exception to the increased coherences in low frequencies is T3-T5/R, and the temporal and parietal coherences of the second head (see Fig. WC-2-CODE 36) agree, in having coherences near their means. There may perhaps be physiological significance to the slight but consistent elevation @ 10-25  $\phi$  in T3-T5/T3-C3 & R - - could this be high-frequency transmission within the temporal lobe, provoked by flashing? Some support for this is offered (Fig. WC-3-CODE 36) by the higher coherences @ 7-10  $\phi$  in F7-T3/T3-T5 & R, and by a curious and quite asymmetric elevation @ 10-25  $\phi$  in T4-F8/F8-F'Z. There is some indication here of a wide-spread reorganization of cerebral transmission and processing, apparently brought on by the flashes.

Code #34, eyes-open clicks, differs very little from the means (which is to say it differs very little from the eyes-open rest coherences), with the exception (see Fig. WC-2-CODE 34) of slightly higher values @ 4-7  $\phi$  in C3-P3/C2-FZ & R. This is a little curious vis-a-vis the variations of intensity, which show quite average intensities in these bands in all three leads here mentioned, whereas in situation #36 (refer back to Fig. WV CODE 36), these frequencies have quite a nice positive variation in C3-P3 & R.

Code #38, eyes-closed taps, also differs very little from the average (and hence from #53 or #34), except for a small but physiologically encouraging elevation of coherences (see Fig. WC-2-CODE #38) @ 17-25  $\phi$  in the ordinarily quite incoherent C3-CZ/R. It seems unlikely that these frequencies are brought into coherence by sharing such high harmonics of the 1  $\phi$  stimulation.

Turning to the slide series, #69 shows small differences in L/R coherences, mainly a reduction @ 7-10  $\phi$  in all pairings in the first head (see Fig. WC-1-CODE 69); on the other hand, the temporal and parietal relations seem uniformly higher especially above 10  $\phi$ , in adjacent pairings (Fig. WC-2-CODE 69) (could this be shared muscle?); all pairs in the longitudinal head (Fig. WC-3-CODE 69) show either reduced 8-10  $\phi$  coherences, or increased values

above 10  $\phi$ , or both. In addition, C3-P3/CZ-FZ & R are quite above average @ 1-5  $\phi$ .

As with the intensities, #79's coherences (Fig. WC-3-CODE 79) represents an exaggeration of the tendencies expressed by #69. Unlike the intensity picture, #119 (Fig. WC-3-CODE 119) appears very similar to both #69 and #79.

There is a small elevation of coherence in #119 versus #79 at most frequencies in C3-P3/CZ-FZ & R (Figs. WC-3-CODE 79 and CODE 119); it would probably not be considered large enough to be noteworthy, were it not that in the discriminant analysis of four subjects (Walter, et al., 1966), the program found that coherence in the 0.5-3.5  $\phi$  range in P3-O1/CZ-FZ was a good discriminator between these two types of situations (these called EO-T-3 & EO-T-1). To qualify as a discriminator, a variable must not only differ between the two situation types on the average; it must also have a small enough standard deviation within the two types to make the difference worth attending to. Unfortunately, the utility of a parameter for discrimination depends not only on those parameters, but also on competition with other variables.

There also seems to be somewhat higher coherence in T4-F8/F8-F'Z (not such a difference in L) @ 11-20  $\phi$ ; this parameter was not included in the list offered as discriminanda in the four-subject study mentioned. Other discriminant studies, on 5 and 10 subjects, did include that parameter, but it was not as good a discriminator for this distinction as RT-RF/RC-RT coherence in the 0.5-3.5  $\phi$  band, or RF-RFP bandwidth in the 2.5-18.5  $\phi$  band.

#### SLEEP HEADS

##### Comparing Waking and Sleeping Averages

It must be remembered that the sleep averages are over 30 subjects of the 50 included in the awake averages, and that each sleep code (and all the sleep codes together) add up to many fewer seconds per subject than could be extracted from the awake records. In the spectra, this makes the estimates somewhat more variable, but not enough so to require much adjustment in our ways of viewing the graphs. In the coherences, however, it may be necessary to



discount the sleep coherences slightly, unless there are several adjacent frequencies in one channel, or several adjacent or symmetric channels showing a similar pattern at the same frequency.

Due to different scales which are most appropriate to these two pattern sets when they are presented separately, it is more convenient to have them plotted together, as in Fig. WS-Average (App. III). Here the scales are the same, and the comparison is immediate. The most general impression is the greater concentration of sleep spectra in the lower frequencies, and their relative lowness in the middle and especially the higher frequencies. In F'1-F7-T3 & R the awake averages are consistently higher than sleep averages, though the contrast is strongest above 15  $\epsilon$ ; the great predominance of the awake records in these leads may be due to their having the strongest muscular component, for most subjects. Of course the sleep averages have very little in the way of an alpha peak (and that little is probably due to the inclusion of one awake case in their average, in order to make the variation comparisons).

A different picture is shown in the standard deviations plotted in WS-Standard Deviation, where several channels (C3-CZ-C4 & CZ-FZ in particular) show a larger deviation in sleep than in waking, in all or many frequencies. It is particularly striking that in all but F'1-F7-T3 & R, the variability in the 9-10  $\epsilon$  alpha band is just about equal in the two states, though again a good part of this may be due to the admixture of a waking code. The coefficient of variation (Fig. WS-Coefficient of Variation) emphasizes the differences between the fronto-lateral group of channels (F'1-F7-T3 & R) and the postero-medial group (all the rest except T3-T5 & R, and T3-C3 & R, which are intermediate between these two groups). The fronto-lateral group has coefficients of variation lower in sleep, except in the alpha range, while the postero-medial group has higher coefficients of variation in sleep at almost all frequencies.

### Variations During Sleep

An attempt was made by Dr. Kellaway and his staff to select typical examples of various stages of sleep for each subject. The sleep was recorded after the subject had had the original set of electrodes removed; later that evening, they were placed again. In order to verify the new application, a recording was taken during eyes-closed rest (Fig. SV-CODE 124). Then he was allowed to sleep naturally, and portions representing drowsiness were selected and dubbed onto our tapes (SV-CODE 125); similarly with light sleep (Fig. SV-CODE 126), intermediate (Fig. SV-CODE 127), deep (Fig. SV-CODE 128), sub-arousal (Fig. SV-CODE 129), and finally waking the subject was recorded (Fig. SV-CODE 130).

The recordings taken under these conditions have been analysed separately from the subjects' waking records, to begin with. Thus an average spectrum, standard deviation between situations, and coefficient of variation for this set of situations has been calculated. Because of the wide range of average spectral intensities, they could only sensibly be represented on a logarithmic scale (Fig. SV-Average). In all leads there is an astonishing similarity of pattern, but one's astonishment is somewhat reduced by realizing that a displacement of 1/8 inch means a difference of a factor of 4! Thus the visually small peak at 10  $\phi$  in some posterior leads is really quite a large one in relative power, but all leads' averages are vastly dominated by their lowest frequencies. These average heads are really of value mainly as bases for the variations to follow.

For sleep variations, of course, the basis is sleep patterns, so that variations for code #124, awake eyes-closed rest (see Fig. SV-CODE 124) mainly represent the differences between sleeping and waking. The fact that the basis is different accounts for the great visual difference between this head, and that for eyes-closed rest on the basis of waking comparisons (see Fig. WV-CODE 25).

Thus, the above-average alpha-band activity posteriorly is much distributed forward, expressing the fact that what alpha there is, in F7-T3 & R, is much above sleep means. Equally notable is the great elevation @ 15-25  $\phi$  in all leads but CZ-FZ, most marked posteriorly.

In drowsiness (Fig. SV-CODE 125), this elevation is still notable, though less extreme, in the frontal leads, but only slightly above mean in all posterior leads; it is greatest now in CZ-FZ. The other frequencies are uniformly depressed below their means, except for residuals of alpha activity posteriorly (making those leads have variations less negative than in other frequencies, but nowhere reaching the mean strength of alpha).

In light sleep (Fig. SV-CODE 126), the frontal leads are subnormal @ 1-15  $\phi$ , but other leads begin to show supernormal @ 4-5  $\phi$ , and the transversal leads have peaks due to spindles, fairly sharply at 15  $\phi$  T3-C3 & R, but @ 14-17, C3-GZ & R. Except for spindles, 15-25  $\phi$  is close to mean.

In intermediate sleep (Fig. SV-CODE 127), there are relative peaks @ 11-15  $\phi$ , especially frontally, becoming narrower and less far out on the variation scale posteriorly. Correspondingly, 3-7  $\phi$  is somewhat above its means, posteriorly and in the vertex, while 16-25  $\phi$  is depressed in all leads.

In deep sleep (Fig. SV-CODE 128), 1-6  $\phi$  is uniformly elevated in all leads which, in view of the extreme dominance of these frequencies in the average spectra, means a strong dominance for them at this time. 15-25  $\phi$  is quite depressed in most leads. But all B-tape leads have very bizarre and unhappy variations in this code @ 6-25  $\phi$ , whose explanation has not yet been found.

The sub-arousal (Fig. SV-CODE 129, putative stage IV sleep) has quite high: 1-7  $\phi$  in all leads, with 8-12  $\phi$  high in front, mean in the middle, and low in back; 15-25  $\phi$  is low everywhere.

Awakening has peaks @ 7-8  $\phi$  everywhere, and @ 12-15  $\phi$  laterally, with a general elevation of frontal leads at all frequencies.

In general we may say that leads vary in larger groups in sleep than in waking ("posterior", "lateral", etc. in sleep, versus mainly some lead & R when awake). This broader covariance accords with the general impression that sleep EEGs are more similar from different parts of the head, than from the same parts during waking.

### Average Coherences During Sleep

Coherences express strength of relationship between brain areas. If they differ substantially between waking and sleeping, this should be interpreted as representing a different organization of transmission within the brain, presumably by the utilization of pathways previously inactive, and the neglect of previously active ones. However, the term "pathways" is a little too restrictive for inter-cortical transmission; "invasion and infiltration trails" would correspond more suggestively to the kind of propagation often apparently observed in cortical inter-area relations.

The inter-area relations expressed on the average during sleep are distinctly in contrast to those seen during waking; the fact that our sleep averages are over a shorter period of time, and over 30 subjects out of the 50 used for waking averages need not bother us, for the number of degrees of freedom even in the smaller sample are quite adequate to keep the known bias of coherence estimates at a negligible level, and to make the sampling variability acceptably small.

Coherences from left to right are generally higher during sleep than during waking; this corresponds with a general impression that brain waves are more similar from side to side during sleep than otherwise, although this impression seems to be one which has not been widely published in the general sleep literature (Brazier, 1963 says so in the cat). This general higher coherence can be attributed to a higher "permeability" of the cortex to infiltration, but it is questionable whether this is more than a semantic transformation. At any rate, the coherences do definitely indicate a different and more permissive organization of the interhemispheric transmission during sleep, as will be clear from the sequel.

The average coherences for the sleep codes can also be described by contrast with those for code #124, eyes-closed rest, with which we are somewhat familiar from the waking series. The L/R coherences (Fig. SC-1-Average) are higher @ 1-5  $\phi$  in the sleep average than in its awake component, and correspondingly

less peaked in the alpha bands. In the temporal and parietal coherences (Fig. SC-2-Average), sleep shows, in its average, none of that rise in T6-T4/C4-T4 and T4-F8/C4-T4 above 15  $\phi$  that is shown in # 124. Longitudinal coherences (Fig. SC-3-Average) are merely lower in the alpha bands than is # 124.

Drowsy coherences (Fig. SC-1-CODE 125) are still very like #124. In light sleep (Fig. SC-1-CODE 126), coherences in the alpha band are low, and coherences are above sleep norms at 2-3  $\phi$  anteriorly, 1-7  $\phi$  posteriorly in L/R relations.

In F1-F7/R, the average coherence @ 1-15  $\phi$  is raised to 0.3 in sleep, versus essentially 0. @ 1, 0.15 @ 2-10, and 0.1 or less @ 10-15  $\phi$ . In other words, about 30% of the activity in either of those leads could be thought of as transmitted from the other (or to both, from elsewhere), in the entire band from 1 through 15  $\phi$ , during sleep, whereas this percentage is never above 15% during wakefulness. In F7-T3/R, the contrast is present but less marked; here the sleep coherences are higher chiefly @ 4-10  $\phi$  and only reach 0.25. In T3-T5/R, a more interesting contrast obtains, in that the coherences are about 0.2 higher than the waking ones, at all frequencies except the alpha range of 9-10  $\phi$ , where they are equal. And a similar description applies to the differences for C3-P3/R, although the levels of coherence for that pair are generally considerably higher than for T3-T5/R. For T5-O1/R, it is mainly in the band 3-8  $\phi$  that sleep is more coherent than waking, whereas for P3-O1/R, the coherences are considerably higher during sleep for all frequencies except 9-10  $\phi$ , and also 20  $\phi$ , perhaps again representing a harmonic of the alpha wave.

The contrast for T3-C3/R is like that for F1-F7/R, in that coherences are stronger @ 1-15  $\phi$ , but the other parietal and temporal coherences are lower in sleep at almost all frequencies, suggesting that the organization of transmission in sleep lacks the moderate relationships among "rolandic" areas which is present when awake.

The longitudinal transmission represented on the third head is lower @ 12-25  $\phi$  in F'1-F7/F7-T3 and R, but higher @ 2-15  $\phi$  (except alpha bands) in F7-T3/T3-T5 & R, and T3-T5/T5-01 & R. Transversal coherences shown in Fig. SC-2-CODE 126 (T3-C3/C3-CZ & R, and the usually incoherent C3-CZ/R) are supernormal @ 2-5  $\phi$ ; that is, slow waves are well shared 'over the top'. A-P transmission, as represented by coherences in the third head for #126 (Fig. SC-3-CODE 126) are close to norms, with a slight elevation @ 1-7  $\phi$  in C3-P3/P3-01 & R.

In #127 (intermediate sleep), coherences (Fig. SC-1-CODE 127) are high @ 1-5 & 10-15  $\phi$  in F'1-F7/R and @ 3-7  $\phi$  in T5-01/R and 1-7  $\phi$  in P3-01/R. In the second head group (Fig. SC-2-CODE 127) there is little deviation from norms, except for a remnant of higher coherence C3-CZ/R @ 3-5  $\phi$ . On the contrary, the A-P transmission (Fig. SC-3-CODE 127) is higher @ 1-7  $\phi$  in several pairings: F7-T3/T3-T5 & R, T3-T5/T5-01 & R, and C3-P3/P3-01 & R. Thus we might suggest that light sleep emphasizes transmission over the transversal, while intermediate emphasizes A-P transmission within the hemispheres.

In stage III sleep (Fig. SC-1-CODE 128) 2-5 and 8-15  $\phi$  are supernormal in F'1-F7/R, but 1-2  $\phi$  are supernormal in all the other L/R pairing of this diagram. The lamentable fluctuations of inter-sity variation affecting B-tape leads in higher frequencies in this code, also affect coherences between them, many of which are essentially zero. Hopefully whatever patches the intensities will also patch these coherences. The transversals (Fig. SC-2-CODE 128) show little deviation from norms, except that T3-C3/R is higher at most frequencies up to 15  $\phi$ . A curious and possibly real small coherence peak is seen at 19  $\phi$  in T3-T5/T3-C3 & R, and T3-C3/C3-CZ & R, but not in C3-CZ/R. A possibly meaningful elevation @ 10-25  $\phi$  is seen (Fig. SC-3-CODE 128) in T6-T4/14-F8, which may be irregularly mirrored on the left.

In the sub-arousal recorded (#129), the coherences F'1-F7/R are quite elevated (see Fig. SC-1-CODE 129) @ 1-13 $\phi$ , especially 1-2 $\phi$ . 1-4 $\phi$  is elevated in all L/R's of the first

head, except T5-01/R, which is rather normal. P3-01/R is somewhat elevated at almost all frequencies (1-25  $\phi$ ), which might suggest a tendency for noisier tape transport in this situation, except that this makes no sense. There is some elevation @ 1-2  $\phi$  in C3-P3/CZ-FZ & R.

During the awakening session, there are several A-P coherences considerably lower than the average, especially @ 10-25  $\phi$ ; contrariwise, C3-P3/CZ-FZ is elevated in coherence @ 8-10  $\phi$ .

## REFERENCES

- Adey, W. R. Computer analysis in neurophysiology. In R. Stacy and B. Waxman (Eds.), Computers in Biomedical Research. Academic Press, New York, 1965: 223-263.
- Brazier, M. A. B. The problem of periodicity in the electroencephalogram: studies in the cat. Electroenceph. clin. Neurophysiology, 1963, 15: 287-298.
- Rhodes, J. M., Reite, M. R., Brown, D. and Adey, W. R. Cortical-subcortical relationships of the chimpanzee during different phases of sleep. In Aspects anatomal-fonctionnels de la physiologie du sommeil. Colloques internationaux du CNRS, No. 127, 1965: 451-473.
- Walter, D. O., Rhodes, J. M., and Adey, W. R. Discriminating among states of consciousness by EEG measurements. Electroencephalog. clin. Neurophysiol., in press (see Appendix II).



APPENDIX I

DEFINITION OF SEGMENTS USED FOR ANALYSIS

```

1 JOB      8016GC 120 500 WALSH NASA NORMATIVE 248B
SID      13,DP1658,7094,RING
$SETUP  15,DP1684,7094
*      LOAD NEEG03
*      DATA
(NOGO)=1B
(NDEN1)=800B
(DATE)H5=16 NOV.19650
(SUBNO)=248B
(H1)H12=HIGH FREQUENCY ANALYSIS FOR 248B0
(BCODE)=-40B (HCODE)=240B (BPULSE)=280B (HPULSE)=250B
(LTAPE1)=15B (LTAPE)=13B
(MAX)=30.1 (DELTA)=1 (OUT)=3B (FS)=400
(NTAPES)=1B
(NCHAN)=13B
(CHAN)H1=LC-LPO H1=RC-RPO H1=LP-L00 H1=RP-R00 H1=FZ-CZO H1=LO-R00
H1=LREGO H1=UDEOGO H1=EKGTMP0 H1=EMGRSP0 H1=PLETH0 H1=G5R0
H1=EXCODE0
(N)=6B
(NX)=-1B
(H2)H12=REST SERIES EYES CLOSED0
(EXPNO)=005B (TEND)=10
*$ END OF CASE
(EXPNO)=010B (TEND)=10$
(EXPNO)=012B (TEND)=10$
(EXPNO)=15B (TEND)=10
*$ END OF CASE
(EXPNO)=017B (TEND)=10$
(EXPNO)=019B (TEND)=10$
(EXPNO)=21B (TEND)=10$
(EXPNO)=023B (TEND)=10$
(EXPNO)=025B (TEND)=10$
(H2)H12=REST SERIES EYES OPEN.0
(EXPNO)=029B (TEND)=10$
(EXPNO)=031B (TEND)=10$
(EXPNO)=033B (TEND)=10$
(EXPNO)=035B (TEND)=10$
(EXPNO)=037B (TEND)=10$
(EXPNO)=040B (TEND)=10$
(H2)H12=STIMULATION ARCHIVE SERIES FLASHES, EYES CLOSED.0
(EXPNO)=011B (PSTART)=1B (BRESP)=0B (TSTART)=0 (PEND)=20B (TEND)=0.01
*$ END OF CASE
(PSTART)=21B (PEND)=40B$
(PSTART)=41B (PEND)=60B$
(PSTART)=61B (PEND)=80B$
(H2)H12=STIMULATION ARCHIVE SERIES TAPS, EYES CLOSED.0
(EXPNO)=016B (PSTART)=1B (BRESP)=0B (TSTART)=0 (PEND)=20B (TEND)=0.01
*$ END OF CASE
(PSTART)=21B (PEND)=40B$
(PSTART)=41B (PEND)=60B$
(PSTART)=61B (PEND)=80B$
(H2)H12=STIMULATION ARCHIVE SERIES CLICKS EYES CLOSED.0
(EXPNO)=018B (PSTART)=1B (BRESP)=0B (TSTART)=0 (PEND)=20B
(TEND)=0.1
*$ END OF CASE
(PSTART)=21B (PEND)=40B$
(PSTART)=41B (PEND)=60B$
(PSTART)=61B (PEND)=80B$

```

1  
59  
60  
61  
62  
63  
64  
65  
66  
67  
68  
69  
70  
71  
72  
73  
74  
75  
76  
77  
78  
79  
80  
81  
82  
83  
84  
85  
86  
87  
88  
89  
90  
91  
92  
93  
94  
95  
96  
97  
98  
99  
100  
101  
102  
103  
104  
105  
106  
107  
108  
109  
110  
111  
112  
113  
114  
115  
116  
117  
118

```

(PSTART)=81B (PEND)=100B$
(H2)H12=STIMULATION ARCHIVE SERIES CLICKS, EYES OPEN.0
(EXPNO)=034B (PSTART)=1B (BRESPI)=0B (TSTART)=0 (PEND)=20B
$* END OF CASE
(PSTART)=21B (PEND)=40B$
(PSTART)=41B (PEND)=60B$
(PSTART)=61B (PEND)=80B$
(PSTART)=81B (PEND)=100B$
(H2)H12=STIMULATION ARCHIVE SERIES FLASHES,EYES OPEN.0
(EXPNO)=036B (PSTART)=1B (BRESPI)=0B (TSTART)=0 (PEND)=20B
$* END OF CASE
(PSTART)=21B (PEND)=40B$
(PSTART)=41B (PEND)=60B$
(PSTART)=61B (PEND)=80B$
(PSTART)=81B (PEND)=100B$
(H2)H12=STIMULATION ARCHIVE SERIES TAPS, EYES OPEN.0
(EXPNO)=038B (PSTART)=1B (BRESPI)=0B (TSTART)=0 (PEND)=20B
$* END OF CASE
(PSTART)=21B (PEND)=40B$
(PSTART)=41B (PEND)=60B$
(PSTART)=61B (PEND)=80B$
(PSTART)=81B (PEND)=100B$
(H2)H12=STIM ARCH. FAST FLASHES, CLICKS, TAPS, EYES CLOSED.0
(EXPNO)=020B (PSTART)=1B (BRESPI)=0B (TSTART)=0
(PSTART)=1B (PEND)=200B
$* END OF CASE
(EXPNO)=022B$
(EXPNO)=024B$
(H2)H12=STIM ARCH. FAST CLICKS, TAPS, FLASHES, EYES OPEN.0
(EXPNO)=028B (PSTART)=1B (BRESPI)=0B (TSTART)=0 (PEND)=200B
$* END OF CASE
(EXPNO)=030B$
(EXPNO)=032B$
(H2)H12=ARCH.CONDIT. 9 SEC EPOCHS 2.11,21.31,40.41,51.61,71.80(19 SEC) 0
(EXPNO)=056B (PSTART)=1B (BRESPI)=0B (TSTART)=2 (TEND)=9
$* END OF CASE
(H2)H12=ARCH.CONDIT. 9 SEC EPOCHS 2.11,21.31,40.41,51.61,71.80(147 SEC) 0
(PSTART)=23B (TSTART)=2.62 $
(H2)H12=ARCH.CONDIT. 9 SEC EPOCHS 2.11,21.31,40.41,51.61,71.80(197 SEC) 0
(PSTART)=48B (TSTART)=2.05 $
(H2)H12=ARCH.CONDIT. 9 SEC EPOCHS 2.11,21.31,40.41,51.61,71.80(147 SEC) 0
(PSTART)=72B (TSTART)=2.49 $
(H2)H12=ARCH.CONDIT. 9 SEC EPOCHS 2.11,21.31,40.41,51.61,71.80(192 SEC) 0
(PSTART)=93B (TSTART)=4.14 $
(H2)H12=ARCH.CONDIT. 9 SEC EPOCHS 2.11,21.31,40.41,51.61,71.80(197 SEC) 0
(PSTART)=96B (TSTART)=2.95 $
(H2)H12=ARCH.CONDIT. 9 SEC EPOCHS 2.11,21.31,40.41,51.61,71.80(247 SEC) 0
(PSTART)=120B (TSTART)=2.38 $
(H2)H12=ARCH.CONDIT. 9 SEC EPOCHS 2.11,21.31,40.41,51.61,71.80(297 SEC) 0
(PSTART)=144B (TSTART)=2.84 $
(H2)H12=ARCH.CONDIT. 9 SEC EPOCHS 2.11,21.31,40.41,51.61,71.80(347 SEC) 0
(PSTART)=168B (TSTART)=3.30 $
(H2)H12=ARCH.CONDIT. 9 SEC EPOCHS 2.11,21.31,40.41,51.61,71.80(392 SEC) 0
(PSTART)=189B (TSTART)=4.95 $
(H2)H12=REST SERIES EYES OPEN TONES SLIDES LAST REST A AND B.0
(PSTART)=1B
(EXPNO)=059B (TSTART)=10 (TEND)=105
(H2)H12 ARCH.SERIES SLIDES A0
(EXPNO)=60B
(TSTART)=0 (NOGO)=1B (TEND)=9$
(TSTART)=0 (NOGO)=0B (TEND)=0$

```

119  
120  
121  
122  
123  
124  
125  
126  
127  
128  
129  
130  
131  
132  
133  
134  
135  
136  
137  
138  
139  
140  
141  
142  
143  
144  
145  
146  
147  
148  
149  
150  
151  
152  
153  
154  
155  
156  
157  
158  
159  
160  
161  
162  
163  
164  
165  
166  
167  
168  
169  
170  
171  
172  
173  
174  
175  
176  
177  
178  
179

```

(EXPNO)=618 (NOGO)=18 (TEND)=9 $
(TSTART)=0 (NOGO)=08 (TEND)=0 $
(EXPNO)=628
(TSTART)=0 (NOGO)=18 (TEND)=9 $
(TSTART)=0 (NOGO)=08 (TEND)=0 $
(EXPNO)=638
(TSTART)=0 (NOGO)=18 (TEND)=9 $
(TSTART)=0 (NOGO)=08 (TEND)=0 $
(EXPNO)=648
(TSTART)=0 (NOGO)=18 (TEND)=9 $
(TSTART)=0 (NOGO)=08 (TEND)=0 $
(EXPNO)=658
(TSTART)=0 (NOGO)=18 (TEND)=9 $
(TSTART)=0 (NOGO)=08 (TEND)=0 $
(EXPNO)=668
(TSTART)=0 (NOGO)=18 (TEND)=9 $
(TSTART)=0 (NOGO)=08 (TEND)=0 $
(EXPNO)=678
(TSTART)=0 (NOGO)=18 (TEND)=9 $
(TSTART)=0 (NOGO)=08 (TEND)=0 $
(EXPNO)=688
(TSTART)=0 (NOGO)=18 (TEND)=9 $
(TSTART)=0 (NOGO)=08 (TEND)=0 $
(EXPNO)=698
(TSTART)=0 (NOGO)=18 (TEND)=9 $
(TSTART)=0 (NOGO)=08 (TEND)=0 $
(EXPNO)=708
(TSTART)=0 (NOGO)=18 (TEND)=9 $
(TSTART)=0 (NOGO)=08 (TEND)=0 $
(EXPNO)=718
(TSTART)=0 (NOGO)=18 (TEND)=9 $
(TSTART)=0 (NOGO)=08 (TEND)=0 $
(EXPNO)=728
(TSTART)=0 (NOGO)=18 (TEND)=9 $
(TSTART)=0 (NOGO)=08 (TEND)=0 $
(EXPNO)=738
(TSTART)=0 (NOGO)=18 (TEND)=9 $
(TSTART)=0 (NOGO)=08 (TEND)=0 $
(EXPNO)=748
(TSTART)=0 (NOGO)=18 (TEND)=9 $
(TSTART)=0 (NOGO)=08 (TEND)=0 $
(EXPNO)=758
(TSTART)=0 (NOGO)=18 (TEND)=9 $
(TSTART)=0 (NOGO)=08 (TEND)=0 $
(EXPNO)=768
(TSTART)=0 (NOGO)=18 (TEND)=9 $
(TSTART)=0 (NOGO)=08 (TEND)=0 $
(EXPNO)=778
(TSTART)=0 (NOGO)=18 (TEND)=9 $
(TSTART)=0 (NOGO)=08 (TEND)=0 $
(EXPNO)=788
(TSTART)=0 (NOGO)=18 (TEND)=9 $
(TSTART)=0 (NOGO)=08 (TEND)=0 $
(EXPNO)=798
(TSTART)=0 (NOGO)=18 (TEND)=9 $
(TSTART)=0 (NOGO)=08 (TEND)=0 $
(EXPNO)=1008
(TSTART)=0 (NOGO)=18 (TEND)=6 $
(TSTART)=0 (NOGO)=08 (TEND)=0 $
(EXPNO)=1018

```

```

160
181
182
183
184
185
186
187
188
189
190
191
192
193
194
195
196
197
198
199
200
201
202
203
204
205
206
207
208
209
210
211
212
213
214
215
216
217
218
219
220
221
222
223
224
225
226
227
228
229
230
231
232
233
234
235
236
237
238
239
240

```

```

(TSTART)=0 (NOGO)=1B (TEND)=6$ 241
(EXPNO)=102B 242
(TSTART)=0 (NOGO)=1B (TEND)=6$ 243
(TSTART)=0 (NOGO)=0B (TEND)=0 244
(EXPNO)=103B 245
(TSTART)=0 (NOGO)=1B (TEND)=6$ 246
(TSTART)=0 (NOGO)=0B (TEND)=0 247
(EXPNO)=104B 248
(TSTART)=0 (NOGO)=1B (TEND)=6$ 249
(TSTART)=0 (NOGO)=0B (TEND)=0 250
(EXPNO)=105B 251
(TSTART)=0 (NOGO)=1B (TEND)=6$ 252
(TSTART)=0 (NOGO)=0B (TEND)=0 253
(EXPNO)=106B 254
(TSTART)=0 (NOGO)=1B (TEND)=6$ 255
(TSTART)=0 (NOGO)=0B (TEND)=0 256
(EXPNO)=107B 257
(TSTART)=0 (NOGO)=1B (TEND)=6$ 258
(TSTART)=C (NOGO)=0B (TEND)=0 259
(EXPNO)=108B 260
(TSTART)=0 (NOGO)=1B (TEND)=6$ 261
(TSTART)=0 (NOGO)=0B (TEND)=0 262
(EXPNO)=109B 263
(TSTART)=V (NOGO)=1B (TEND)=6$ 264
(TSTART)=0 (NOGO)=0B (TEND)=0 265
(EXPNO)=110B 266
(TSTART)=0 (NOGO)=1B (TEND)=6$ 267
(TSTART)=0 (NOGO)=0B (TEND)=0 268
(EXPNO)=111B 269
(TSTART)=0 (NOGO)=1B (TEND)=6$ 270
(TSTART)=0 (NOGO)=0B (TEND)=0 271
(EXPNO)=112B 272
(TSTART)=0 (NOGO)=1B (TEND)=6$ 273
(TSTART)=0 (NOGO)=0B (TEND)=0 274
(EXPNO)=113B 275
(TSTART)=0 (NOGO)=0B (TEND)=0 276
(EXPNO)=114B 277
(TSTART)=0 (NOGO)=1B (TEND)=6$ 278
(TSTART)=0 (NOGO)=0B (TEND)=0 279
(EXPNO)=115B 280
(TSTART)=0 (NOGO)=1B (TEND)=6$ 281
(TSTART)=0 (NOGO)=0B (TEND)=0 282
(EXPNO)=116B 283
(TSTART)=0 (NOGO)=1B (TEND)=6$ 284
(TSTART)=0 (NOGO)=0B (TEND)=0 285
(EXPNO)=117B 286
(TSTART)=0 (NOGO)=1B (TEND)=6$ 287
(TSTART)=0 (NOGO)=0B (TEND)=0 288
(EXPNO)=118B 289
(TSTART)=0 (NOGO)=1B (TEND)=6$ 290
(TSTART)=0 (NOGO)=0B (TEND)=0 291
(EXPNO)=119B 292
(TSTART)=0 (NOGO)=1B (TEND)=6$ 293
(TSTART)=0 (NOGO)=0B (TEND)=0 294
$SEND OF JOB 295

```

APPENDIX II  
DISCRIMINATING AMONG STATES OF  
CONSCIOUSNESS BY EEG MEASUREMENTS--A STUDY OF  
FOUR SUBJECTS<sup>1</sup>

by

Donald O. Walter, Ph.D., J. M. Rhodes<sup>2</sup>, Ph.D.  
and W. Ross Adey, M. D.

Departments of Physiology and Anatomy  
and the Brain Research Institute,  
University of California at Los Angeles  
Los Angeles, Calif. (U.S.A.)

## INTRODUCTION

The approximate definition of "states of consciousness" of a subject or patient has long interested electroencephalographers. By combining the mathematical techniques of spectral analysis (Walter, 1963) and of multi-group discriminant analysis (Anderson, 1958) such definitions can be studied objectively. We offer here an illustrative example of the power of these methods.

## METHODS

Spectral analysis (Walter, 1963) was applied to segments of EEG recorded from four normal adult human males as part of an extensive normative library of physiological recordings; the segments represented five types of situations extracted from a 1 h pre-recorded experiment. During the first type of situation, the subjects were resting with eyes closed, between periods of stimulation; the second type of situation was similar, except that the subjects had their eyes open. In the third, the subjects, with eyes closed, were listening to a series of tones, and had to respond intermittently by pushing a button. In the fourth and fifth types of situations, the subjects viewed a series of slides, in order to make a visual discrimination. First they viewed the slides for 3 sec each; later, for 1 sec each; subjects stated that both of these tasks were somewhat stressful, the second one, of course, more so. There were about twice as many segments of the fourth and fifth

types of situations for each subject, as there were of the first three types. No attempt was made to eliminate segments containing movement artifact or muscle interference.

Two digital computer programs<sup>3</sup> were devised to calculate and examine certain measurements on each EEG segment, and on the basis solely of the values of these measurements, to construct formulas to assign each segment to the correct type of experimental situation. The measurements were derived from: left and right parieto-occipital leads (P3-01 and P4-02), vertex (CZ-FZ), and bioccipital (O1-02). Each channel's activity was analyzed into four frequency bands, 0.5-3.5 c/sec (' $\delta$ '), 3.5-7.5 (' $\theta$ '), 7.5-12.5 (' $\alpha$ '), and 12.5-25.5 (' $\beta$ '). In each of these bands, for each channel, three parameters were measured: 'power' (better called mean-square intensity--proportional to the square of the amplitude if there is a dominant wave in this band and channel); the mean frequency within the band (which will be close to the dominant frequency if there is one); and the band-width within the band (which expresses the variability of the dominant frequency. Rhodes, et al. 1965). Also measured were coherences<sup>4</sup>, which are quantities expressing the strength of relationship between each pair of channels, in each band (Walter, 1963).

The discriminant analysis program initially considers all the measurements for all the segments, and from these selects that parameter which can be expected to discriminate best between segments recorded in different situations. Then the program reexamines all the remaining measurements, and chooses that parameter which can be expected to add most to the power of the first selection. It also derives 5 linear



formulas (one for each type of situation), based on the 2 selected parameters; each formula is applied to the measurements from each segment; finally, the segment is categorized as having come from that type of situation for whose formula it gives the highest value. The iteration of examining, selecting, and deriving formulas is repeated until an additional selection cannot be expected to give enough improvement in categorization to justify its inclusion.

A fuller explanation of discriminant analysis for several groups is given in (Anderson, 1958); briefly, that parameter is selected, at each stage, whose conditional distributions in the different types of situations (conditioned on all other selected variables) are least likely to differ as much as they do, by chance. The optimality of this choice is mathematically demonstrable only under various normality assumptions known to be violated to some extent by this data; we regard the selections made as indicative of worthwhile parameters for further study, not as definitive. The linear formulas, derived at each stage, are very complicated functions of the values of selected and unselected parameters, whose justification must be left to the experts. However, since these functions generate the automatic categorizations reported, we regard them as being justified by their fruits.

The discriminant analysis program was first applied to the data for all 4 subjects together ('ensemble' study); then the same program was applied separately to the data from each subject ('solo' studies). It may be pointed out that such studies are not small undertakings: approximately 1.6 million voltage readings constituted the primary data, which were transformed into about 35,000 parameter values utilized in the discriminant studies.

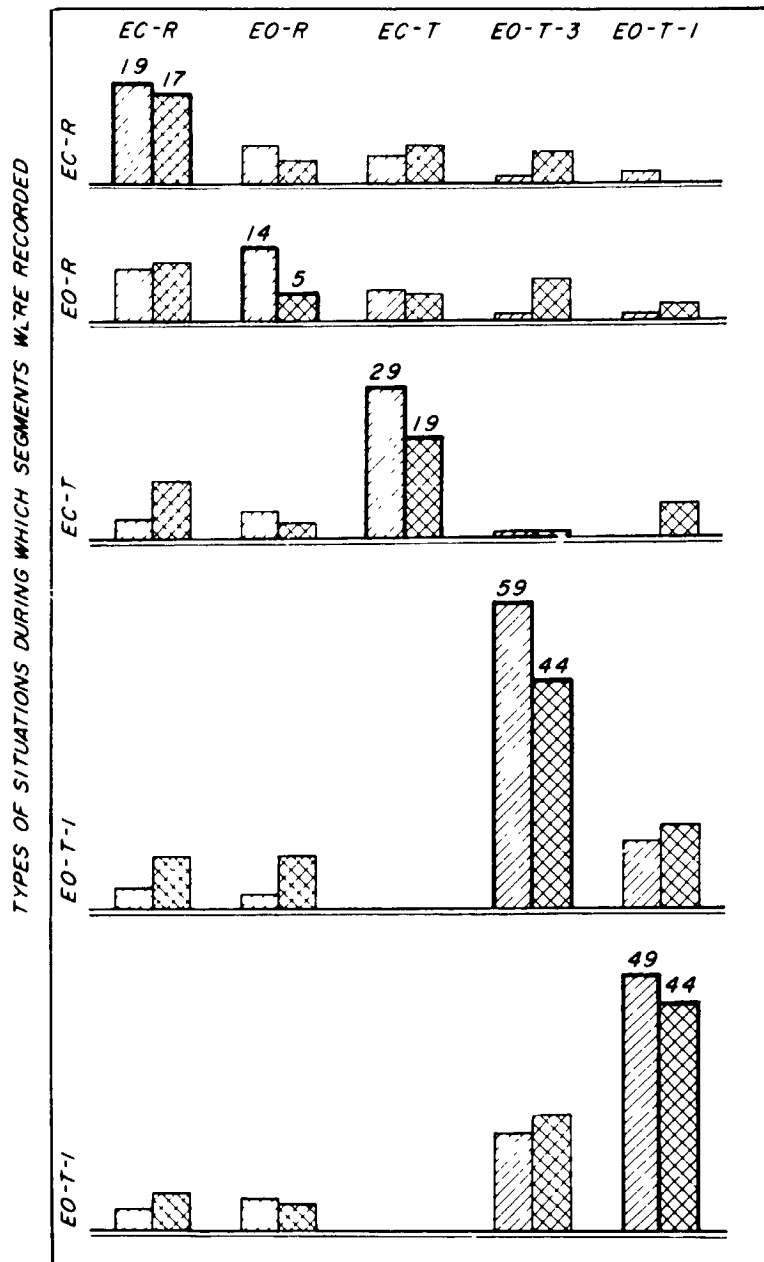
## RESULTS

Fig. 1 shows the results for the 4 solo studies and the ensemble study, stopped for illustrative purposes at an early stage, when the program has selected only 4 parameters in each study. After the program has selected the 4 parameters, it derives five linear formulas containing them (one formula for each type of situation); it then calculates, for each segment, the value attained by each of those linear functions; finally, the segment is classified as belonging to that type of situation whose linear function had the highest value. The Figure shows that the total correctly classified in solo studies is greater than the number so classified in the ensemble study, for every type of situation. This is one aspect of the cost of generalizing. Even so, the plurality of segments are correctly categorized in that study, for 4 of 5 types of situations, and a majority for the situations which might be expected to be least distinguishable, the two visual tasks. The particular difficulty in correctly recognizing EC-R may be due to the fact that those segments were recorded during short rest periods between periods of stimulation, and often appeared to contain more alpha-wave activity than might be expected in other situations of alert, eyes-open rest.

Many of the errors of classification accord with the similarities among the situations: eyes-open rest is chiefly misclassified as either eyes-closed rest or as eyes-open discrimination, eyes-closed task as eyes-closed rest; and the two discriminations are chiefly misclassified as each other. Even with only four parameters, almost half of the samples from these four subjects have been assigned correctly

## ACCURACY OF AUTOMATIC CLASSIFICATION

TYPE OF SITUATION INTO WHICH SEGMENTS WERE CLASSIFIED  
BY BEST\* COMBINATION OF 4 BEST\* PARAMETERS



\*BEST BY CRITERIA FOR STEP-WISE DISCRIMINANT ANALYSIS

▭ SUM OF FOUR SOLO STUDIES

▩ RESULT OF ENSEMBLE STUDY

Figure 1. Distribution of EEG segments by an automatic discrimination program. Segments recorded in 5 situations: EC-R, eyes closed, rest periods (34 segments); EO-R, eyes open, rest (32 segments); EC-T, eyes closed, listening to tones to which a response is intermittently required (40 segments); EO-T-3, eyes open, examining slides exposed for 3 sec each, to make a size discrimination (80 segments); EO-T-1, the same, with 1 sec exposure (78 segments). Five related studies are summarized: in 4 'solo' studies, each subject's records were evaluated separately, and the 4 parameters which would best categorize his records were selected; in the other, 'ensemble' study, records from all subjects were treated as if from a single subject, and the 4 parameters which would best categorize them all were selected. The rows of bars of the Figure represent the type of situation in which the segments were recorded; the columns represent the categorizations made on the basis of the selected parameters, optimally weighted and combined, in the attempt to imitate the actual type; thus, bars on the diagonal (outlined heavily) represent correct categorizations. As indicated, the single shading represents the sum of categorizations made in the 4 solo studies (for instance, a total of 29 segments out of the 40 recorded during EC-T were correctly so categorized in solo studies), while the cross shading represents the categorizations of of ensemble study (19 of the same 40 correctly so categorized in that study).

in the ensemble study, to the situation in which they were recorded. We emphasize that no attempt was made to eliminate segments containing non-cerebral potentials due to movement or muscle. When an objective method of editing out such segments is developed, no doubt our score will increase even at this early stage, of only four selections.

In the ensemble study, the four variables which best distinguish among the five situations are: intensity ('power') in the  $\alpha$  band in the left parieto-occipital channel, the mean frequency of the  $\theta$ -band activity in the vertex, and two less anticipated measures: the coherence in the  $\theta$  band between left parieto-occipital and vertex, and the coherence in the  $\delta$  band between left parieto-occipital and the bioccipital channels. This is not entirely an expected list; but further examination makes it more understandable.

Table I gives, for the ensemble study, characteristics of some initially improbable parameters. Those listed are most of the parameters whose initial probability of being, by chance, distributed as observed, was less than approximately 0.05; a few other parameters had initial probabilities between 0.02 and 0.05, but they were quickly eliminated in later steps, and are not shown in the Table. The initially most improbably distributed parameter was left parieto-occipital  $\alpha$  intensity, whose values would have served chiefly to distinguish the eyes-closed task situation (in which P3-01  $\alpha$  intensity, as shown in Table I, had values around a mean of  $2200 \mu V^2$ , with standard deviation  $1700 \mu V^2$ ), from all other situations (wherein its mean value was  $730 \mu V^2 \pm 725$ ). In this first selection step, lumping all other situations is not an adequate summary of the utility of this parameter; the best summary evaluator is the probability shown.

TABLE I. Initially Improbable Parameters, and Their Principal Discriminations

Prob.	Parameter	Types <sup>(1)</sup>	Values <sup>(2)</sup> $\pm$ s.d.
0.0040	P3-01 $\alpha$ intensity	(A) <sup>(3)</sup> EC-T/others	2200 $\mu V^2 \pm 1700/730$ $\mu V^2 \pm 725$
0.0043	01-02 $\alpha$ intensity	(b) EC-T/others	2200 $\mu V^2 \pm 1500/865$ $\mu V^2 \pm 920$
0.0080	CZ-FZ $\theta$ mean freq.	(C) E0-T-1&3/EC-R&E0-R	5.00 c/sec $\pm 0.30/5.29$ c/sec $\pm 0.31$
0.0090	P4-02 $\alpha$ intensity	(D) EC-T/others	1560 $\mu V^2 \pm 1180/650$ $\mu V^2 \pm 700$
0.0110	CZ-FZ $\theta$ intensity	(E) E0-T-1&3/EC-R&E0-R	1080 $\mu V^2 \pm 1100/314$ $\mu V^2 \pm 220$
0.0120	P3-01/CZ-FZ $\theta$ coherence	(F) E0-T-1/EC-R, E0-R&E0-T-3	0.13 $\pm 0.11/0.05 \pm 0.06$
0.0130	CZ-FZ $\theta$ bandwidth	(G) E0-T-1&3/EC-R&E0-R	2.23 c/sec $\pm 0.51/2.61$ c/sec $\pm 0.53$
0.0470	P4-02/01-02 $\theta$ coherence	(H) E0-T-1/E0-T-3	0.12 $\pm 0.12/0.07 \pm 0.08$
0.0510	P3-01/01-02 $\delta$ coherence	(I) E0-T-1/E0-T-3	0.23 $\pm 0.19/0.14 \pm 0.11$

- (1) Types of situations which the parameter would chiefly serve to discriminate, if selected.
- (2) Values of indicated parameter in the two types (or groups of types) of situations given in previous column.
- (3) The letters are arbitrary labels, given here to assist the reader in following later tables.

TABLE II. Distribution Probabilities of Initially Improbable Parameters, after Allowing for Optimum Prediction by Selected Parameters.

Part a. Probabilities after allowing for first selection (P3-01  $\alpha$  intensity)

Prob.	Parameter
0.0060	CZ-FZ $\theta$ intensity (C) selected
0.0130	P3-01/CZ-FZ $\theta$ coherence (F)
0.0200	CZ-FZ $\theta$ intensity (E)
0.0202	CZ-FZ $\theta$ bandwidth (G)
0.0400	P3-01/01-02 $\delta$ coherence (I)
0.0500	P4-02/01-02 $\theta$ coherence (H)
0.1700	01-02 $\alpha$ intensity (B) ignored hereafter
0.3700	P4-02 $\alpha$ intensity (D) ignored hereafter

Part b. After allowing for 2 first selections (P3-01  $\alpha$  intensity and CZ-FZ  $\theta$  intensity)

0.0150	P3-01/CZ-FZ $\theta$ coherence (F) selected
0.0400	P3-01/01-02 $\delta$ coherence (I)
0.0505	P4-02/01-02 $\theta$ coherence (H)
0.2000	CZ-FZ $\theta$ intensity (E) ignored hereafter
0.3000	CZ-FZ $\theta$ bandwidth (G) ignored hereafter

Part c. After 3 selections

0.0400	P3-01/01-02 $\delta$ coherence (I) selected
0.0500	P4-02/01-02 $\theta$ coherence (H)

Other parameters were quite improbably distributed at the stage before the first selection. Only bioccipital or right parieto-occipital  $\alpha$  intensities would have served the same discrimination, but as can be seen approximately from the values given, or from the probabilities, these competing  $\alpha$  intensities would not be expected to discriminate quite as well as the selected one.

After the first selection is made, the probabilities of the remaining parameters are recalculated, making allowance for how much of their variation could be predicted from the chosen P3-01  $\alpha$  intensity. Those, such as O1-02  $\alpha$  intensity and P4-02  $\alpha$  intensity, which are well correlated with the selected parameter can, of course, be predicted by it to a considerable extent; thus their recalculated probabilities are much increased, as shown in Table 11a. Others, such as CZ-FZ  $\theta$  mean frequency, or P3-01/CZ-FZ  $\theta$  coherence, which are scarcely correlated with the first selection, are little changed in calculated probability. It is interesting to note, in connection with the discrimination between E0-T-1 & -3 accomplished by CZ-FZ  $\theta$  mean frequency, that these two visual tasks, said by the subjects to have been somewhat stressful, result in  $\theta$ -band activity in the vertex becoming lower in frequency (parameter C), higher in power (parameter E), and narrower in bandwidth (i.e., more regular or sinusoidal (parameter G)). In any case, the parameter selected second is the one (CZ-FZ  $\theta$  mean frequency), whose conditional probability (of being distributed as observed, after taking account of the predictability from the first selection) is the least.

Again the probabilities of the remaining variables are recalculated, this time taking account of their predictability from both the previously selected parameters. Again, two of the previously improbably distributed parameters were well correlated with the selected one, so their conditional probability is considerably raised, as shown in Table 11b. For the third selection, we again take the parameter with minimum conditional probability, which, as it happens, was not highly correlated with any other parameters (Table 11c.). Finally, the fourth selection is made in the same way; it is the parameter which was ninth in line in the initial competition. The third and fourth measurements selected by the program,  $\theta$ -band coherence between left parieto-occipital and vertex, and  $\delta$ -band coherence between left parieto-occipital and bioccipital, both served to distinguish between the two degrees of stress, there being higher coherence in the higher degree of stress. We may have encountered here a valuable new observation about EEGs. To rephrase the finding concerning  $\theta$ -band coherence between left parieto-occipital and vertex records: during 1 sec, the strength of relationship between the  $\theta$ -band activity in two areas of subjects' scalps was stronger than during the period when they had 3 sec for similar discriminations. A reasonable interpretation might be that a deep generator of  $\theta$  waves, perhaps the hippocampus, was more active during the greater stress; being deep, it radiated to the two fairly separated leads, parieto-occipital and vertex. The fact that the fourth selection,  $\delta$ -band coherence, P3-01/01-02, had its utility mainly in aiding the difficult differentiation between E0-T-3 and -1, but is in a different frequency band and location from the previous selection, makes it seem that a different, additional process has been detected, which aids in distinguishing these epochs.

The record from each of the 4 subjects was separately analyzed in the same way, with somewhat different results. With his own best 4 measurements, 52, 52, 56 or 59% of a single subject's samples were correctly classified, as contrasted with 40% for the subjects simultaneously. An even greater disparity was noticeable after 15 measurements were selected: 95, 93, 96, and 90% were correct in solo studies while for the ensemble study, only 55% were. A great disparity is also noticeable in the lists of measurements selected as the best 4. Only one subject's list contains P3-01  $\alpha$  intensity, another's contains CZ-FZ  $\theta$  mean frequency, a third's contains P3-01/01-02  $\delta$  coherence (selected, respectively 1st, 2nd and 4th in the ensemble study); the fourth subject's list shares no parameter with the ensemble study's list. Three subjects' solo selection lists contain CZ-FZ  $\theta$  intensity, two subjects' lists contain 01-02  $\alpha$  intensity, both of which were competitors in the ensemble study. Two subjects' solo lists contain P4-02  $\theta$  intensity, which was neither selected nor competing in the ensemble study. Six other parameters complete those selected in some subject's solo study, none of them shared with the ensemble study, or with another's solo study.

#### DISCUSSION

The present results, while exploratory, do appear to have suggestive implications for our ways of thinking about the EEG, particularly in regard to what frequency bands, and which features of activity in those bands, may be useful indicators for differentiating the EEG response to various inputs. The utility of alpha activity as an indicator appears to be supported, at least in the ensemble study; it is curious to note,



however, that, while three subjects' solo lists contain alpha intensity, in two it is bioccipital alpha intensity which is the better discriminating index; and for one subject of our four, no alpha intensity was a good index. Similar remarks apply to the other parameters selected in the ensemble study, so that a summary description of the results might be that those aspects of EEG activity and reactivity which 'generalize' across subjects (and hence were worthy of selection in the ensemble study) are seldom the same aspects which are best indices when a subject is considered separately. From the complementary point of view, we may view the subjects' solo lists as constituting spatially and numerically characterizable EEG 'signatures', which show those aspects of EEG reactivity which do not 'generalize' so broadly.

To study individual subjects' records does capitalize to some extent on chance variations. An experimental design in which the same subject is re-tested on a later day would be useful, but was not available to us in this case. In the absence of a widely accepted method, we are attempting to develop a statistical test for inferring the generalizability of these discriminant formulas, by removing each case sequentially from the corpus of those classified, and treating that case as a "retest" sample.

Several extensions of this pilot study immediately suggest themselves, and are being pursued. Additional channels and measurements are being submitted to the same competition. The method is being applied to objective discrimination among sleep states, and between EEGs recorded during "correct" and "incorrect" responses to a conditioned discrimination task (all in preparation). Another value of the method lies in its ability

to compare competing analysis techniques, at least as far as concerns their effectiveness in defining "states" of the subject. Additional parameters derived from our present spectral analysis, as well as from more simplified analytic procedures, are being submitted to competition in this way.

Many improvements and adaptations of the discriminant method also suggest themselves. Among those we are implementing at this time are an option to consider "difference scores" for each individual, so that average values of all parameters are equalized between individuals, and an option to "transform" each parameter, in such a way as to bring its distribution function closer to a Gaussian shape (which should improve the program's effectiveness).

The discrimination program applied here in effect constructs planar surfaces (in a space whose axes are the selected parameters) for separating the points which represent the EEG segments arising from the differing situations. Often we can see in test plottings that curved surfaces would better separate the situations, with the same selection of variables. Fitting the simplest curved surfaces (quadratic surfaces) requires the optimum combination of parameter values, their squares and products; programs to offer such functions of parameters as additional parameters are being written. It may be that this improvement will also reduce the disparity between solo and ensemble classifications, since it is sometimes the points representing a single subject's segments which intrude curvilinearly into the domain of other situations' points. A related technical improvement, in some applications, would be automatic inclusion of the

proper combination of competing variables, which would improve both the repeatability and the generalizability of particular examples. This can perhaps be accommodated by the device of canonical variables, already available by manual control of the planar program.

#### SUMMARY

Intensity of activity, mean frequency, equivalent band-width, and coherence values in four frequency ranges ( $\delta$ ,  $\theta$ ,  $\alpha$ ,  $\beta$ ) were calculated for four channels of EEG recorded from each of four normal adult human males, in five experimental situations, including periods of rest and of attention. Stepwise discriminant analysis was applied to the calculated values for all subjects simultaneously, to develop formulas for automatic categorization of records into the situation in which they were recorded. After selecting only four parameters, the program correctly categorized 49% of the records; the erroneous categorizations were mainly into related situations.

When the records from each subject were separately analyzed, and the four parameters best for discriminating his own records were applied, a higher proportion of records was correctly categorized; the parameters chosen were only partially overlapping with those chosen for the simultaneous discrimination. Thus an objective method of identifying parameters of the EEG which are important in distinguishing subjects' responses to differing situations has shown its value for developing criteria applicable to many individuals; it has also shown that individuals differ substantially in the list of parameters most distinguishing for their own records.

## FOOTNOTES

- i. Supported in part by various federal agencies. Some of the calculations were done on a digital computer (Scientific Data Systems, Model 930) by the Data Processing Laboratory of the Brain Research Institute, partially supported by USPHS Grant NB02501 through the NINDB, by AFOSR Contract AF 43(638)-1387, and ONR Contract 233(91). The spectral and the discriminant computations were done on an IBM 7040-7094, by the Health Sciences Computing Facility, sponsored by NIH Grant FR-3. The normative library analysis was supported in part by NASA Contract 9-1970; we are also happy to acknowledge assistance from NASA Grant NsG 237-62. The stimulus-control devices were designed and constructed in our laboratory by R. T. Kado and others; the EEGs were recorded in the laboratories of Dr. P. Kellaway, Methodist Hospital, Houston. Methods of data acquisition and treatment are further explained in Walter et al (1966).
2. Present address: Department of Psychology, University of New Mexico, Albuquerque.
3. Measurements made by the spectral analysis program, NEEG, of which further description is available from D. O. Walter; stepwise discriminant analysis program, BMD07M (Dixon, 1965).

4. To illustrate the concept of coherence, suppose that the vertex and bioccipital voltage records were to be passed through two similar filters, responding only in the 3.5-7.5 c/sec band. Suppose further that the filters' output records appeared relatively similar, except for a phase lag; let the optimum phase compensation be applied; then the ordinary coefficient of correlation between the filtered and phase-compensated filter output records is the coherence between vertex and bioccipital records in the  $\theta$  band. If it is near 1, there is a close linear relationship between the records, in this band; if it is near 0, there is almost no linear relationship (Koopmans, 1964).

## REFERENCES

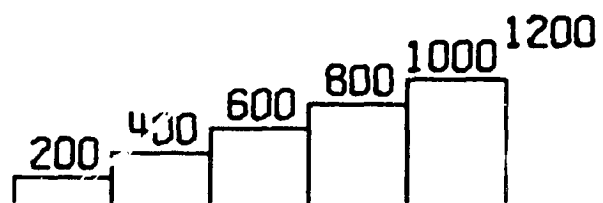
- Anderson, T. W. Introduction to Multivariate Statistics, New York Wiley, 1958, pp. 142-153.
- Dixon, W. J., Ed. BMD. Biomedical Computer Programs, Health Sciences Computing Facility, Dept. Preventive Medicine and Public Health, School of Medicine, UCLA. Revised Sept. 1, 1965, pp. 507-605. Available from UCLA student store, 308 Westwood Blvd., Los Angeles, California, 90024.
- Koopmans, L. H. On the coefficient of coherence for weakly stationary stochastic processes. Annals Math. Stat. 1964, 35: 532-549.
- Rhodes, J. M., Reite, M. R., Brown, D., Adey, W. R. Cortical-subcortical relationships of the chimpanzee during different phases of sleep. In: Aspects Anatomofonctionnels de la Physiologie du Sommeil; Colloques Internationaux, No. 127, Editions CNRS Paris, 1965 pp. 451-473.
- Walter, D. O. Spectral Analysis for Electroencephalograms: Determination Neurophysiological Relationships from Records of Limited Duration. Exp. Neurol., 1963 8: 155-181.
- Walter, D. O., Rhodes, J. M., Brown, D., and Adey, W. R. Comprehensive Spectral Analysis of Human EEG Generators in Posterior Cerebral Regions. Electroenceph. clin. Neurophysiol. 1966 (in press).

## APPENDIX I.I

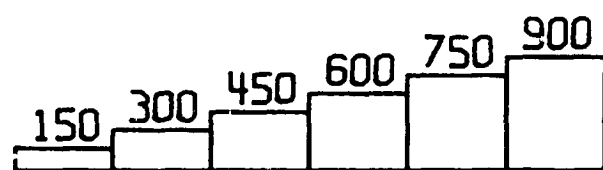
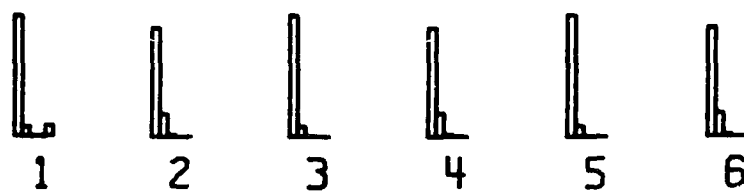
### FIGURES

For the contour maps of intensity, such as Fig. LFP-LF (p.111), the contour curves are drawn at 10, 30, 100, 300, 1000, 3000  $(\mu V)^2/(c/sec)$ , the 10-unit curve being labeled with X's. For contour maps of variations, such as LFP-LF Variations (p.111), the contour curves are drawn at -1 and +1 standard deviations (see text, p. 32).

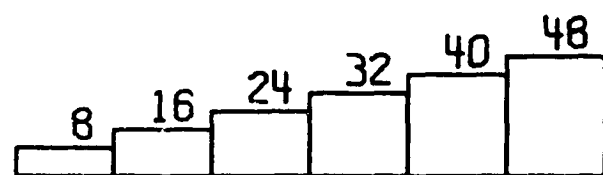
FIG. VM



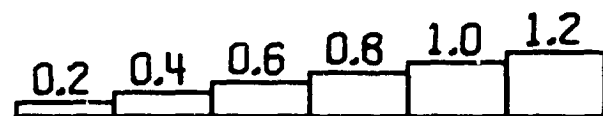
DATA



MEAN



ST DEV

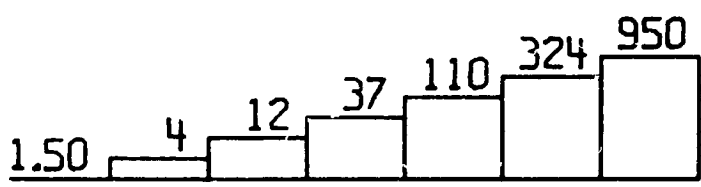


COEF OF VAR

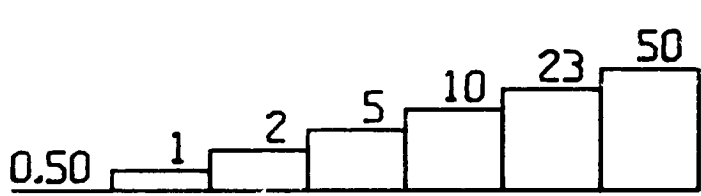




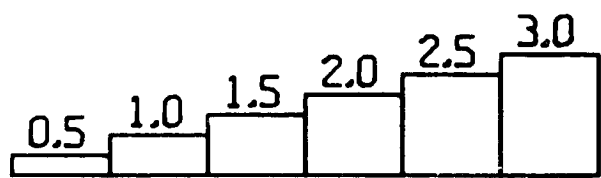
FIG. V0



MEAN



ST DEV



VARIATIONS



1



2



3



4



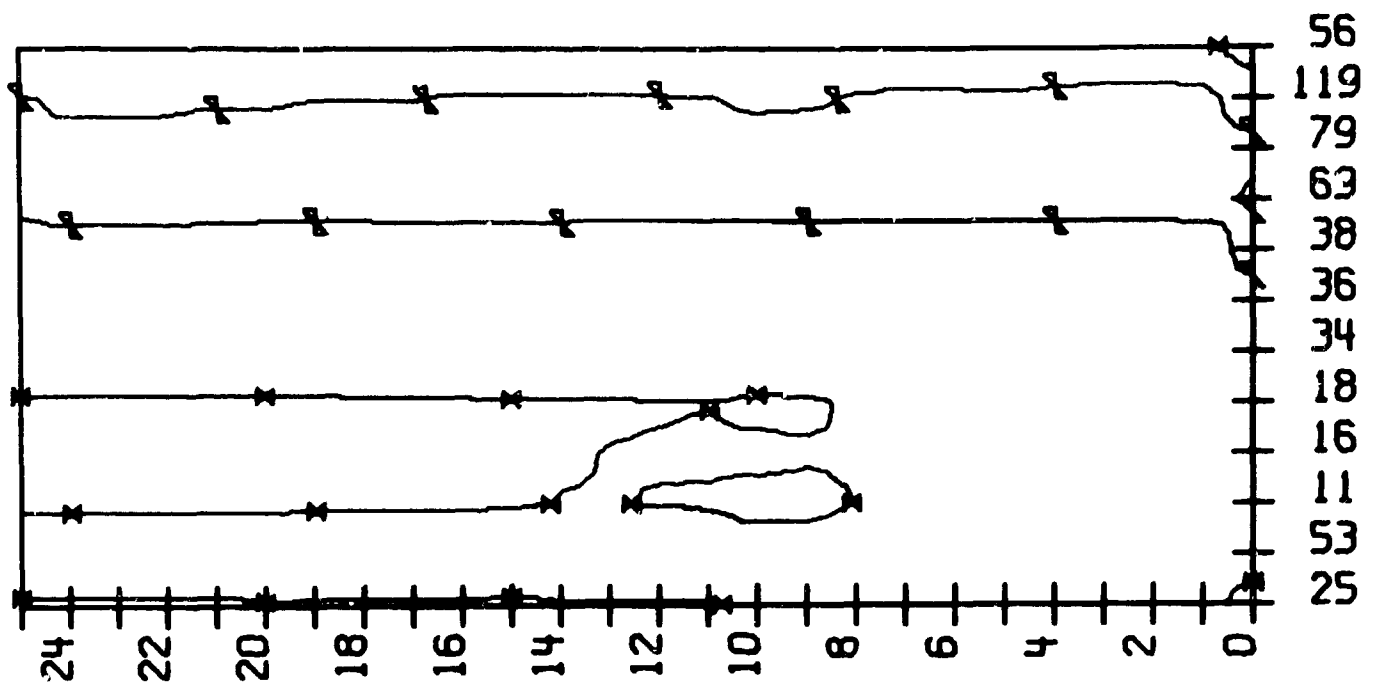
5



6

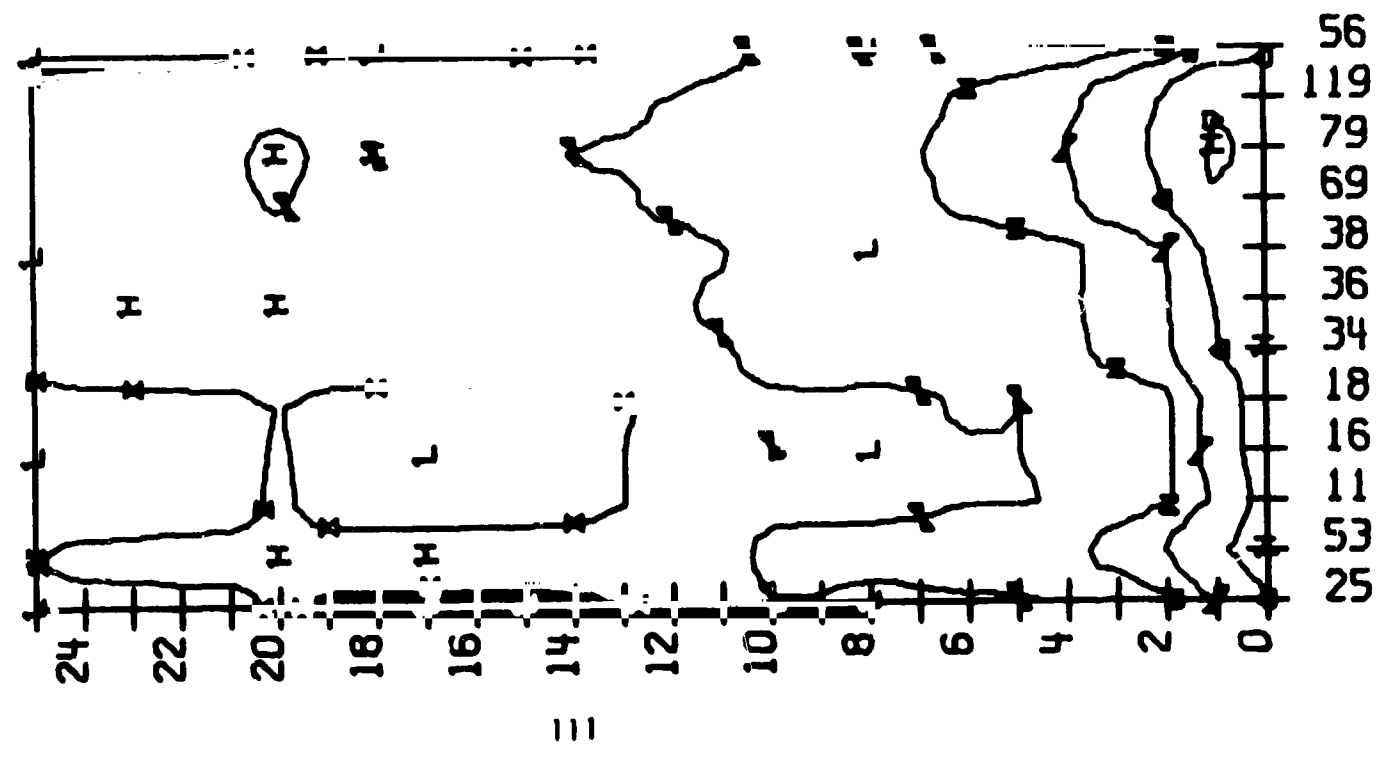
50 A

LFP-LF



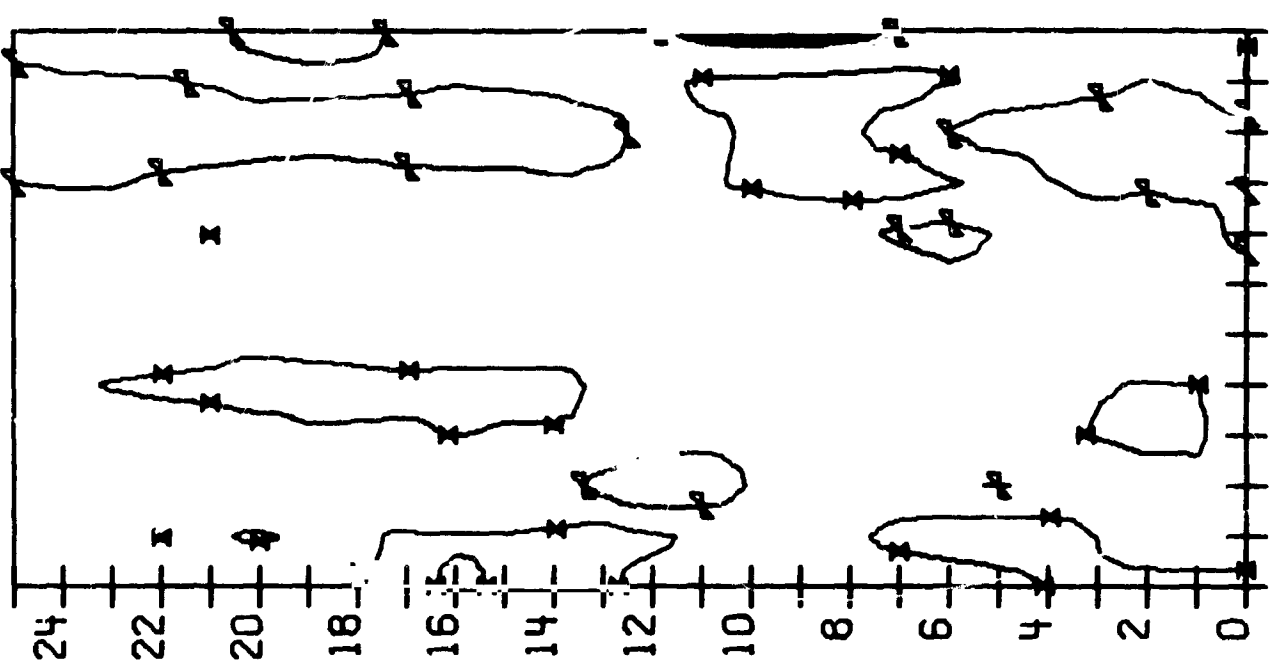
50 A

LFP-LF



VARIATIONS  
50 A

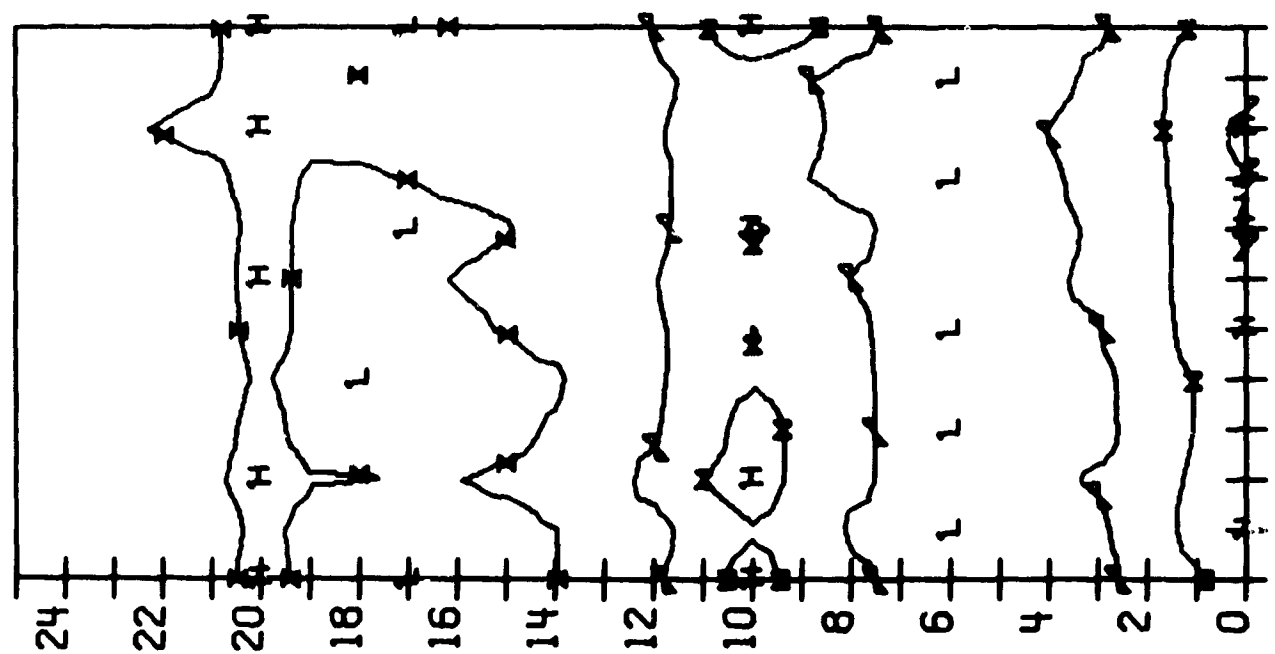
LTP-LO



56  
119  
79  
69  
38  
36  
34  
18  
16  
11  
53  
25

50 A

LTP-LO



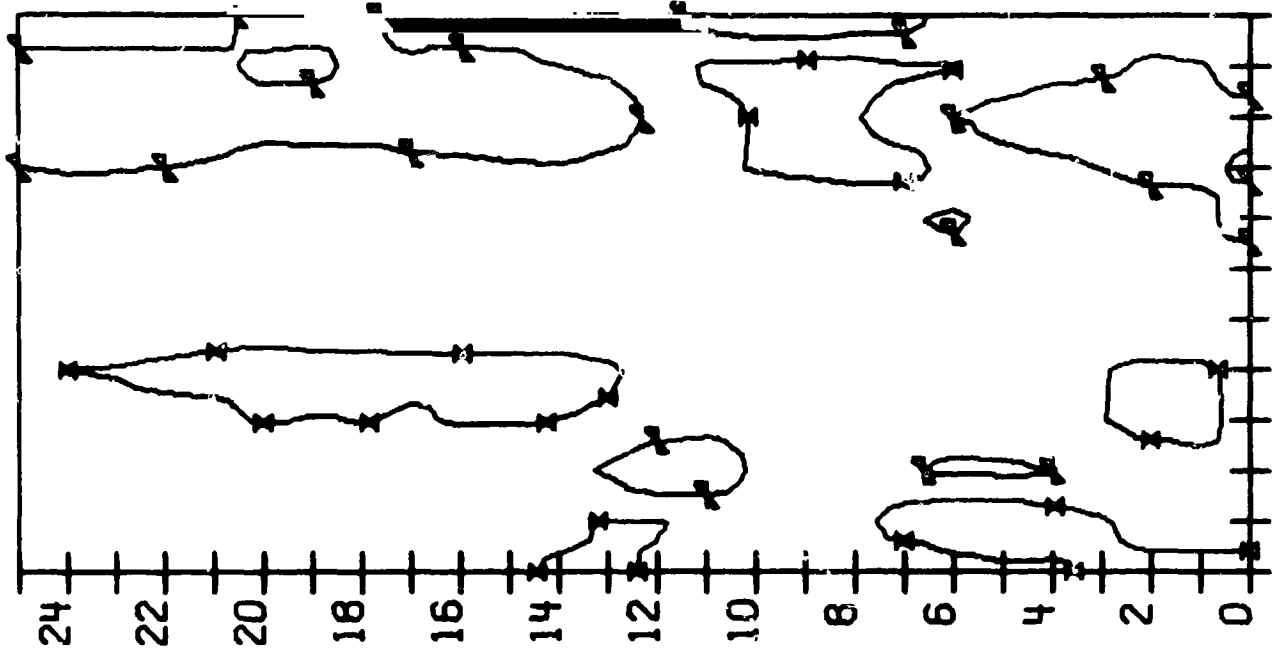
56  
119  
79  
69  
38  
36  
34  
18  
16  
11  
53  
25

56  
119  
79  
69  
38  
36  
34  
18  
16  
11  
53  
25

56  
119  
79  
69  
38  
36  
34  
18  
16  
11  
53  
25

VARIATIONS  
50 A

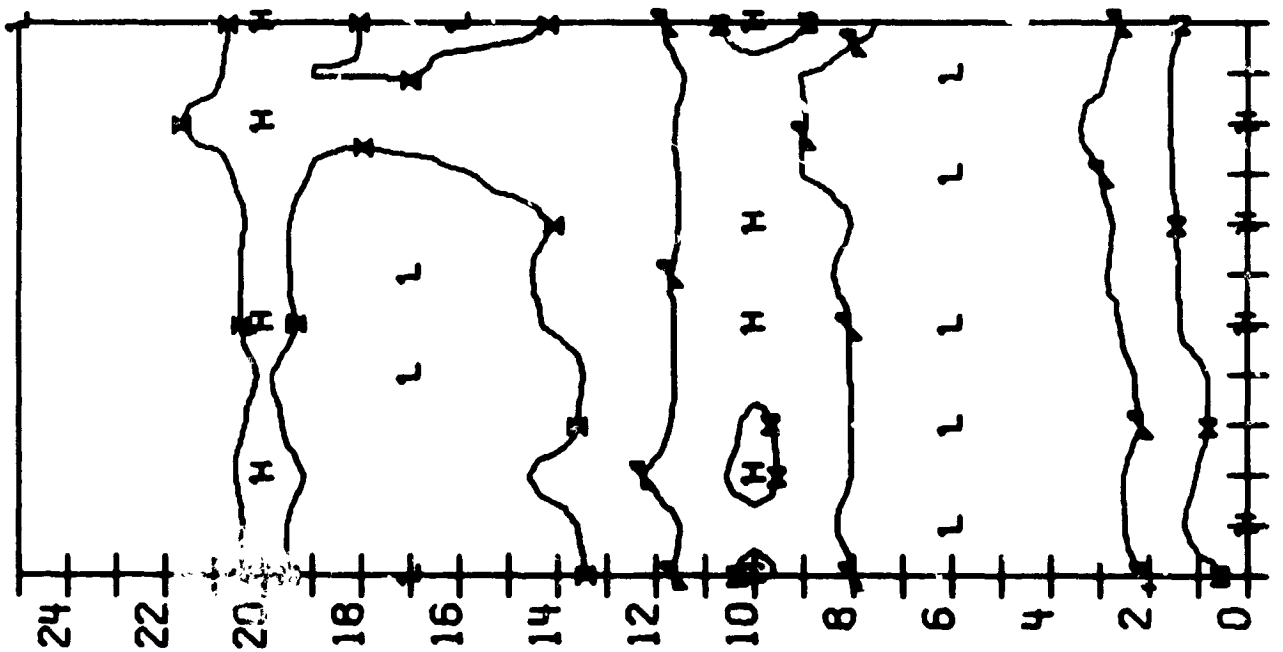
RO-RTP



56  
119  
79  
69  
38  
36  
34  
18  
16  
11  
53  
25

50 A

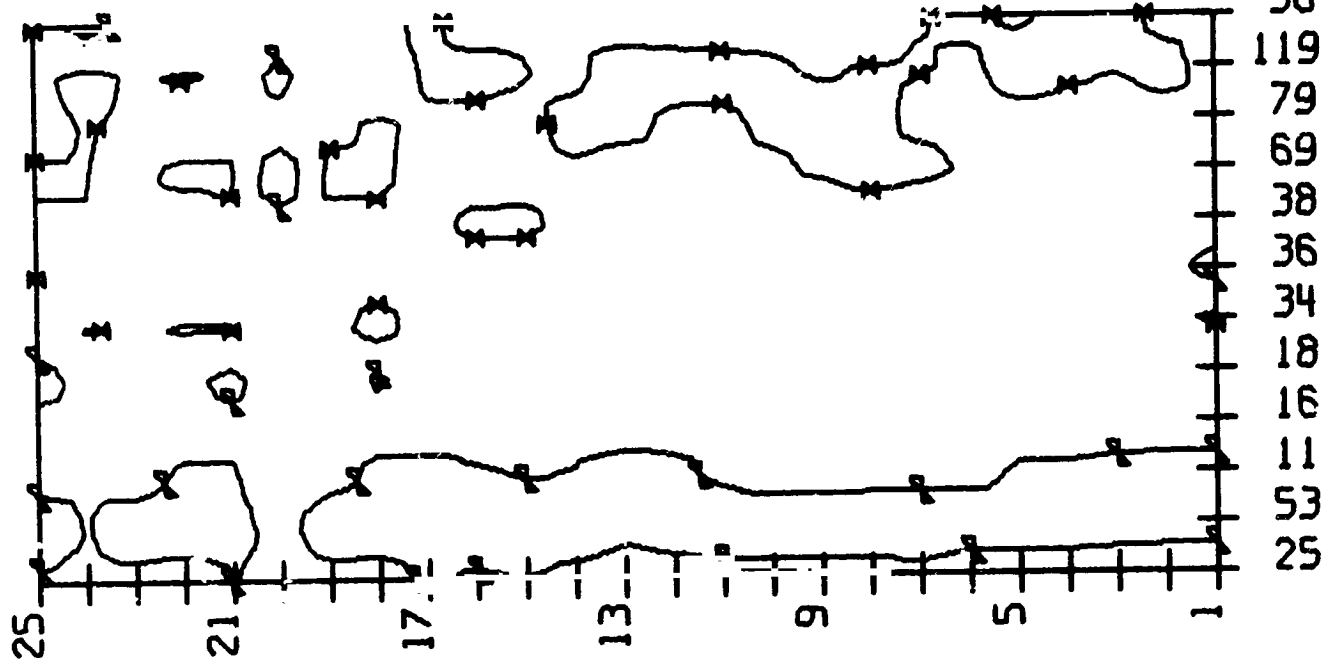
RO-RTP



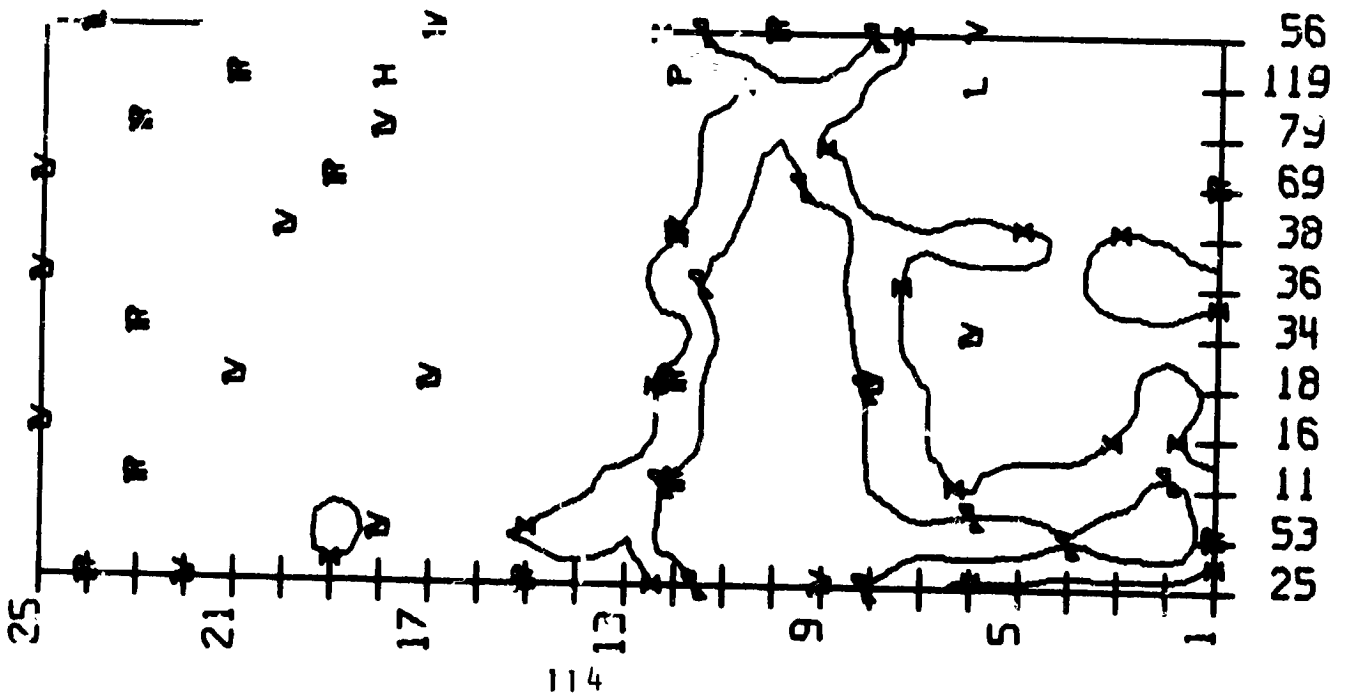
56  
119  
79  
69  
38  
36  
34  
18  
16  
11  
53  
25

VARIATIONS  
50 A

LTP-LO/RO-RTP

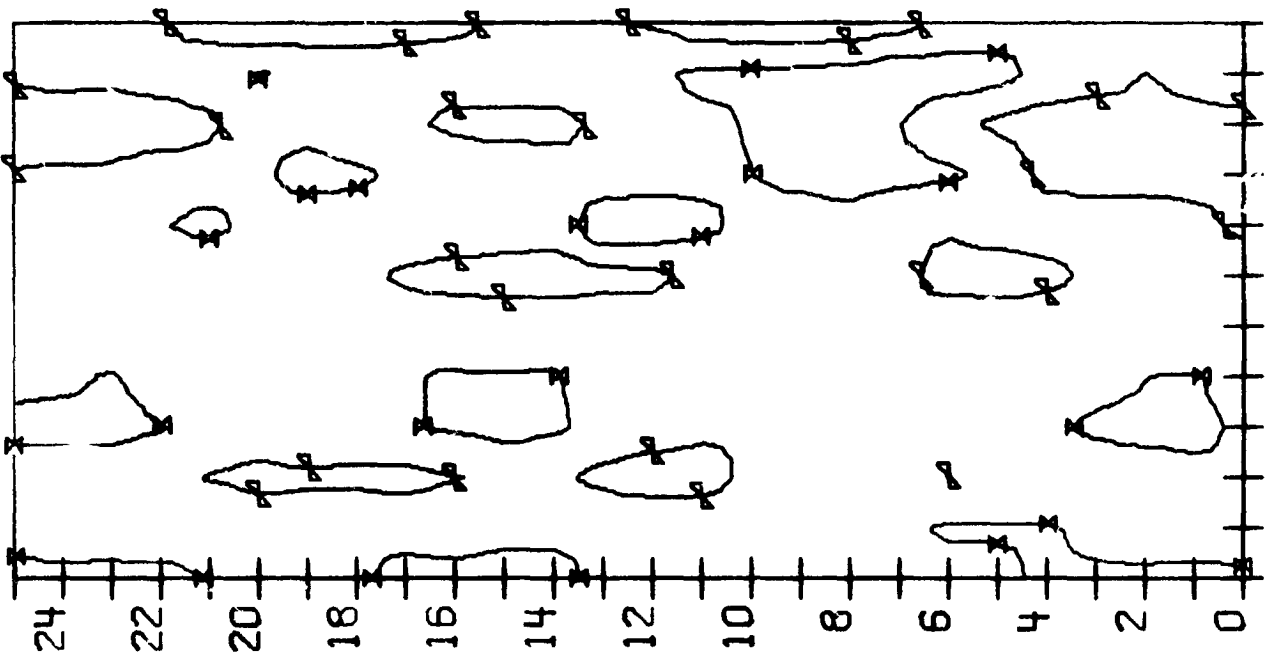


50 A  
LTP-LO/RO-RTP



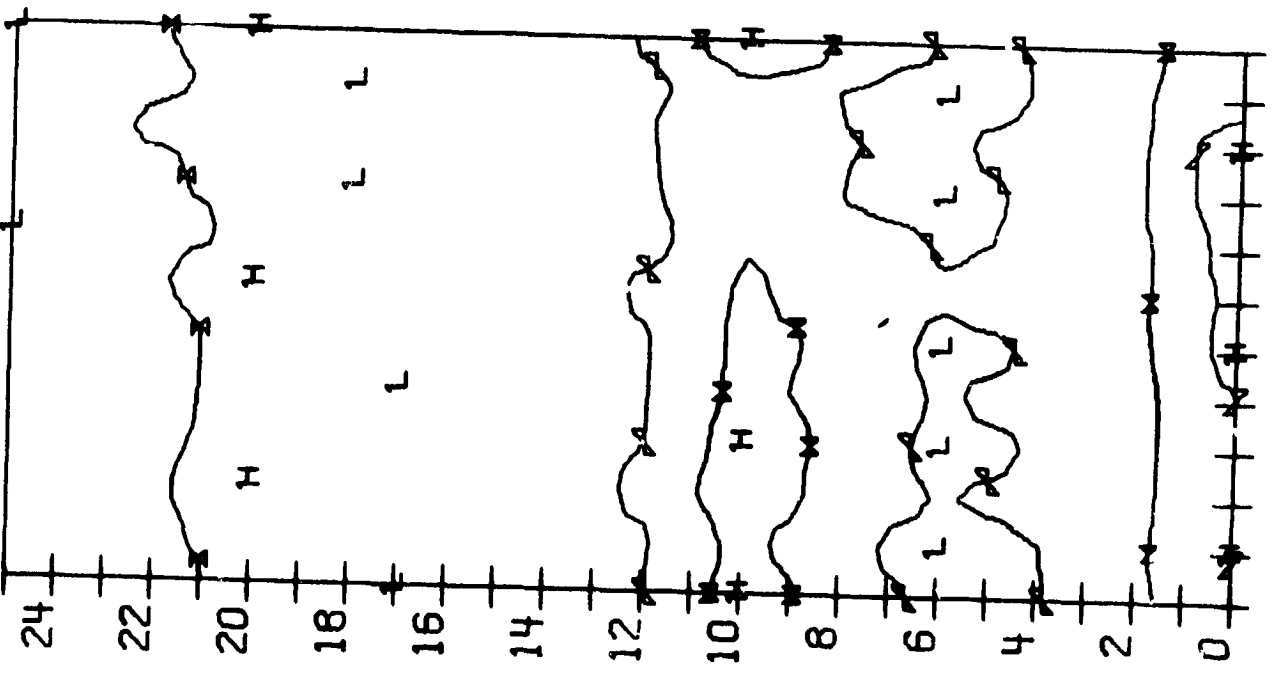
50 SUB

LP-L0



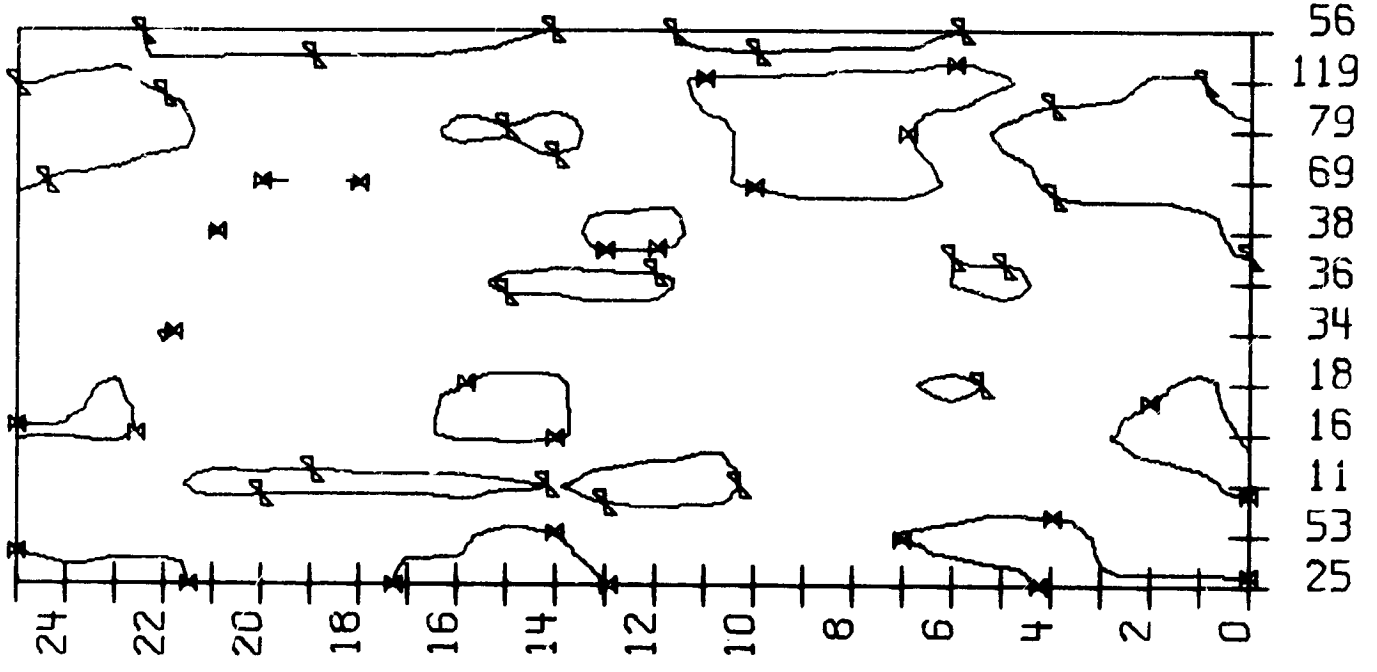
50 SUB

LP-L0



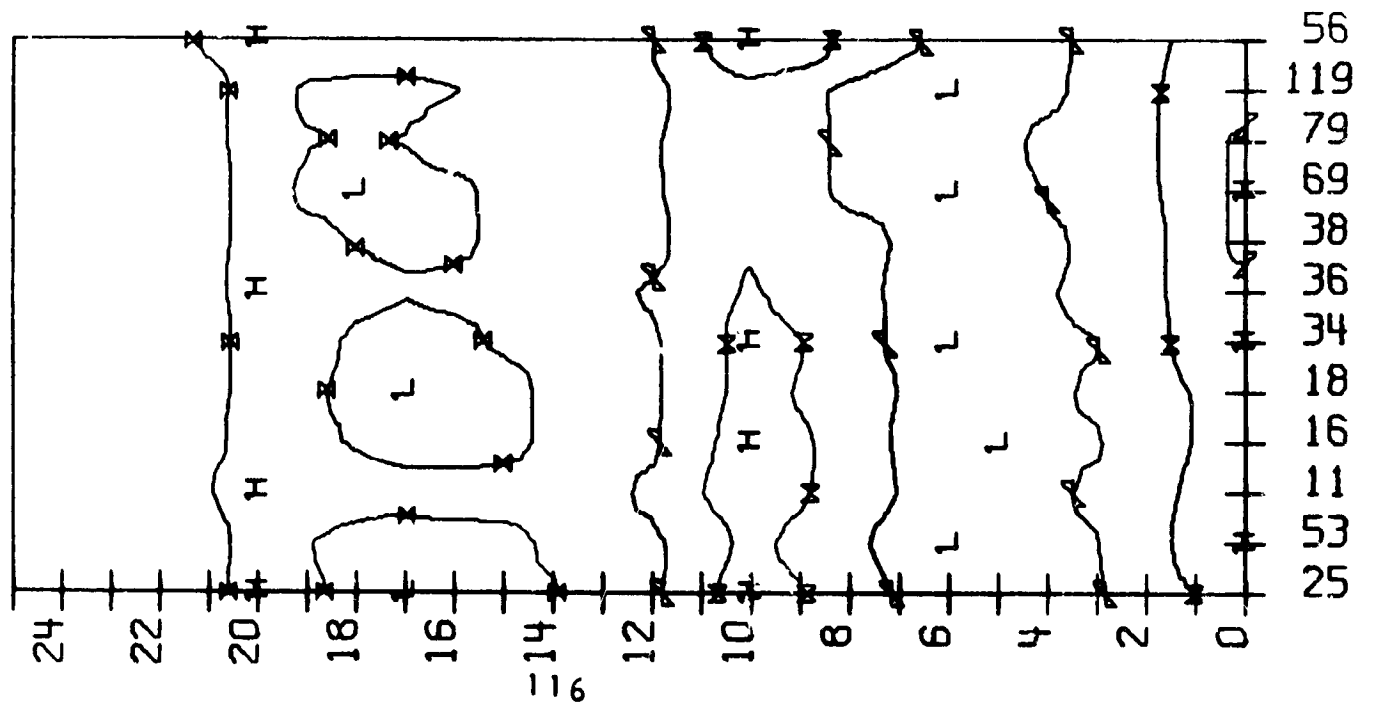
VARIATIONS  
50 SLB

RP-RO



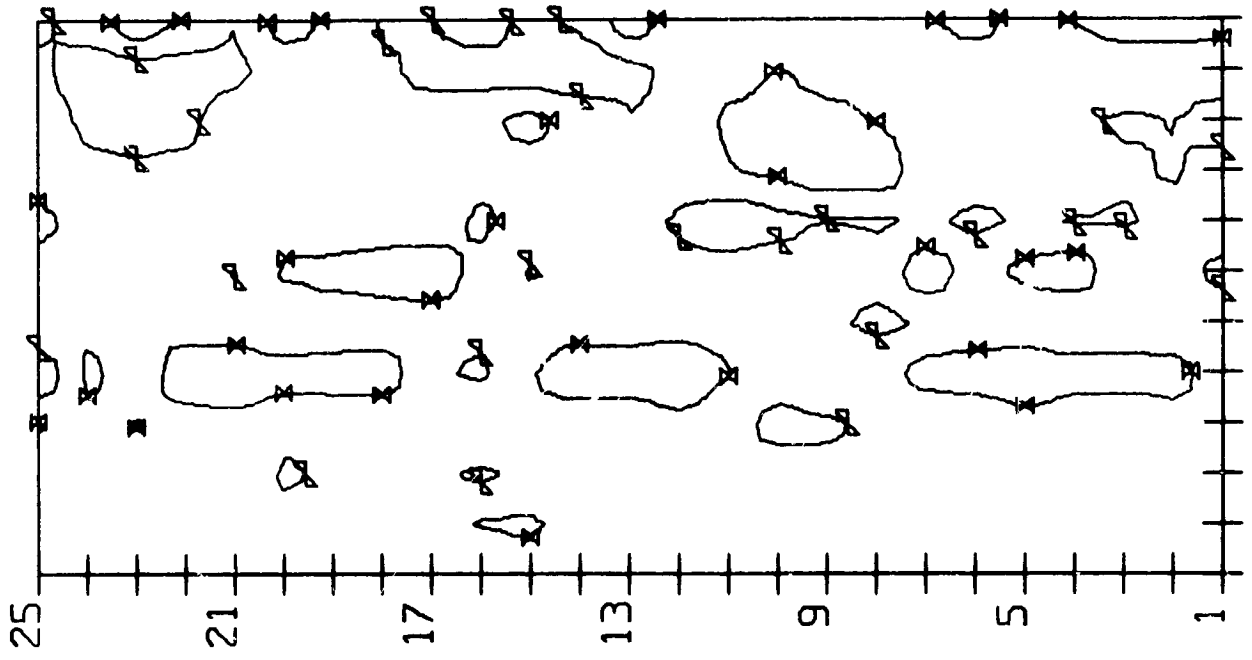
50 SUB

RP-RO



VARIATIONS  
50 SUB

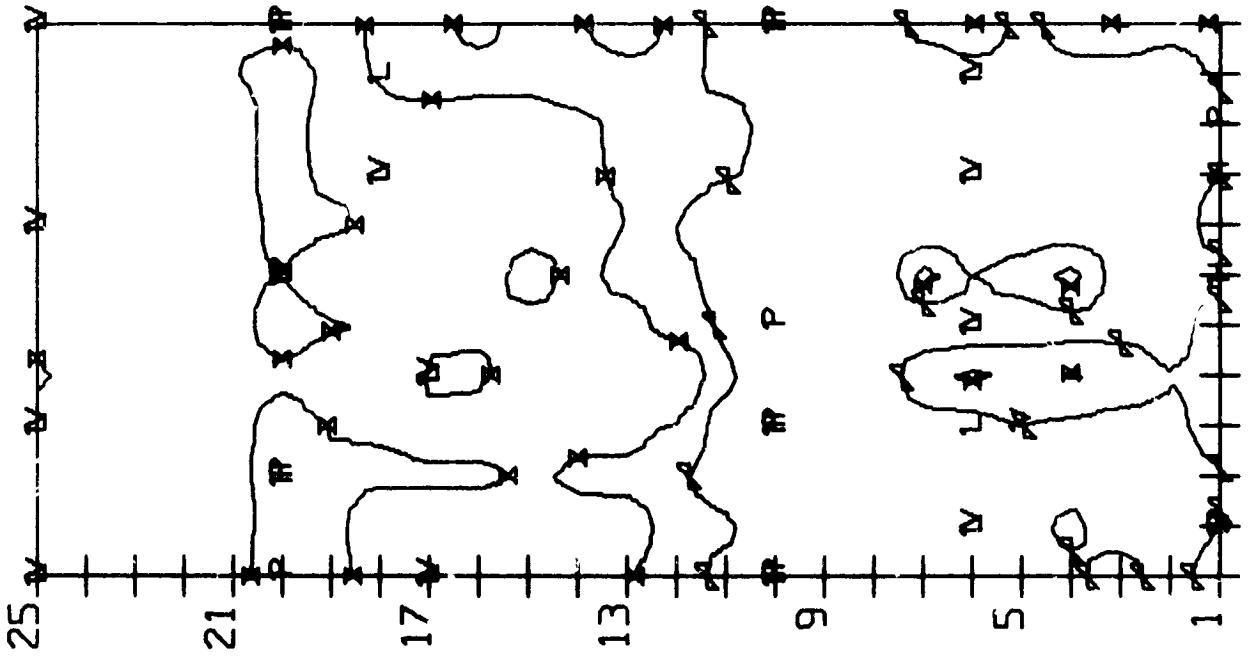
LP-LO/RP-RO



56  
119  
79  
69  
38  
36  
34  
18  
16  
11  
53  
25

50 SUB

LP-LO/RP-RO

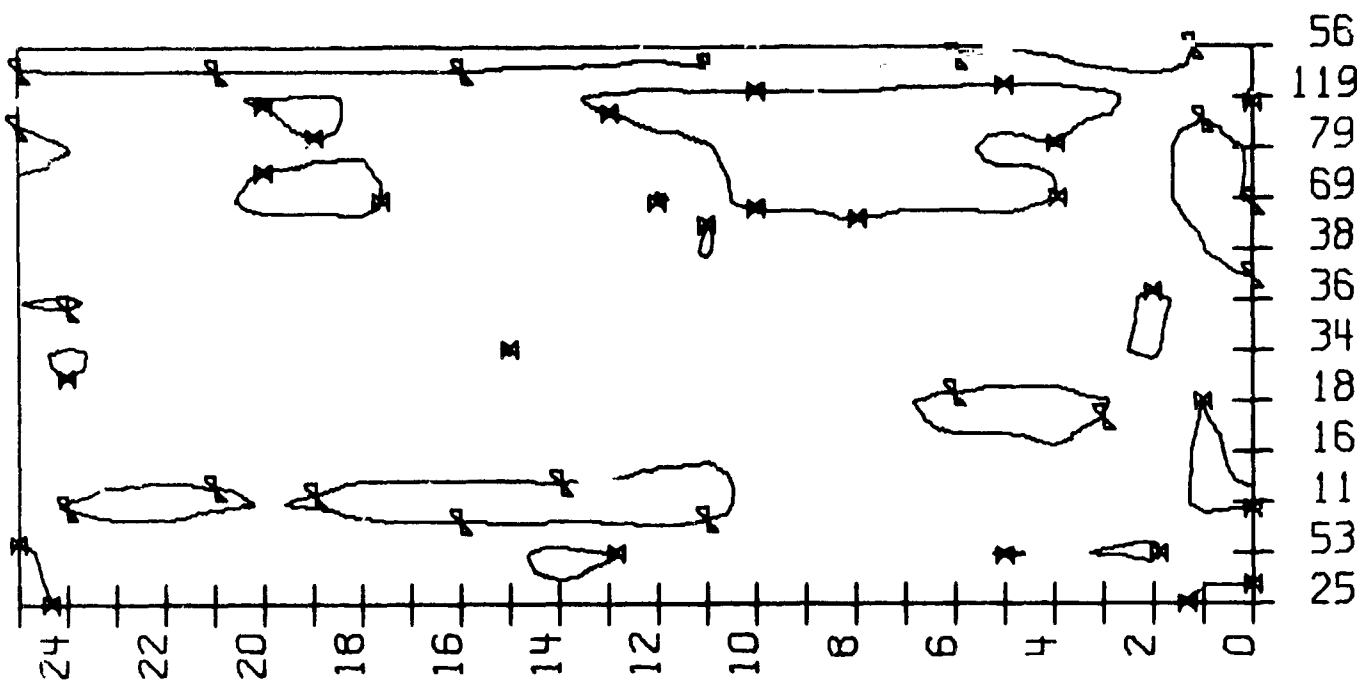


56  
119  
79  
69  
38  
36  
34  
18  
16  
11  
53  
25



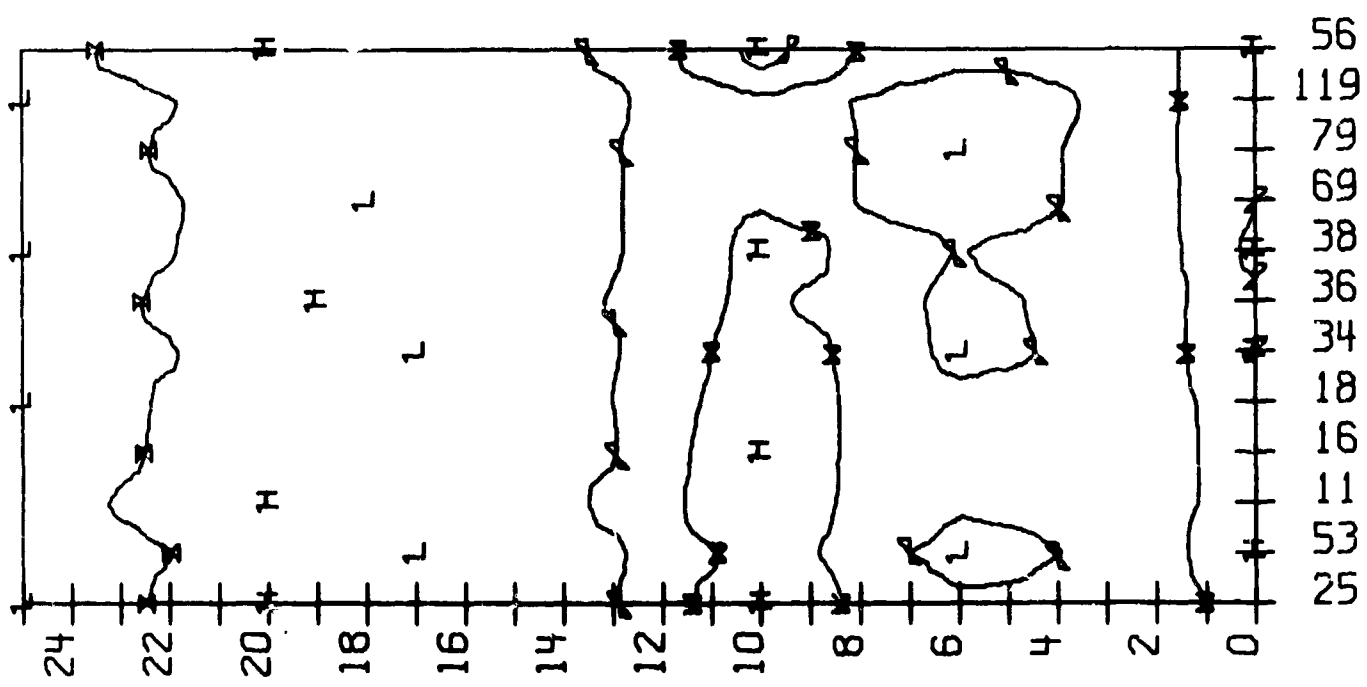
VARIATIONS  
50 SUB

LO-RO



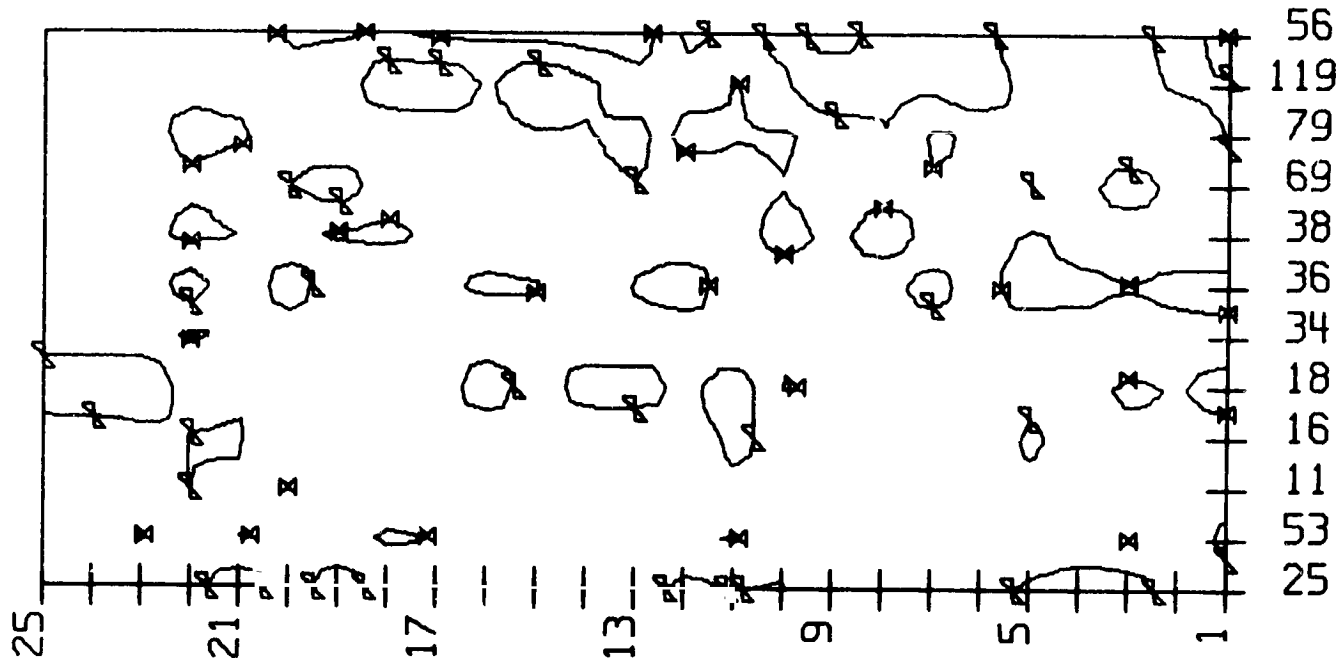
50 SUB

LO-RO



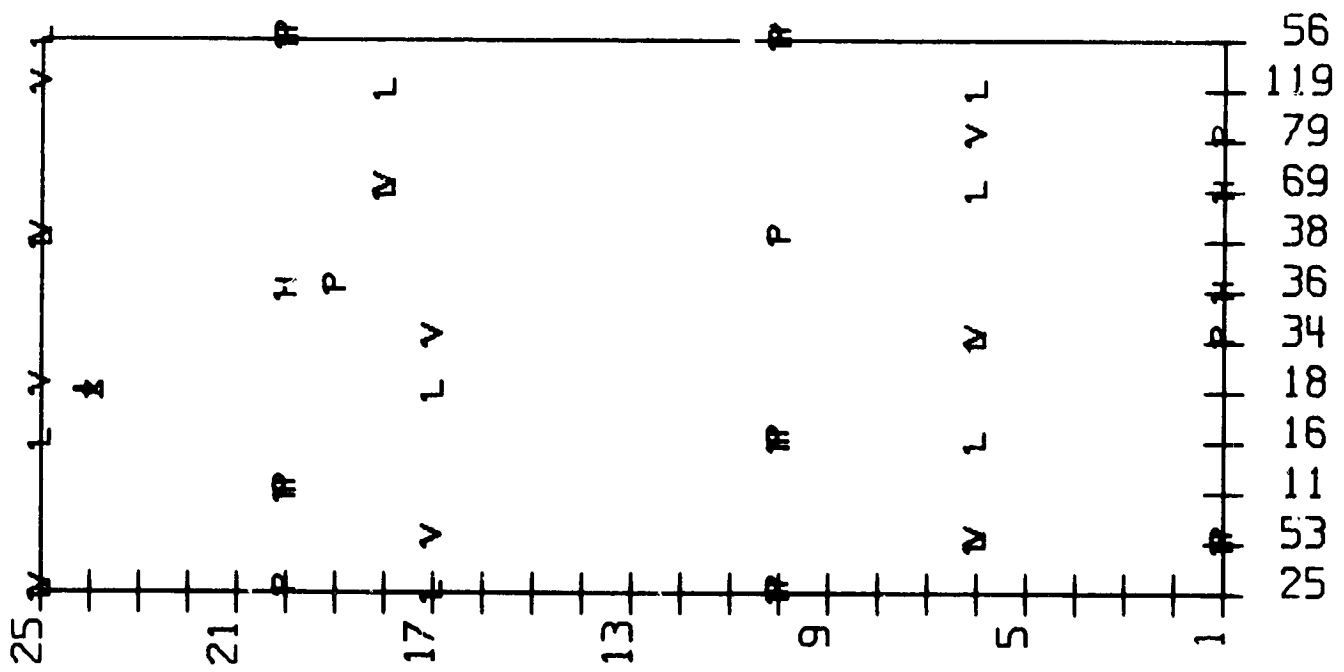
VARIATIONS  
50 SUB

LP-LO/LO-RO



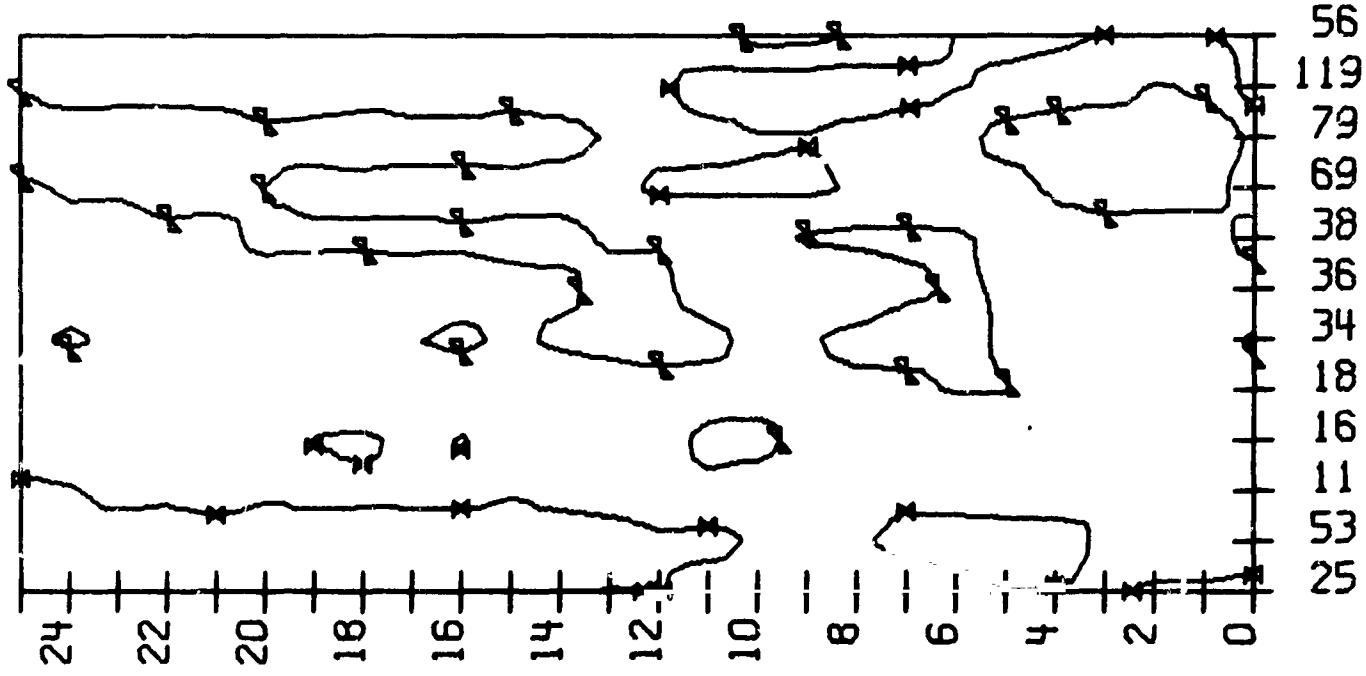
50 SUB

LP-LO/LO-RO



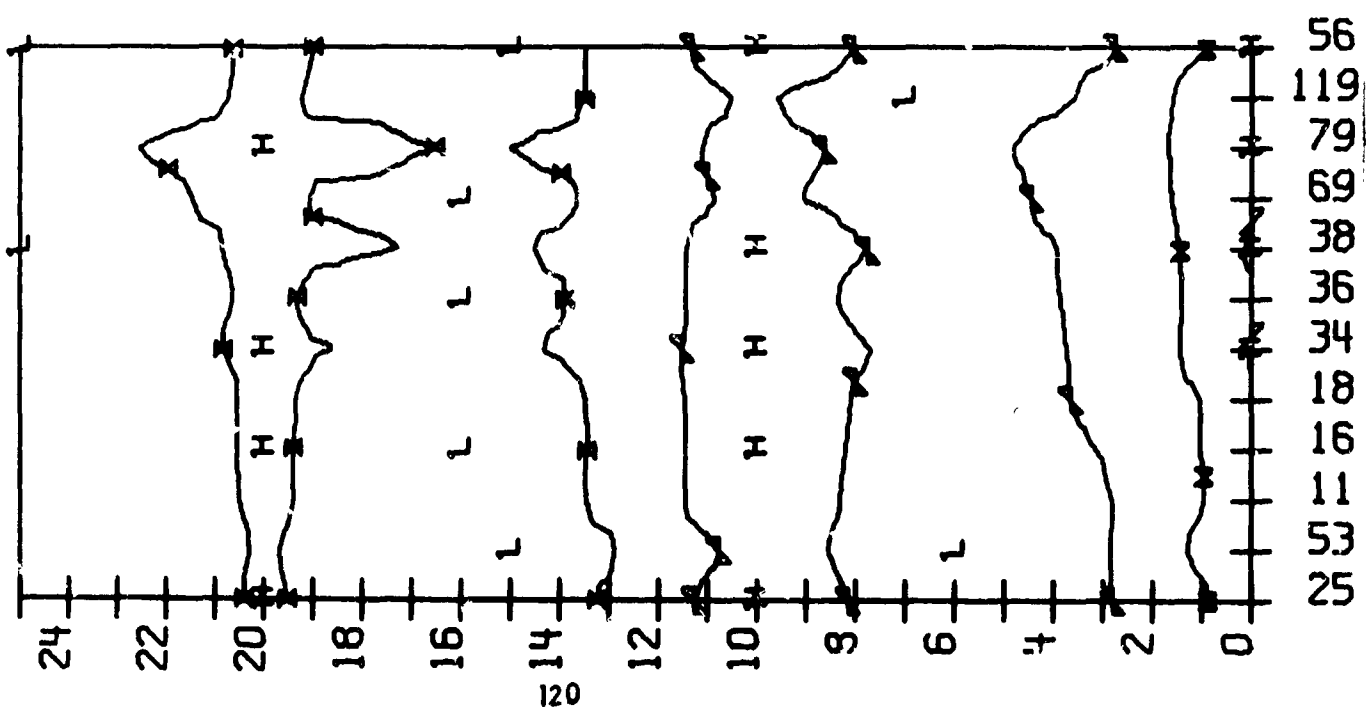
VARIATIONS  
50 A

LC-CZ



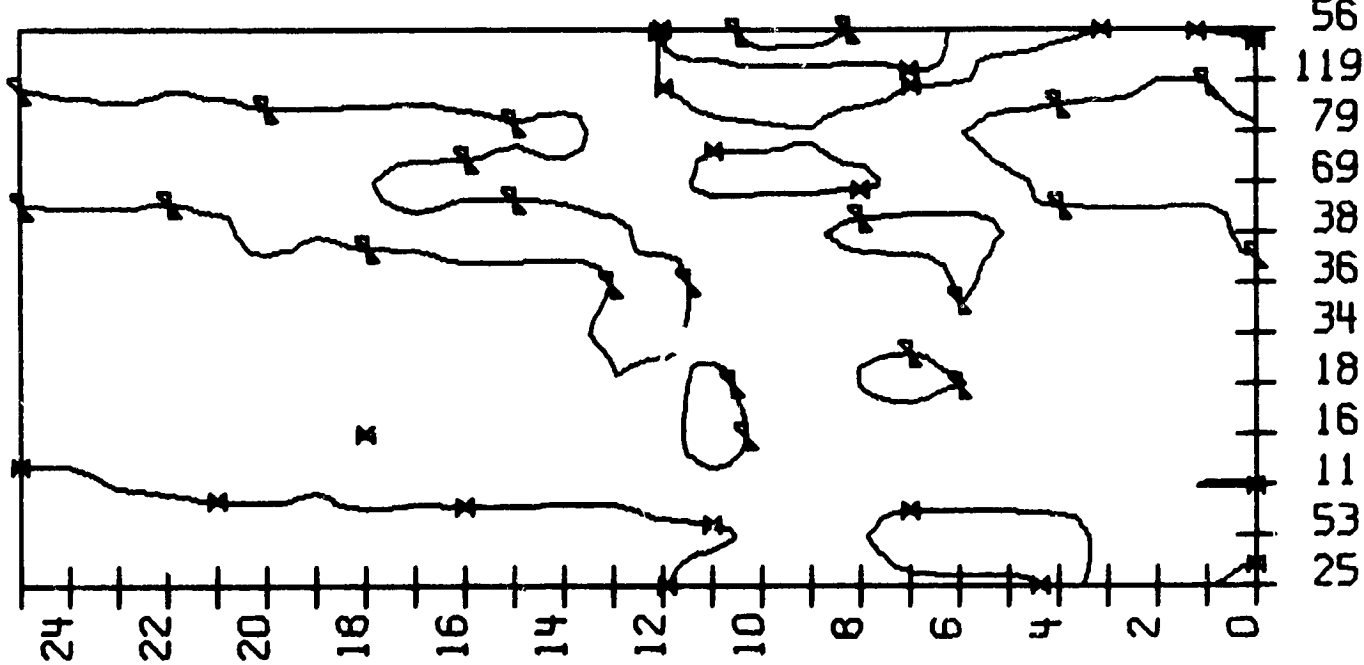
50 A

LC-CZ



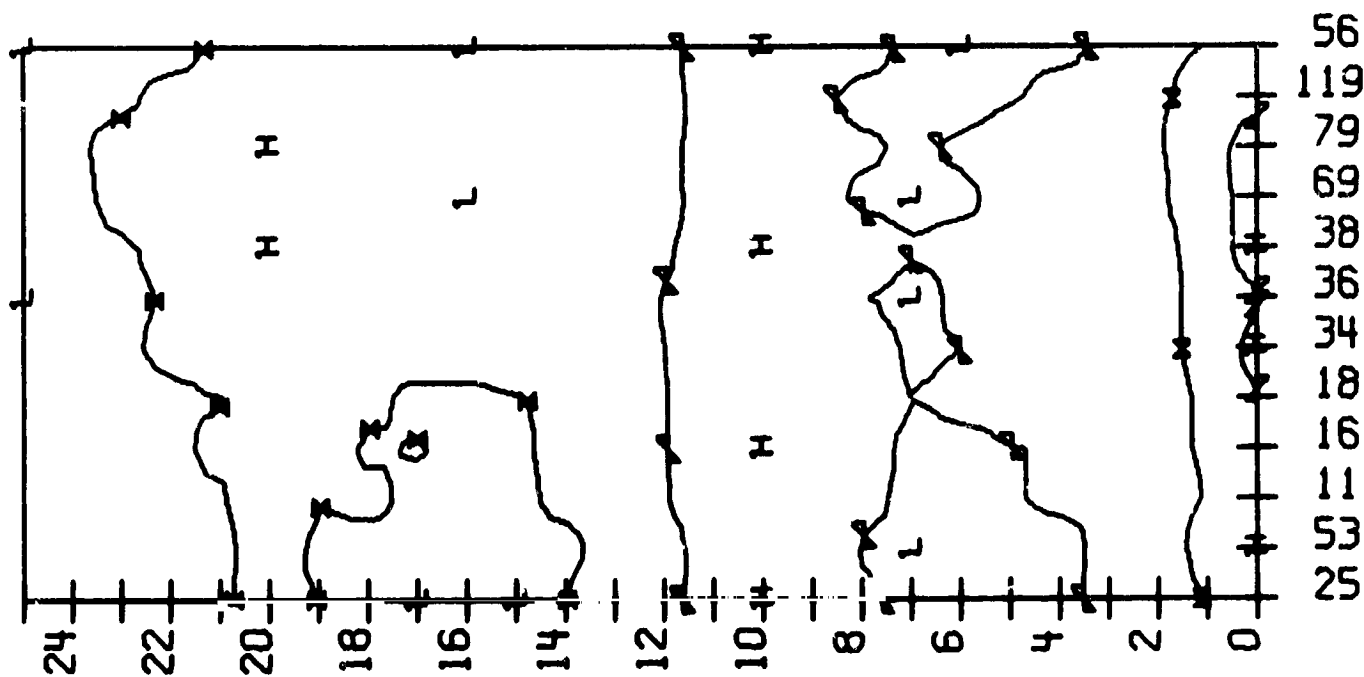
YHRHILUNIS  
50 A

CZ-RC



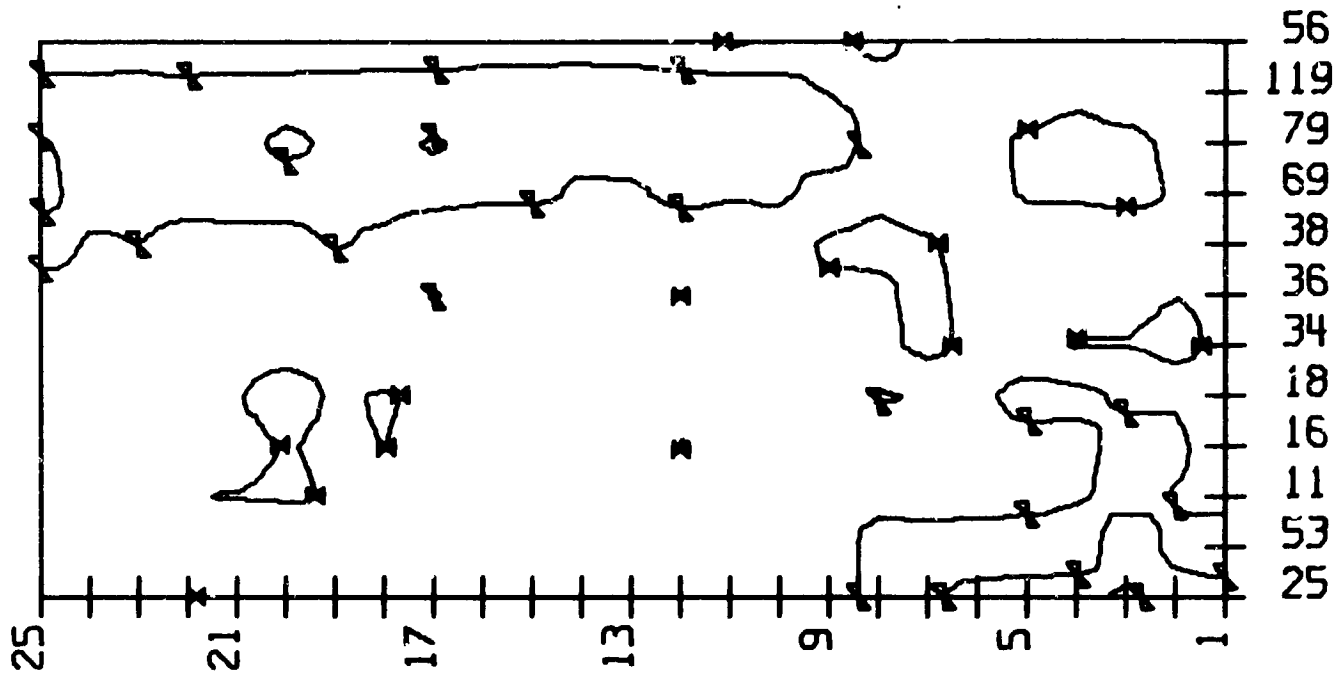
50 A

CZ-RC



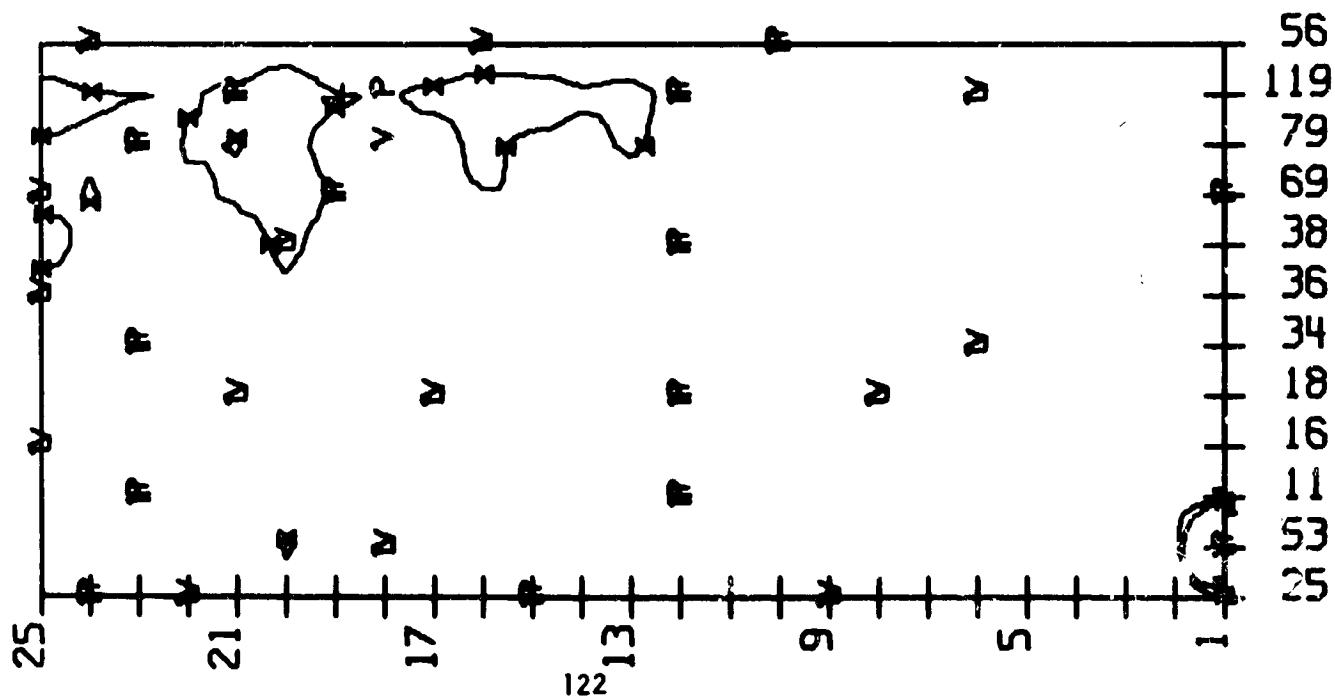
VARIATIONS  
50 A

LC-CZ/CZ-RC



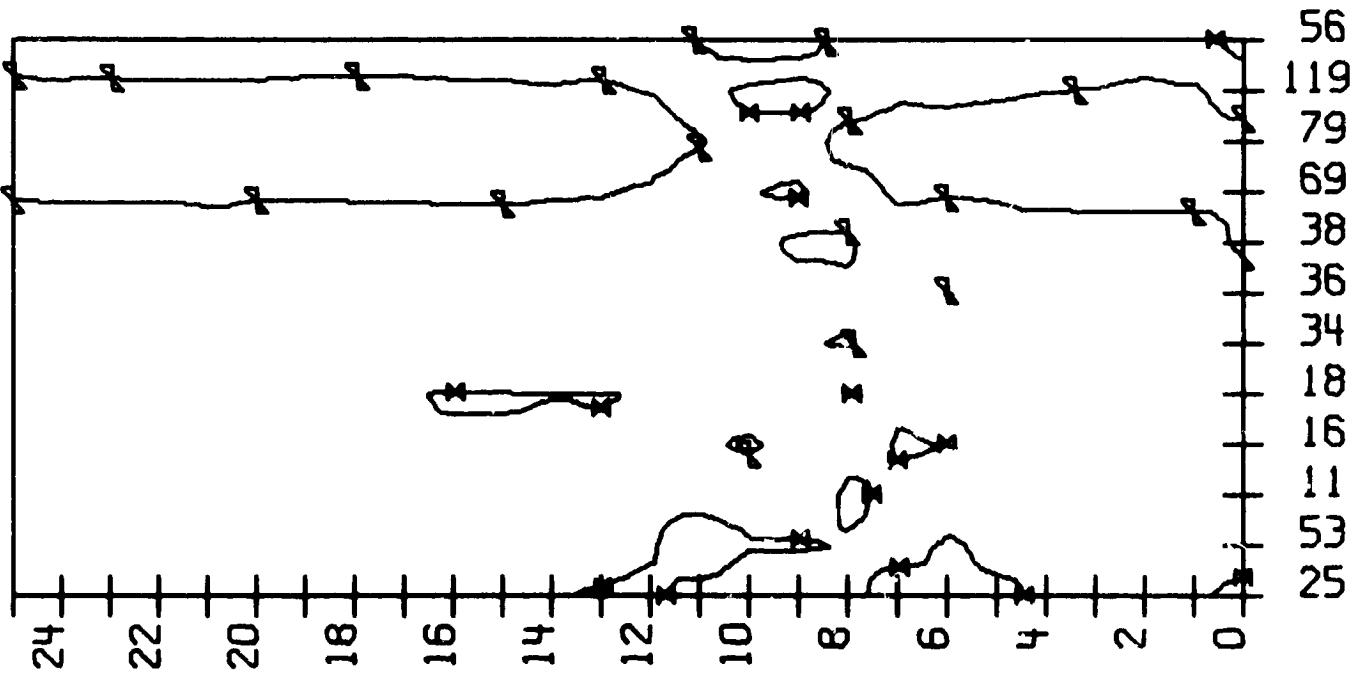
50 A

LC-CZ/CZ-RC



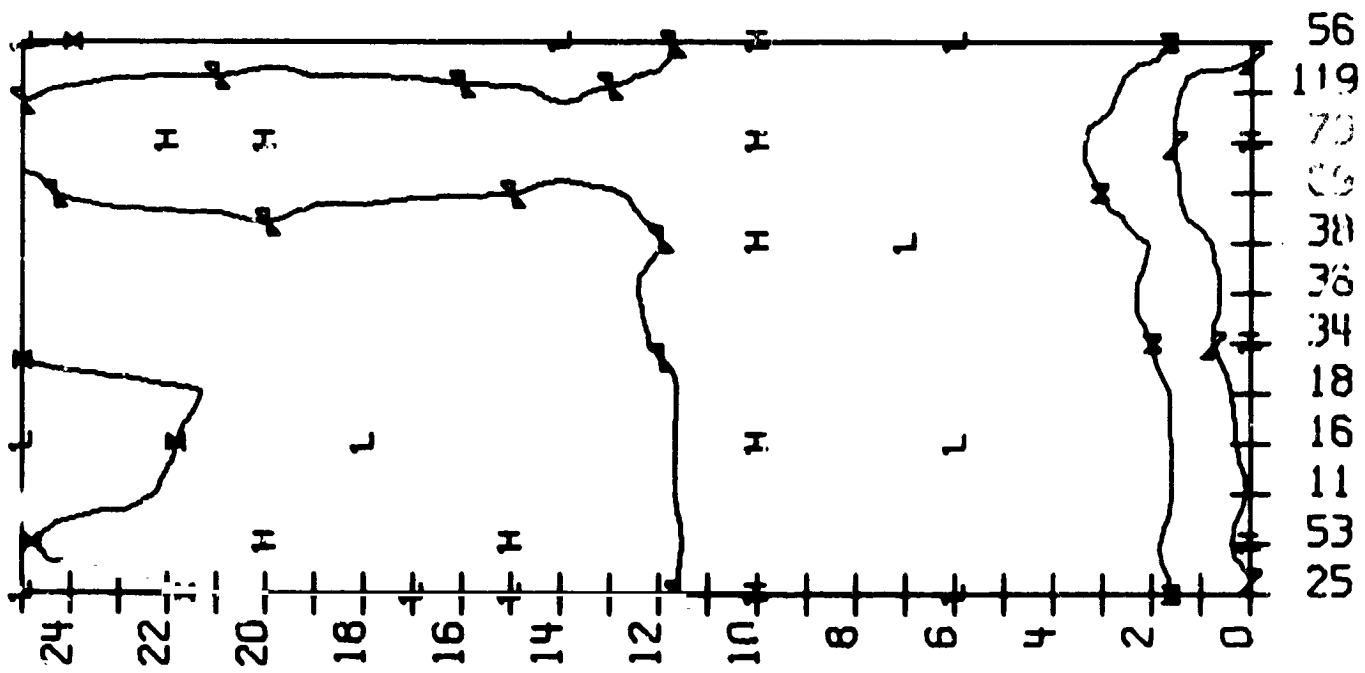
50 A

LT-LC



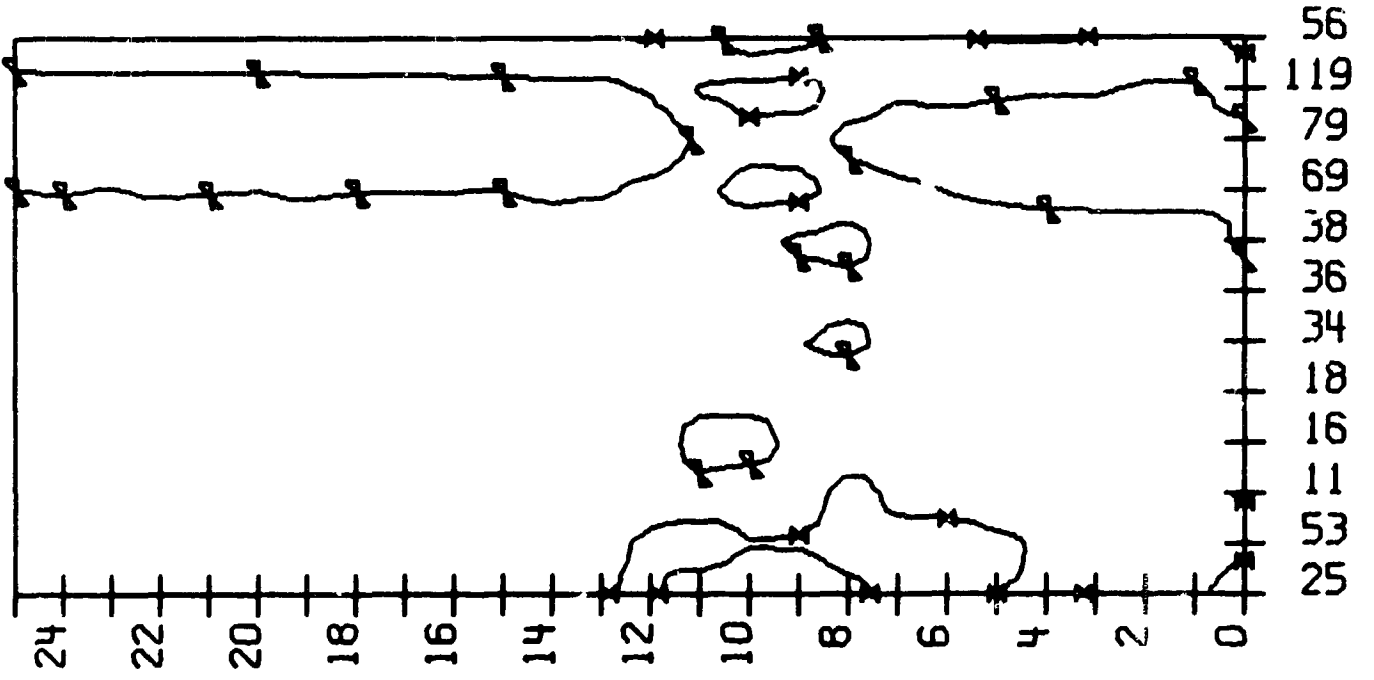
50 A

LT-LC



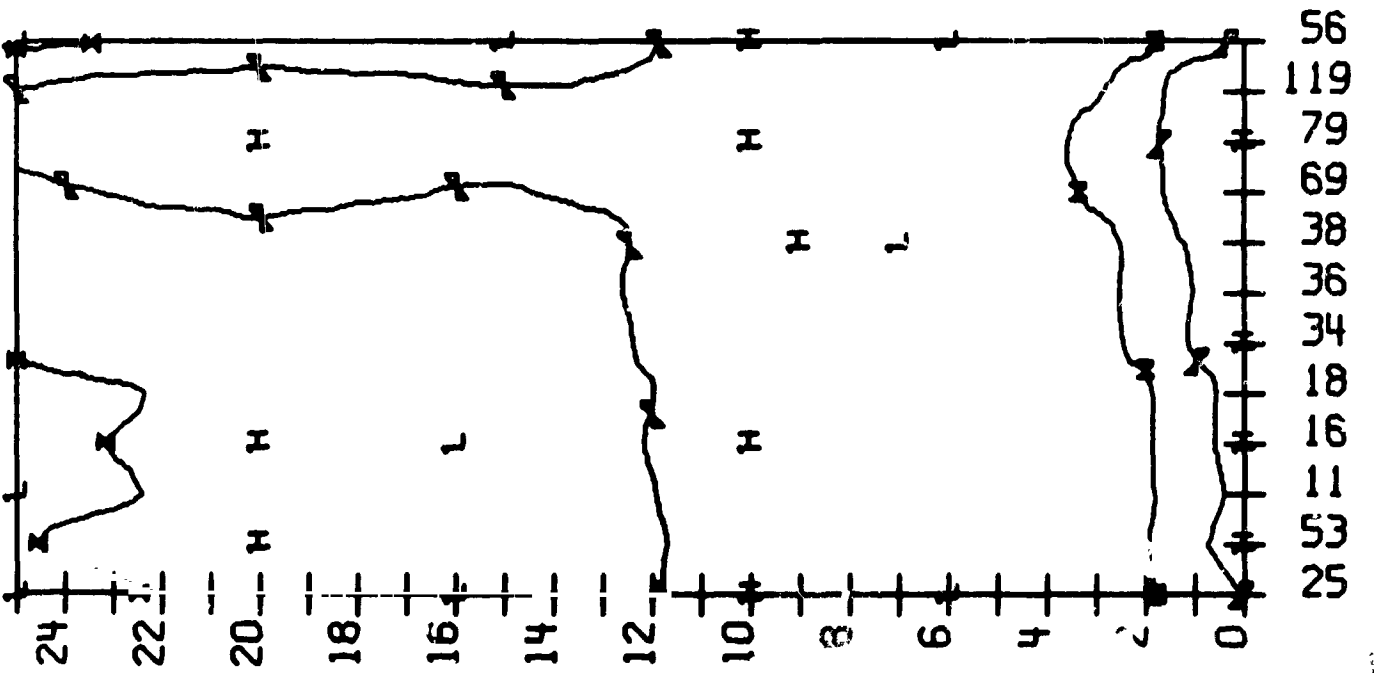
UHKHILJUNS  
50 A

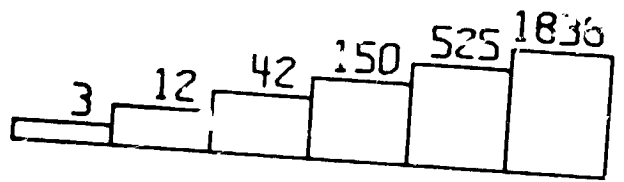
RC-RT



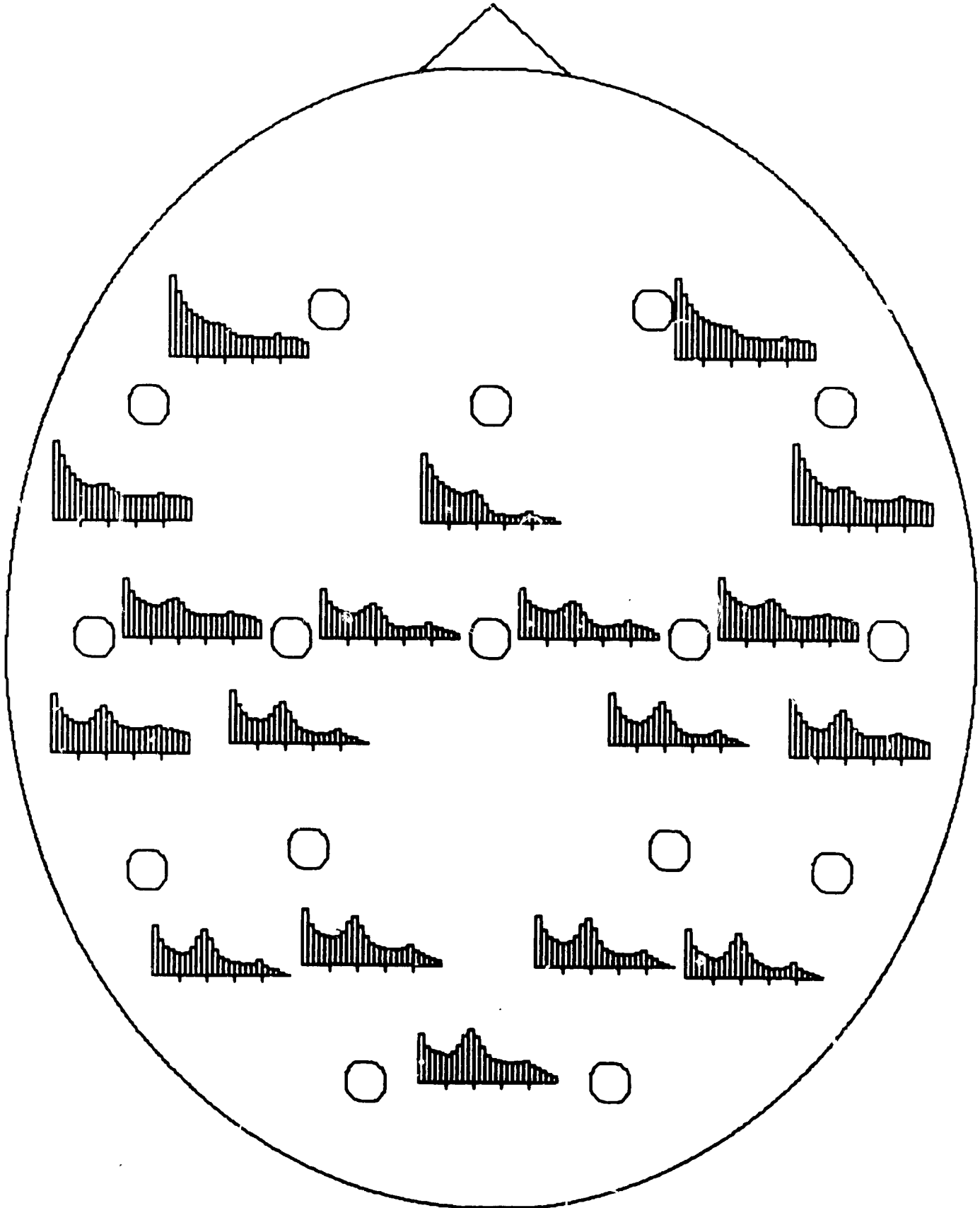
50 A

RC-RT

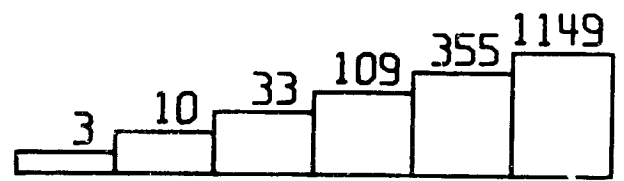




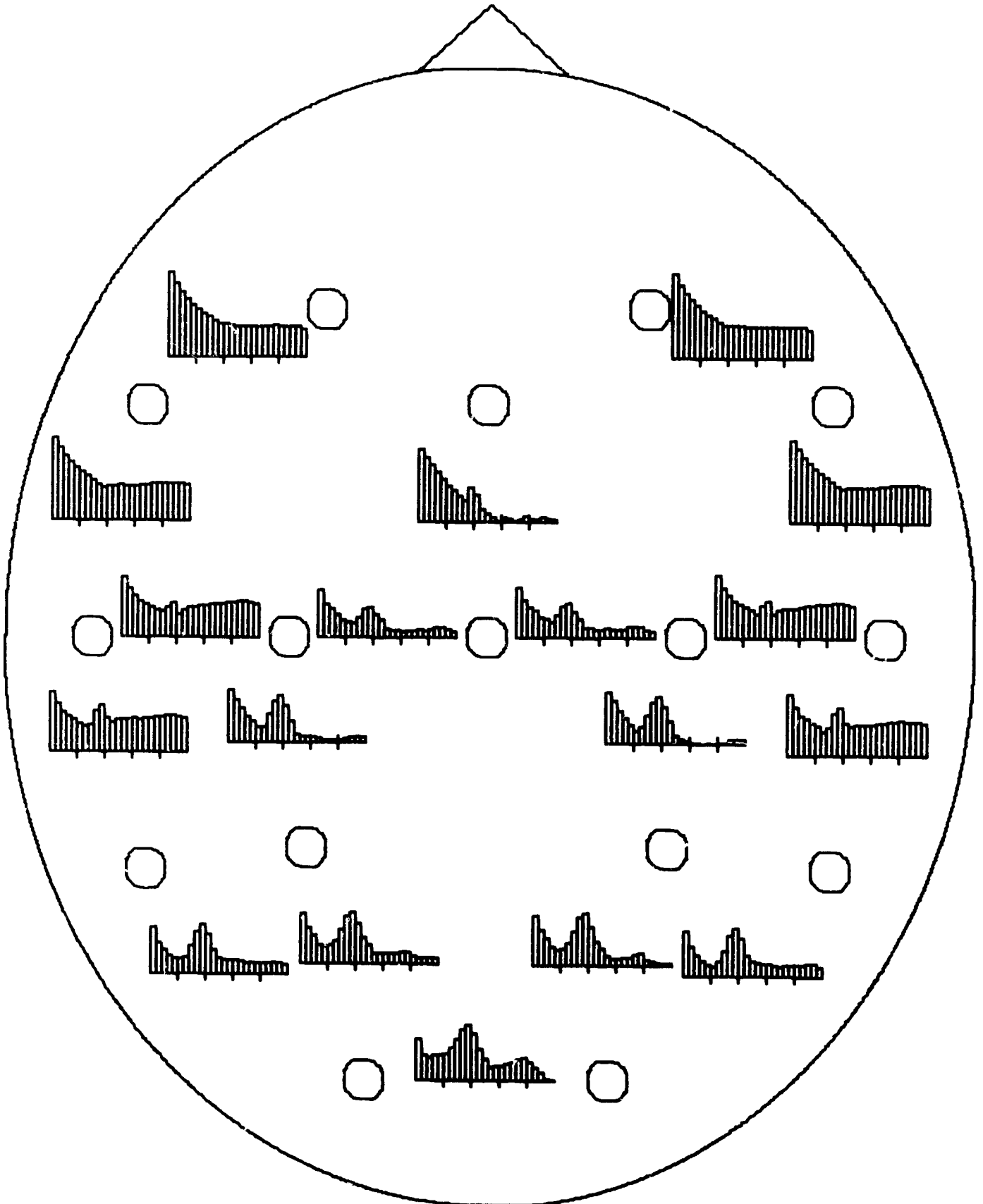
WV - AVERAGE

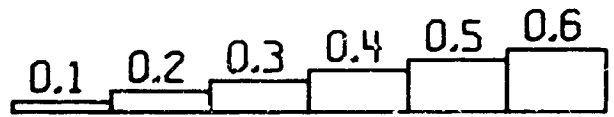




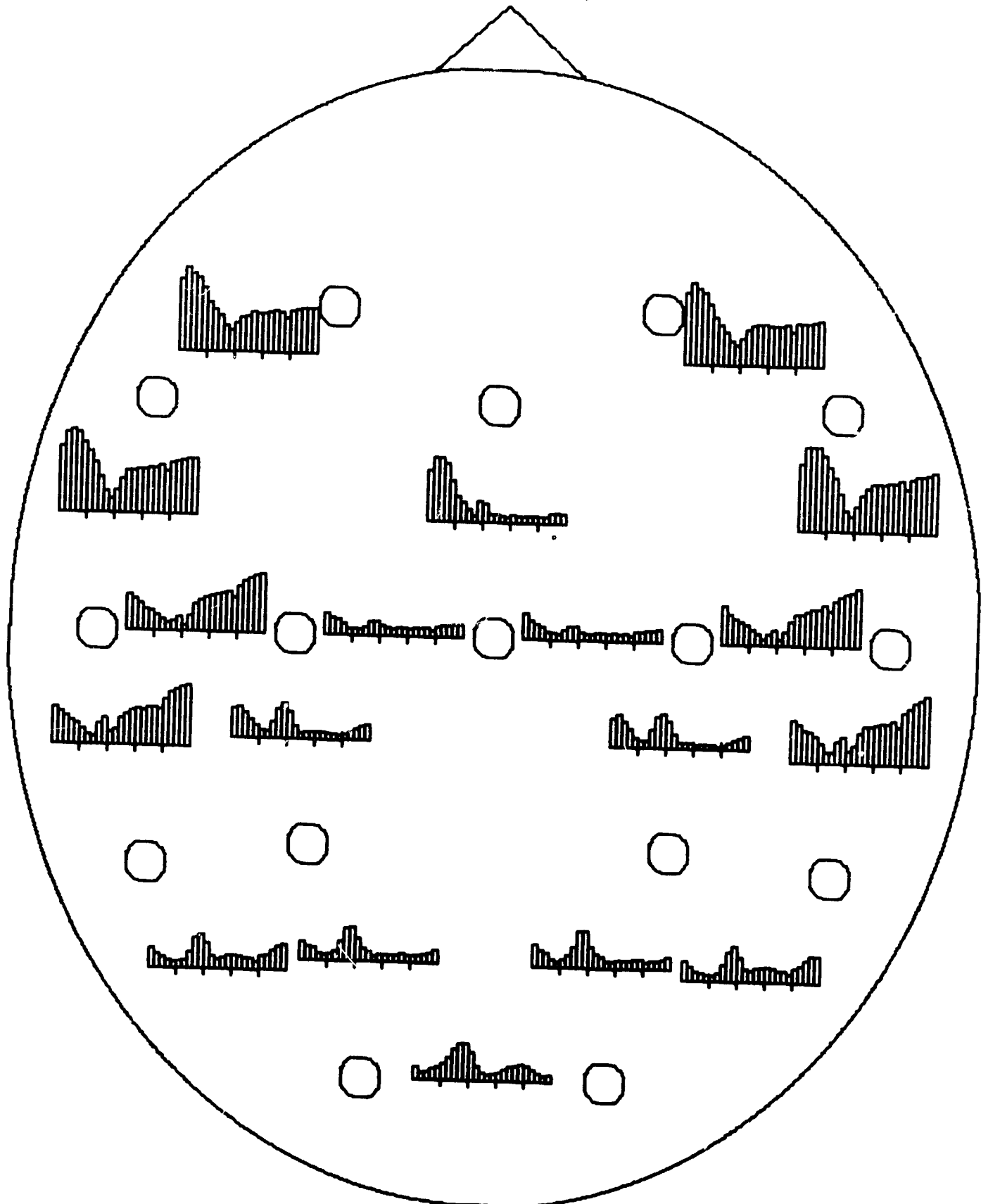


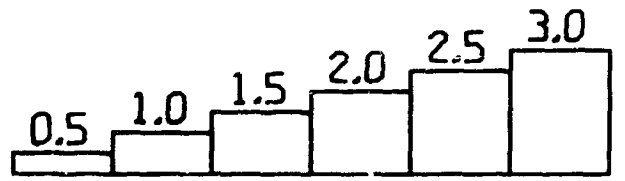
WV - STD. DEV.





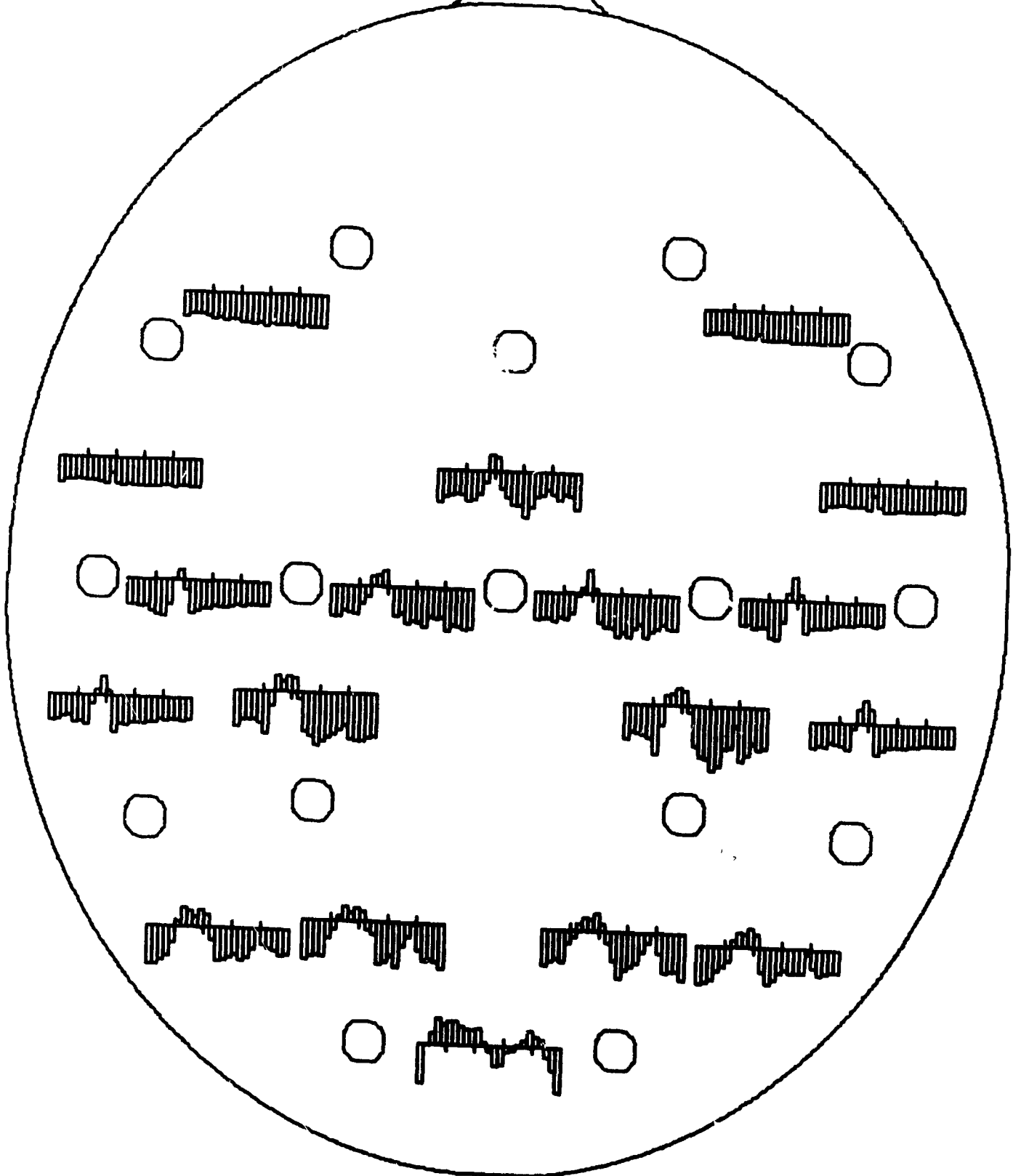
WV-COEF. OF VAR.



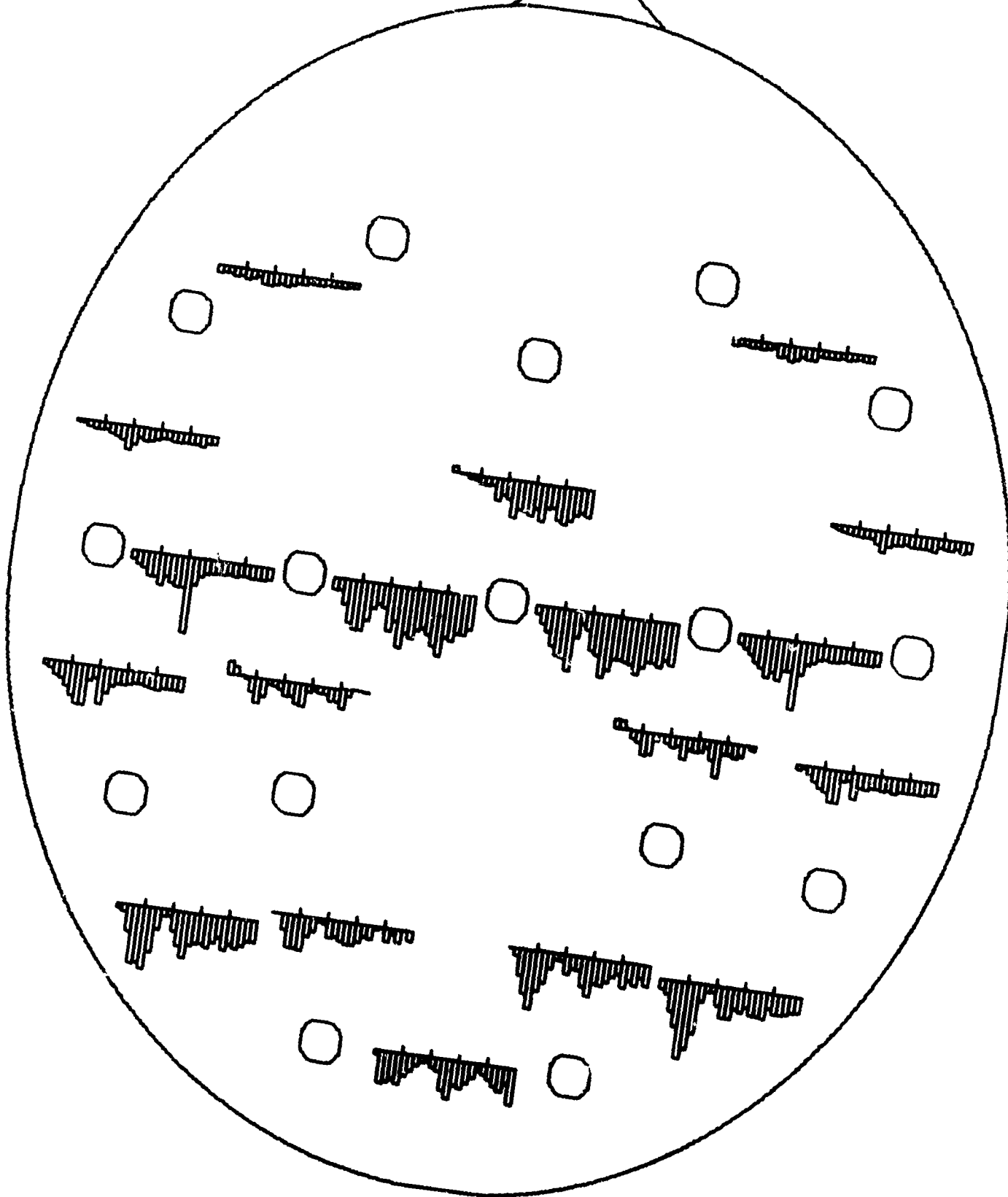


WV - CODE 25

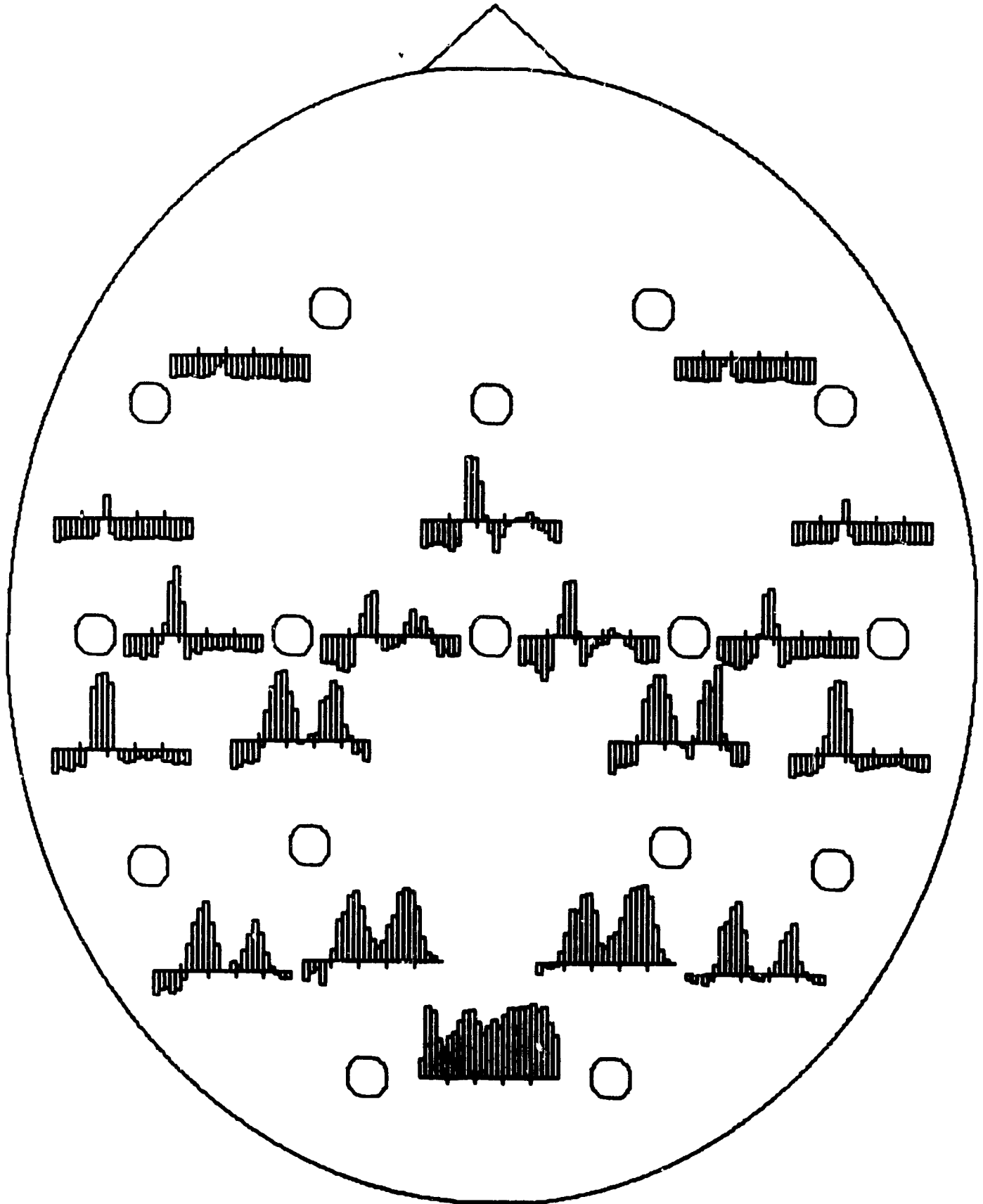
50 SUB + NEW 53



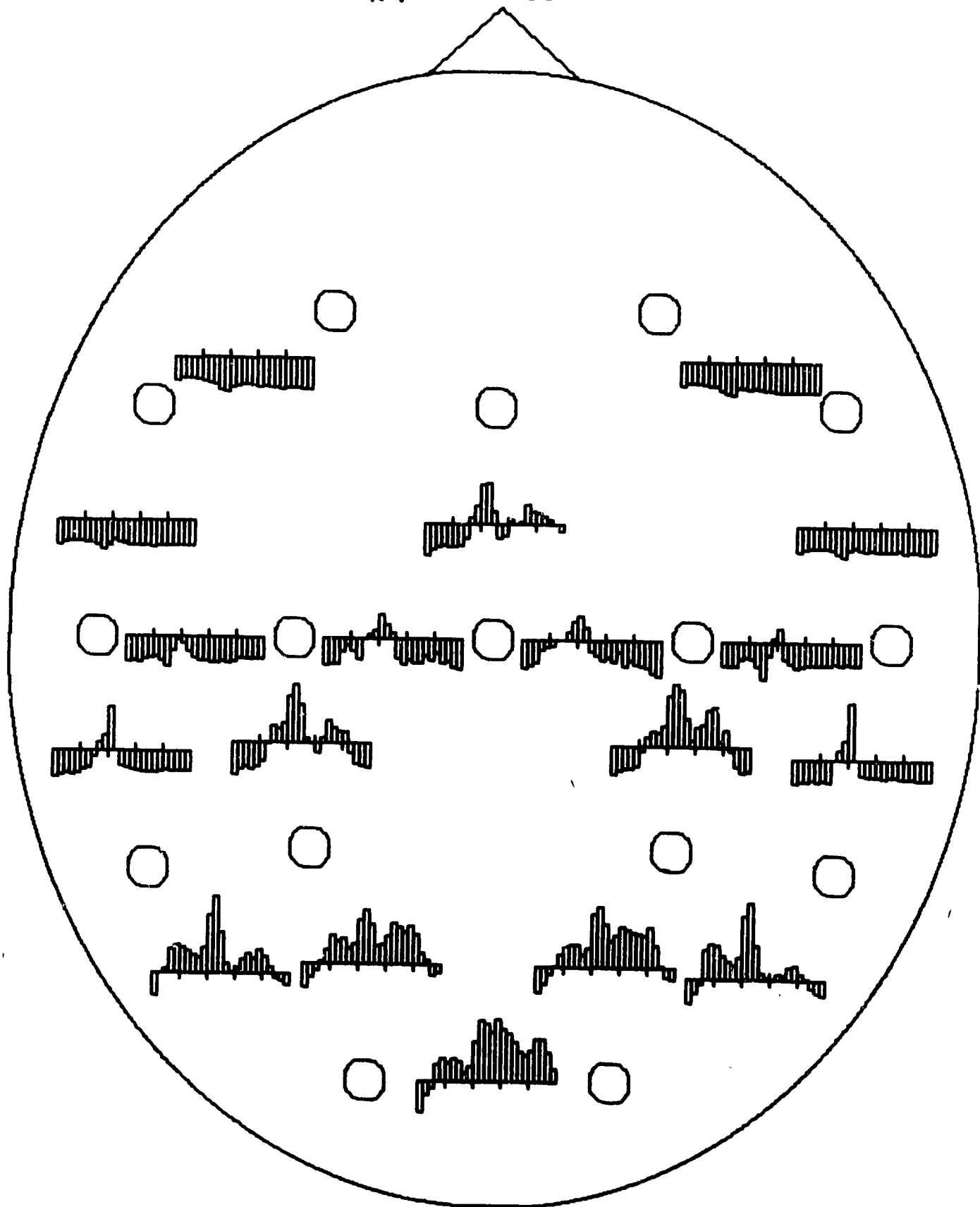
WV - CODE 53



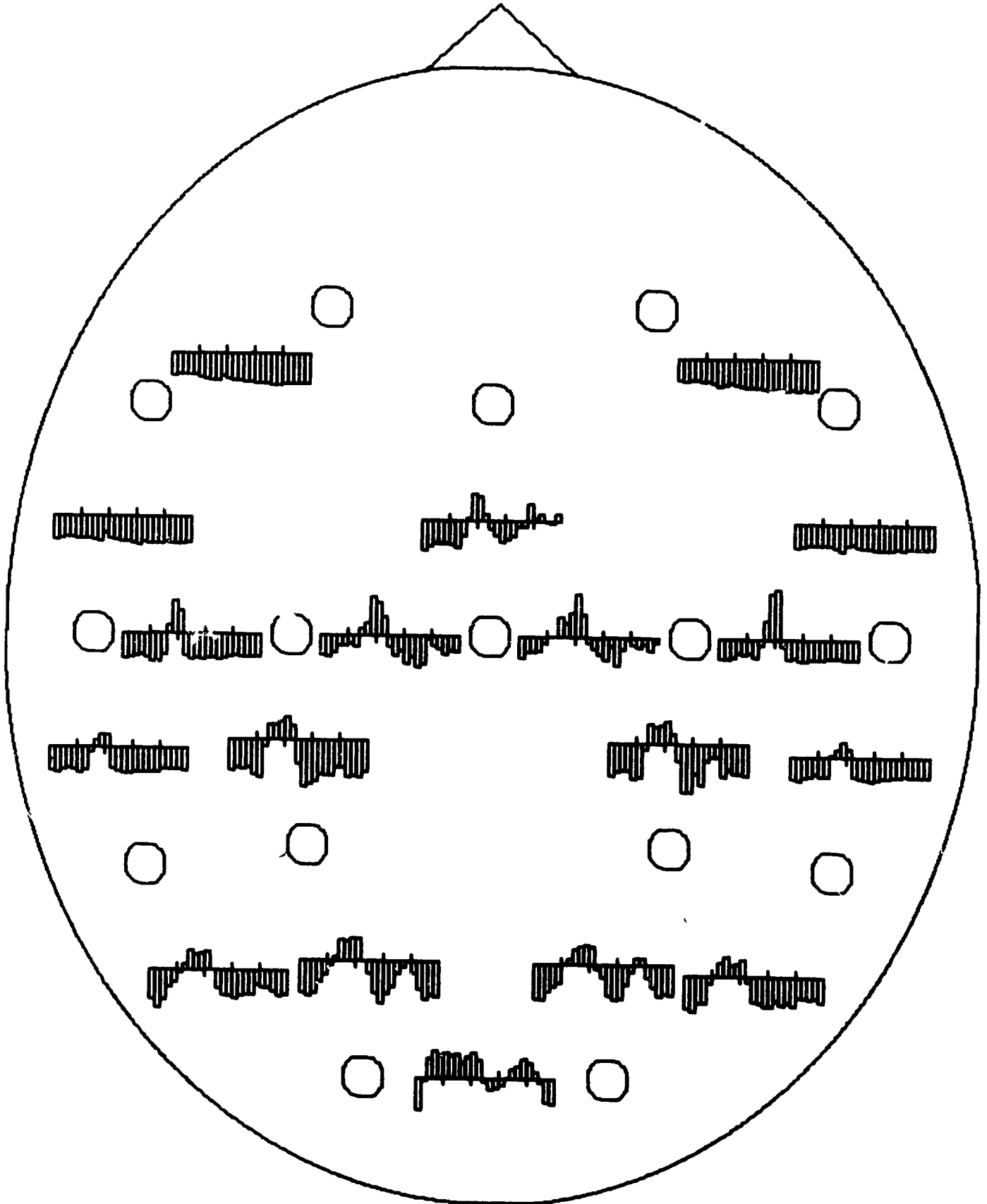
WV-CODE 56



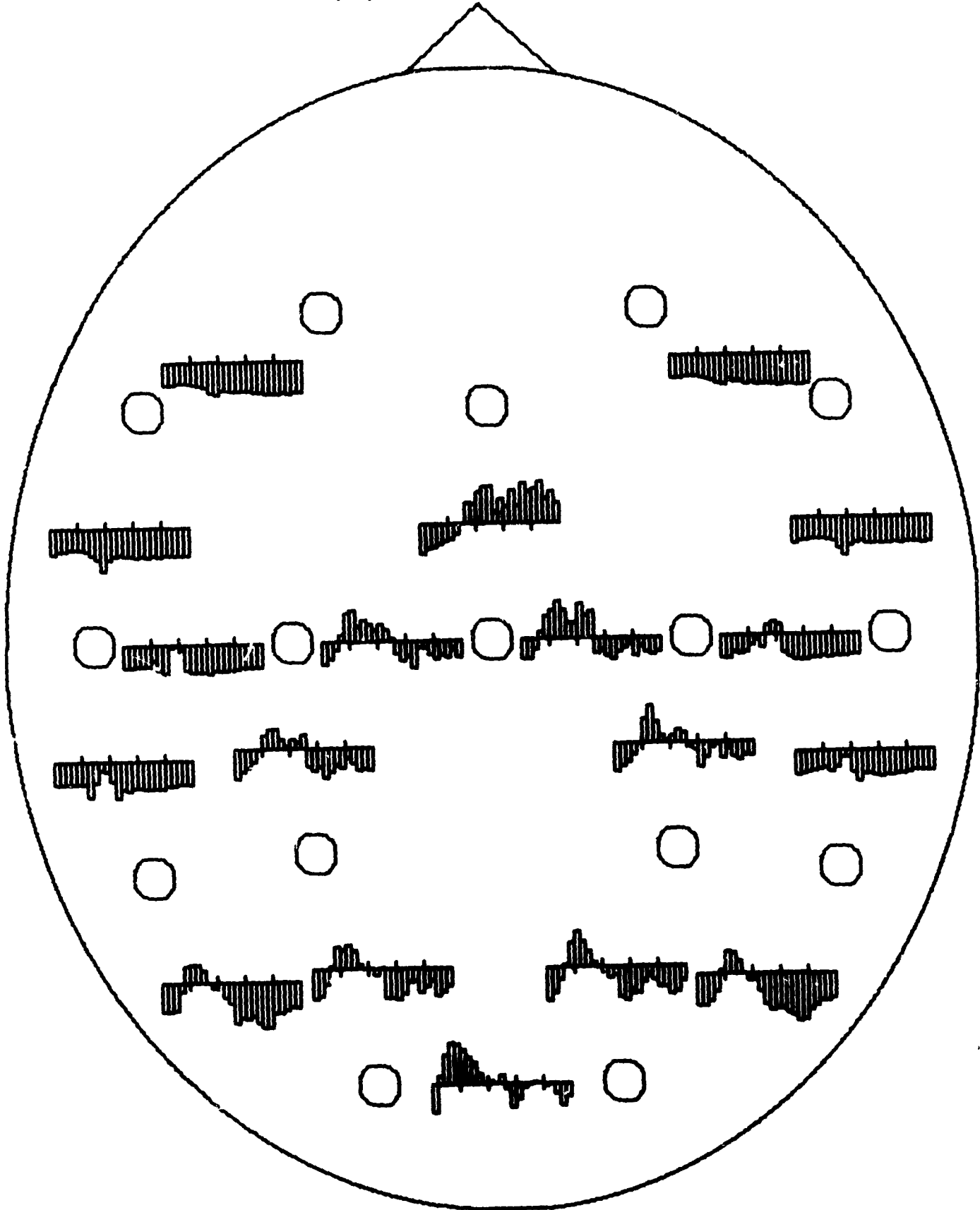
WV-CODE 11



WV - CODE 16

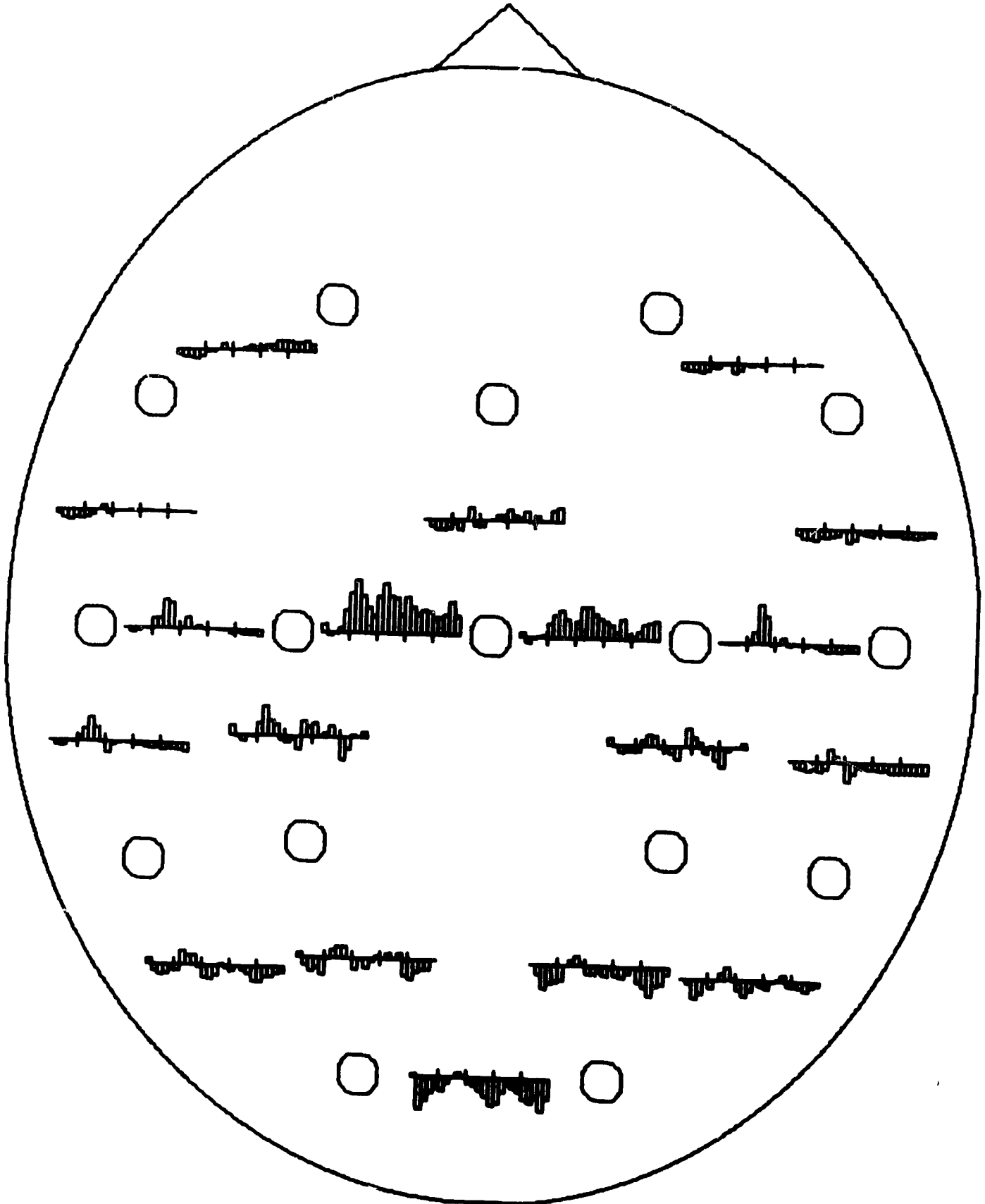


WV-CODE 18

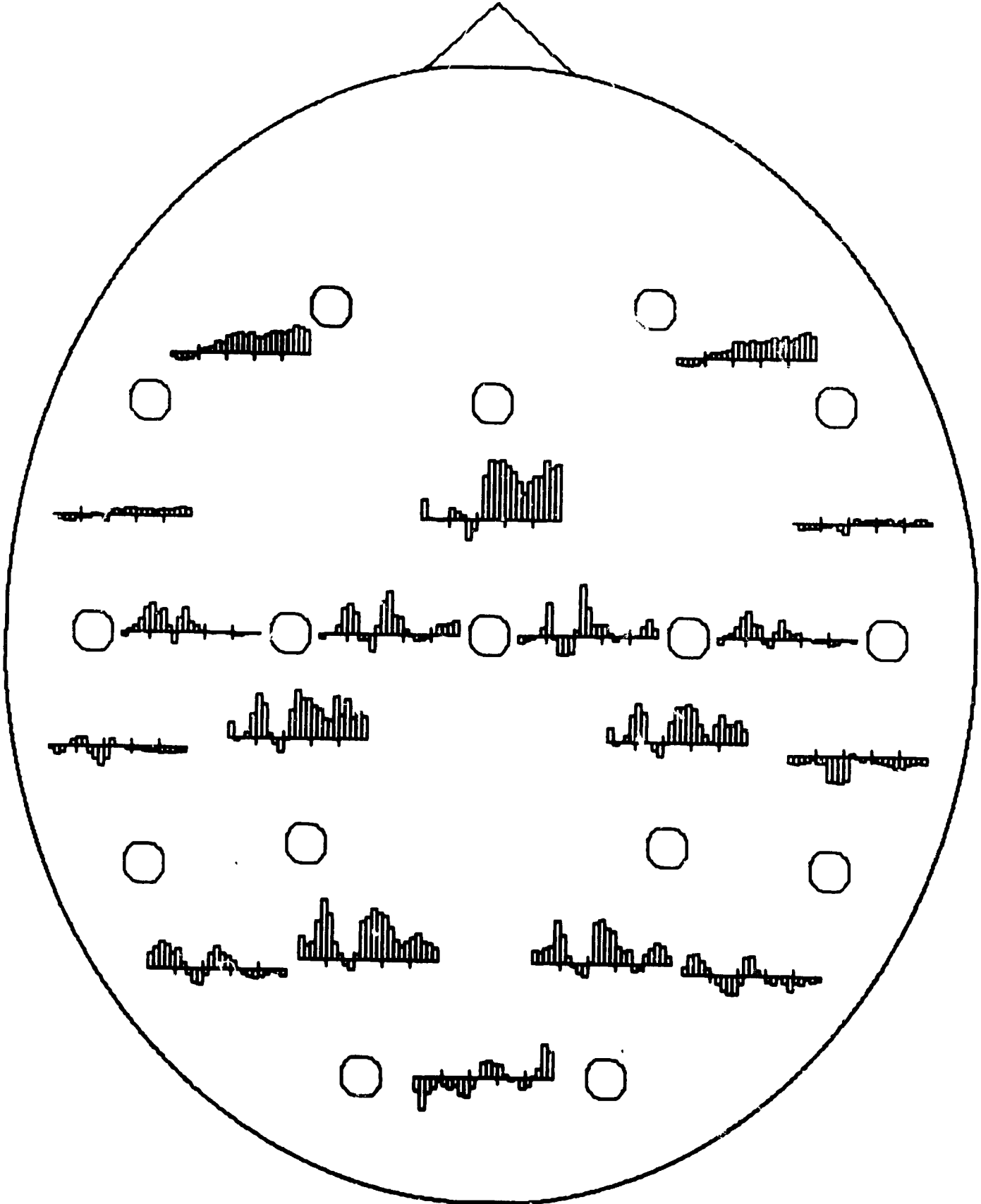




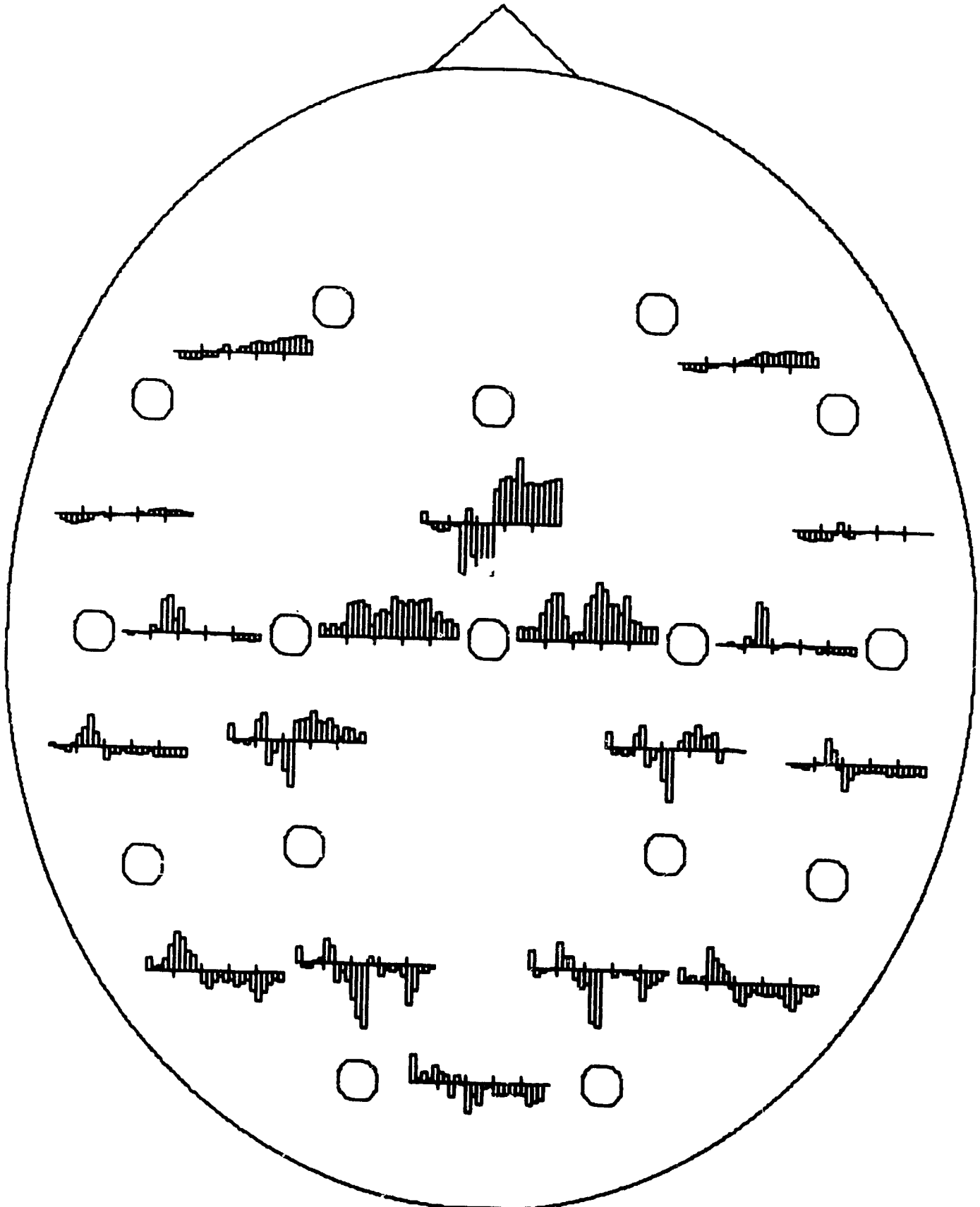
WV-CODE 34



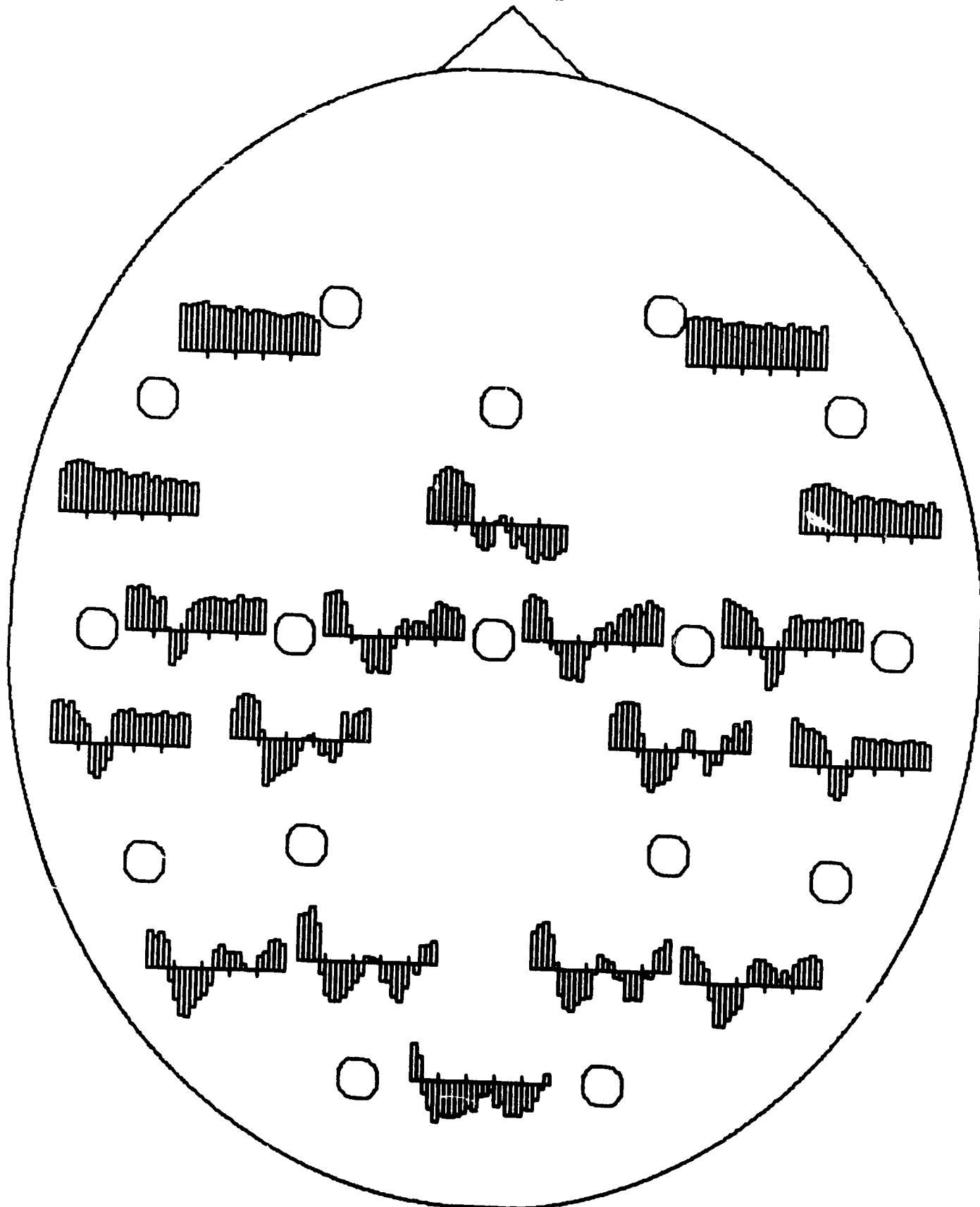
WV - CODE 36



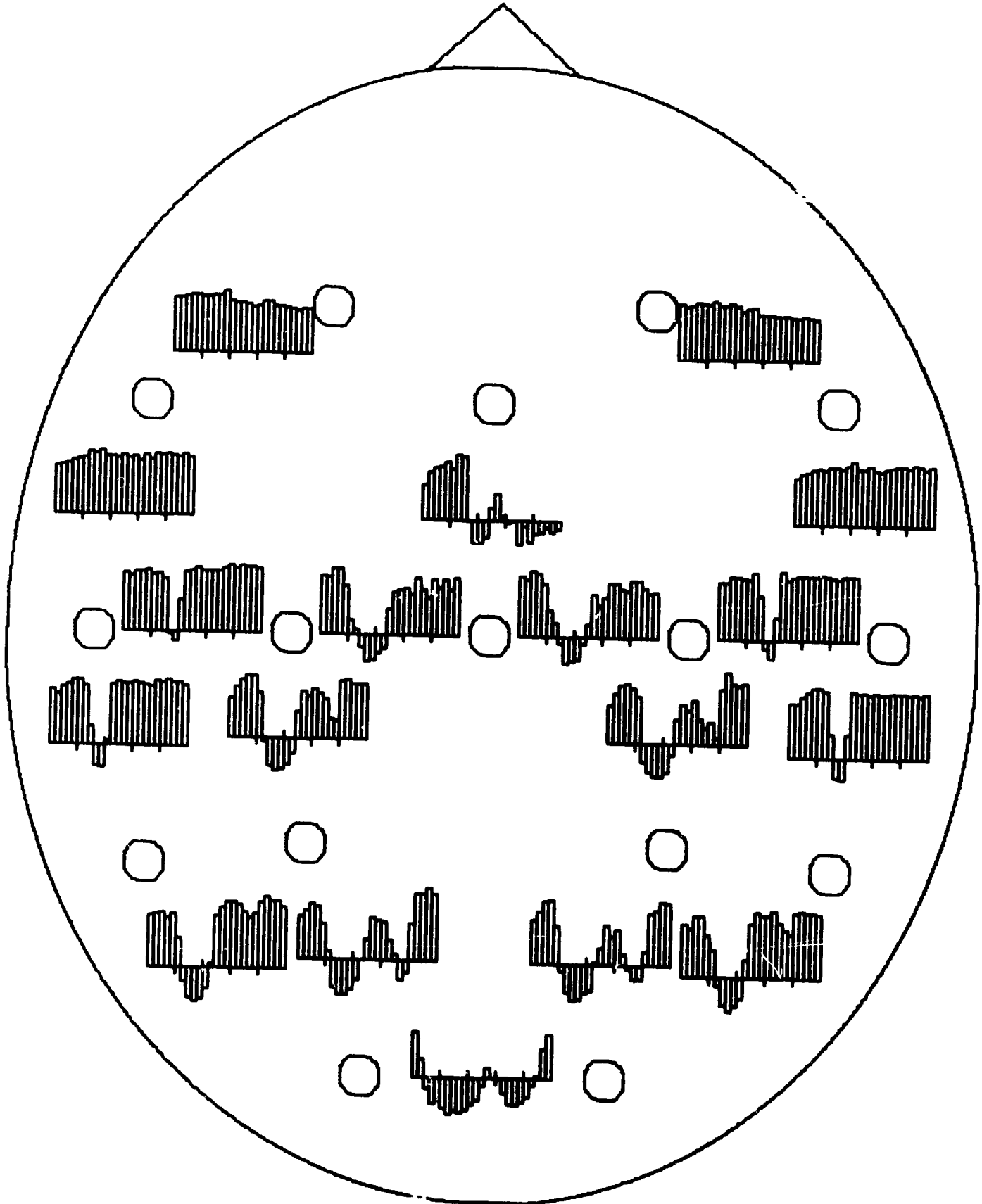
WV-CODE 38



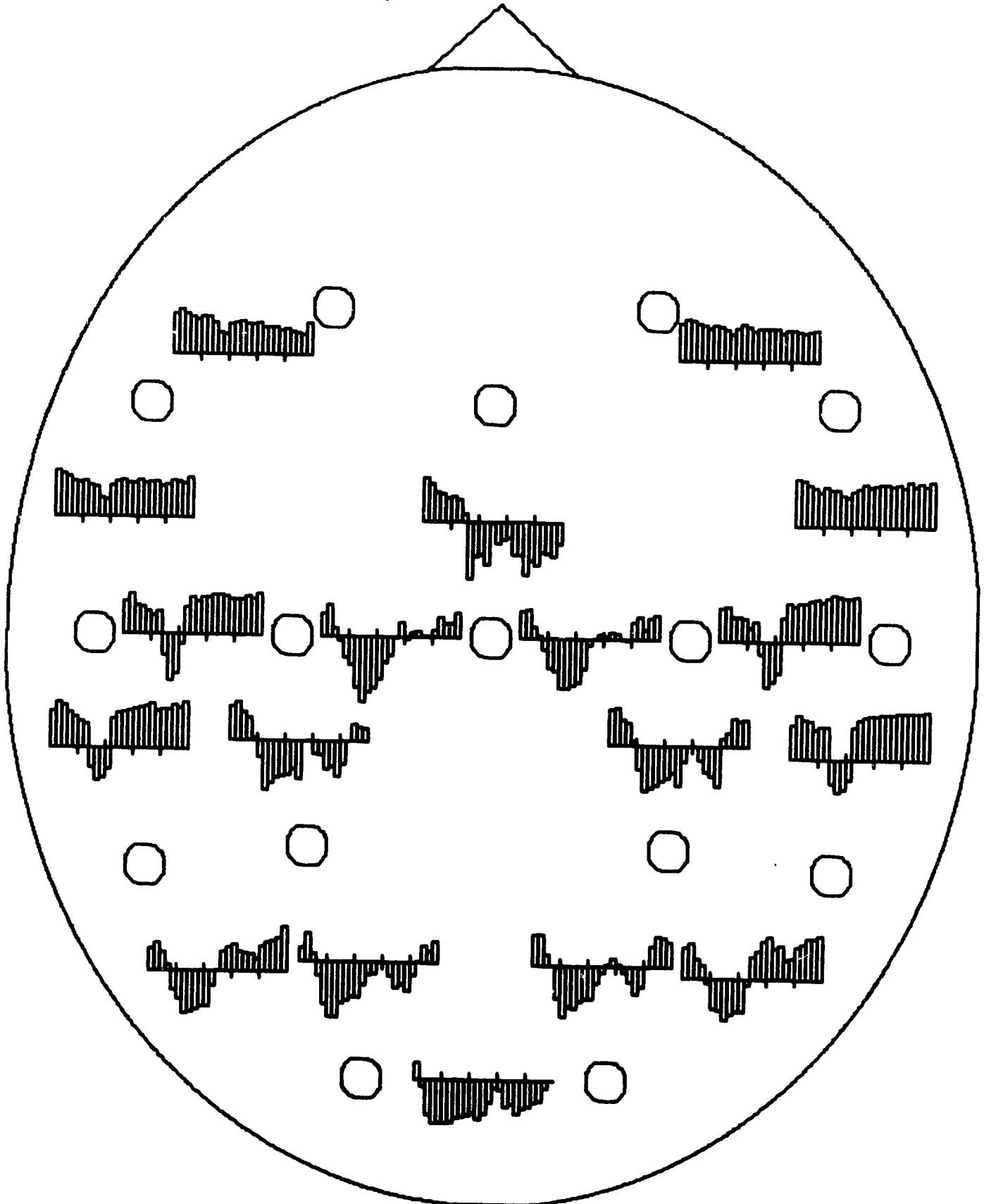
WV - CODE 59

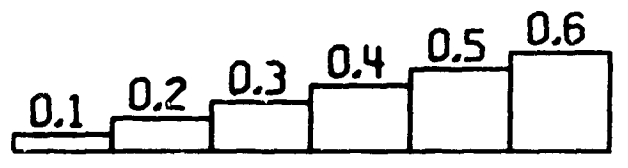


WV - CODE 79

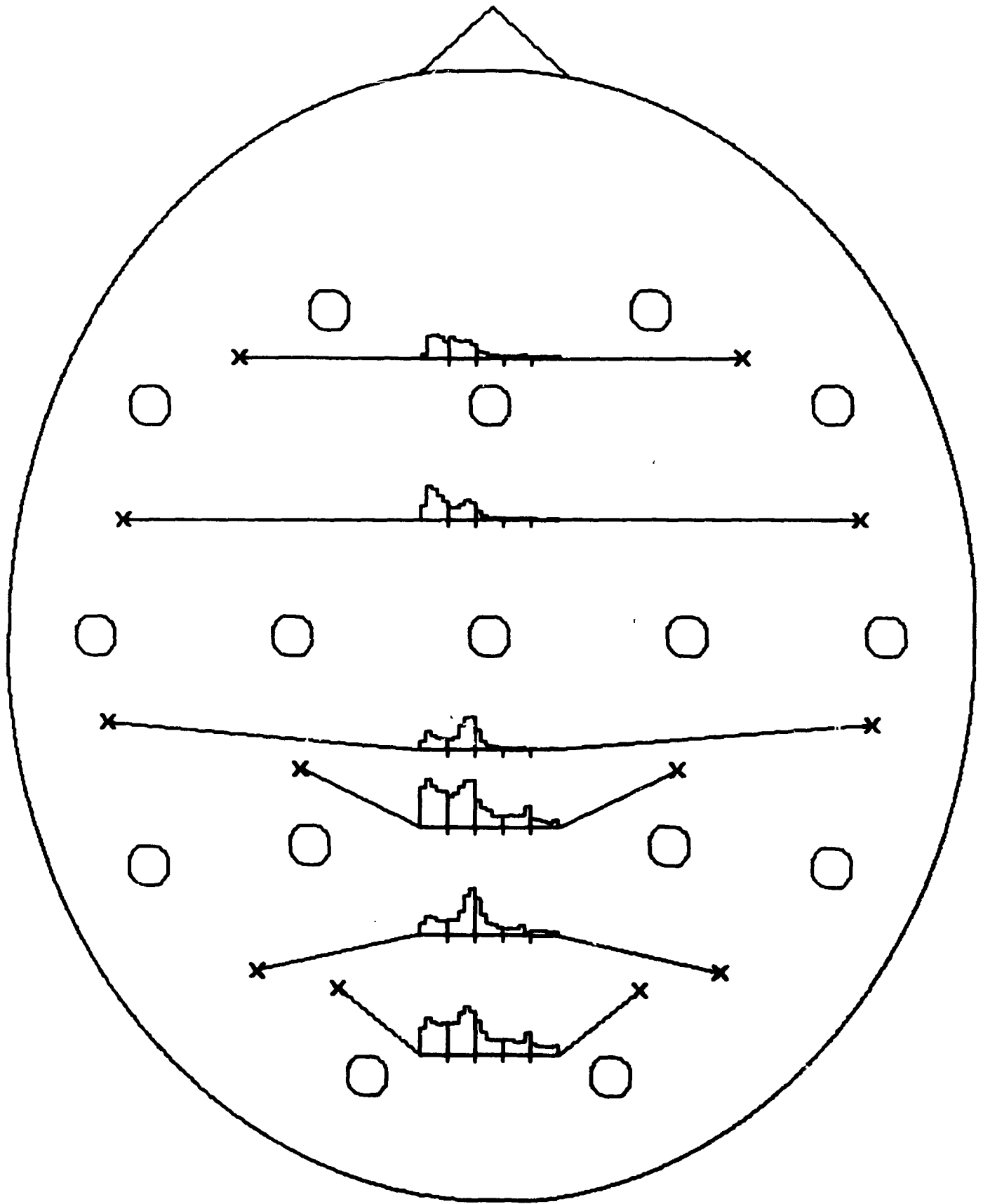


WV - CODE 119





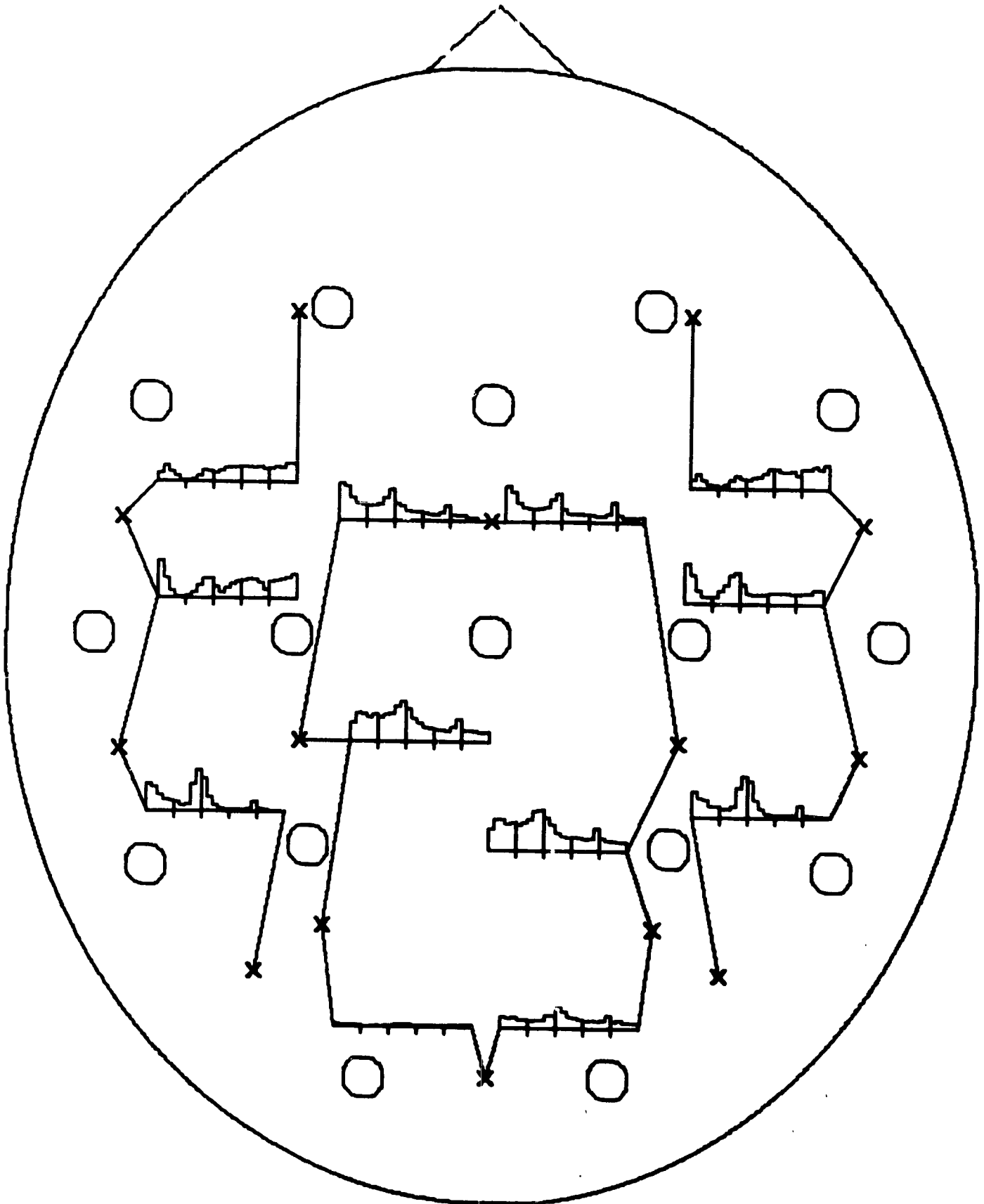
WC-1-AVERAGE



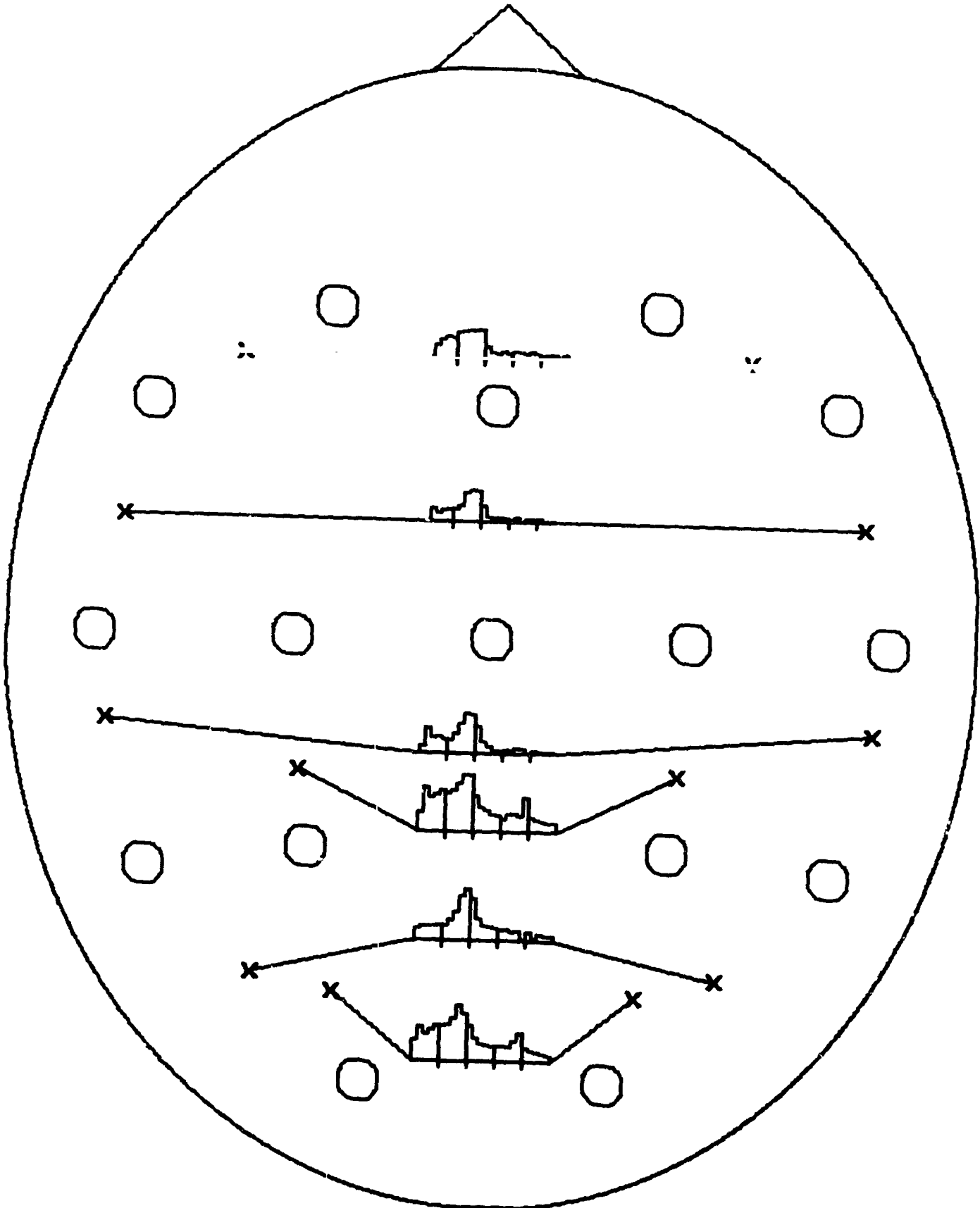




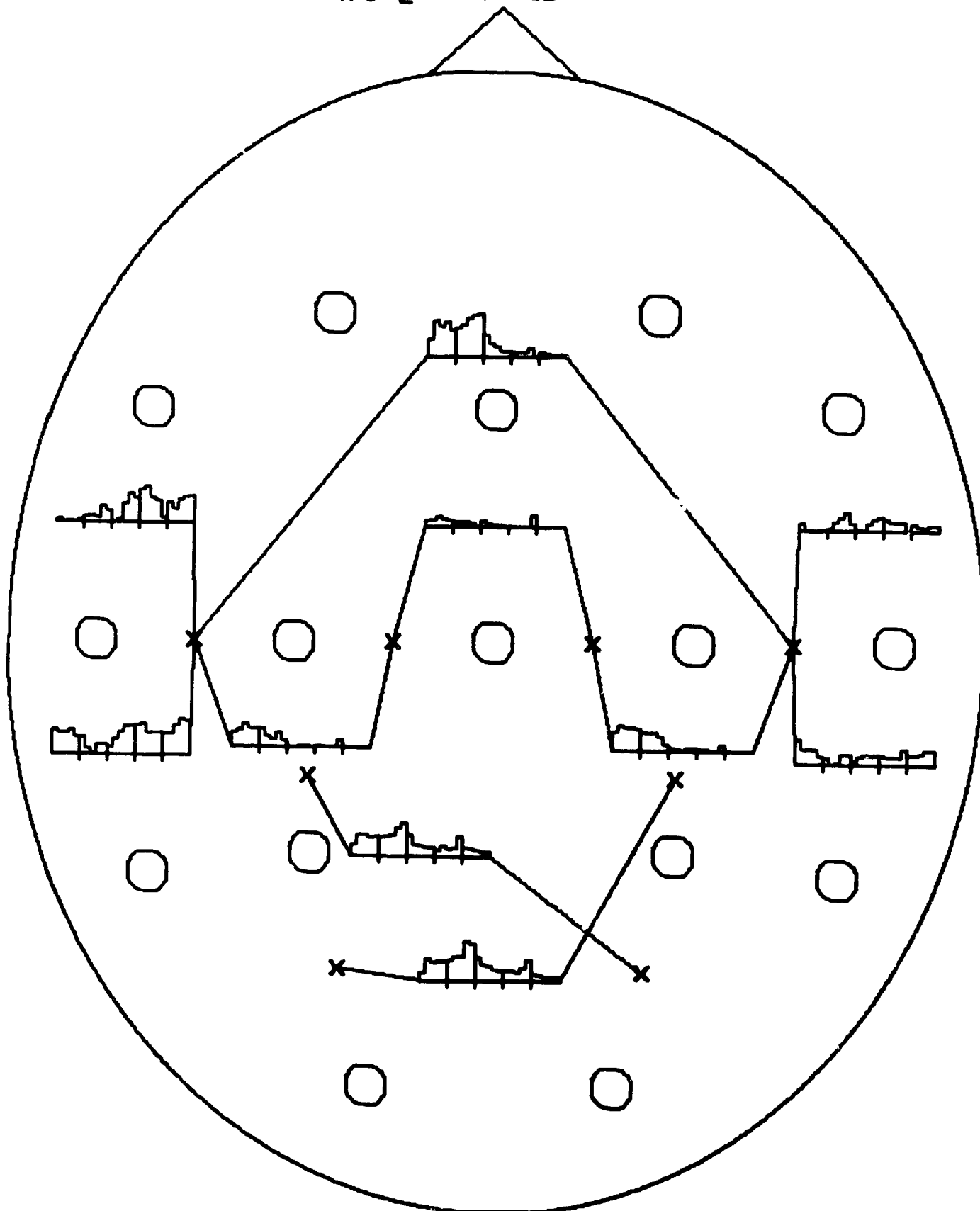
WC-3-AVERAGE



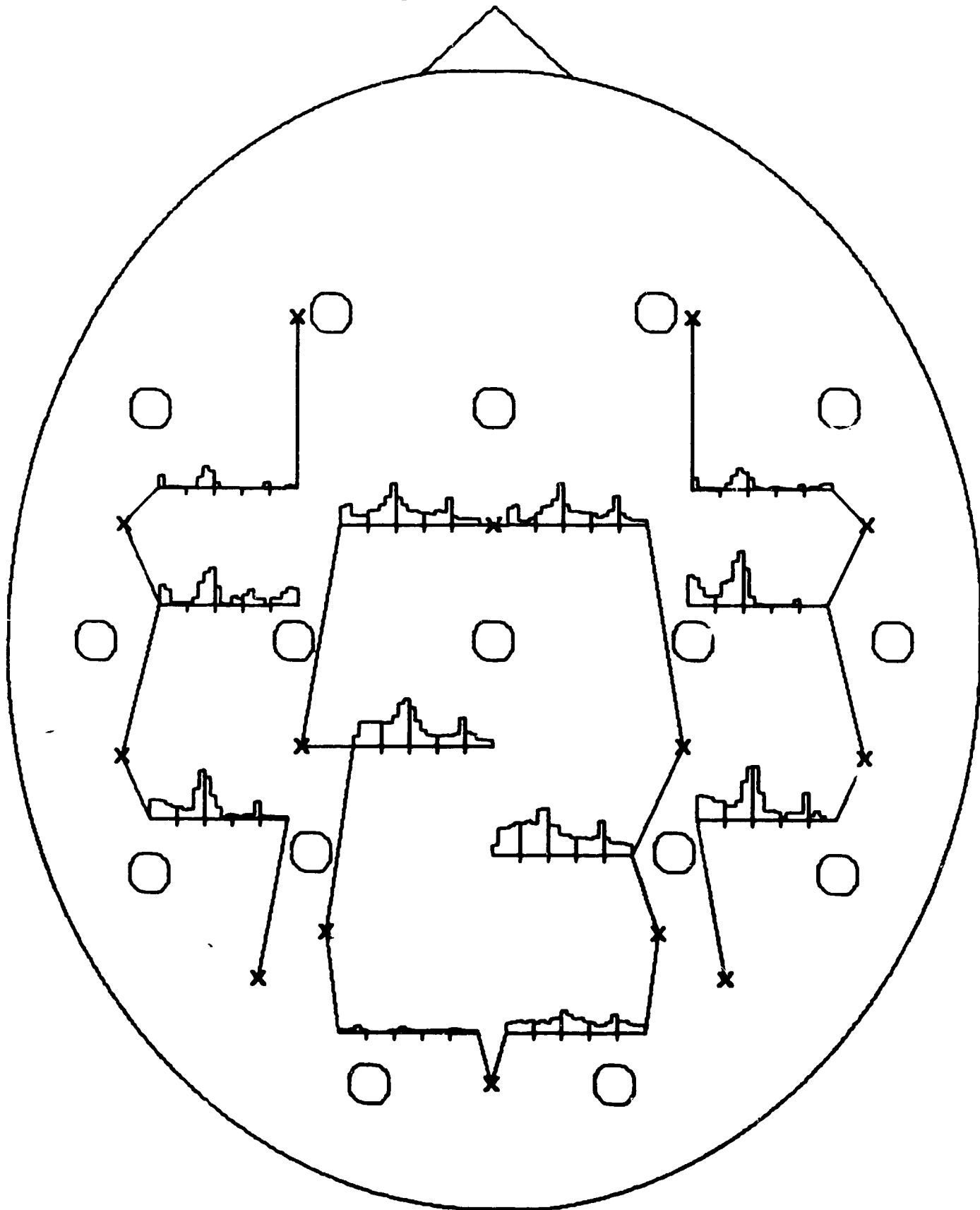
WC-1-CODE 25



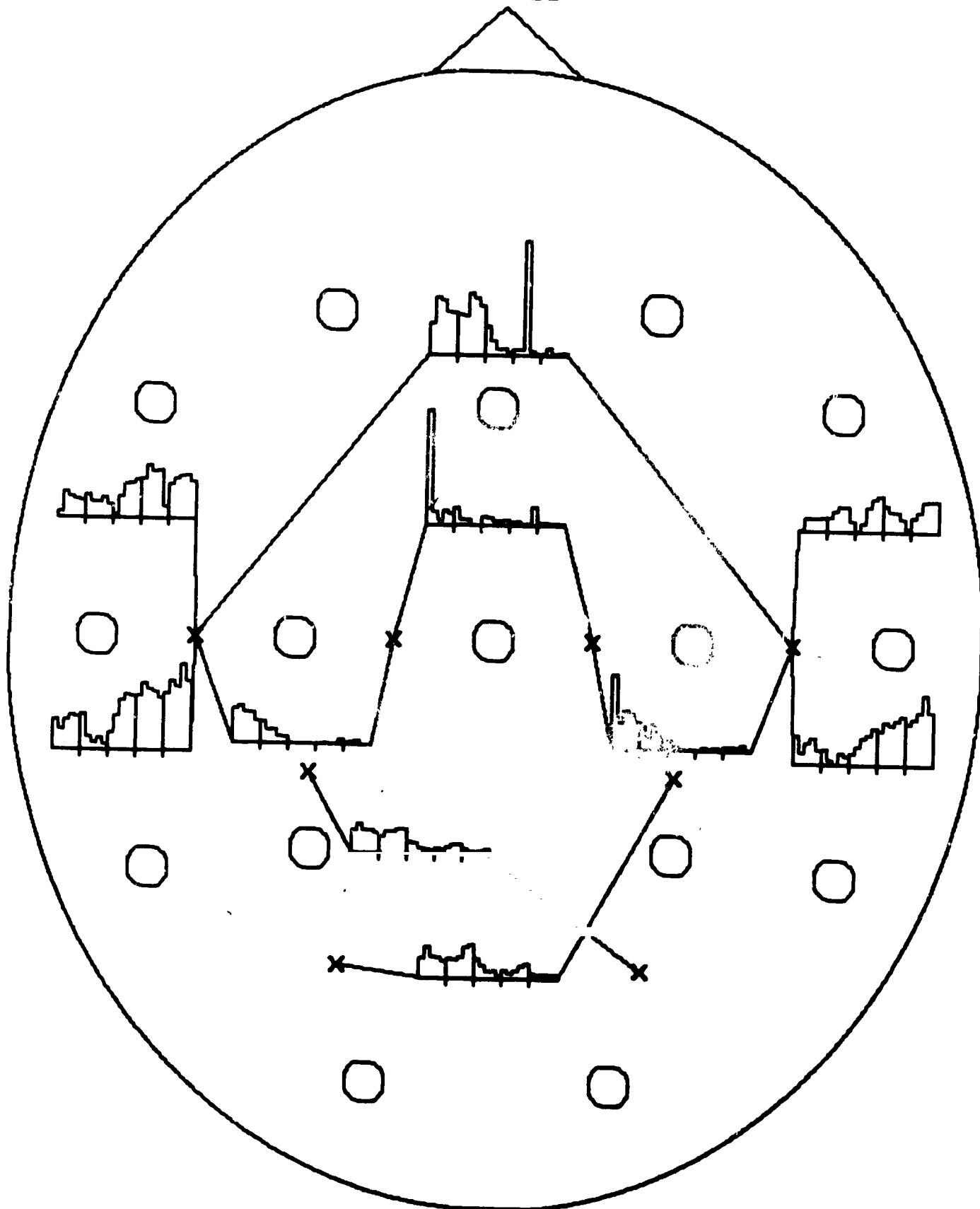
WC-2-CODE 25



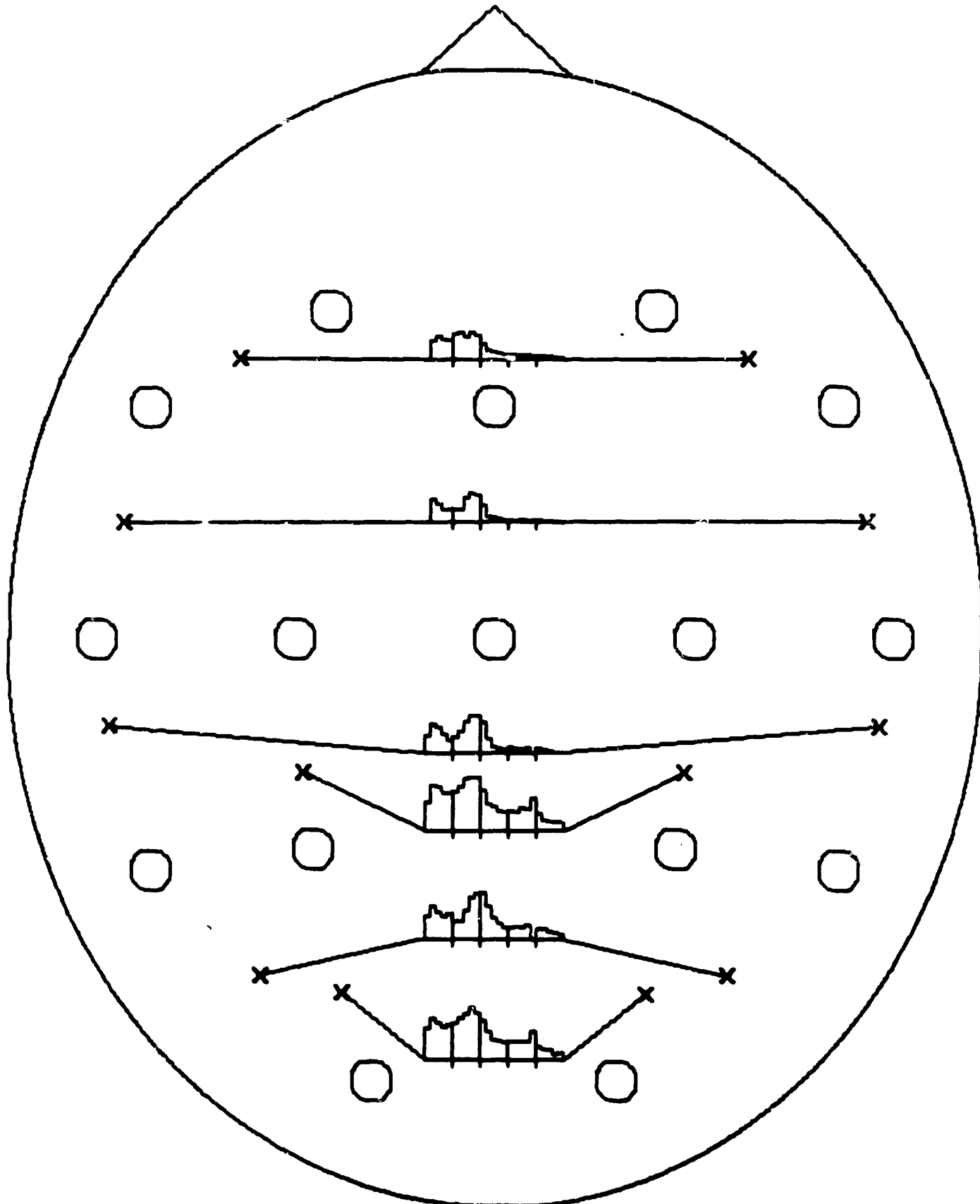
WC-3-CODE 25



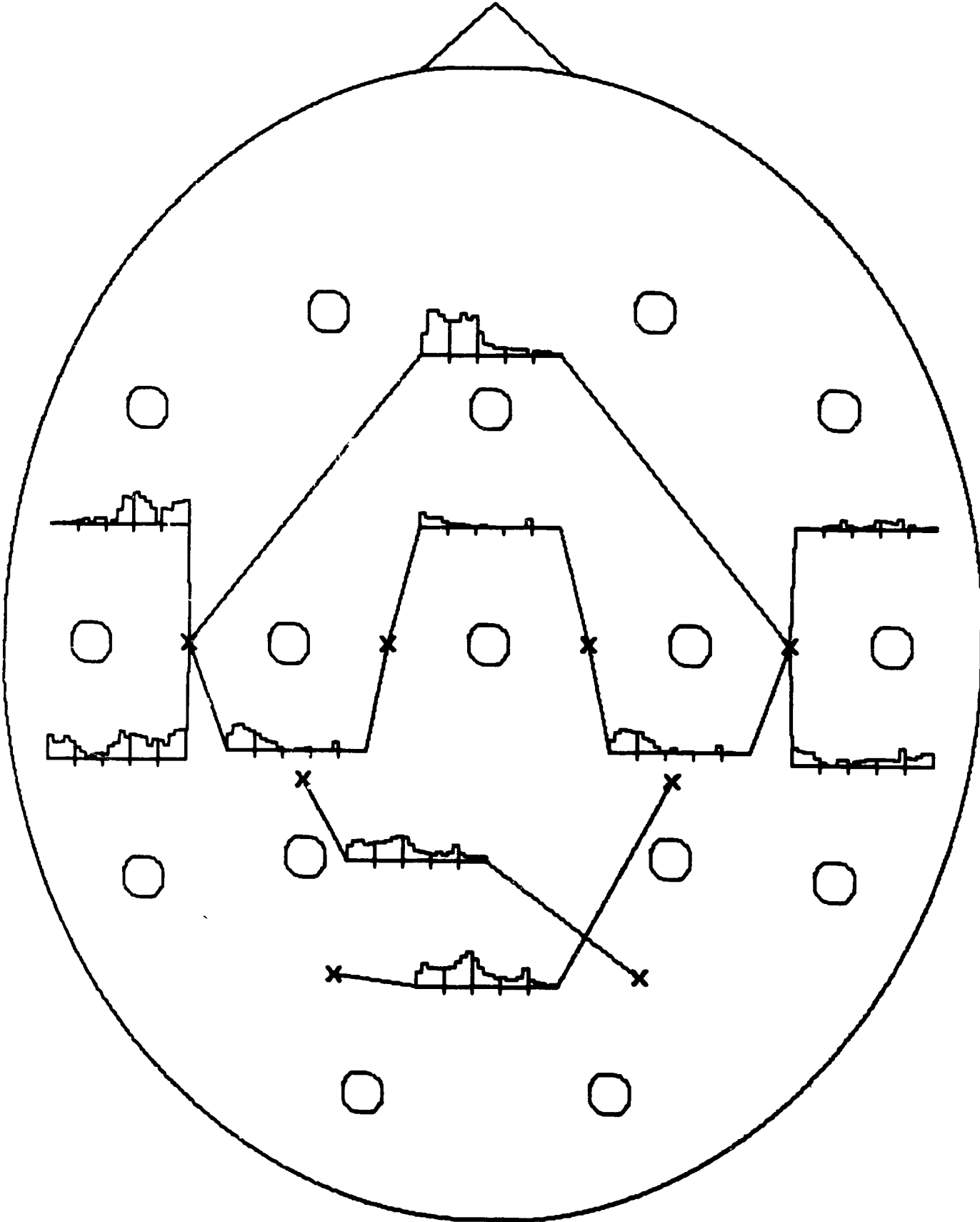
WC-2-CODE 53



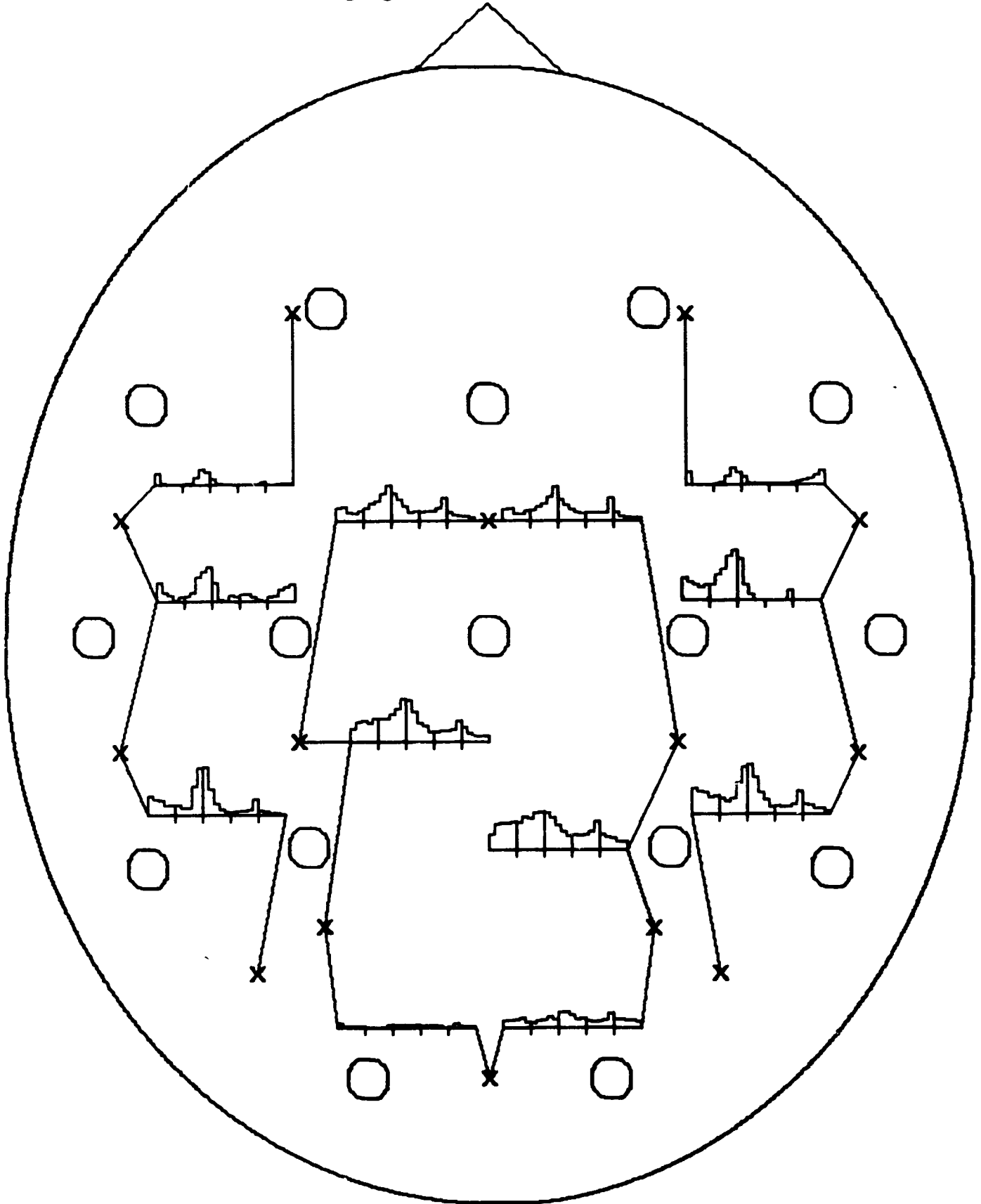
WC-1-CODE 11



WC-2-CODE 11

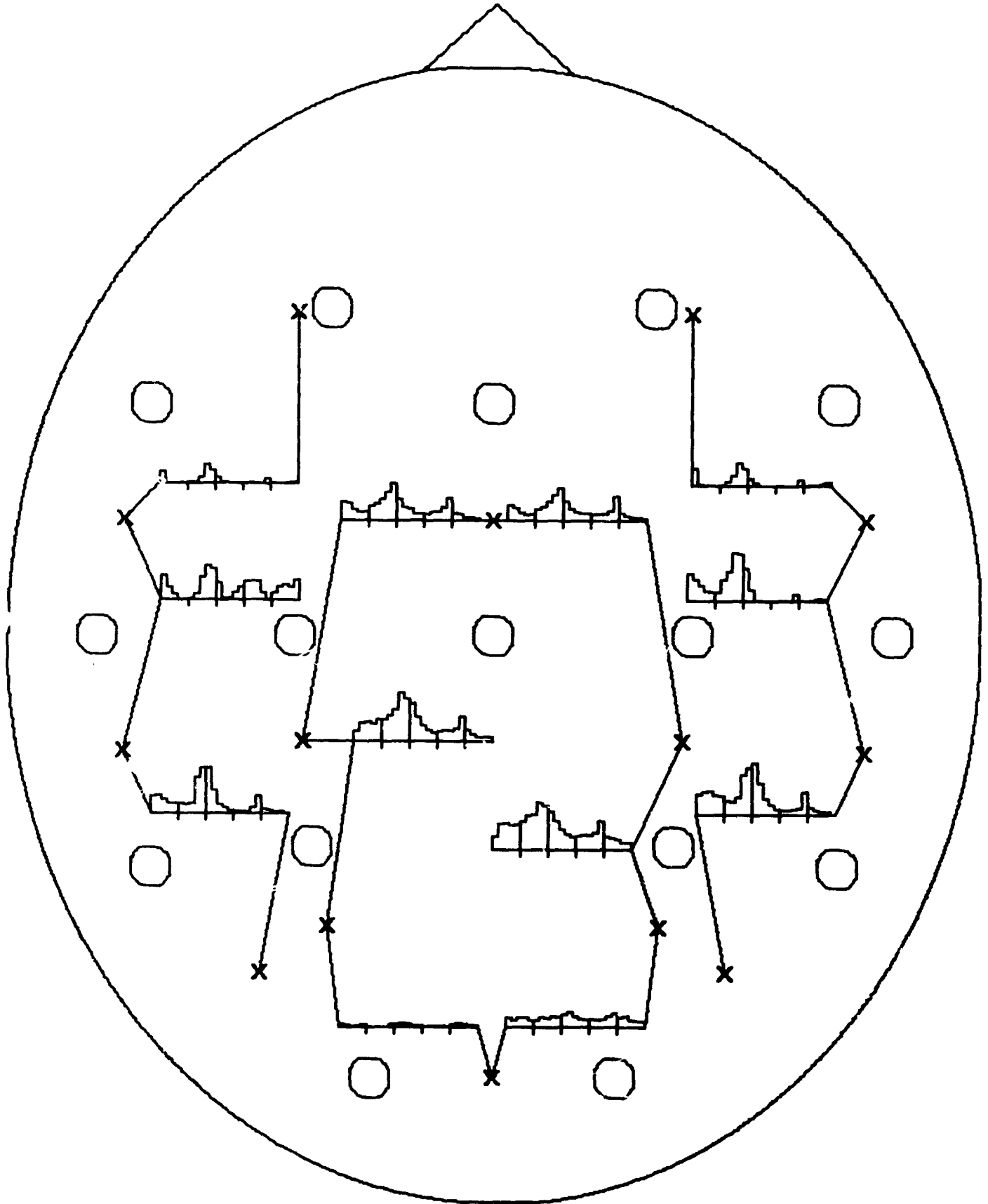


WC-3-CODE 11

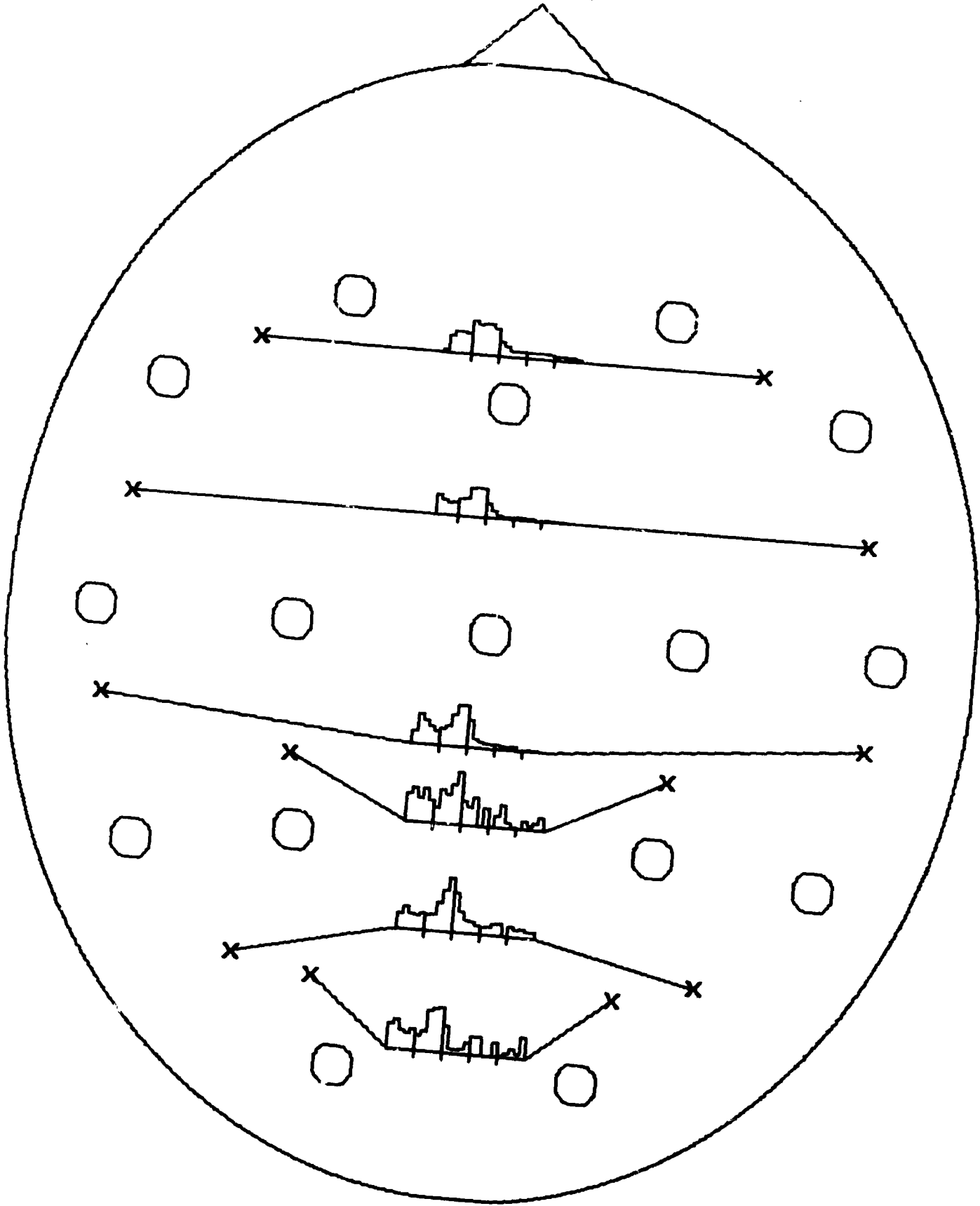




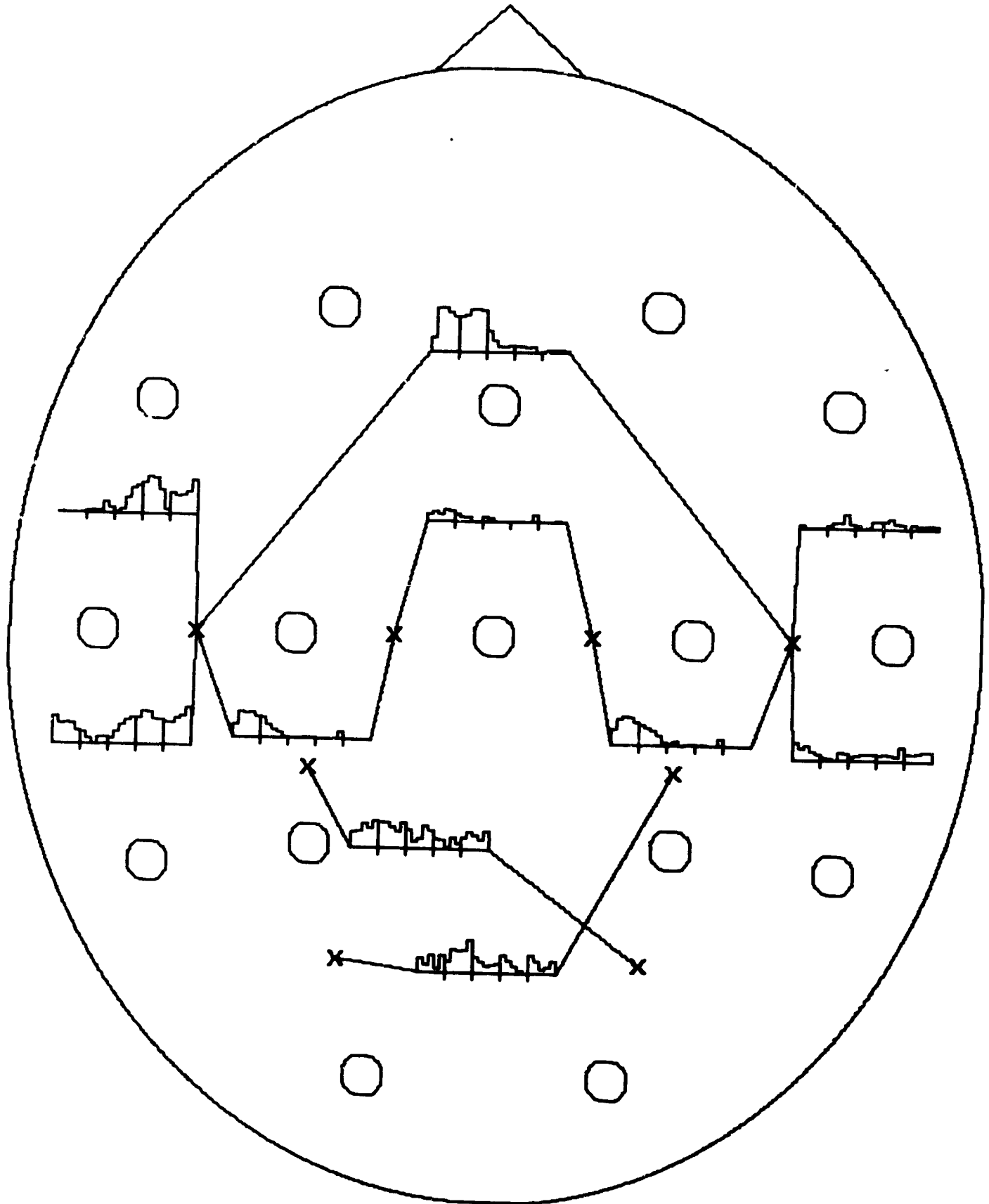
WC-3-CODE 16



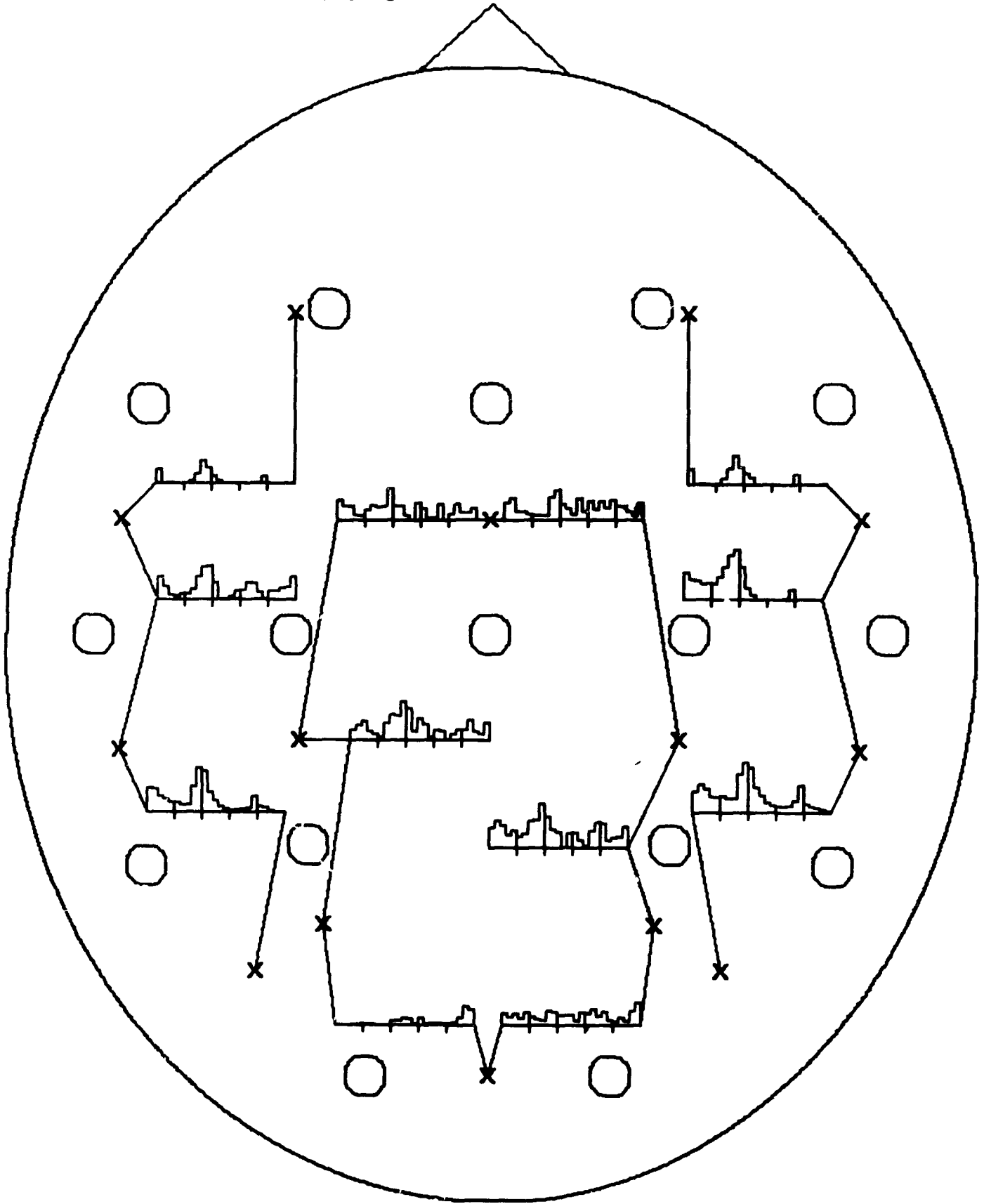
WC-1-CODE 18



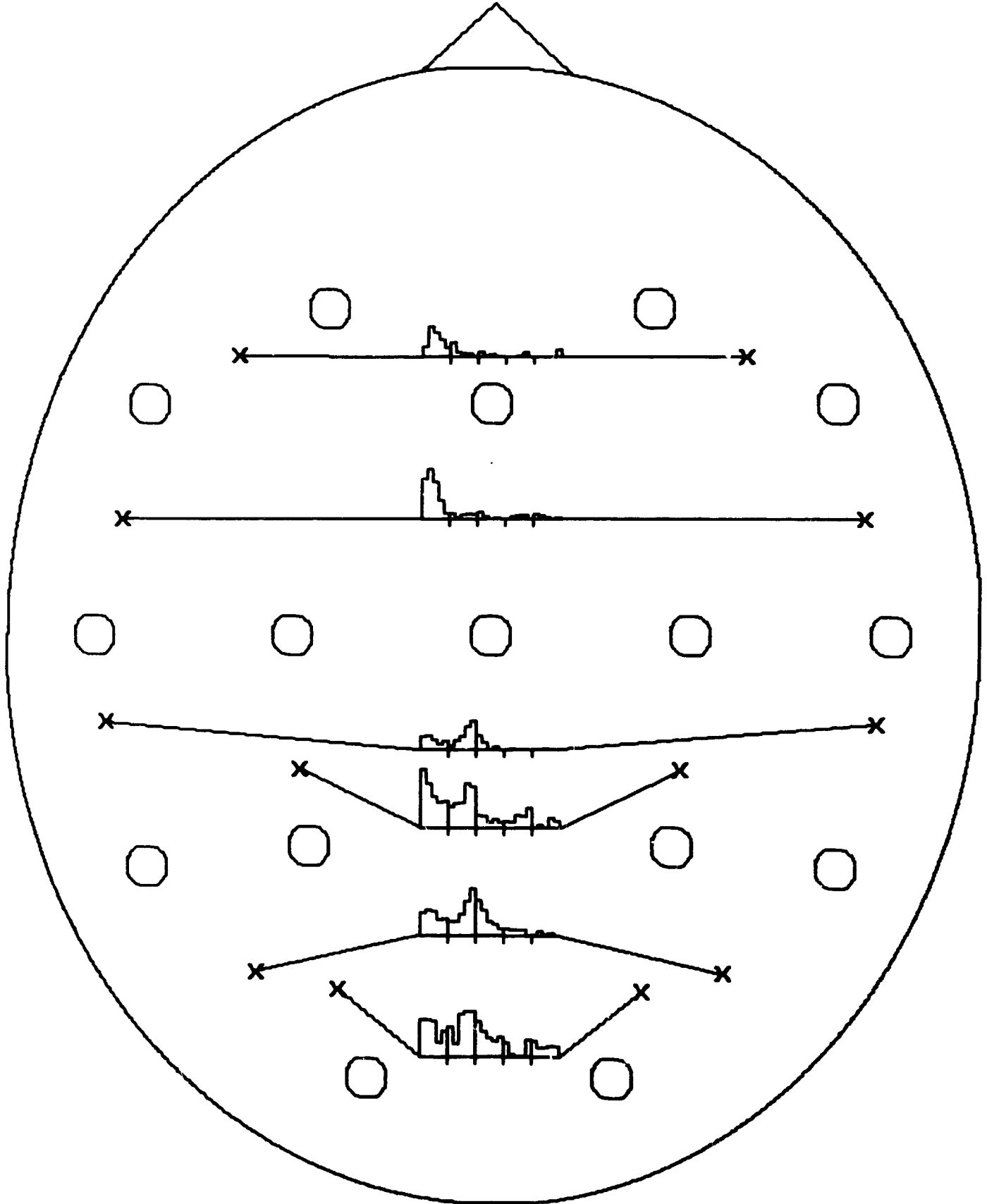
WC-2-CODE 18



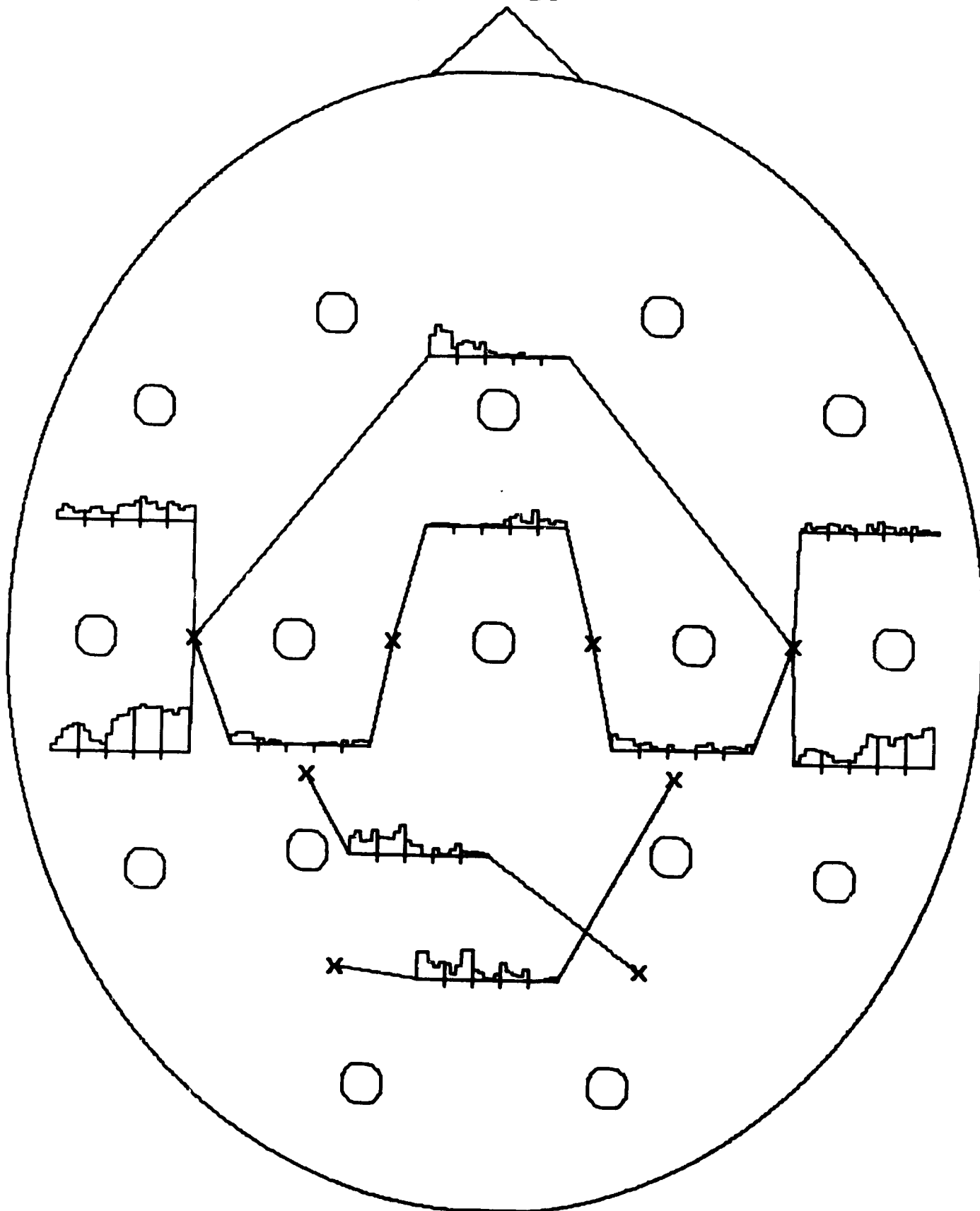
WC-3-CODE 18



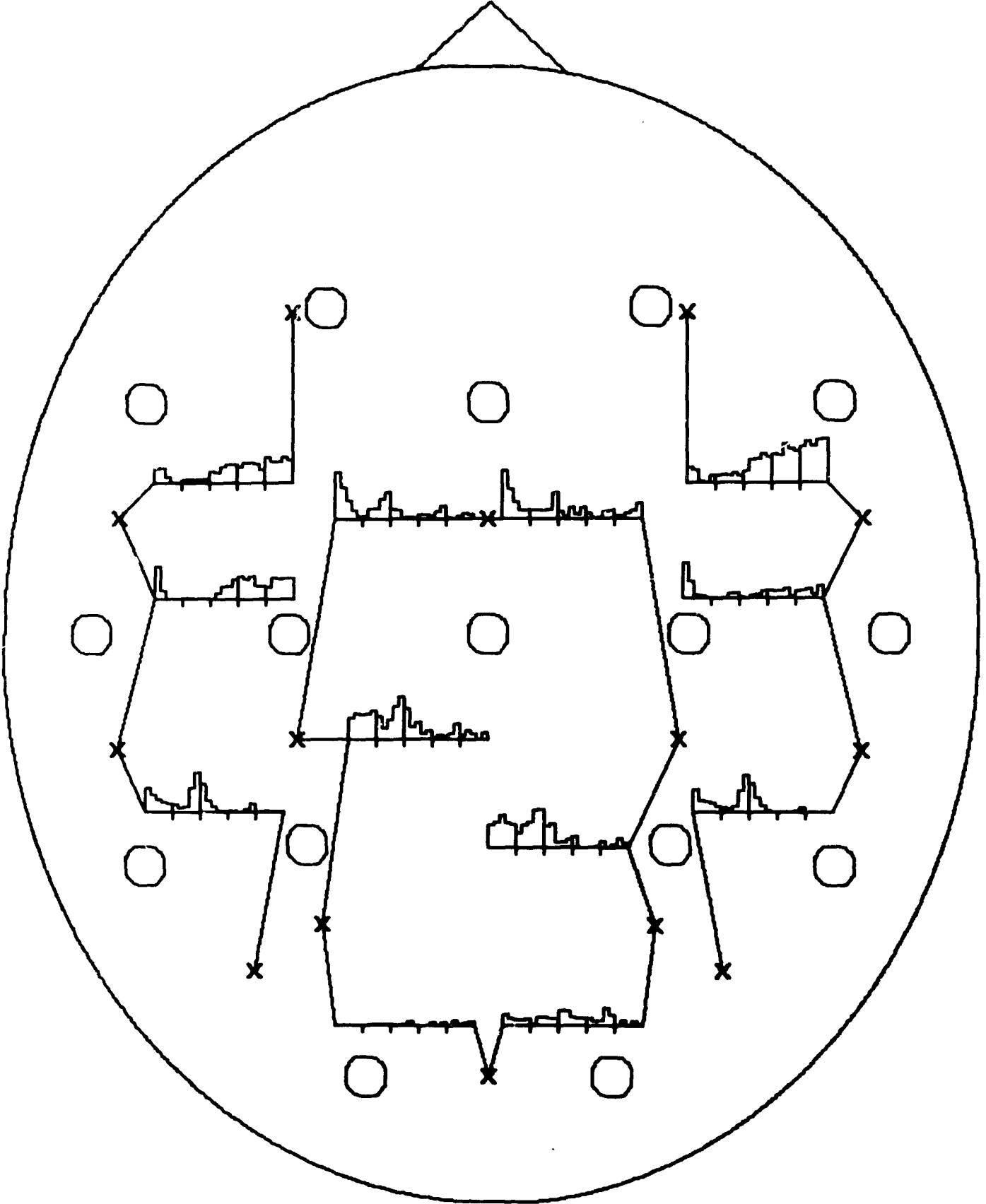
WC-1- CODE 36



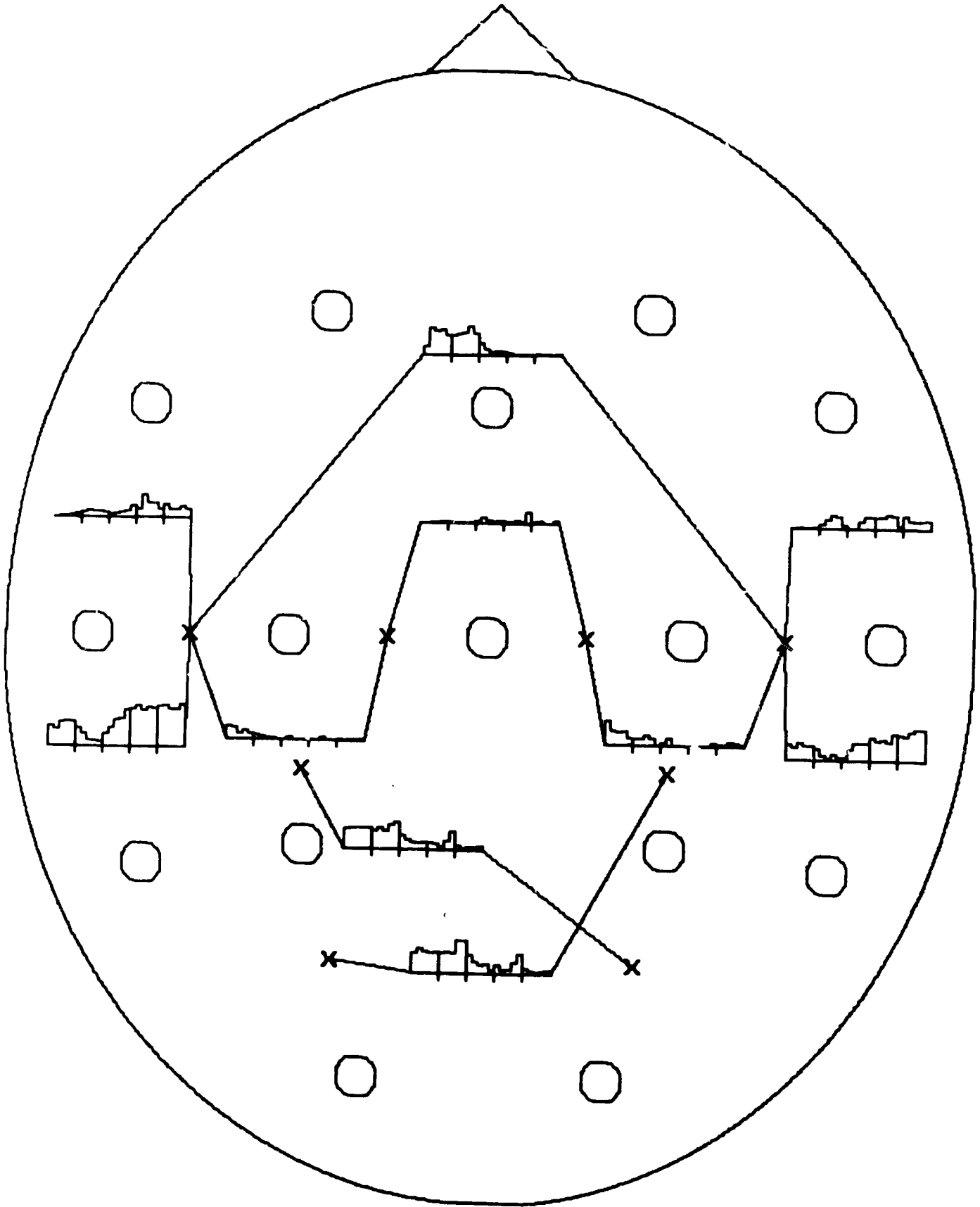
WC-2-CODE 36



WC-3-CODE 36

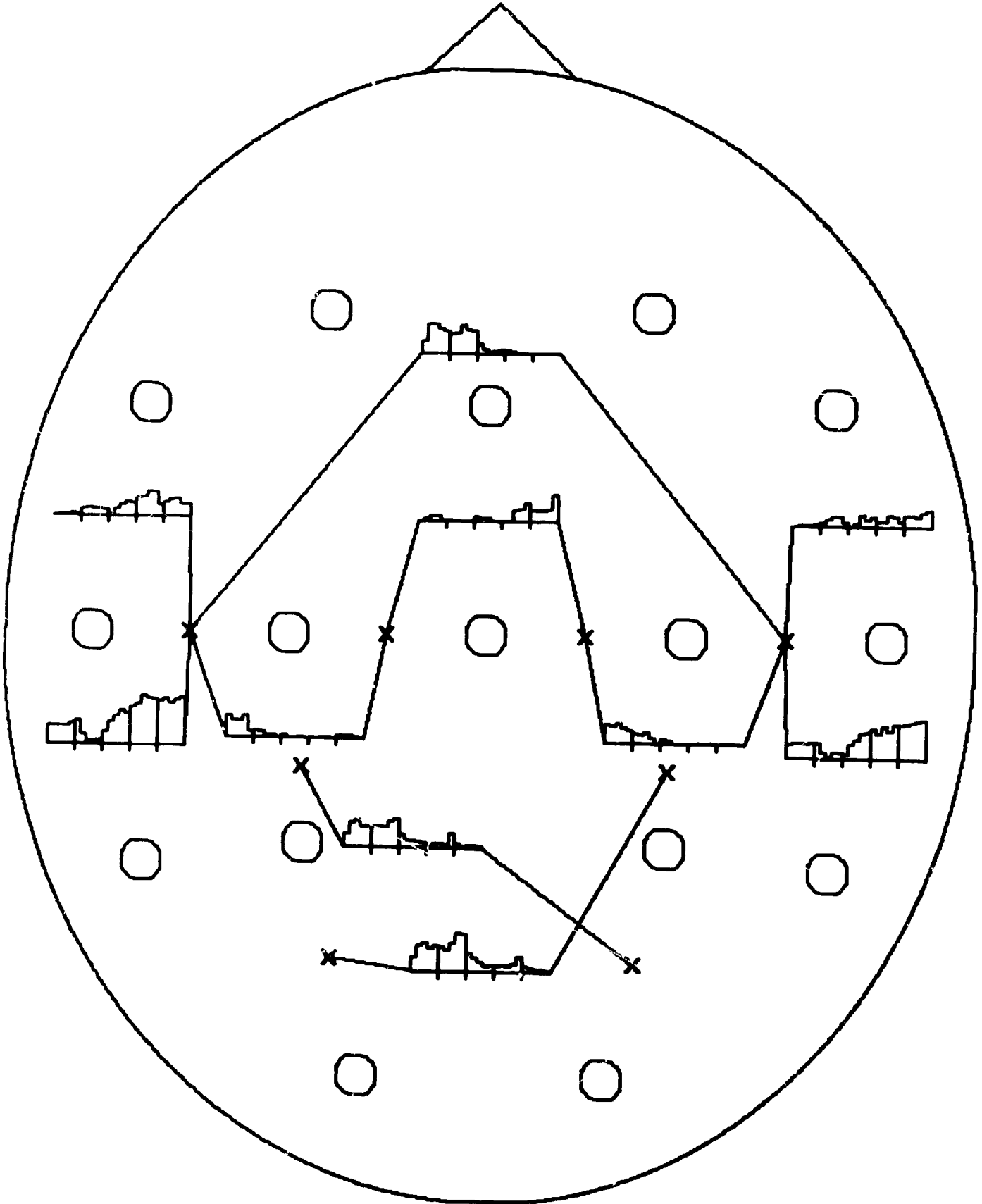


WC-2-CODE 34

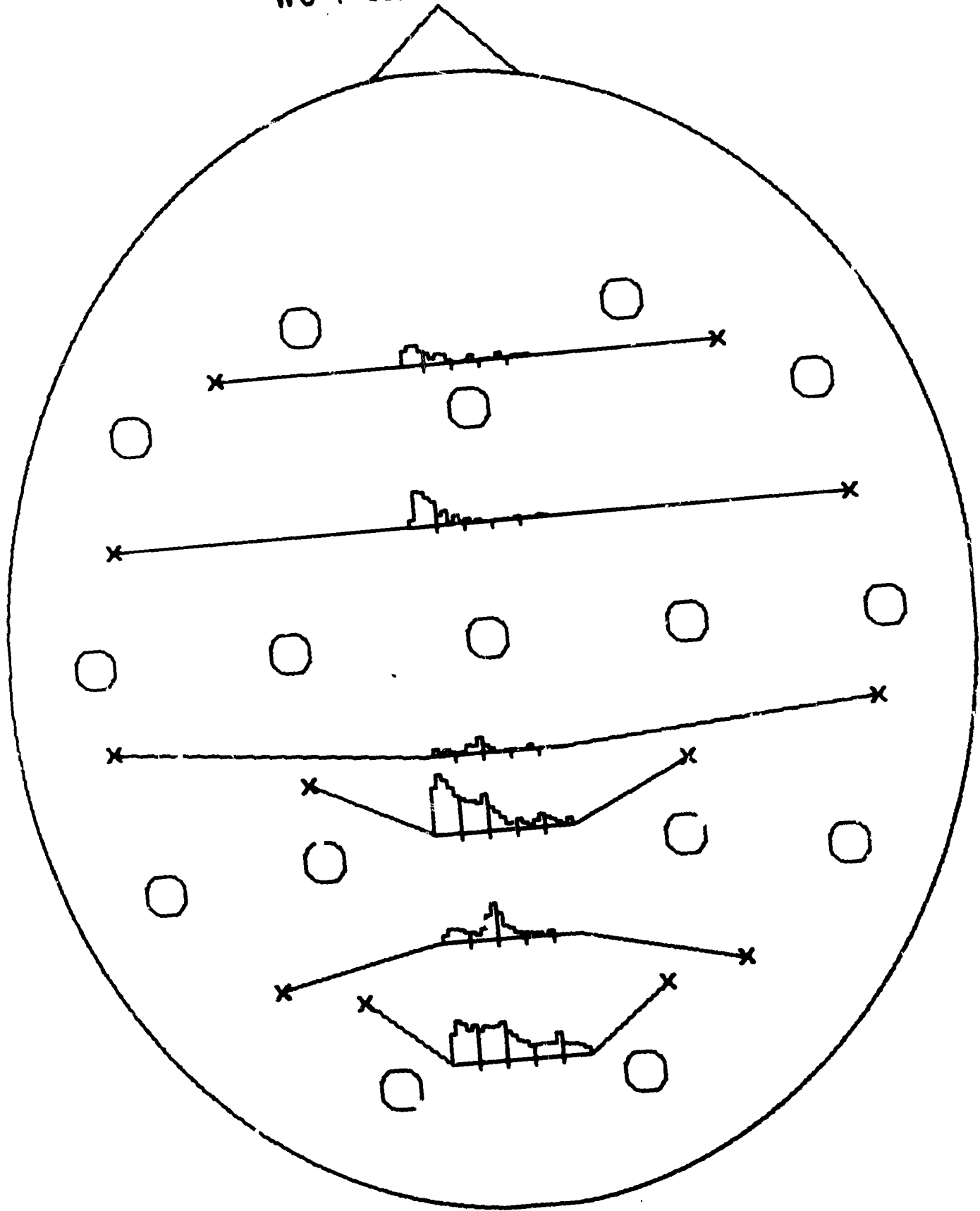




WC-2-CODE 38

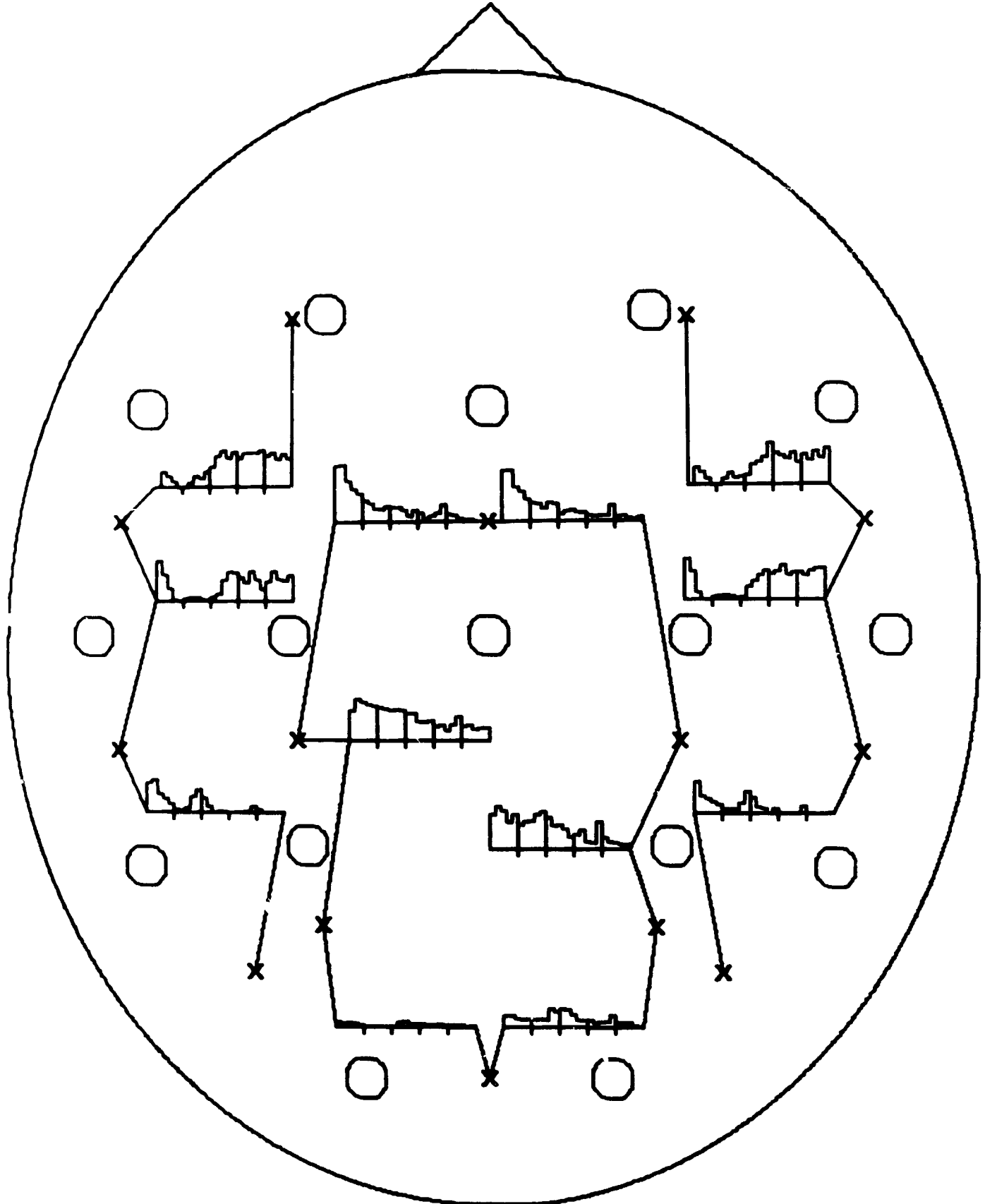


WC-1-CODE 69

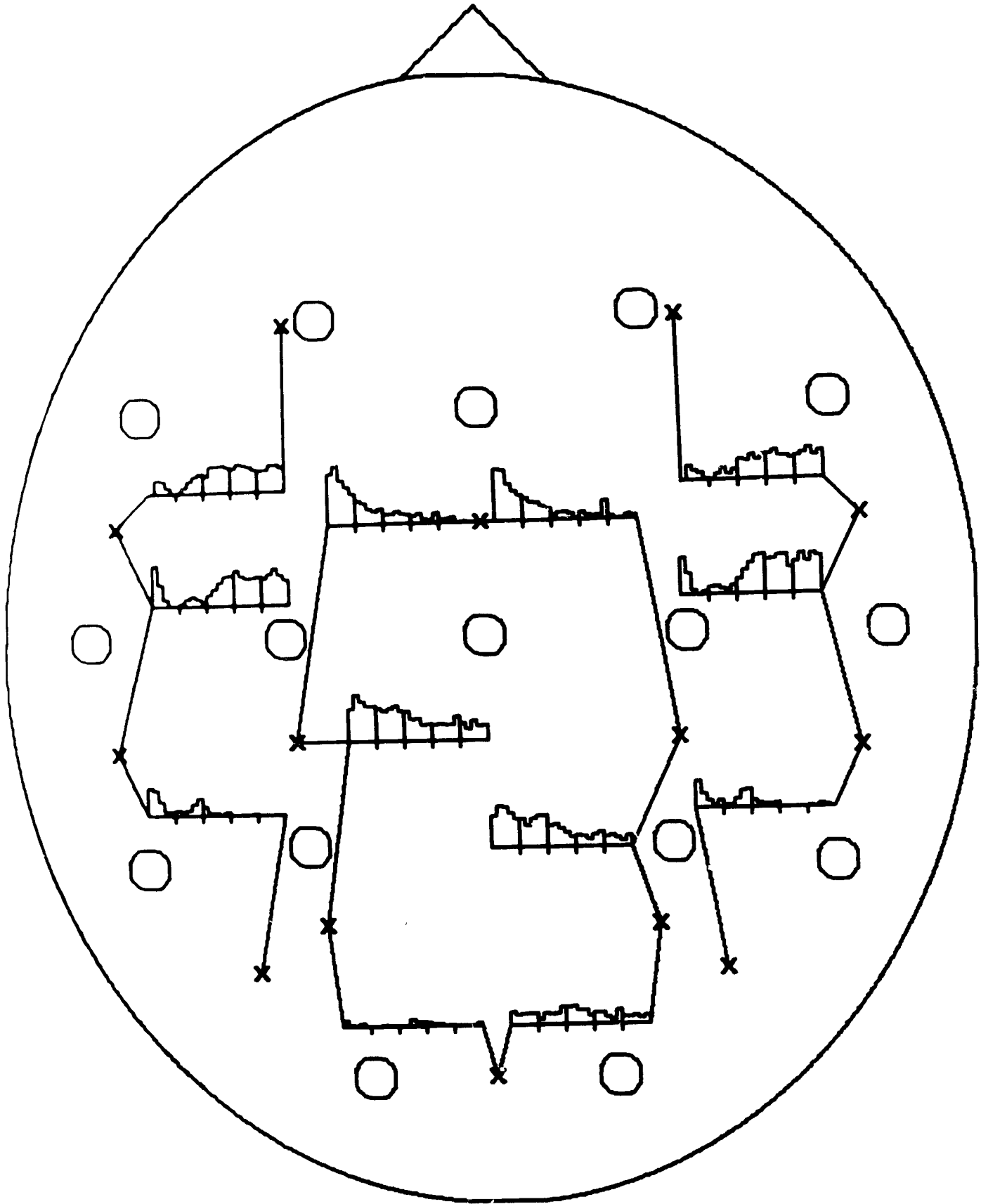




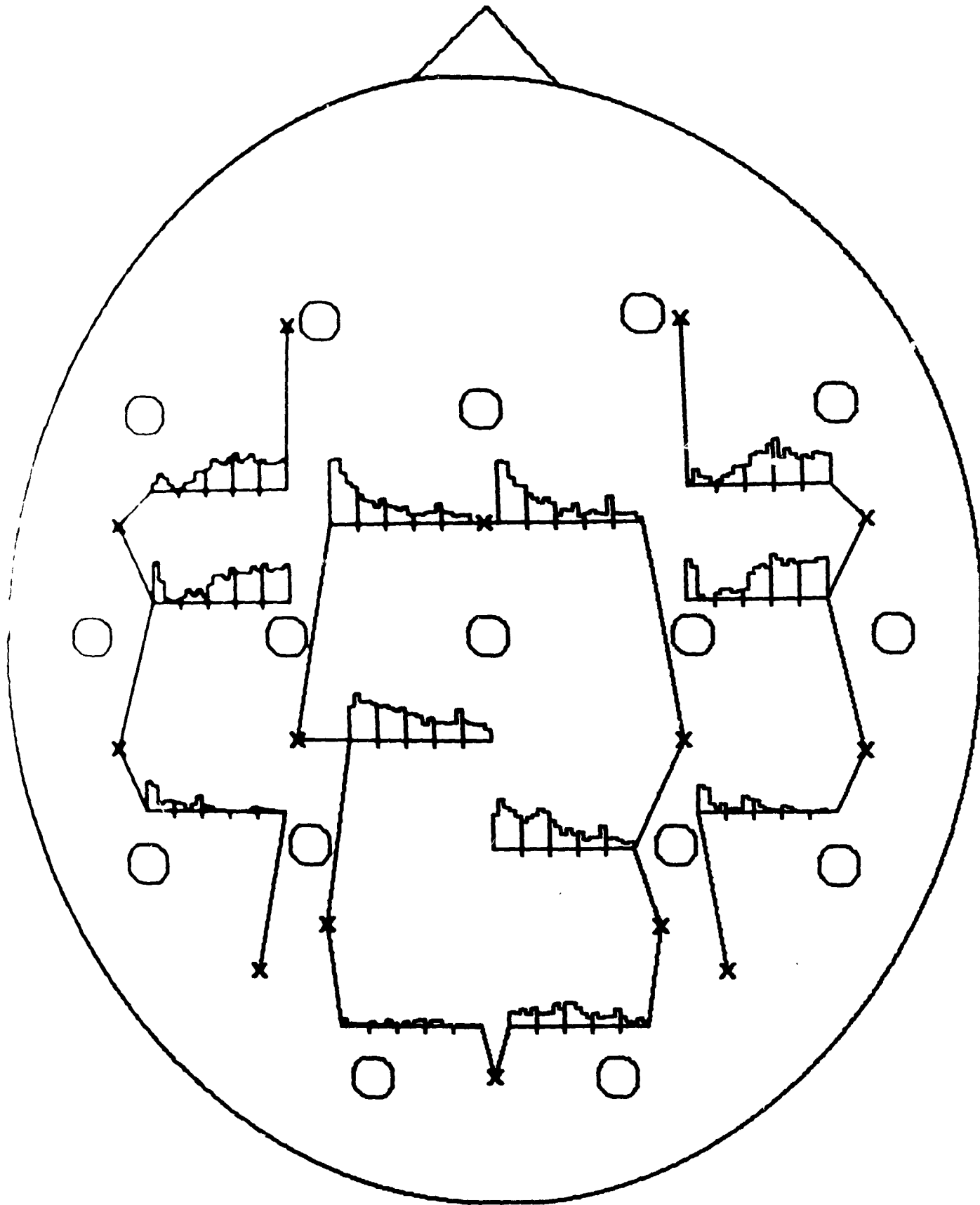
WC-3 - CODE 69



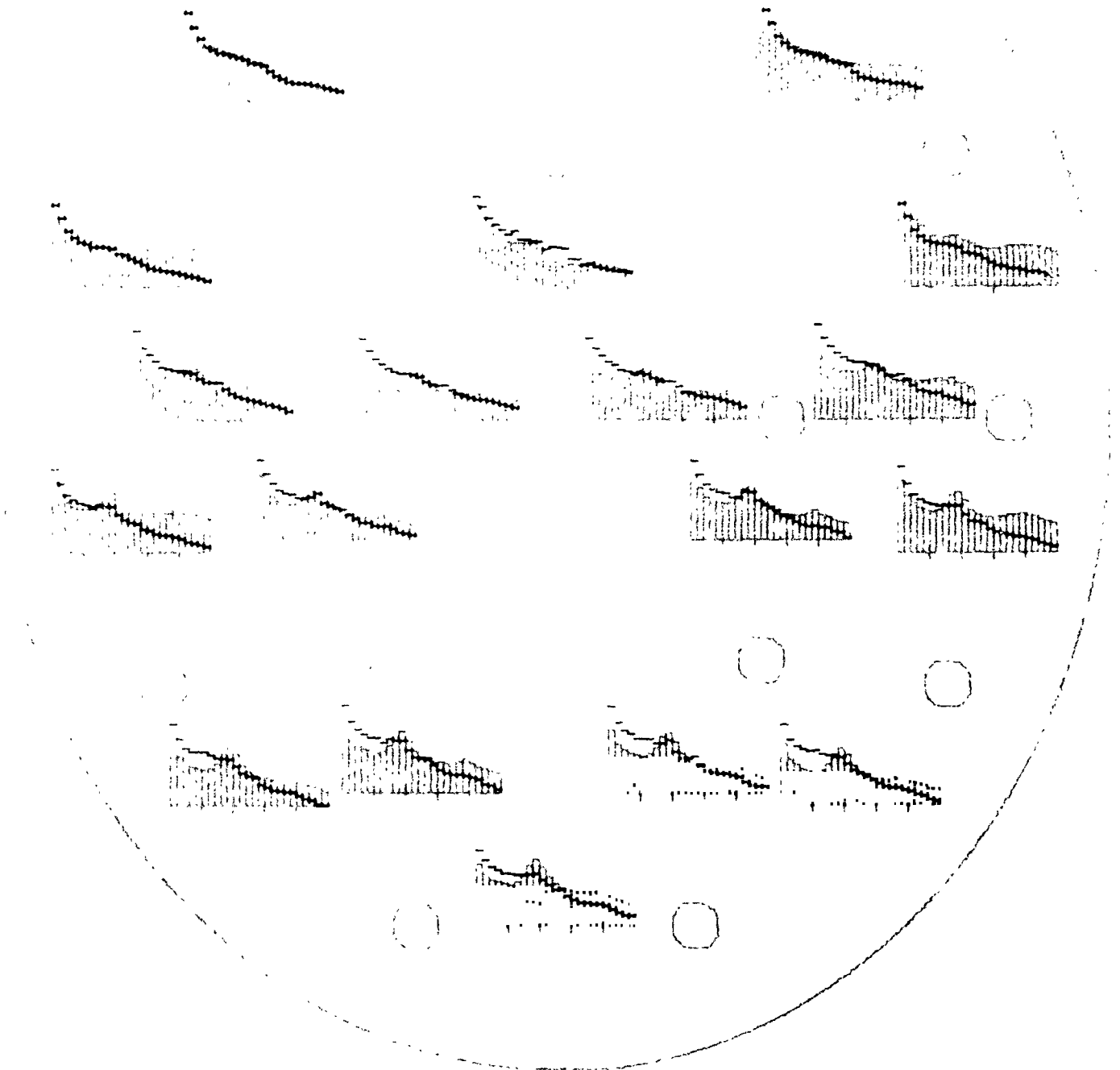
WC-3-CODE 79

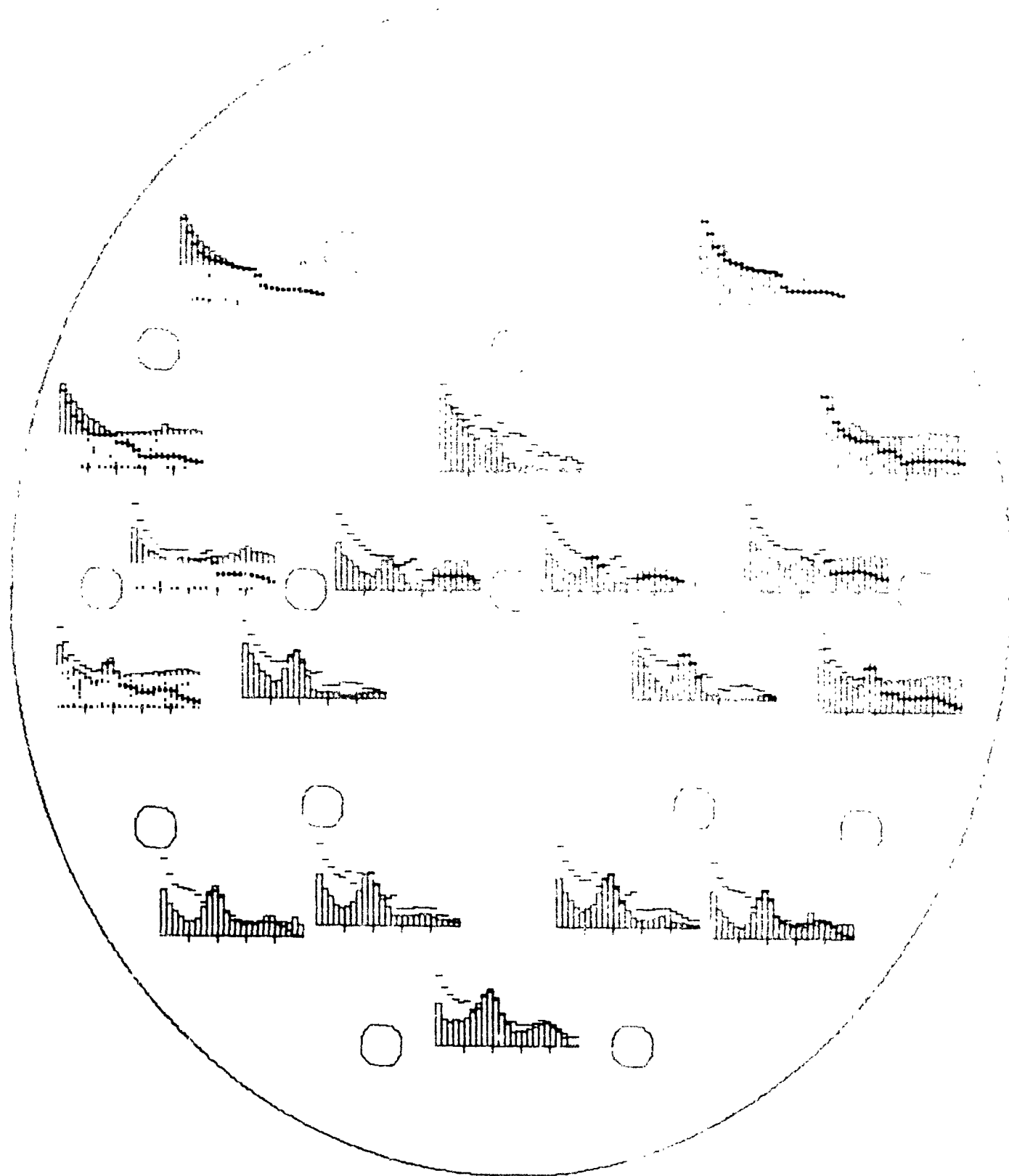


WC-3-CODE 119



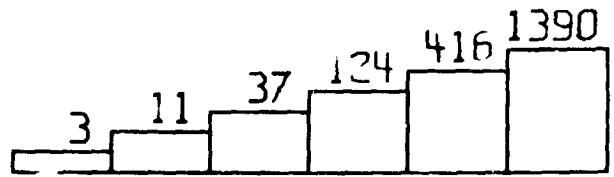
30 SUB SLEEP RED



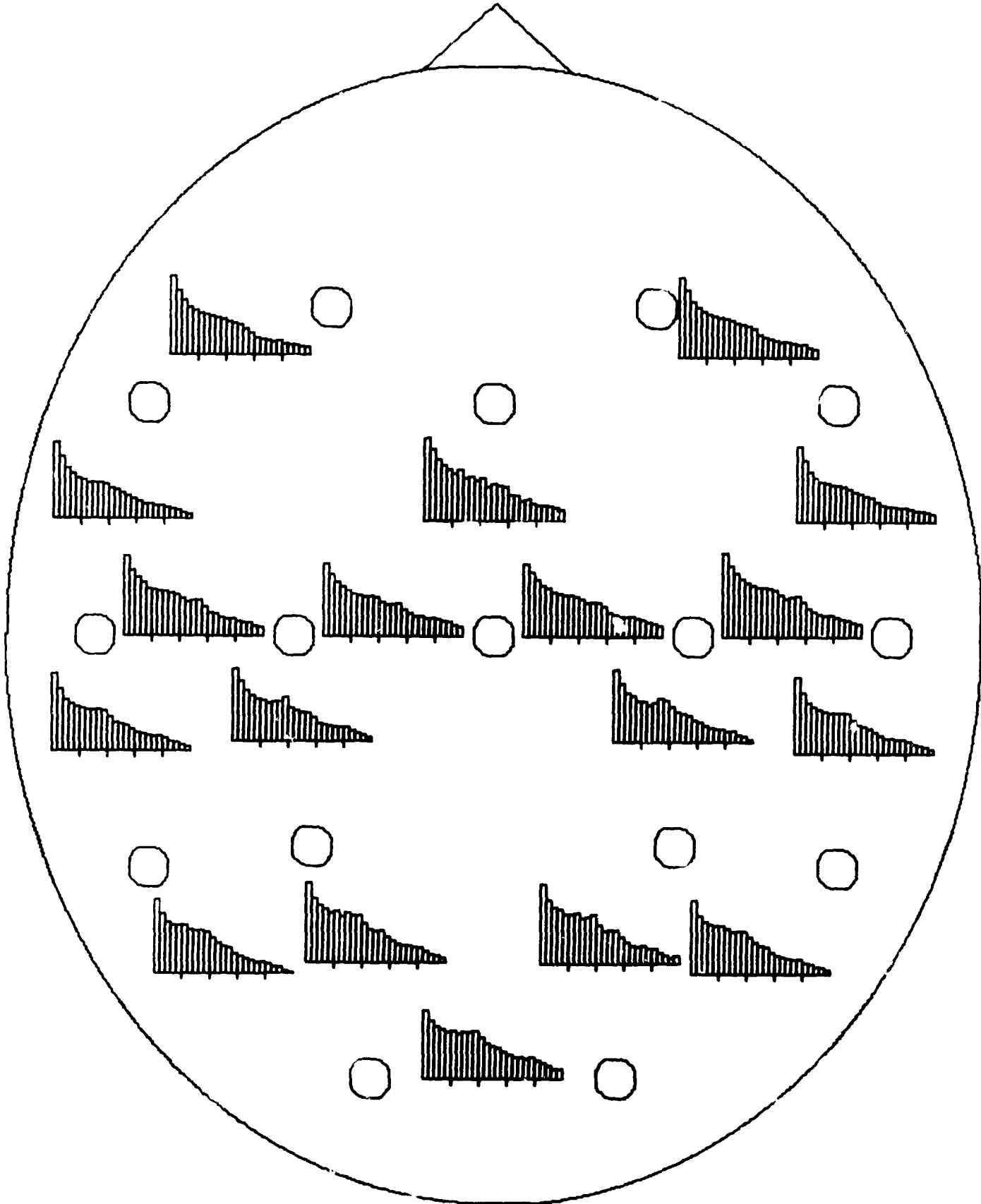




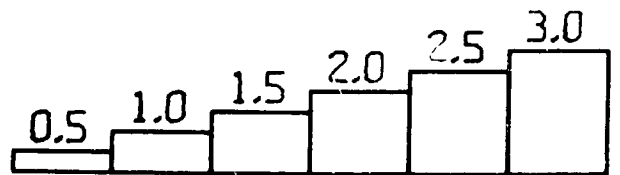




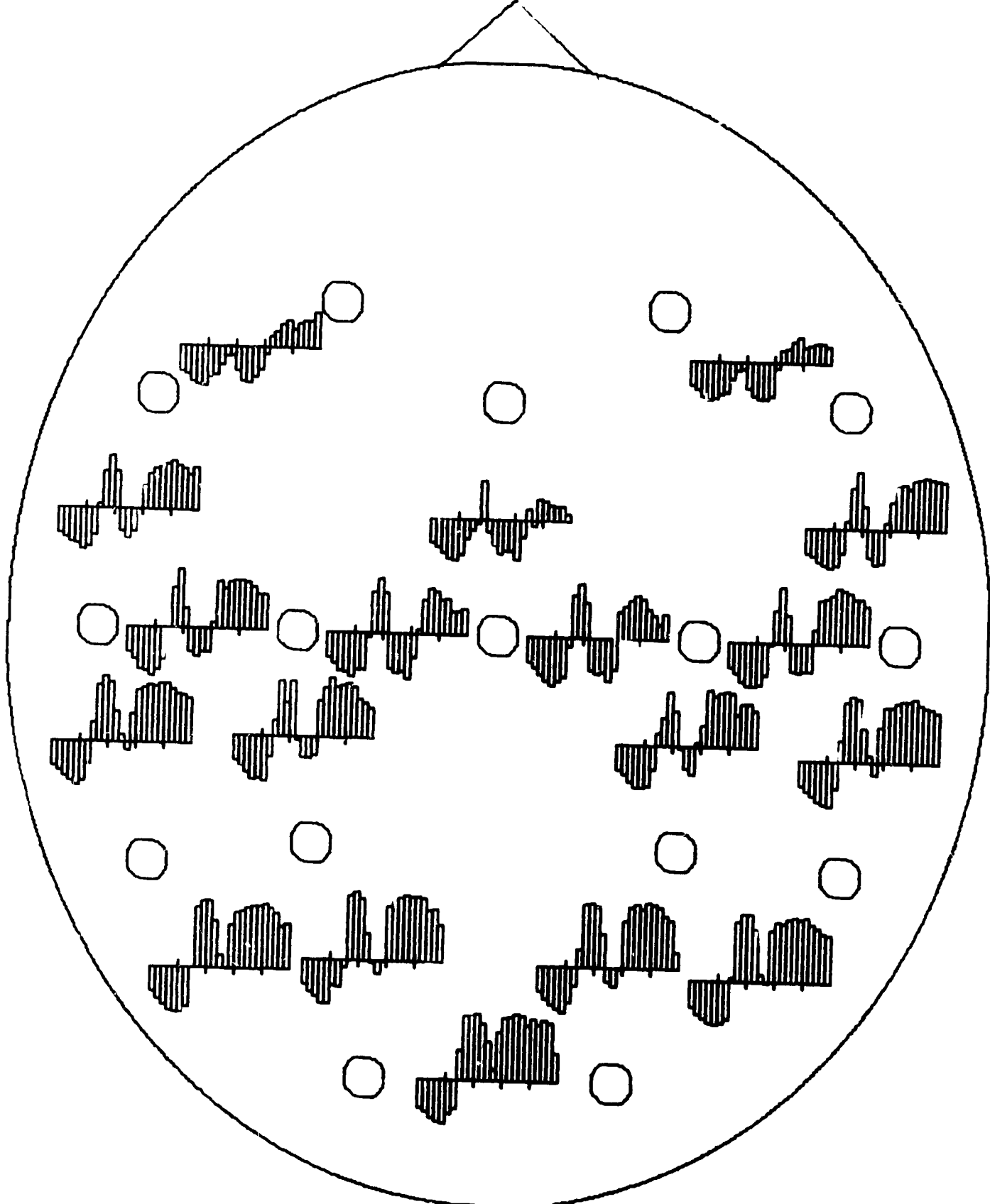
SV - AVERAGE



WITHIN VAR-NS



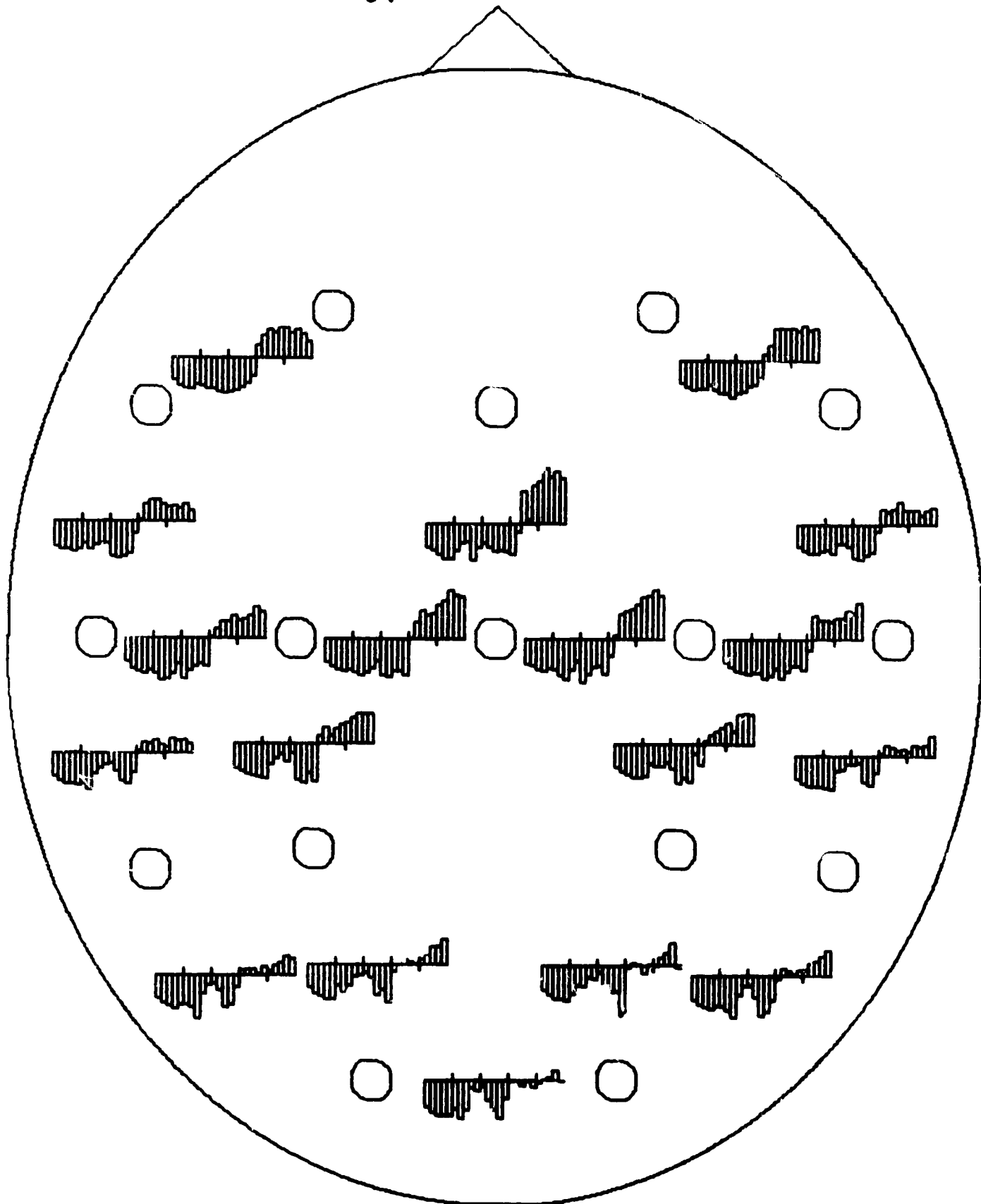
SV - CODE 124



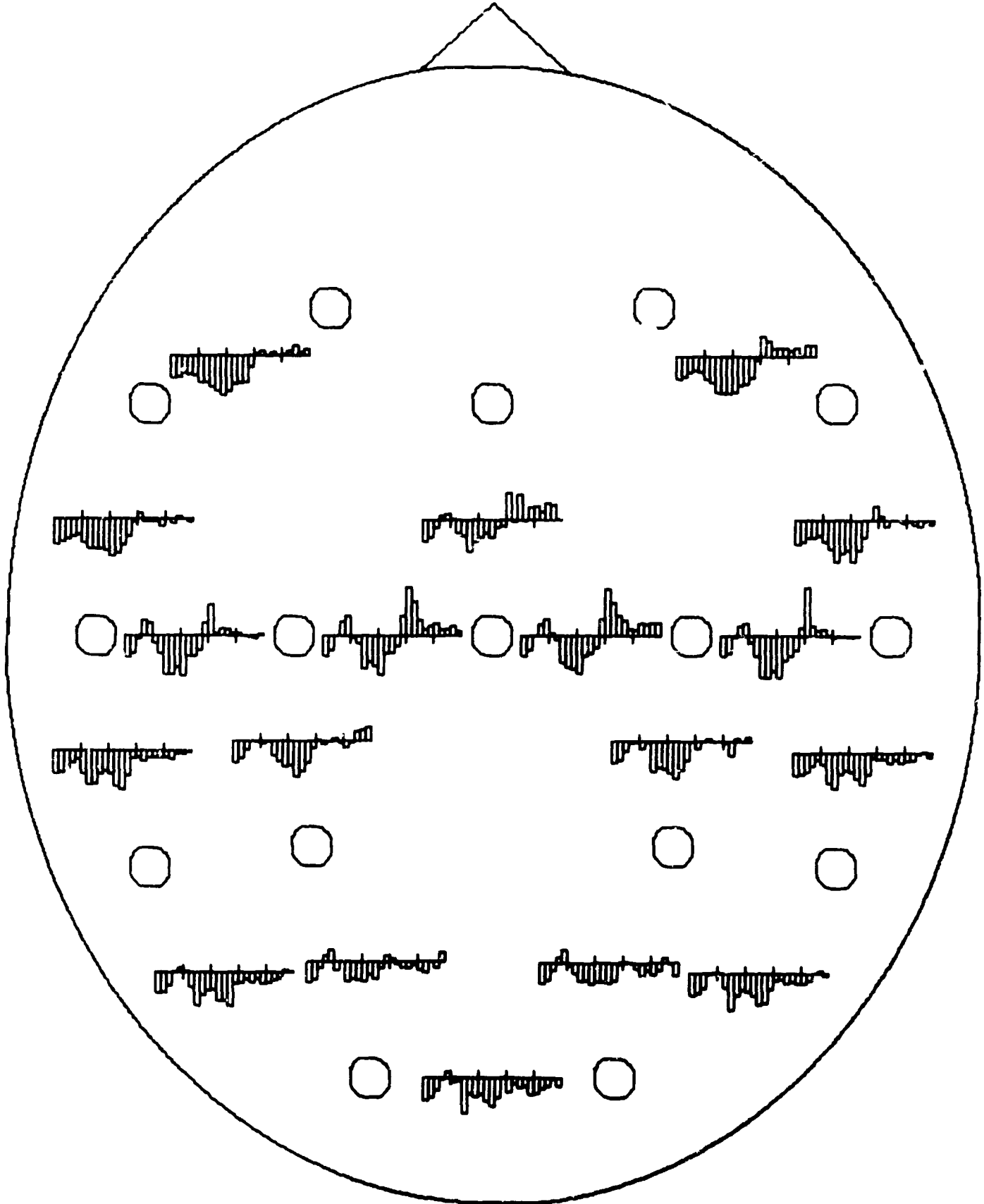
1

WITHIN UAR-NS

SV-CODE 125

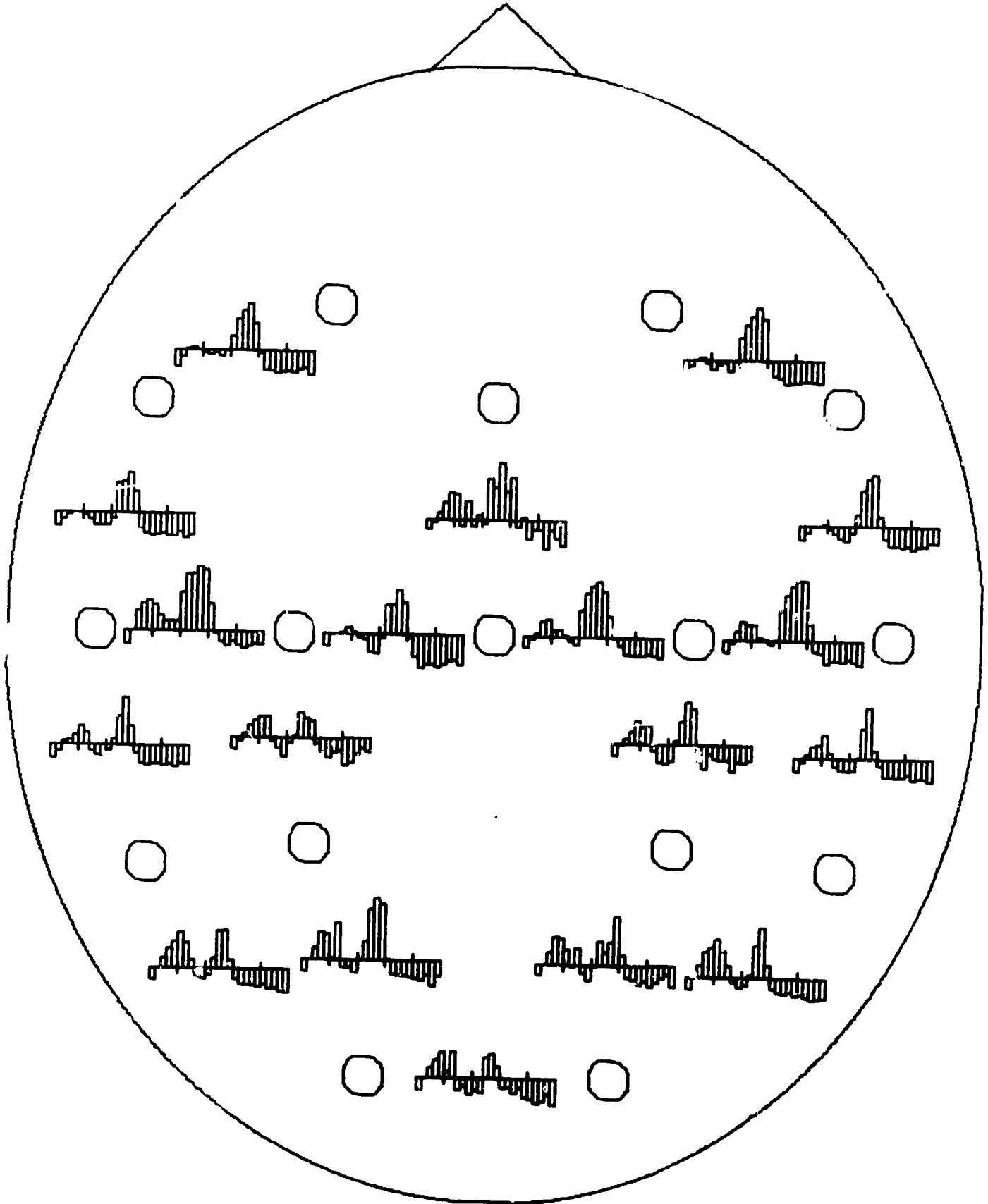


SV - CODE 126



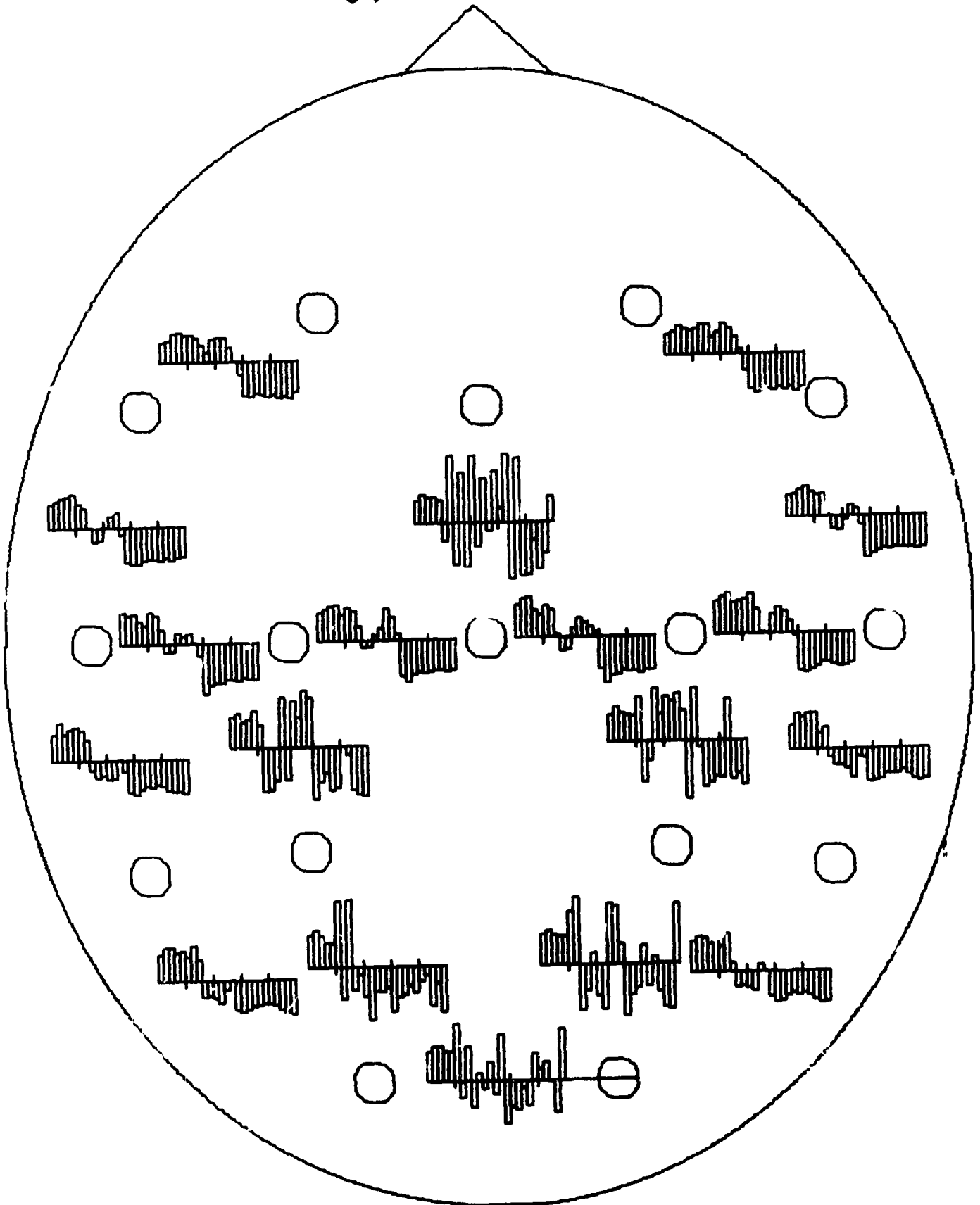
WITHIN UAR-NS

SV - CODE 127



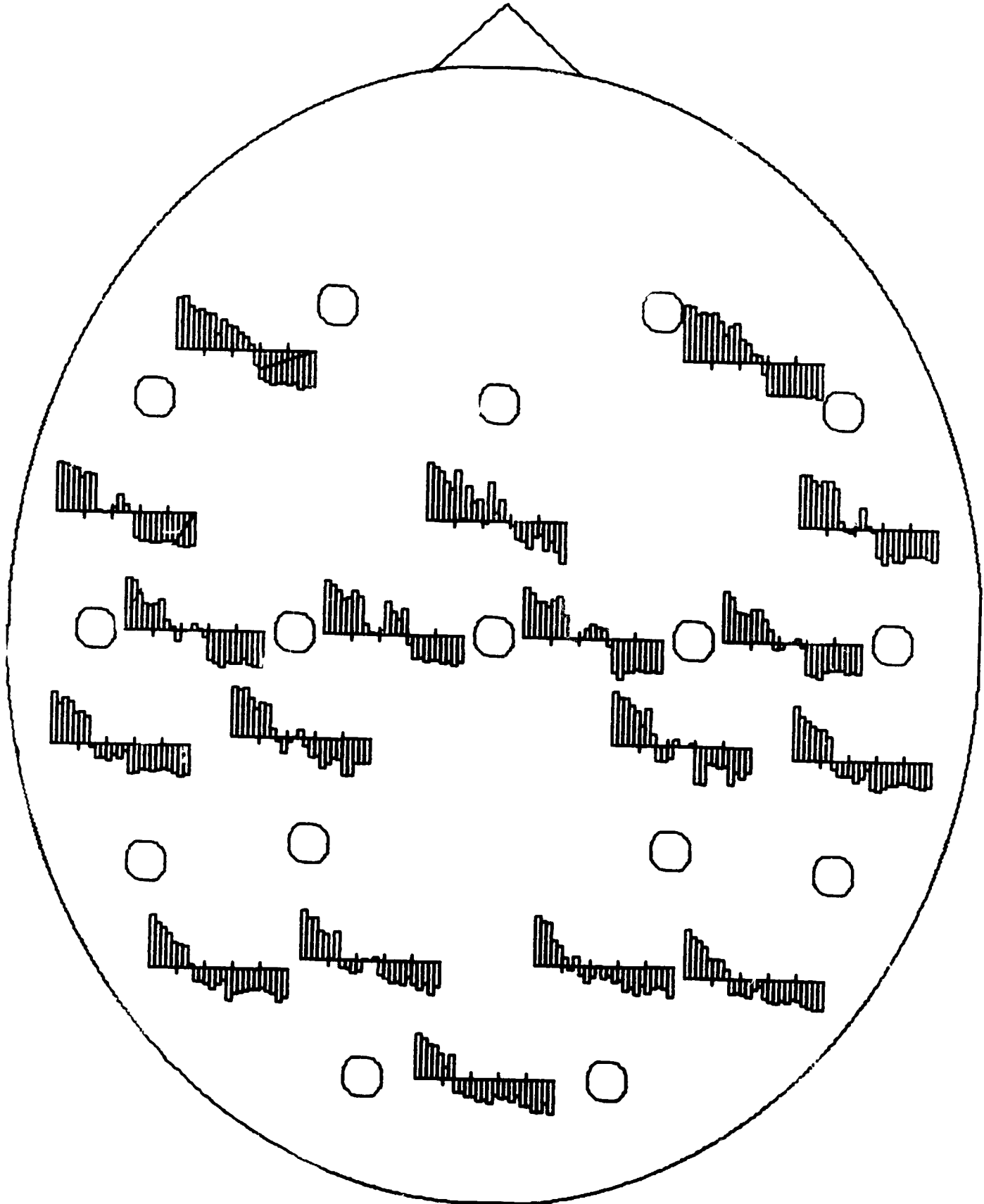
WITHIN VAR-NS

SV-CODE 128



WITHIN VAR-NS

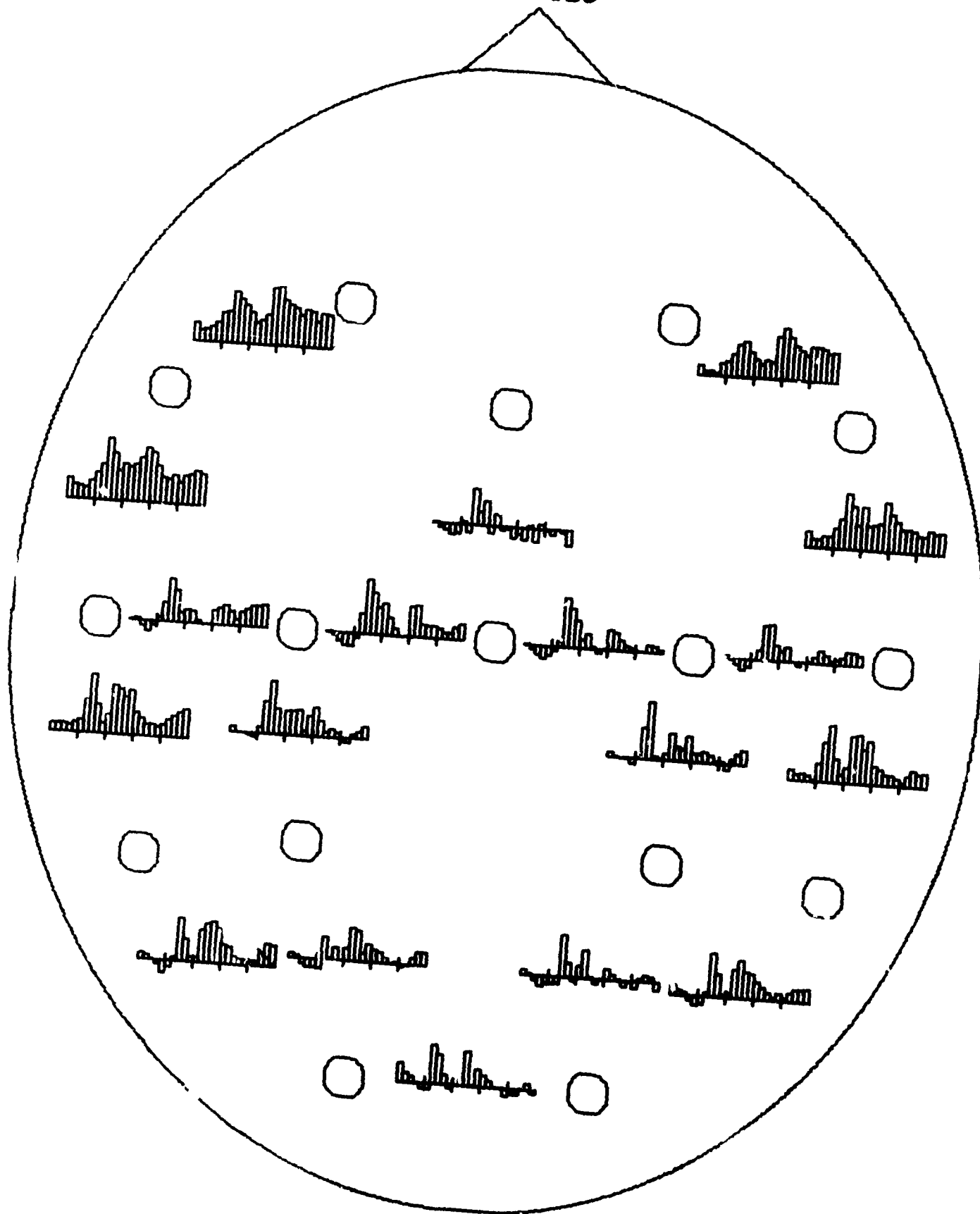
SV-CODE 129

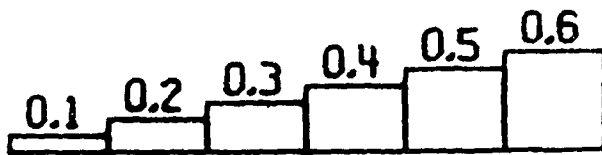




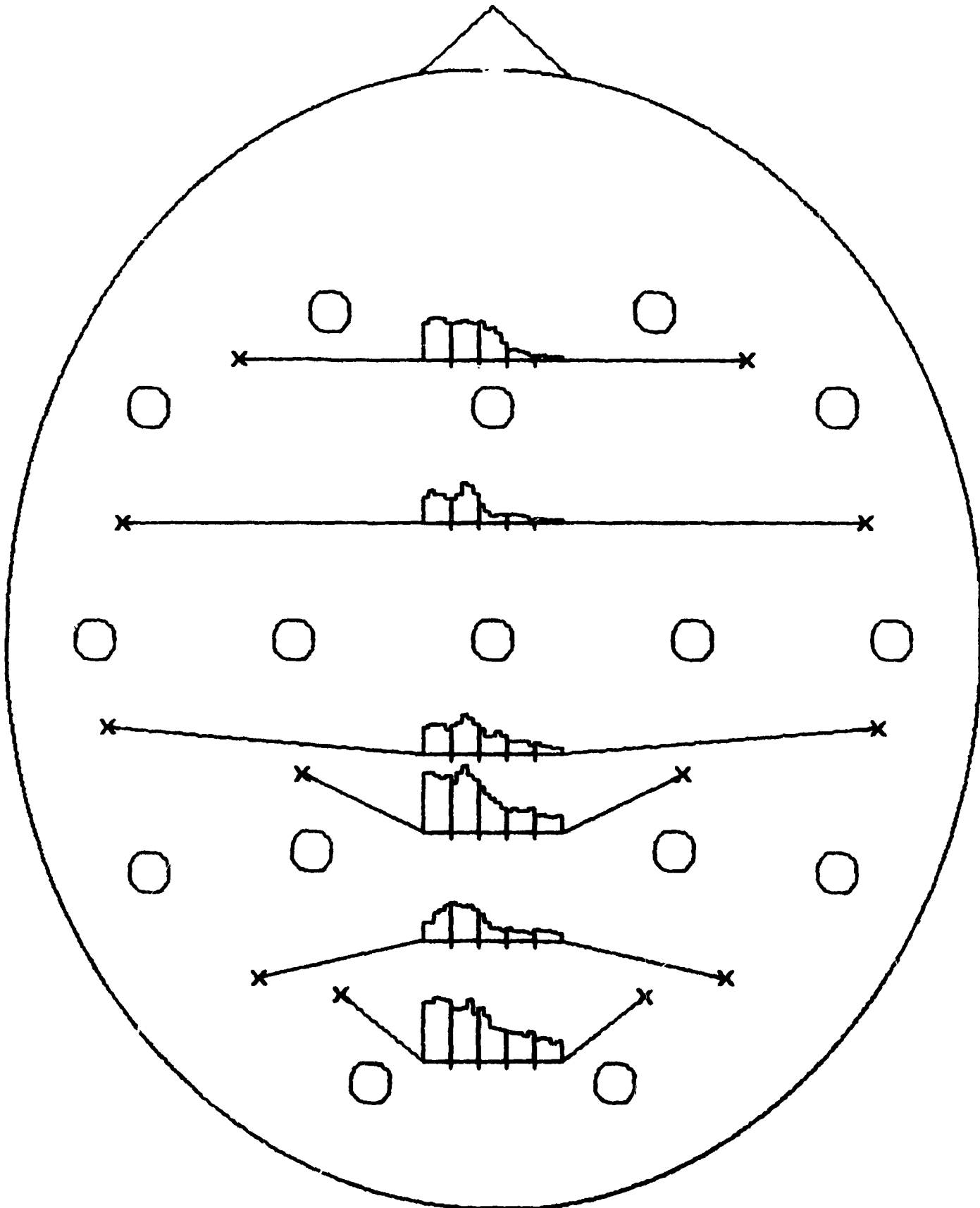
WITHIN UAR-NS

SV-CODE 130



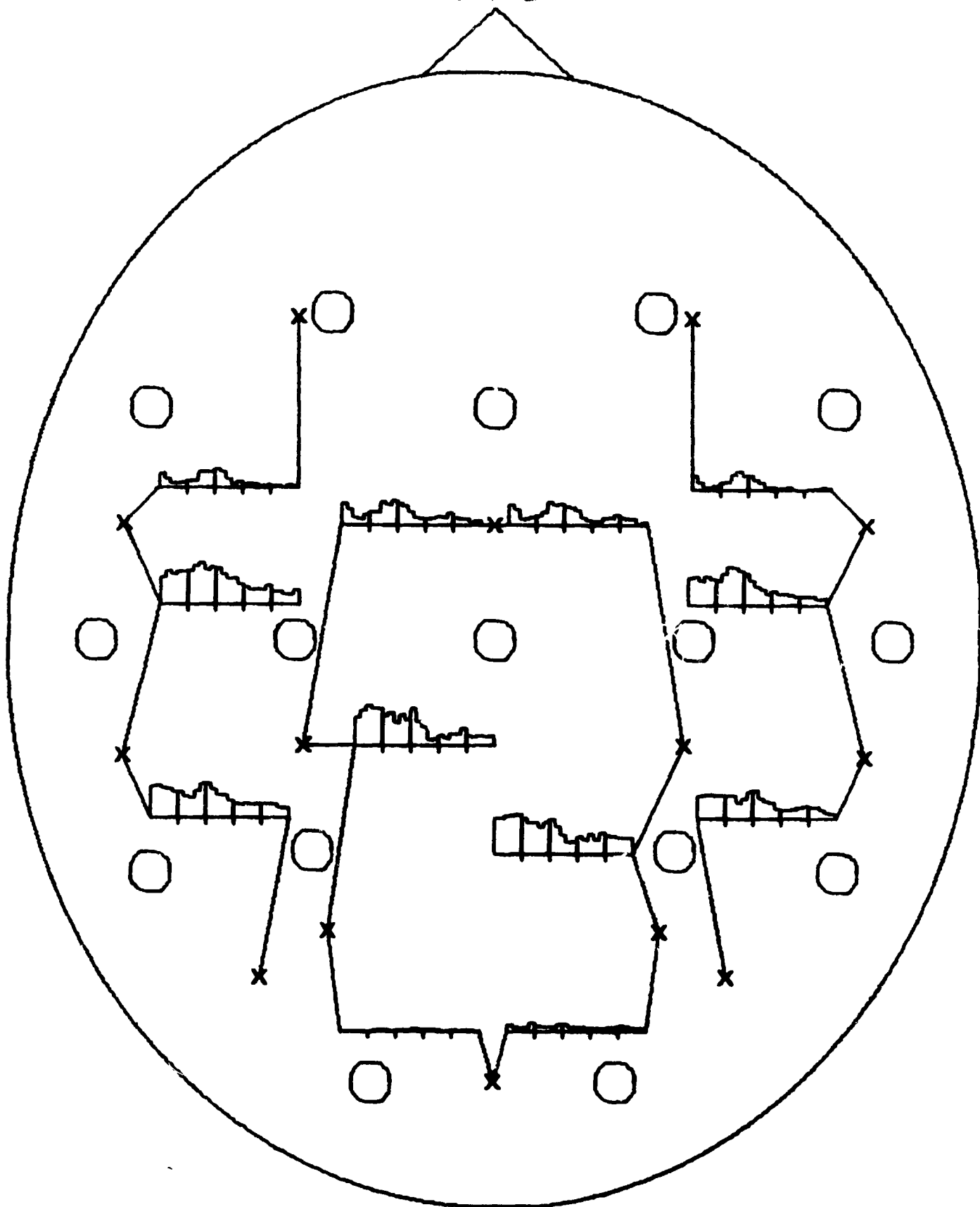


SC-1-AVERAGE

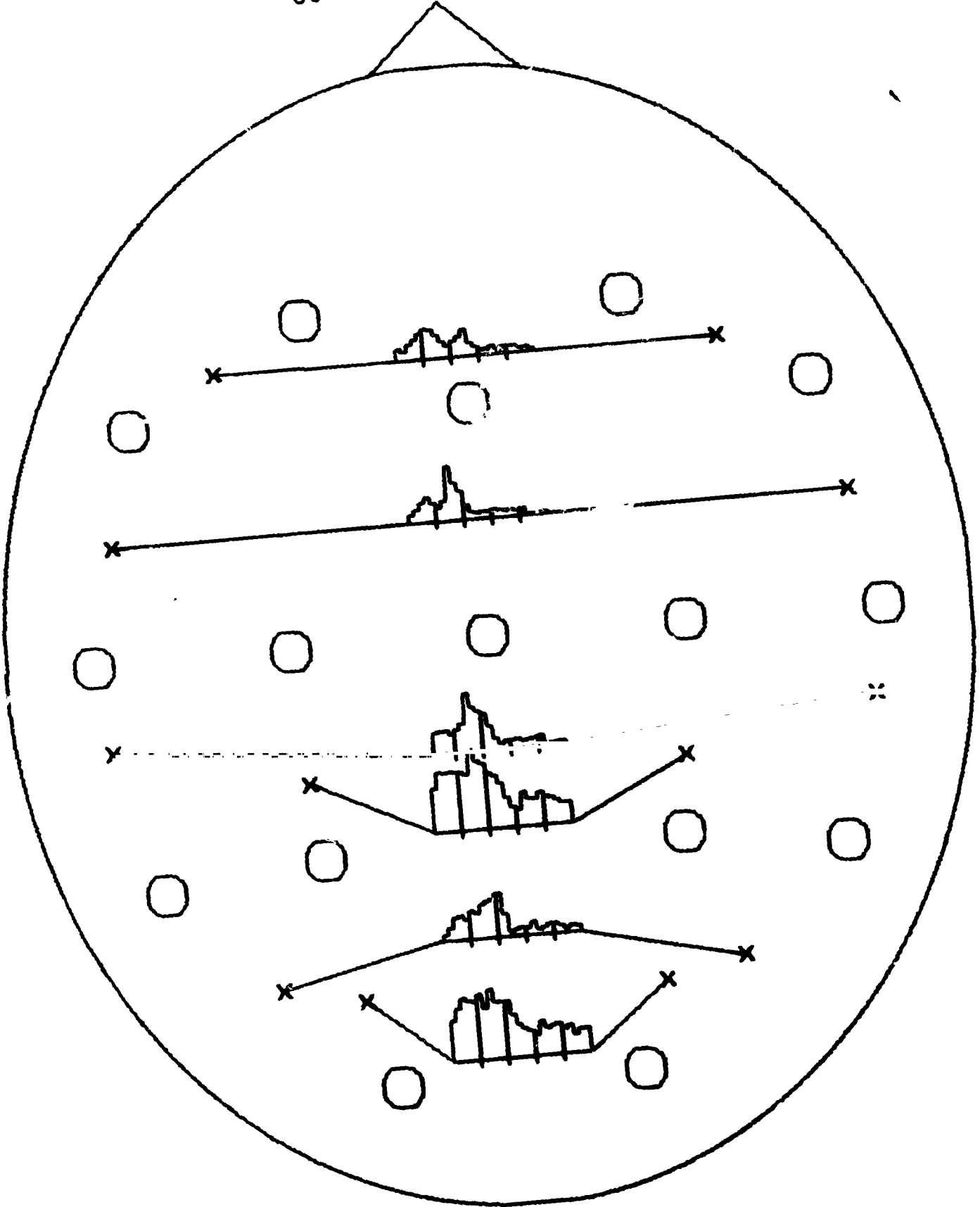




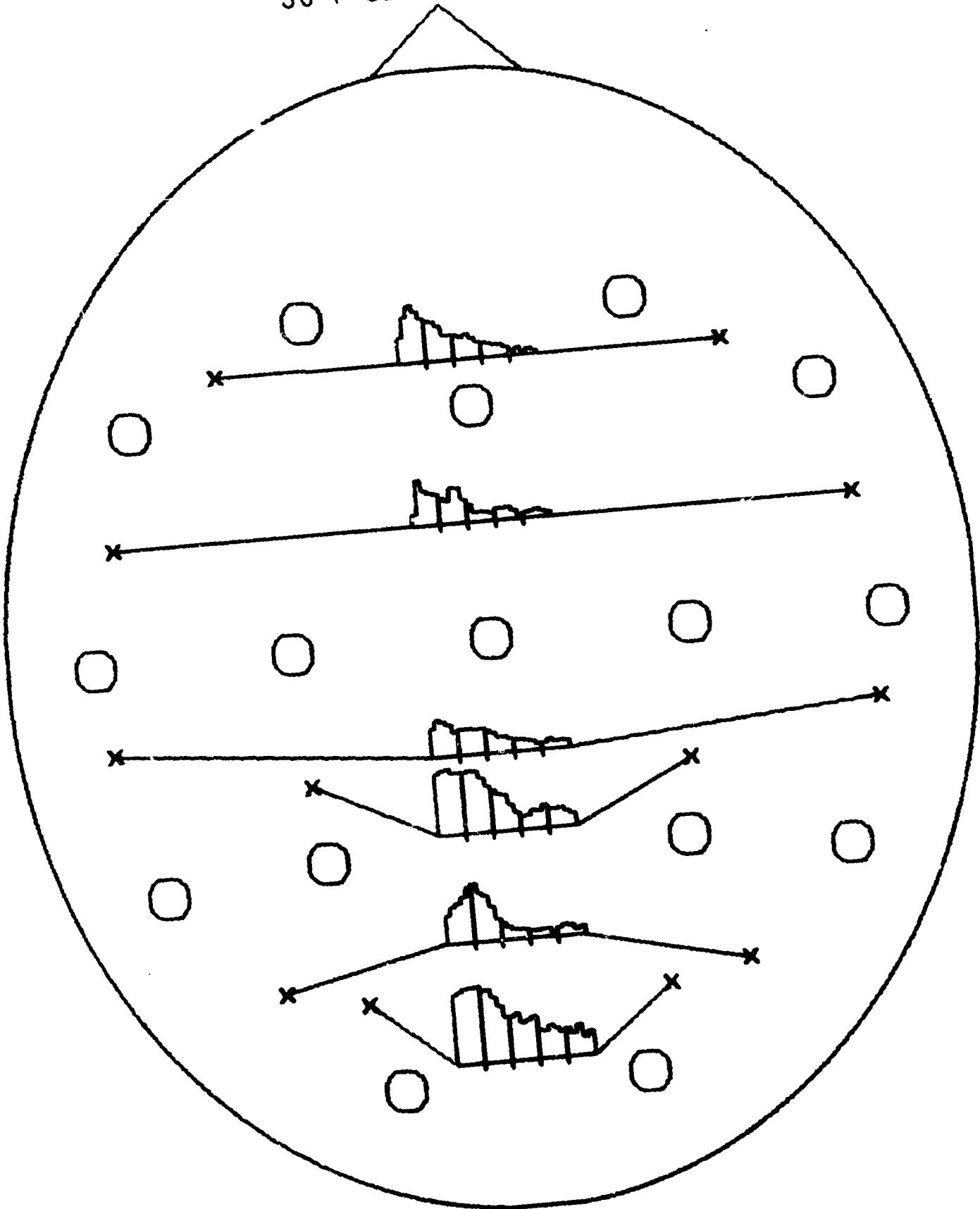
SC-3-AVERAGE



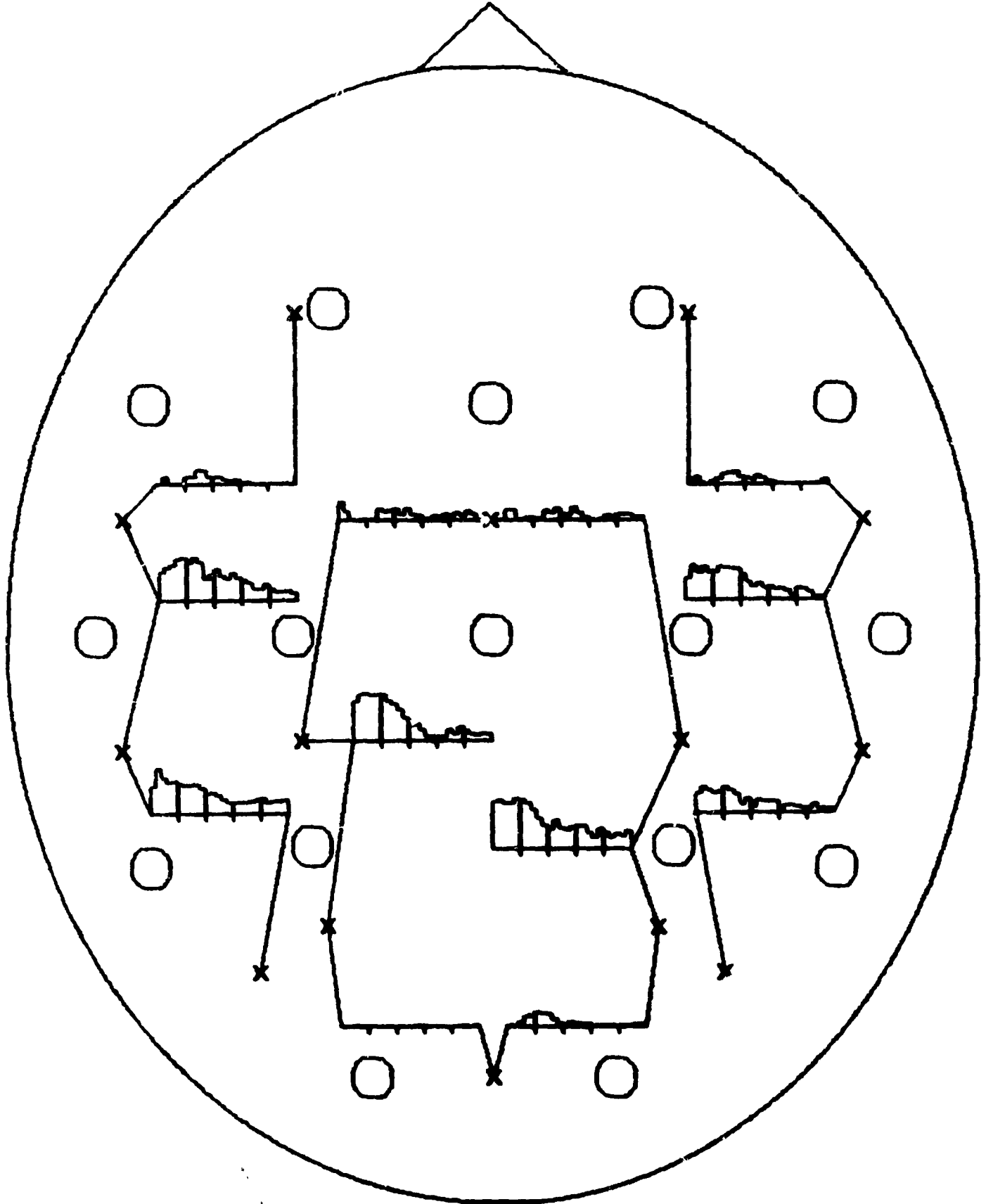
SC-1- CODE 125



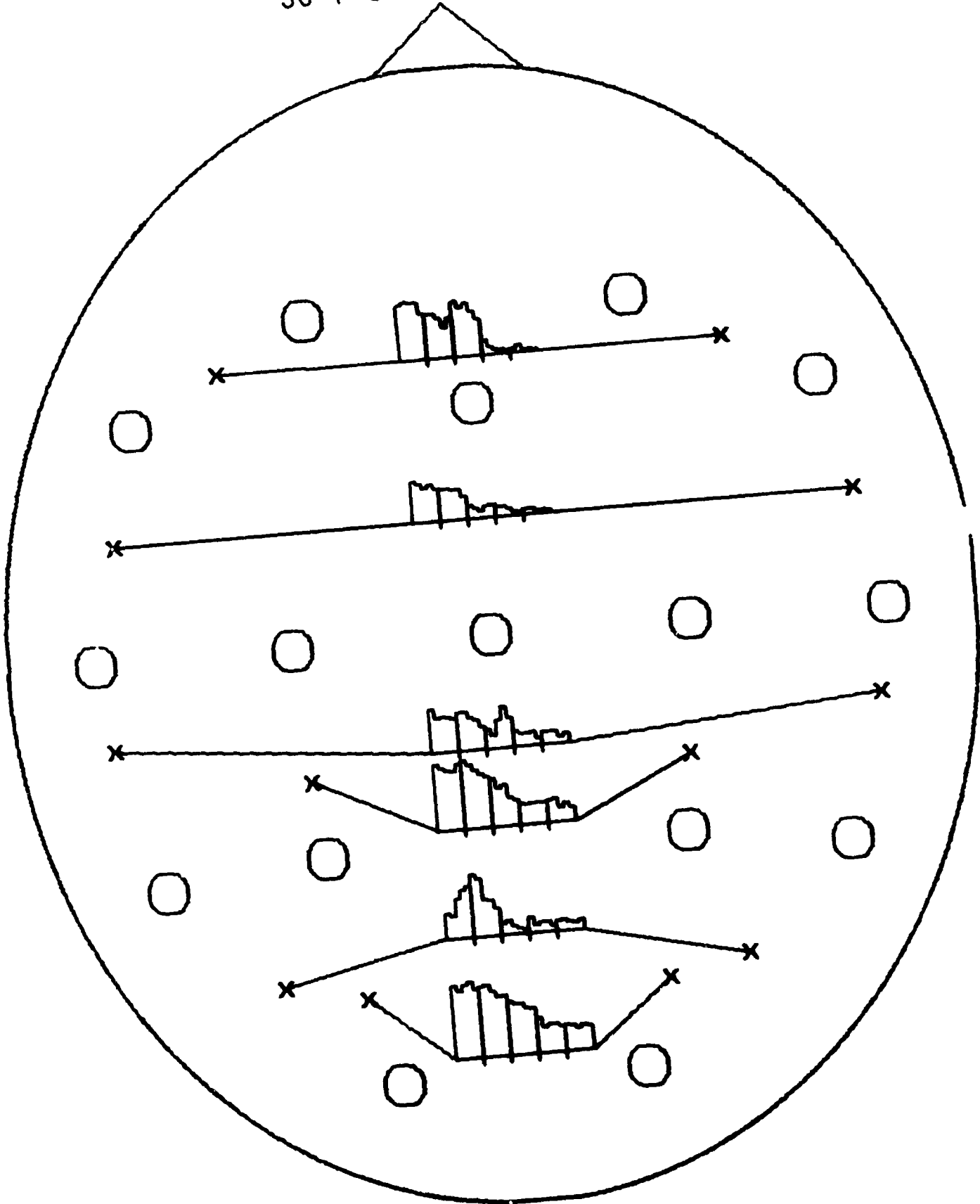
SC-1-CODE 126



SC-3-CODE 126

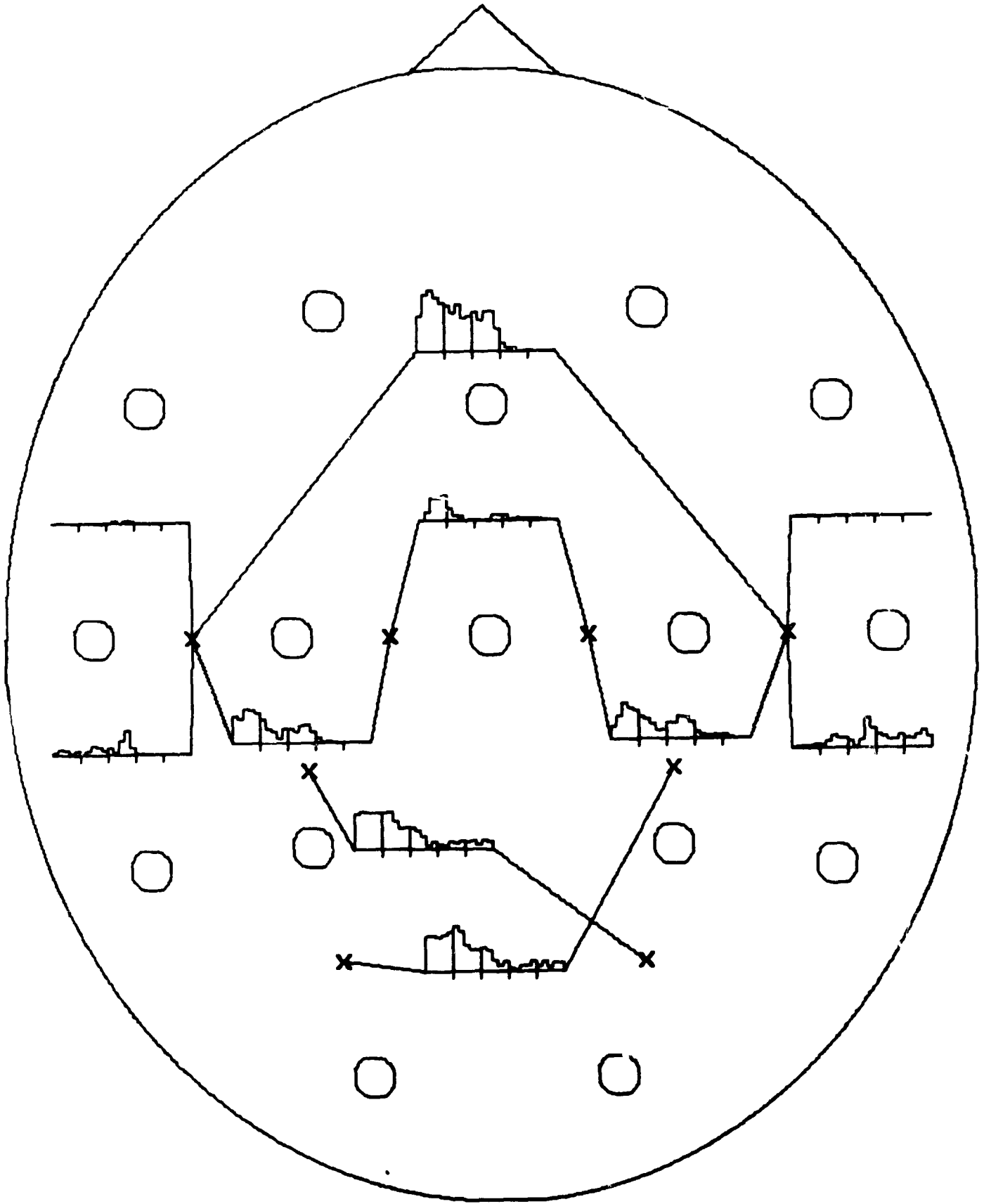


SC-1-CODE 127

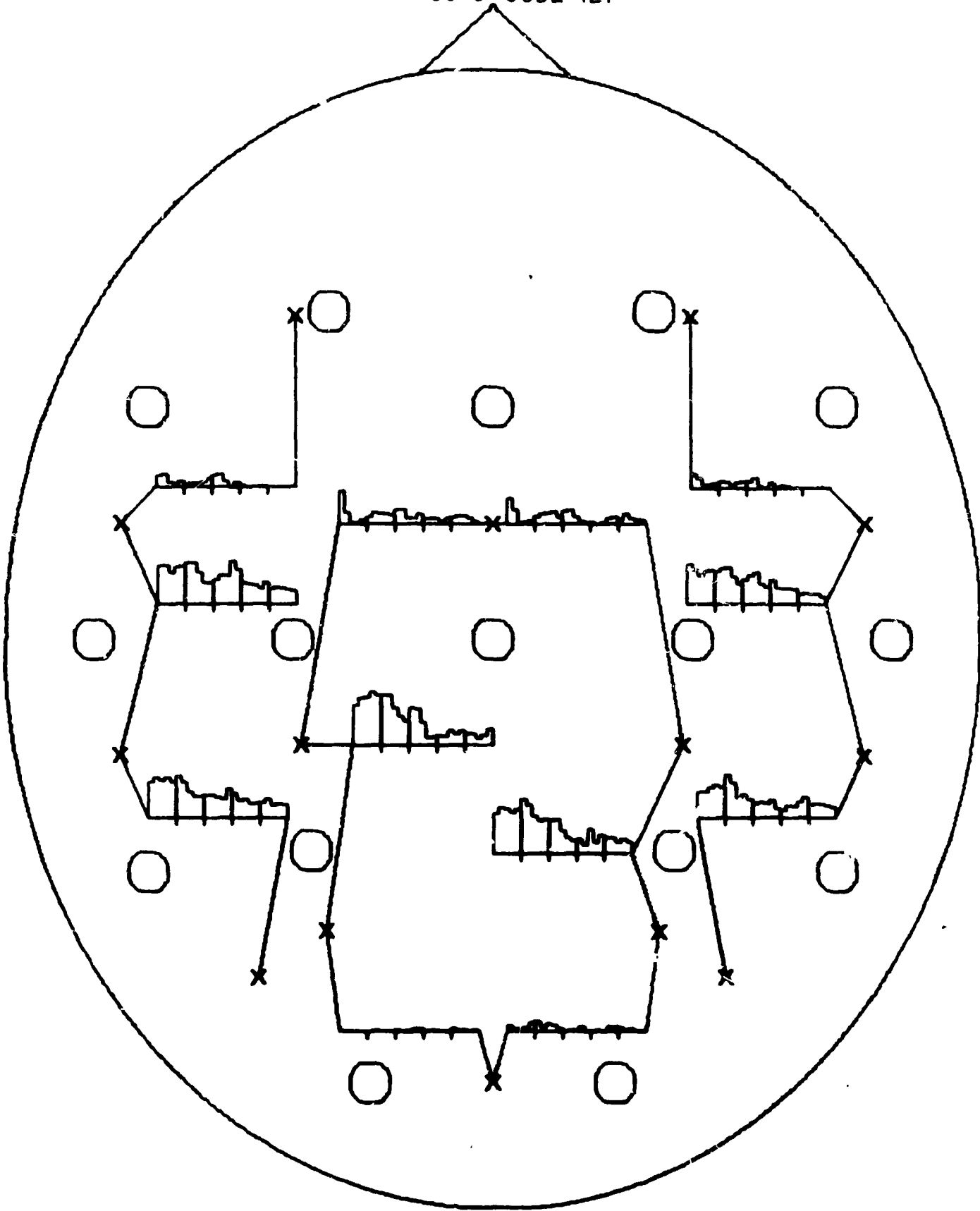




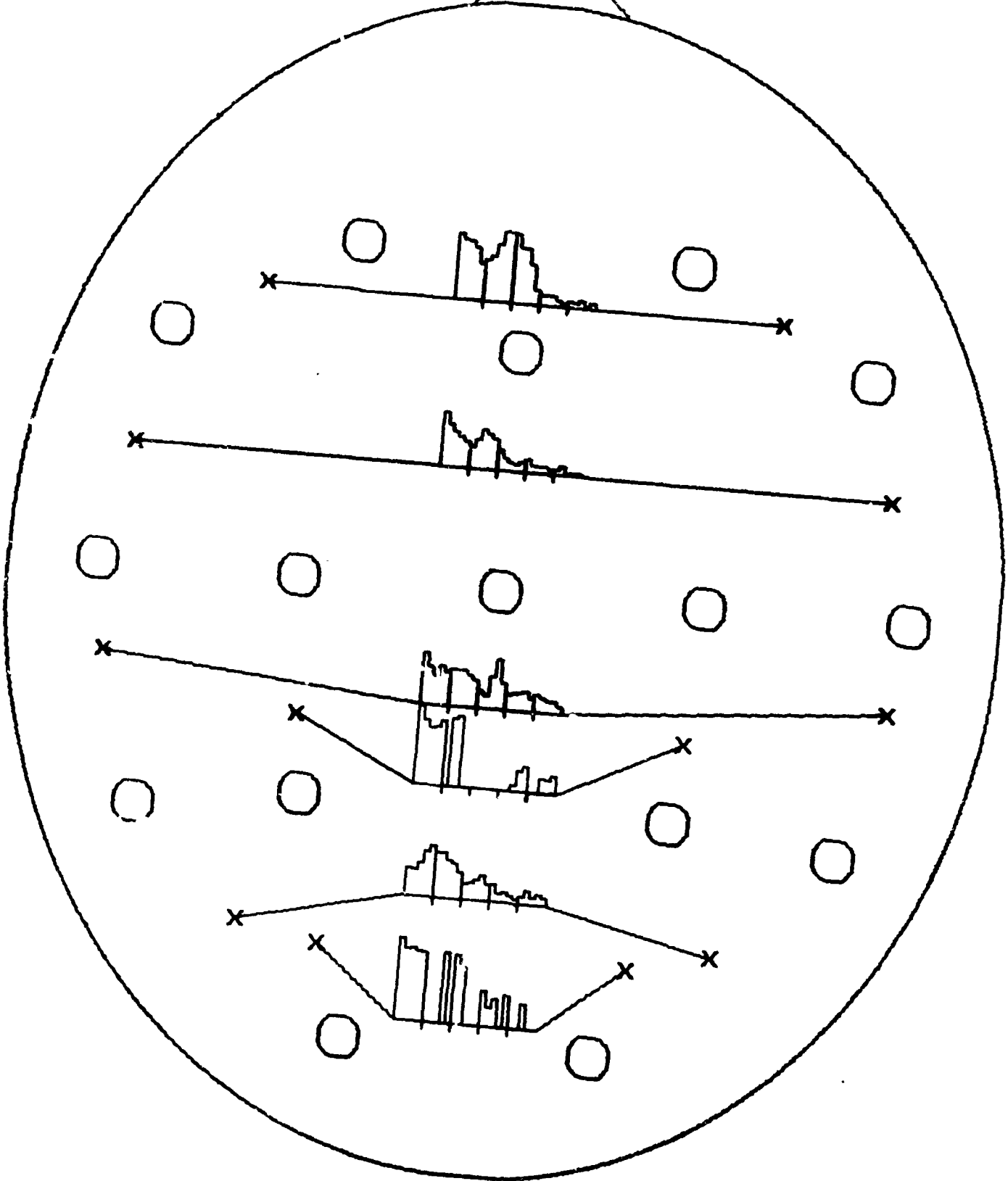
SC-2 - CODE 127



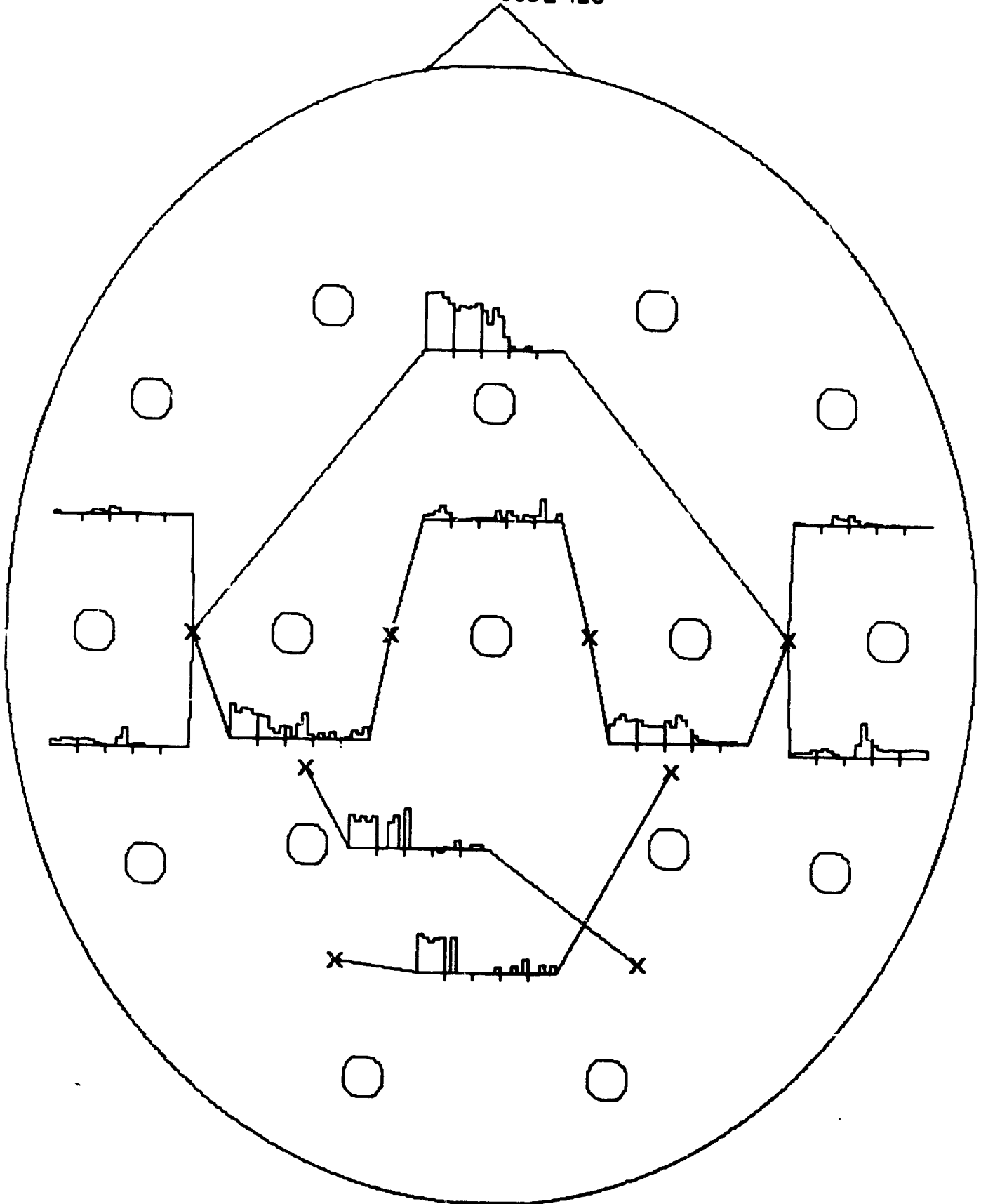
SC-3- CODE 127



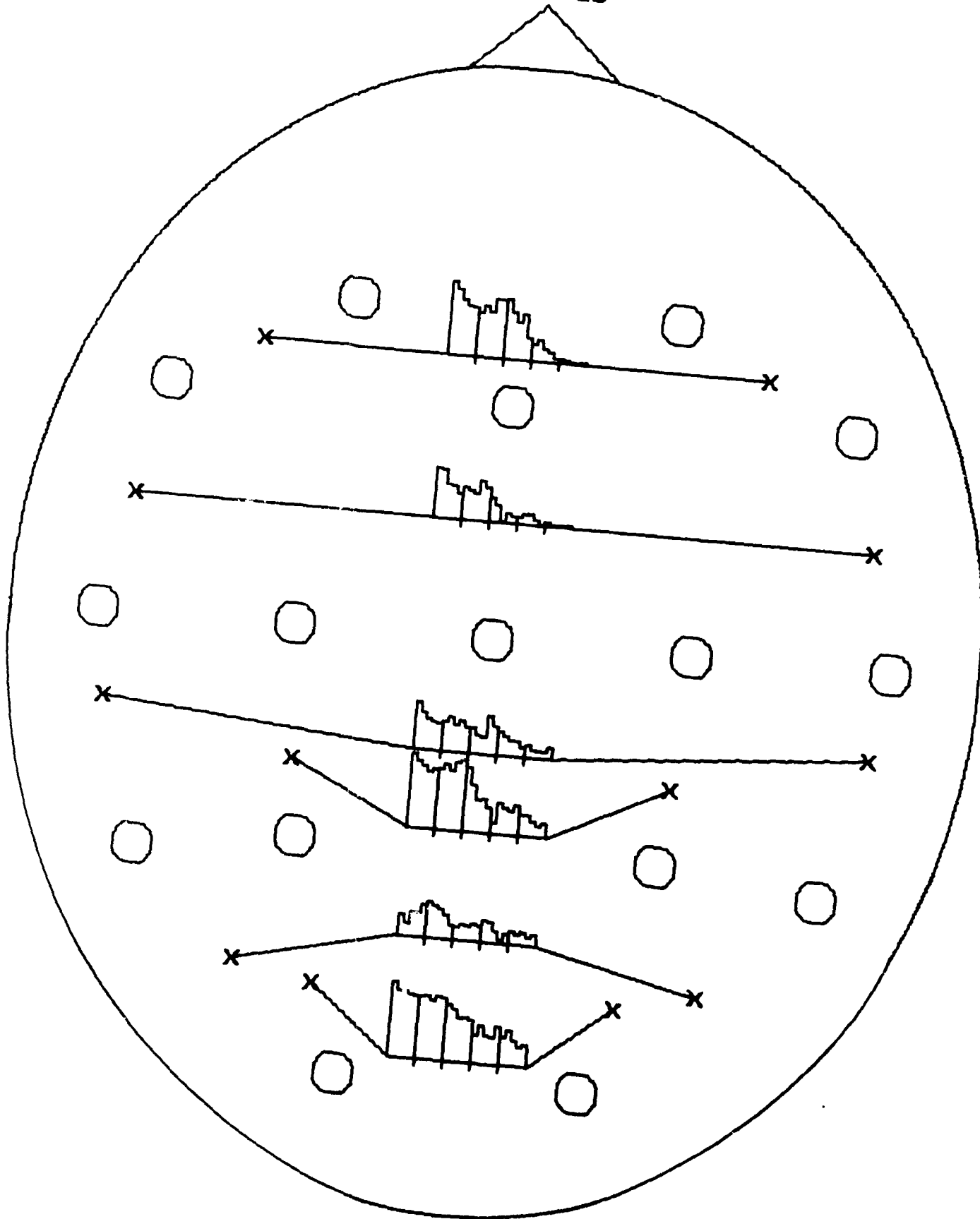
SC-1-CODE 128



SC-2-CODE 128



SC-1- CODE 129



SC-1- CODE 129

